Motivational salience, the clinical highrisk state for psychosis and acute modulation by cannabidiol

Wilson, Robin

Awarding institution:
King's College London

Motivational salience, the clinical high-risk state for psychosis and acute modulation by cannabidiol

Dr Robin Paul Wilson

MBBS, BSc, MRCPsych

Thesis for the degree of

Doctor of Medicine (Research) by Publication

King's College London

Department of Psychosis Studies

Institute of Psychiatry, Psychology and Neuroscience

King's College London

This thesis is dedicated to my long-suffering wife Ali, who has inspired, challenged, comforted, re-assured and just plain put up with me for the duration, and to my two favourite chaps, Barnaby and Rory, who constantly remind me that there's more to life than work.

Acknowledgements

First and foremost, I'd like to express deep gratitude to my supervisor Sagnik, who has the patience of a saint and wisdom of a guru. I'd like to thank Matt Kempton, Matthijs Bossong, Paul Allen and the rest of 'Team Sagnik' (you know who you are) for listening, advising, encouraging, assisting, collaborating, organising and generally making this work possible. Finally, I'd like to thank my parents for their unwavering support on this journey.

Contents

Abstract **6**

Chapter 1. Introduction **9**

Psychosis 10

Early intervention 11

Reward processing and motivational salience in psychosis 13

The endocannabinoid system, motivational salience and psychosis 16

Cannabidiol 20

Thesis rationale 21

Chapter 2. General methodology **22**

Imaging activity in the brain: functional magnetic resonance imaging (fMRI) 23

The BOLD signal 24

Analysing images: Statistical Parametric Mapping (SPM) 25

Preprocessing *25*

Modelling and the general linear model (GLM) *26*

Statistical inference *27*

Capturing reward processing with fMRI: the monetary incentive delay task 28

Publication 1. The neural substrate of reward anticipation in health: a meta-analysis of fMRI findings in the monetary incentive delay task 29

Publication 2. Cannabidiol attenuates insular dysfunction during motivational salience processing in subjects at clinical high risk for psychosis 31

Population sample *31*

Design *32*

Chapter 3. The neural substrate of reward anticipation in health: a meta-analysis of fMRI findings in the monetary incentive delay task. Wilson, R. P., Colizzi, M., Bossong, M. G., Allen, P., Kempton, M. & Bhattacharyya, S., 25 Sep 2018, Neuropsychology Review **34**

Addendum 46

Bias in coordinate-based data *46*

Between-group linear comparison *47*

Conclusion *49*

Chapter 4. Cannabidiol attenuates insular dysfunction during motivational salience processing in subjects at clinical high risk for psychosis. Wilson, R. P., Bossong, M. G., Appiah-Kusi, E. M., Petros, N., Brammer, M., Perez, J., Allen, P., McGuire, P. & Bhattacharyya, S., 2019, Translational Psychiatry **50**

Chapter 5. Discussion **61**

Summary of findings 62

The MS meta-analysis 62
The CBD study 64
Limitations and methodological considerations 68
The fMRI/cognitive task paradigm 68
MS meta-analysis 68
CBD study 69
Implications for clinical practice 70
Future research 71
Chapter 6. References 72
Appendices 94
Appendix 1 95
Supplementary References 1: Monetary Incentive Delay Task Analysis Consortium (MTAC) listed in alphabetical order 95
Supplementary Table 1. Available demographics for all 33 studies included in omnibus analysis including coordinate-based and group map data sources 96
Supplementary Table 2: Monetary incentive delay task parameters for all 33 studies included in omnibus analysis including coordinate-based and group map data sources 100
Supplementary Table 3: fMRI data acquisition and analysis parameters for all 33 studies included in omnibus analysis including coordinate-based and group map data sources 103
Supplementary Figure 1: Funnel plots for the highest peaks in AWAN and ALAN with Egger's test for asymmetry 107
Supplementary Table 4: Omnibus results for text coordinates and maps combined- main peaks 111
Supplementary Table 5: Only Group Map Results 113
Supplementary Table 6: Between Group Linear Comparison anticipation win-vs-neutral minus anticipation lose-vs-neutral 127
Supplementary Table 7: Hetereogeneity QH Stats Converted to SDM z-scores 128
Supplementary Figure 2: Binarised thresholded overlay map of heterogeneity and mean map activation and deactivation 129
Supplementary Figure 3: Binarised Jacknife density maps with mean maps of activation and deactivation separated out to enhance visual inspection 129
Supplementary Figure 4: Meta-regression for placebo effect with mean map heterogeneity overlaid 130
Supplementary Table 8: Meta-regression for Placebo Effect 131
Supplementary Figure 5: Meta-regression for Field Strength with Mean Map Heterogeneity Overlay 132
Supplementary Table 9: Meta-regression for Field Strength 132
Appendix 2 135

Figure 1. Example of MIDT visual cue sequence *135*
Table 1. Brain regions activated by the monetary incentive delay task in healthy controls..... *136*
Table 2. Wholebrain analysis for salience-vs-neutral contrast *137*
Figure 2. Whole-brain analysis of salience>neutral contrast..... *138*
Supplementary Analysis *139*

Abstract

Functional psychosis is a severe mental illness with often devastating consequences for individuals and a high cost to society. One leading aetiopathological hypothesis is the 'aberrant salience theory' whereby abnormal salience is attributed to stimuli leading to psychotic symptoms mediated by striatal dopamine. Reward processing is also thought to be mediated by striatal dopamine and is disrupted in psychosis. One aspect of reward processing is motivational salience, whereby perception of an incentivising stimulus leads to approach behaviour in an organism. Accumulating data points to a role for the endocannabinoid system in both psychosis and reward processing. In particular, the phytocannabinoid cannabidiol (CBD) is a promising candidate as a novel antipsychotic. At the core of this thesis are two published articles using functional magnetic resonance imaging (fMRI) to investigate the neural substrate of motivational salience in health, how it is affected in psychosis and the neurocognitive effects of CBD.

The first article is an international meta-analysis of fifteen original fMRI group maps sourced from healthy adult participants (n=346) undertaking the Monetary Incentive Delay Task (MIDT). We analysed the anticipation of monetary reward and loss contrasted with the neutral condition. In both contrasts there was consistent activation of the striatum and salience network, with more complex patterns of activation and deactivation in the central executive network, default network and cerebellum. We subsequently compared the anticipation of reward with loss and found significantly greater relative deactivation in the left inferior frontal gyrus.

The second publication reports a randomised double-blind placebo-controlled study using the MIDT in which thirty-three participants at clinical high risk for psychosis (CHR) were administered either 600mg oral CBD or placebo and compared with nineteen healthy controls (HC). CHR subjects represent a population of help-seeking individuals who have experienced psychotic-like symptoms or have significant genetic risk of developing a psychotic illness, but they remain antipsychotic-naïve. Reward and loss anticipation conditions were combined to create a condition of motivational salience, subsequently contrasted with neutral. Region-of-interest analysis was confined to two masks consisting of striatum/midbrain/hippocampus and the core salience network (anterior cingulate/insula). Differences were detected between CHR-placebo and HC groups and CHR-placebo and CHR-CBD groups within the core salience network but not within the mask containing the striatum. There was increased activation in a region of posterior left insula/parietal operculum in CHR-placebo compared to HC. Activation in this area in the CHR-placebo group positively correlated with psychotic symptoms and negatively correlated with salience perception, as indexed by reaction time difference between salient and neutral stimuli. Thus, psychopathology and aberrant salience were

linked to increased activation in the same region of brain in CHR. Increased activation in the left insula/parietal operculum in CHR was attenuated by CBD.

In conclusion, this thesis establishes that the salience network is activated in motivational salience, and that the neurocognitive dysfunction associated with reward processing in psychosis may be based in the salience network, in particular insula/operculum regions. Moreover, the effect of CBD in attenuating activity in the insula/operculum suggests a potential antipsychotic mechanism-of-action by normalising aberrant motivational salience.

Chapter 1

Introduction

Psychosis

Psychosis is a severe mental disorder involving the breakdown of evaluation of external reality. There are many different diagnostic categories of psychotic disorder, the most well-known being schizophrenia, a lifelong disorder characterised by a combination of positive symptoms, such as thought disorder, delusions and hallucinations, and negative symptoms, such as avolition, anhedonia and blunting of affect. It's a big problem. The global and lifetime prevalence of primary psychotic disorders have been estimated at 0.46% and 0.75% respectively (Moreno-Küstner, Martin et al. 2018), the global disability-adjusted life years of schizophreniform disorders at 0.51% (James, Abate et al. 2018), and the global economic burden can be up to 1.65% of national GDP (Chong, Teoh et al. 2016). The incidence of psychotic disorders peaks in the third decade of life. In males, incidence is higher in youth, with a steep decline compared to females, for whom there is a smaller secondary peak in the fifth decade of life (Kirkbride, Errazuriz et al. 2012, Eranti, MacCabe et al. 2013). Objective recovery including clinical and social domains has been estimated from between 14 to 38% (Jääskeläinen, Juola et al. 2012, Lally, Ajnakina et al. 2017). Life expectancy is significantly reduced (worse for males) (Hjorthøj, Stürup et al. 2017), attributed mainly to vascular disease, cancer and respiratory disease, with between five to ten times elevated mortality due to suicide (Das-Munshi, Chang et al. 2017).

The aetiopathology of schizophreniform disorders remain elusive. There are established associations with childhood adversity, such as trauma and abuse, measures of 'urbanicity' and ethnicity (such as black Caribbean and black African in the UK) (Kirkbride, Errazuriz et al. 2012, Matheson, Shepherd et al. 2012). There is a strong genetic component with high estimated heritability, up to 81% in twin studies (Sullivan, Kendler et al. 2003). 108 independent genetic loci have been identified through genome-wide association study including the dopamine receptor 2 (D_2-R) gene, glutamatergic genes and genes involved in immunity (Schizophrenia Working Group of the Psychiatric Genomics, Ripke et al. 2014), although the presence of such genes confers risk only, being 'neither necessary nor sufficient' to cause psychosis. The longstanding 'neurodevelopmental hypothesis' (Weinberger 1987) posits that early insults to the developing brain impact on normal maturation. This is supported by evidence of increased risk in low birthweight, obstetric complications, prenatal exposure to viral infection and malnutrition (Murray, Bhavsar et al. 2017). Further supporting evidence is now emerging for epigenetic effects during pre and post-natal development (Jaffe, Gao et al. 2015).

Two neurotransmitter systems are at the forefront of aetiological theory and treatment- glutamate (Glu) and dopamine (DA) (Howes, McCutcheon et al. 2015). One dominant aetiological theory is the 'aberrant salience hypothesis', whereby hyperdopaminergia in the mesostriatal pathway (from midbrain to striatum) results in aberrant attribution of salience to stimuli causing psychotic symptoms

(Kapur 2003). Evidence for hyperdopaminergia is robust: all licensed effective antipsychotics block D_2-R, the D_2-R affinity of antipsychotics is related to clinical response, antipsychotics have a therapeutic index based on D_2-R occupancy between 50 to 65%, and presynaptic DA-ergic function is elevated in both PET (positron emission tomography) and SPECT (single-photon emission computed tomography) studies (Howes, Egerton et al. 2009, Howes, Kambeitz et al. 2012).

However, in around 20 to 30% of people with schizophrenia, psychotic symptoms do not respond to D_2-R blockade with conventional antipsychotics. The exact clinical criteria for this 'treatment-resistant' group are not yet fully codified, though consensus guidelines have been published (Howes, McCutcheon et al. 2017). Neuroimaging has identified some differences from treatment-responsive groups, including reduced frontotemporal perfusion and grey matter volume, increased white matter perfusion, increased basal ganglia perfusion, relatively normal striatal DA synthesis and elevated Glu in the anterior cingulate gyrus (ACG) (Demjaha, Murray et al. 2012, Demjaha, Egerton et al. 2014, Mouchlianitis, McCutcheon et al. 2016).

Glu-ergic involvement is predominantly based on the NMDA-R (N-methyl-D-aspartate receptor) hypofunction theory, whereby the afore-mentioned leads to disinhibition of GABA-ergic (gamma-aminobutyric acid) neurons, elevating cortical Glu and leading to excitotoxicity and neurodegeneration in key regions of the brain (Olney and Farber 1995, Stone, Morrison et al. 2007). There is some evidence for this including genetic studies and the finding of elevated Glu-ergic metabolites in the basal ganglia, thalamus and medial temporal lobe (MTL) (Merritt, Egerton et al. 2016). Yet, to date, there are no effective Glu-ergic antipsychotics.

The immune system has also been implicated in the pathogenesis of schizophrenia, by genetic studies, findings of increased microglia density and expression of pro-inflammatory genes in post-mortem studies (van Kesteren, Gremmels et al. 2017), and by elevated cytokines in vivo (Miller, Buckley et al. 2011). These theories are not mutually exclusive. In fact, immunopathogenesis is linked to NMDA-R hypofunction by the finding of NMDA-R autoantibodies in a significant minority of cases of schizophreniform disorder (Pollak, McCormack et al. 2013). Moreover, DA and Glu dysfunction are linked by the rodent-derived MAM (methylazoxymethanol) model of psychosis, in which MTL dysfunction leads to striatal hyperdopaminergia (Modinos, Allen et al. 2015).

Early intervention

Early intervention in psychosis has clinical roots in the Buckingham Project in the UK (Shanahan, Falloon et al. 1990), set up to rapidly identify and treat severe mental illness in the community, and

the EPPIC (Early Psychosis Prevention and Intervention Centre) program in Melbourne, Australia, developed to reduce morbidity in first-episode psychosis (FEP) (McGorry 1993). Early intervention in FEP has been found to significantly improve outcomes, including lower relapse, higher remission and higher recovery rates, lower treatment discontinuation, lower risk of hospitalisation, reduction of symptoms, and improved quality of life and global functioning (Correll, Galling et al. 2018), although good outcomes may not be sustained on transfer to standard treatment (Nordentoft, Rasmussen et al. 2014). The 'duration of untreated psychosis' (DUP) is defined as the time from development of the first psychotic symptom to treatment with an antipsychotic. A longer DUP is associated with worse prognosis in terms of symptoms, remission, social functioning and global outcome (Penttilä, Jääskeläinen et al. 2014). The clinical significance of reducing DUP is now recognised by NHS England with the introduction of a 2-week waiting time standard from referral to treatment (Excellence 2016). However despite great leaps in clinical service provision, 23% of FEP remain treatment-resistant at 10 years (84% since illness onset) (Demjaha, Lappin et al. 2017).

'An ounce of prevention is worth a pound of cure' (Henry de Bracton, De Legibus c.1240). One of the most robust predictors of poor prognosis is premorbid difficulties (Díaz-Caneja, Pina-Camacho et al. 2015). The 'prodrome' of relatively mild non-specific symptoms and change in general functioning prior to the onset of schizophrenia has long been recognised (Docherty, Van Kammen et al. 1978), necessitating the codifying of minimum duration and severity of symptoms into the current diagnostic classification systems (Keith and Matthews 1991). The first clinical attempt to address the prodrome phase started with the opening of the PACE (Personal Assistance and Crisis Evaluation) clinic for young people in Melbourne, Australia, in 1994. Three core characteristics were thought to elevate risk for developing psychosis in young people, as operationalised in the Comprehensive Assessment of At Risk Mental States (CAARMS) (Yung, Yuen et al. 2005): trait-state factors (presence of drop in function and first or second degree relative with diagnosed psychotic disorder), subthreshold attenuated psychotic symptoms (APS) and brief limited intermittent psychotic symptoms (BLIPS) lasting less than one week (Yung, McGorry et al. 1996). Services for people at clinical high-risk (CHR) have since blossomed internationally, stimulating research into transition, intervention, the development of further diagnostic tools and leading to the controversial inclusion of the Attenuated Psychosis Syndrome in the DSM V (Davies, Oliver et al. 2017).

However, CHR services have been criticised as an ineffective approach to preventing the onset of psychosis (van Os and Guloksuz 2017, Ajnakina, David et al. 2018). It is now known that psychotic experiences are relatively common in the general population, with prevalence estimated at 7.2% (Linscott and Van Os 2013). Psychotic experiences span both psychotic and non-psychotic states, and

may predominantly represent a marker of severity of non-psychotic disorders (van Os and Reininghaus 2016, van Os and Guloksuz 2017), particularly in adolescence (Kelleher, Keeley et al. 2012). The vast majority of CHR subjects do not transition to psychosis and actually have anxiety and/or depression (Addington, Piskulic et al. 2017). Initially, there were high rates of transition to psychosis between 30 to 54% in the first 24 months, but more recently rates appear to have fallen as low as 8 to 17% (Ajnakina, David et al. 2018). There are also discrepancies between CHR and FEP populations, for example only a fraction of FEP patients in a South London clinic had transferred from the local CHR service (Ajnakina, Morgan et al. 2017), males may be under-represented in CHR compared to FEP services internationally (Wilson, Patel et al. 2016) and ethnic minorities are under-represented in CHR subjects who transition (Valmaggia, Byrne et al. 2018). To date there is no evidence for any effective intervention in preventing transition to psychosis (Davies, Cipriani et al. 2018).

Nonetheless, early intervention in CHR has delivered important aetiological insights, particularly for individuals who have transitioned to a psychotic disorder, including: evidence of increased activity in the prefrontal cortex, left hippocampus and subcortical structures (Allen, Luigjes et al. 2012), elevated hippocampal Glu levels (Bossong, Antoniades et al. 2019), correlation between medial prefrontal GABA levels and left hippocampal perfusion (Modinos, Şimşek et al. 2018), progressive increase in striatal DA synthesis (Howes, Bose et al. 2011), and progressive grey matter volume loss in the frontal cortex (Cannon, Chung et al. 2015). Moreover, CHR research promises new pharmacological interventions such as cannabidiol (Bhattacharyya, Wilson et al. 2018) and oxytocin (Davies, Paloyelis et al. 2019).

Reward processing and motivational salience in psychosis

Reward-seeking behaviour is found across the animal kingdom (Barron, Søvik et al. 2010). At its core it consists of goal-directed behaviour and adaptive decision-making. It is an iterative learning process, whereby perception of an incentivising stimulus induces goal-directed behaviour towards consummation of reward. This, in turn, increases the likelihood of the behaviour re-occurring on perception of the same stimulus. The intrinsic value or 'valence' of an incentive creates salience in an organism. Incentives may be innate/intrinsic/primary (such as food) or may be learnt/extrinsic/secondary (such as money). The anticipation of a reward following incentive presentation creates 'motivational salience' and prepares approach behaviour. Motivational salience is subsequently reinforced by reward consumption.

In mammals, the reward mechanism is thought to be mediated by DA-ergic neurons in the striatum (Schultz, Dayan et al. 1997) and closely fits an algorithm described by the 'reward prediction error' (RPE) hypothesis (Schultz 2017). In RPE the difference between the value of the anticipated reward and the value of the received reward generates a DA-ergic signal in the striatum which subsequently informs future value anticipation. If the same stimulus and reward are presented repeatedly, the DA-ergic signal propagates earlier in time to the presentation of an incentive, contributing to motivational salience.

Abnormal reward processing is implicated in multiple psychiatric disorders and is at the root of addiction psychiatry, whereby an extrinsic chemical (and learnt cues) creates pathological motivational salience, aberrant goal-directed behaviour and recurrent consumption of the chemical, leading to a three-stage repeating cycle of binge/intoxication, withdrawal/negative affect and preoccupation/anticipation mediated by emotional state and executive function (Koob and Volkow 2016). Abnormal striatal activity and DA-ergic function are consistent findings in animal and human studies of substance use disorders (SUD) (Leyton and Vezina 2013). At the same time, aberrant salience mediated by striatal DA-ergic neurons is the leading theory of psychotic disorders (Kapur 2003, Winton-Brown, Fusar-Poli et al. 2014), and fMRI meta-analyses of both SUD and psychotic disorders have found abnormal striatal function (Radua, Schmidt et al. 2015, Luijten, Schellekens et al. 2017), suggesting there may be a common neural substrate.

There is epidemiological evidence for a common neural substrate. For decades it been observed that people with psychotic mental illness have a high prevalence of SUD (Regier, Farmer et al. 1990, Degenhardt and Hall 2001). A recent comprehensive international meta-analysis of 165,811 subjects with schizophreniform disorder estimated the prevalence of comorbid SUD (excluding tobacco) at 41.7%, identifying cannabis (26.2%) and alcohol (24.3%) as the most prevalent substances (Hunt, Large et al. 2018). Tobacco use also has long been established as being high in prevalence compared to the general population (Mitchell and Dahlgren 1986). SUD prevalence is high in both FEP and CHR with rates of cannabis and alcohol use consistently elevated (Cantwell, Brewin et al. 1999, Lambert, Conus et al. 2005, Barnett, Werners et al. 2007, Mazzoncini, Donoghue et al. 2010, Wisdom, Manuel et al. 2011, Addington, Case et al. 2014, Colizzi, Carra et al. 2016, Brunette, Mueser et al. 2018).

Applied research has demonstrated that reward processing and motivational salience are disrupted in psychosis. One behavioural measure of motivational salience is an 'accelerated motor response' to increasing probability of reward receipt. Using the Cued Reinforcement Reaction Time task, Murray et al have demonstrated impairment of this effect in both medicated and unmedicated FEP patients (Murray, Clark et al. 2008). Roiser et al also reported this in medicated patients with schizophrenia

using the Salience Attribution Test (SAT), termed 'implicit adaptive salience' (Roiser, Stephan et al. 2008). Using an instrumental learning monetary reward task, Murray et al also reported faster reaction time to neutral stimuli in both medicated and unmedicated FEP (Murray, Corlett et al. 2007).

Observing the SAT with fMRI, Smieskova et al found that reduced implicit adaptive salience was associated with clusters of reduced activation in multiple brain regions at whole-brain level in unmedicated FEP (straddling left dorsal ACG, left middle frontal gyrus and left precentral gryus), medicated FEP (right insula, right ACG, right precentral gyrus, right paracingulate gyrus), and both FEP combined (right precentral gyrus/inferior frontal gyrus and right insula) (Smieskova, Roiser et al. 2015). Furthermore, they reported a negative correlation between hallucination severity and right anterior insula activation in unmedicated FEP. Using a variant of the Monetary Incentive Delay Task (MIDT), Nielsen et al found that healthy controls improved their accuracy more than unmedicated schizophrenia patients following motivationally salient cues, associated with attenuated activation in the striatum, ACG, midbrain, thalamus and cerebellum in patients. Furthermore, ventral striatum (VS) activation on region-of-interest (ROI) analysis correlated to positive psychotic symptoms (Nielsen, Rostrup et al. 2012). After 6 weeks of antipsychotic treatment, ROI-analysis revealed that patients had increased activation in the right VS from an attenuated baseline and signal change correlated with change in psychotic symptoms (Nielsen, Rostrup et al. 2012). Using the SAT, Schmidt et al found reduced ACG-right insula connectivity in adaptive reward prediction in unmedicated FEP correlating with unusual thought content on the BPRS (Schmidt, Palaniyappan et al. 2016), an effect not found in treated patients. A meta-analysis of monetary reward anticipation in schizophrenia spectrum disorder reported bilateral VS hypoactivation and correlation between negative symptoms and the left VS (Radua, Schmidt et al. 2015).

There is also evidence of disrupted motivational salience in CHR. Using the SAT, Roiser et al reported increased attribution of reward probability to irrelevant stimuli on visual analogue scale estimation, correlating to unusual thought content on CAARMS. On analysing striatal DA synthesis capacity with PET, they reported negative correlation between hippocampal activity during irrelevant stimuli in CHR and positive correlation in healthy controls (Roiser, Howes et al. 2012). Using the MIDT, Wotruba et al found increased activation in reward anticipation in the posterior cingulate, middle frontal gyri and superior frontal gyri at the whole-brain level, but no difference in ROI-analysis for VS, right anterior insula or medial orbitofrontal cortex (Wotruba, Heekeren et al. 2014). Smieskova et al reported relatively less activation in a cluster spanning the right supramarginal gyrus and right inferior parietal lobule in CHR compared to healthy controls but without any behavioural difference using the SAT

(Smieskova, Roiser et al. 2015). In the same meta-analysis as above, Radua et al also found bilateral VS hypoactivation in CHR (Radua, Schmidt et al. 2015).

The endocannabinoid system, motivational salience and psychosis

The story of the endocannbinoid system (ECS) starts with cannabis. Cannabis sativa is an ancient domesticated crop. There is evidence of its use as a fibre since the Paleolithic era (Adovasio, Soffer et al. 1996), and it has been called a 'camp follower' of pre-agrarian hunter-gatherer nomadic groups (Anderson 1952). Documented medicinal use stems back at least four millennia in China (Abel 1980) and Ancient Egypt (Russo 2007), where in particular it is reported that women used it to improve their mood (Carod-Artal 2013). Fast-forward to the twenty-first century, and it is still being use as a fibre for manufacturing worldwide, but nearly 200 million people now consume it primarily for its psychotropic effects (UNODC), attributed to the main psychoactive molecule Δ9-tetrahydrocannabinol (Δ9-THC).

Δ9-THC is not the only chemical unique to the plant. At least 113 phytocannabinoids have now been isolated (Aizpurua-Olaizola, Soydaner et al. 2016) since the first molecule (cannabinol) was identified at the end of the nineteenth century (Mechoulam, Hanuš et al. 2014). Δ9-THC itself was first isolated in 1964 (Gaoni and Mechoulam 1964). The first cannabinoid receptor (CB1) was cloned in 1990 (Gerard, Mollereau et al. 1990, Matsuda, Lolait et al. 1990), the first endogenous lipid ligand or 'endocannabinoid' (ECB) arachidonoyl ethanolamide (AEA-'anandamide') identified in 1992 (Devane, Hanus et al. 1992), the CB2 receptor was cloned in 1993 (Munro, Thomas et al. 1993), and the second ECB 2-arachidonoylglycerol (2-AG) was identified in 1995 (Mechoulam, Ben-Shabat et al. 1995). We now understand that the ECS is involved in many aspects of physiology, that ECB's interact with a wide range of receptors beyond CB1 and CB2, and a number of ECB-related lipid mediators have been identified (Iannotti, Di Marzo et al. 2016).

In relation to mental illness, the most studied parts of the ECS are CB1, CB2, AEA and 2-AG. CB1 is primarily expressed in the central and peripheral nervous system, whereas CB2 is primarily expressed on immunocytes (Pertwee 2008). Within the CNS, CB1 is observed throughout the cortex, but it is found in high density in the cingulate, frontal, secondary somatosensory and secondary motor cortex. It is also found in high density in the hippocampus and amygdala. Density varies in the basal ganglia: high in the internal globus pallidus and substantia nigra pars reticulata, moderate in the external globus pallidus, caudate and putamen, and low in the VS/nucleus accumbens (NAcc). CB1 is notably absent on DA-ergic projections from the ventral tegmental area (VTA) to the NAcc (the mesostriatal

pathway), but it is present on GABA-ergic projections from the NAcc to the VTA. CB1 is also found in high density in the cerebellum on basket cell axon terminals, climbing fibres and parallel fibres mediating glutamatergic and GABA-ergic inputs to Purkinje neurons (Hu and Mackie 2015).

Both CB1 and CB2 are inhibitory G-protein coupled receptors. CB1 is located presynaptically as part of a retrograde messenger system (Pertwee 2015). Activation inhibits the release of other neurotransmitters such as Glu and GABA from the presynaptic terminal. AEA is a partial agonist at CB1, whereas 2-AG is a full agonist at CB1. Both are synthesised on demand and released postsynaptically following calcium influx (Di Marzo, Bisogno et al. 2005). AEA is metabolised by fatty acid amide hydrolase (FAAH) which is found in dendritic spines on the membranes of mitochondria and other organelles (Piomelli 2014). 2-AG is metabolised mainly by monoacylglycerol lipase (MAGL) in axon terminals, but also by FAAH (Piomelli 2014). Of note, 2-AG is found in significantly higher concentrations than AEA in the rat brain (Stella, Schweitzer et al. 1997) implying a more significant role than AEA.

Evidence of ECS dysfunction in psychosis continues to accumulate. Epidemiologically, cannabis consumption is implicated in the both the onset and prognosis of psychotic mental illness. To date, at least five independent longitudinal cohort studies have comprehensively demonstrated the association between cannabis use and development of psychotic mental illness (Andréasson, Allebeck et al. 1987, Arseneault, Cannon et al. 2002, Van Os, Bak et al. 2002, Callaghan, Cunningham et al. 2012, Nielsen, Toftdahl et al. 2017). A meta-analysis of 66,186 subjects has confirmed a dose-response relationship between level of cannabis use and psychotic outcomes (Marconi, Di Forti et al. 2016). Several meta-analyses have identified differences between psychotic disorders associated with cannabis use and without, including an earlier onset of psychosis in cannabis users (Large, Sharma et al. 2011), higher relapse rates in ongoing cannabis use, longer hospital admissions, more severe positive symptoms, worse overall functioning (Schoeler, Monk et al. 2016) and worse adherence to medication (Foglia, Schoeler et al. 2017). Schoeler et al reported that continued use of high versus low potency (higher Δ9-THC concentration) cannabis increased risk and frequency of relapse, reduced time between relapses and required more intensive care (Schoeler, Petros et al. 2016). Furthermore, a recent multicentre case-control study across Europe has estimated that up to 30% of FEP in London (50% in Amsterdam) is attributable to high potency cannabis use (Di Forti, Quattrone et al. 2019).

It is broadly accepted that the molecule responsible for these effects is Δ9-THC, a partial agonist at CB1 (Pertwee 2008). Cannabis potency, as assessed by Δ9-THC concentration or the Δ9-THC:CBD ratio, is a potentially modifiable risk factor in the aetiology of psychosis. Experimental studies have repeatedly demonstrated that Δ9-THC can induce psychotic-like symptoms in healthy subjects

(D'Souza, Perry et al. 2004, Morrison, Zois et al. 2009, Bhattacharyya, Morrison et al. 2010, Colizzi, McGuire et al. 2018). Psychotic symptoms in cannabis users have been linked to polymorphisms of the AKT1 and COMT genes (Caspi, Moffitt et al. 2005, Morgan, Freeman et al. 2016). Independent of psychosis and as a stand-alone SUD in its own right, cannabis use can lead to a dependence syndrome (Budney, Roffman et al. 2007, Hall and Degenhardt 2007) with a recognised withdrawal (Budney, Hughes et al. 2004), development of tolerance (Colizzi and Bhattacharyya 2018), evidence of harm (Moore, Augustson et al. 2005, Fergusson and Boden 2008) and disruption of Glu metabolism (Colizzi, McGuire et al. 2016). Yet despite growing medical concern, there has been a trend toward increasing concentrations of ∆9-THC in cannabis over the last few decades (Mehmedic, Chandra et al. 2010, Cascini, Aiello et al. 2012, ElSohly, Mehmedic et al. 2016, Dujourdy and Besacier 2017), prompting calls for global monitoring (Freeman and Swift 2016).

Aside from the effects of exogenous ∆9-THC, internal ECS abnormalities are also associated with psychosis. AEA has been shown to be elevated in the cerebrospinal fluid (CSF) of antipsychotic-naïve patients with schizophrenia (Leweke, Giuffrida et al. 1999), a finding repeated more than once and inversely correlated with psychotic symptoms (Giuffrida, Leweke et al. 2004, Leweke, Giuffrida et al. 2007). AEA is also elevated in prodromal subjects, where, counterintuitively, lower levels predict a higher transition risk (Koethe, Giuffrida et al. 2009). AEA is in fact low in otherwise-healthy cannabis users, and levels correlate negatively with psychotic-like symptoms on abstinence (Morgan, Page et al. 2018). Additionally, PET has shown that CB1 binding and availability are altered in schizophrenia both cortically and subcortically (Ceccarini, De Hert et al. 2013, Ranganathan, Cortes-Briones et al. 2016).

The ECS is also involved in reward processing, including motivation for primary rewards such as food and sex (Laredo, Marrs et al. 2017), and also in SUD (Manzanares, Cabañero et al. 2018). Thus far, genetic studies are inconclusive for the role of the CB1 gene (CNR1) in psychosis (Gouvêa, Santos Filho et al. 2017), but polymorphisms of both CNR1 and the FAAH gene have been associated with SUD (López-Moreno, Echeverry-Alzate et al. 2011). CB1 is found in key areas associated with reward including the GABA-ergic projections from the NAcc to the VTA as already mentioned, and DA signalling may be mediated by presynaptic CB1 on GABA-ergic terminals in the VTA (Mátyás, Urbán et al. 2008, Melis, Muntoni et al. 2012).

Rodent studies have suggested a direct role of the ECS in motivational salience. In an operant sensation seeking task, CNR1-knockout mice engaged in goal-directed behaviour less than wild-type mice, and FAAH-knockout mice engaged in more (Helfand, Olsen et al. 2017). CB1 agonism by AEA and 2-AG increases DA in the NAcc (Solinas, Justinova et al. 2006, De Luca, Valentini et al. 2014). CB1

agonism by 2-AG in the VTA increases cue-evoked DA release in the NAcc and goal-directed behaviour (Oleson, Beckert et al. 2012). CB1 agonism with 2-AG and noladin changes appetite for specific dietary components in free-feeding rats (Deshmukh and Sharma 2012). The administration of the CB1 agonist 'WIN' prior to conditioning enhanced approach behaviour to a conditioned stimulus (Brancato, Cavallaro et al. 2018). Administration of AEA optimises effort:reward decisions in a free-choice food processing task (Zona, Fry et al. 2017). In the inherited neurodegenerative condition Huntington's Disease (HD), there is characteristic degeneration of striatal medium spiny neurons (GABA-ergic inhibitory cells, comprising 95% of neurons in the striatum) associated with apathy. In the HD mouse-model, behavioural deficits are present in higher effort:reward choices, but the MAGL inhibitor JZL-184 has been shown to restore motivation to overcome higher cost rewards by elevating 2-AG [105]. In contrast, CB1 antagonism with rimonabant reduces cue-evoked dopamine release in the NAcc and goal-directed behaviour (Oleson, Beckert et al. 2012), and also inhibits cue-induced reinstatement of learned goal-directed behaviour (Hernandez and Cheer 2011).

In humans, behavioural and neuroimaging studies have implicated the ECS in reward processing, salience and motivational salience. Acute ∆9-THC challenge impairs salience processing in non-psychotic subjects (Bhattacharyya, Crippa et al. 2012). In healthy controls, ∆9-THC administration reduces the likelihood of high effort choices in the 'Effort Expenditure for Rewards Task' (Lawn, Freeman et al. 2016). In healthy subjects, ∆9-THC induces DA release in the striatum (Bossong, Mehta et al. 2015) and has been shown to attenuate activation of bilateral inferior temporal gyrus and left inferior parietal cortex during reward feedback in the MIDT (van Hell, Jager et al. 2012). Using the novel method of presenting visual followed by gustatory stimuli of rewarding (sight and taste of chocolate) and aversive (sight and taste of unpalatable strawberries) food, rimonabant has been shown to attenuate activation in the right orbitofrontal cortex during anticipation of reward and in right VS/putamen during consummation of an aversive stimulus (Horder, Harmer et al. 2010).

Regarding chronic cannabis users, motivational salience is enhanced behaviourally in response to cannabis cues (Wijayendran, O'Neill et al. 2016). Using the MIDT with fMRI, there are multiple regions of attenuation including bilateral NAcc, caudate and left putamen, and enhanced activation in bilateral middle temporal gyri, right cuneus and parahippocampal gyrus (van Hell, Vink et al. 2010). On PET scanning, Bloomfield et al reported reduced DA synthesis capacity in the striatum (Bloomfield, Morgan et al. 2014), correlating with diminished goal-directed behaviour (Bloomfield, Morgan et al. 2014). Using the SAT, Bloomfield et al reported a positive correlation between psychotic-like symptoms and explicit (consciously experienced) aberrant salience, an association between severity of cannabis

dependence and implicit aberrant salience, and a loss of correlation between implicit aberrant salience and striatal DA synthesis capacity (Bloomfield, Mouchlianitis et al. 2016).

Cannabidiol

Intriguingly the cannabis plant appears to be a 'pharmakon', offering both poison and cure. The antipsychotic effect of the phytocannabinoid cannabidiol (CBD) was first reported in the case study of a 19 year-old female with schizophrenia (Zuardi, Morais et al. 1995). In regular cannabis users, there is evidence that CBD content in cannabis reduces the psychotic-like symptoms induced by higher levels of Δ9-THC (Morgan and Curran 2008). In healthy subjects, CBD administration curbs the psychotomimetic effects of Δ9-THC (Bhattacharyya, Morrison et al. 2010, Englund, Morrison et al. 2013). There is now clinical evidence of the potential efficacy of CBD as a novel antipsychotic agent in psychotic mental illness (Leweke, Piomelli et al. 2012, McGuire, Robson et al. 2018), and it may normalise MTL, midbrain and striatal dysfunction in CHR subjects (Bhattacharyya, Wilson et al. 2018).

Oral administration of CBD is subject to significant first-pass effect with bioavailability estimated between 13 to 19% (Scuderi, Filippis et al. 2009). The time to maximum plasma concentration of oral CBD is around four to five hours after administration, and there is a large volume of distribution (high tissue distribution) (Taylor, Gidal et al. 2018). It is protein-bound, highly lipophilic and readily crosses the blood brain barrier with rapid distribution to the brain and adipose tissue (Gaston and Friedman 2017). CBD is subject to hepatic metabolism, mainly by CYP (cytochrome P450) enzymes 3A4 and 2C19 (Jiang, Yamaori et al. 2011). It is also an inhibitor of CYP enzymes, including its own major metabolisers 2C19 and 3A4 (Zendulka, Dovrtelová et al. 2016). The main circulating metabolites have been reported as follows: 7-carboxy-CBD, CBD, 7-hydroxy-CBD, 6-hydroxy-CBD (Taylor, Gidal et al. 2018). In a study of repeated oral administration in healthy subjects, steady state was achieved after 2 days. Elimination was multiphasic, with effective elimination half-life (of the dose) between 10 to 17 hours and terminal elimination half-life of steady-state plasma concentration around 60 hours (Taylor, Gidal et al. 2018). Excretion of metabolites is mostly through faeces, though a small proportion is via urine (Gaston and Friedman 2017).

Remarkably, CBD has low affinity at CB1 and CB2 and is active at many alternative sites, including other metabotropic receptors and ion channels within the emerging ECS, adenosine A_{2A}, serotonin 5-HT_{1A}, α_2-adrenoceptors, D_2-R,, $GABA_A$, μ and δ-opioid receptors (McPartland, Duncan et al. 2015). Accordingly, there are a number of different potential mechanisms of action, for example augmentation of endocannabinoid tone by inhibition of FAAH or a putative 'anandamide transporter',

or by encouraging synthesis of AEA and 2-AG by stimulating arachidonic acid release (McPartland, Duncan et al. 2015). Specifically concerning activity at CB1, it has recently been reported to act as a negative allosteric modulator (Laprairie, Bagher et al. 2015, Tham, Yilmaz et al. 2018).

The relationship between CBD and ∆9-THC is complex. CBD may potentiate the effects of ∆9-THC as well as acting as a functional antagonist (McPartland, Duncan et al. 2015). There is evidence of an augmentation of psychoactive effects and alteration of ∆9-THC pharmacokinetics in one animal study (Klein, Karanges et al. 2011). However, CBD has a favourable safety profile; the most common side effects are tiredness, diarrhoea and appetite changes, although there is a lack data for chronic administration (Iffland and Grotenhermen 2017).

Thesis rationale

What is the neural substrate of motivational salience in humans in health? Is there a relationship between altered motivational salience in psychosis and psychopathology? How are differences in motivational salience in psychosis affected by CBD? What is the neurocognitive mechanism of the putative antipsychotic effect of CBD? The main aim of this MD(res) is to investigate abnormalities in motivational salience in psychosis and the neurocognitive effects of cannabidiol, detected by fMRI.

In order to meaningfully interpret any reward processing differences in psychosis, it is crucial to have some understanding of normal functioning in health. The MIDT was designed to capture brain function during reward processing. It is well established and confers the advantages of adaptability and flexibility, breaking down processing into discrete stages of anticipation and feedback. The anticipation stage represents a form of motivational salience. In order to determine the neural substrate of motivational salience, we conducted the first ever meta-analysis of original group map data of the anticipation phase of the MIDT.

The clinical high-risk state offers access to the neural substrate of psychosis, without modification by antipsychotic medication and without severe loss of evaluation of reality. Given the evidence of disrupted motivational salience in CHR and guided by findings from the meta-analysis of motivational salience in health, we investigated differences in motivational salience between CHR subjects and matched healthy controls using the MIDT. The endocannabinoid system is involved in psychosis and motivational salience, and cannabidiol promises a potentially ground-breaking non-DA-ergic form of treatment. We therefore subsequently investigated the acute effect of CBD on motivational salience in CHR participants.

Chapter 2

General methodology

This thesis involved the application of functional magnetic resonance imaging (fMRI) to index the neurophysiological response of brain regions during the processing of rewarding stimuli. The methodologies of the two constituent publications are contained within each articles and respective supplementary materials. The core methodologies and techniques are evaluated in this chapter, but first the principles of fMRI and the chosen reward processing task are explained below.

Imaging activity in the brain: functional magnetic resonance imaging (fMRI)

Magnetic resonance imaging is a technique of producing non-invasive images of tissue inside the body. It involves the creation of a powerful magnetic field, the 'B0' field, by an MRI scanner typically between 1.5 to 7 Tesla in strength. In nature, protons, such as the nucleus of the hydrogen atom, spin generating their own magnetic field. The axis of spin also rotates and is known as 'precession' creating a local net magnetic field. An MRI scanner applies a magnetic field aligning proton spin (both parallel and antiparallel to the field), creating net magnetisation in the same direction as the field. A radio frequency (RF) pulse is then emitted. The frequency of this pulse is known as the 'Larmor frequency' and is the precise frequency to change a proton's energy state in a given magnetic field by resonating at the same frequency as precession. This causes phase alignment of precession and 'spin-flip' whereby the number of antiparallel magnetic moments equals parallel and the net magnetic vector shifts to 90 degrees from the spin axis. The protons then release this energy in the form of 'T1' or 'spin-lattice' relaxation, losing spin-flip and emitting a radio frequency signal detected by a receiver coil in the MRI scanner. The rate of T1 relaxation differs between tissues, being faster in fat than in water. This signal decays more quickly than expected from this process alone because of 'dephasing' of protons, known as 'T2' or 'spin-spin' relaxation. Most of the protons generating this signal are contained in water molecules. Bodily tissues contain many tiny regional differences in magnetic field which enhance dephasing. The combined decay of all dephasing is known as 'T2* relaxation' (McRobbie, Moore et al. 2003, Kempton 2006, Vink, van den Heuvel et al. 2007).

To create 3-dimensional images, additional magnetic field gradients are superimposed on the main B0 field across the brain so that different regions precess at different frequencies and phases depending on their spatial location. The brain is divided into planes or 'slices' whereby a narrow range RF pulse is emitted which affects protons in a narrow range of magnetic field strength. This 'slice excitation pulse' initiates a spin-flip in protons in that slice without affecting other slices. Within this 2D plane, a 'phase encoding' magnetic field gradient is applied in one direction, e.g. posterior-anterior, then turned off leaving different phases of precession depending on spatial position. A 'frequency

encoding' magnetic field gradient is then applied orthogonally across the remaining dimension, e.g. left-right, such that there is different resonant frequency depending on location (McRobbie, Moore et al. 2006). The signal detected by the coil from each step in the sequence contains both phase and frequency spatial information, building an image in 'k-space'. In turn the k-space image can be decomposed into the constituent frequencies and amplitudes by Fourier transformation into a 2D image of the slice (McRobbie, Moore et al. 2003, Kempton 2006, Vink, van den Heuvel et al. 2007).

MRI is not without drawbacks. There are significant problems with artefact in MRI. For example, magnetic susceptibility varies between tissues, and boundaries can generate local magnetic field gradients. Most striking are air-tissue boundaries such as sinuses near the brain which render regions including the lateral temporal lobe and orbitofrontal cortex sensitive to signal distortion. Head movement by the subject in the scanner can also lead to misleading changes in signal intensity.

The BOLD signal

As neurons generate action potentials and synaptic transmission, so metabolic demand increases and more oxygen is required. Local vasodilation is triggered increasing oxygenated blood flow to the area, in excess of need. This is called the haemodynamic response. Functional MRI is based on the ground-breaking discovery that the T2 relaxation signal in blood vessels and perfused brain tissue decreases with deoxygenation of haemoglobin (Ogawa, Lee et al. 1990). Because oxygenated blood exerts a weaker effect on surrounding magnetic field than 'paramagnetic' deoxygenated blood, it exhibits slightly more stability in the local magnetic field and prolonged T2* relaxation. This is known as the blood oxygenation level-dependent (BOLD) signal. The BOLD signal peaks at about 5 to 6 seconds, representing around 1 to 5% increase in intensity of signal of the area, returning to zero after about 20 seconds. This signal allows in vivo study of physiological activity in the brain (McRobbie, Moore et al. 2003, Kempton 2006, Vink, van den Heuvel et al. 2007).

The physiological mechanism underlying the BOLD signal is generally assumed to be related to synaptic activity (Attwell and Iadecola 2002), but understanding is far from comprehensive. The relationship between neuronal activity and change in blood flow is known as 'neurovascular coupling', and a number of cellular mechanisms have been proposed, for example that increasing local glutamate stimulates metabotropic glutamate receptors on astrocytes ultimately leading to local prostaglandin release and local vasodilation, or that cortical interneurons release of vasoactive substances (Hillman 2014).

fMRI relies on contrasting the BOLD signal from two physiological states in the brain known as the 'subtraction paradigm'. This could be the difference between two related conditions induced by a cognitive task thought to involve a similar set of cognitive processes, and the difference in signal represents one or more cognitive processes of interest. This is based on assumption that cognitive processes can simply be added or subtracted, known as 'cognitive subtraction' (Harrison and Pantelis 2010).

Analysing images: Statistical Parametric Mapping (SPM)

SPM (https://www.fil.ion.ucl.ac.uk/spm/) is a freely available software package providing a framework for the analysis of neuroimaging data (Penny, Friston et al. 2007). It was originally created by Karl Friston in 1991 and developed by co-authors associated with the Wellcome Trust Centre for Neuroimaging. It is comprised of three main processes: spatial transformation of data known as 'preprocessing', the application of the parametric general linear model (GLM) to each voxel to describe effects, and statistical inference to create a statistical parametric map whereby voxels represent statistics.

Preprocessing

In order to study a group of subjects, fMRI data must be preprocessed. Initially, this is broken down into four discrete stages: realignment, coregistration, normalisation and smoothing. All subjects will naturally move their head during an MRI scan described by six parameters- three 'translations' (up-down, left-right, forward-backward) and three 'rotations' (x/y/z axes). All functional images are *re-aligned* to the first functional image by rigid body transformation. This involves determination of the specific parameters needed for each image to be realigned, then resampling and interpolation of the data to obtain new values. The realigned functional images are then *coregistered* (realigned again) with the structural T1 image, so that the BOLD signal is superimposed on the correct anatomical location. Because no two brains are exactly the same, the images must then be *normalised* to a standard template, such as MNI space (Montreal Neurological Institute). In this process, the differences between the template and original brain are minimalised by adjusting in twelve parameters: translation (3), rotation (3), scaling and skewing on the x/y/z axis. Finally, the images are intentionally blurred, known as *'smoothing'*, in which data is convolved with a Gaussian kernel described by the term 'full width at half maximum' (FWHM; width in mm at 50% of the peak value). This results in a single voxel representing not only its own signal but also that of neighbouring voxels,

reducing the signal:noise ratio and increasing overlap between subjects, of benefit in group analysis and increasing statistical validity (Kempton 2006, Vink, van den Heuvel et al. 2007).

Finally, data is subject to slice-time correction. The brain is scanned continuously during fMRI, and each whole-brain volume contains approximately 30 slices in a specific temporal order. The time elapsed from the start of a whole-brain scan to the end is known as the 'repetition time' (TR), which could be up to 3000ms. However, during analysis it is assumed that all slices are from the same time-point. Considering the duration of the BOLD response is only 5 to 6 seconds, a 3 second difference between the first and last slice is considerable. To correct for this, slices are shifted in time to a reference time point by interpolation of data collected before and after the reference time-point.

Modelling and the general linear model (GLM)

Experimental tasks designed for fMRI are traditionally categorised as 'block design' or 'event related'. In a block design, task conditions are maintained for an extended period of time to stimulate robust cognitive engagement resulting in a relatively large BOLD signal. For an event related design, conditions are shorter and more discrete allowing randomisation of timing and order. During an experimental task, a whole-brain scan is performed every few seconds (TR) creating a 'timeseries' of data points at each voxel. In a typical fMRI scan, there may be around 100,000 to 200,000 voxels. A 'brain mask' must be created which excludes voxels below a specific signal intensity, i.e. voxels outside the brain. The BOLD signal is modelled by the 'haemodynamic response function' curve (see Lindquist et al for further discussion (Lindquist, Meng Loh et al. 2009)), which is convolved with experimental parameters to create predictor variables. Of note the BOLD series varies within and between individuals, for example in duration and onset.

The signal detected from an individual voxel naturally varies over time and consists of the sum of effects of interest, effects of no interest and random error. Effects of interest refers to signal variation induced by the task. Effects of no interest are known sources of error such as drift of the magnetic field over time, physiological noise (e.g. head movement, breathing) and low frequency noise due to heating. The GLM assumes a linear relationship between a predictor variable and the signal, whereby

y (=signal) = xb (x=predictor variable, b = 'b-value'/parameter estimate/beta/effect size) + e (=error)

Predictor variables are the variables defined by experimental design and potential confounds, and they are expressed in the design matrix. The b-value is an estimated multiplication scalar or 'regression coefficient' for each predictor variable, indicating how strongly a predictor variable changes the signal.

It is calculated for each voxel by finding the weighted predictor variable that best fits the observed data by yielding the smallest residual error using the ordinary least squares method. The residual error is the part of the signal not explained by the model, known as the residual mean square. The final model xb is actually the combined contribution of all weighted predictor variables. Activation due to the model (i.e. the combined relative contribution of predictor variables) is expressed in the form of a t-value which depends on the b-value and the ratio of explained versus unexplained variance in signal data: t = b* √(explained variance due to model/unexplained variance).

Explained variance is signal variability described by the prediction model, whereas unexplained variance is created from the observed timeseries data minus the model prediction, known as the residuals. If more variance can be explained, there is less unexplained variance, and the t-value increases. In SPM, unexplained variance is depicted as the residual mean square error image.

Statistical inference

The b-value determined by the GLM can be used for statistical inference by testing the null hypothesis that either a linear combination of b-values is zero (t-test) or that all the b-values are zero (f-test). The former is calculated by means of subtraction of one b-value from another creating a contrast. The corresponding weighted vector is known as the contrast vector. A 't-value' or 't-statistic' is then calculated by dividing the contrast vector by the standard error of the contrast, estimated with the residual mean square error of the entire model. All t-values are combined in the 'SPM(t)' file with the coordinates of each corresponding voxel to produce a 3D image. The traditional p-value for each voxel can then be calculated using a one-sample t-test.

However, given the thousands of individual voxels being tested, the threshold for individual significance must be raised to maintain the probability of type 1 error at the standard 5% for the whole-brain image, known as 'family-wise error correction'. One such method is the traditional Bonferroni correction, whereby each p-value is divided by the number of tests (voxels). However, this is based on an incorrect assumption that all observations are independent. Random Field Theory (RFT) is a correction technique based on volume and smoothness which is more sensitive and less conservative. Briefly in RFT, voxel sizes are discounted and search volume expressed in terms of smoothness or 'resels' (resolution elements) consisting of a number of voxels falling within the FWHM. The final statistical parametric map (SPM) is thresholded by height (t-value) and spatial extent, yielding three groups of inferences: set-level (number of clusters exceeding height and volume thresholds), cluster-level (number of activated voxels in a cluster, spatial extent) and height within a cluster (peak

local maxima). When testing a single group of subjects, p-values are calculated by standard one-sample t-test. The two-sample t-test is used to compare two groups.

Capturing reward processing with fMRI: the monetary incentive delay task

The monetary incentive delay task (MIDT) was developed by Brian Knutson and colleagues in the 1990's to capture the neural substrate of reward processing. Money was chosen as an incentive, because it is a more universal and consistent incentive stimulus than other forms such as imagery, taste or sound (Knutson and Heinz 2015). In essence, the MIDT is a time-dependent visuo-motor task involving rapid incentivised response to a learned visual cue. It involves presentation of a sequence of three visual stimuli- a cue indicating monetary value, a target indicating that the subject should press a button on time, and visual feedback informing the participant of success, failure and winnings. When combined with fMRI, t-maps of activity can be created for the anticipation of reward/punishment, feedback of success/failure and associated 'neutral' conditions where the monetary value is zero. Each of these can be subsequently contrasted to gain insight into the different patterns of activation. It is well-suited to practical experimental manipulation, allowing modification of valence magnitude and distinction between the behaviourist concepts of reward and punishment through delivery or deduction of reward. The MIDT (and modified variants) is capable of capturing multiple aspects of reward processing including initial presentation of an incentive, approach/avoidance behaviour, reward learning, delayed reward discounting (Lutz and Widmer 2014) and even reward prediction error (Abler, Walter et al. 2006).

The MIDT has now been used to investigate underlying pathology of numerous psychiatric disorders, contributing data to several major meta-analyses in addiction (Luijten, Schellekens et al. 2017), major depression (Zhang, Chang et al. 2013), bipolar disorder (Chen, Suckling et al. 2011), psychosis (Radua, Schmidt et al. 2015) and ADHD (Plichta and Scheres 2014). It has been used in psychoactive drug challenge studies (van Hell, Jager et al. 2012) and to investigate mechanisms of action of therapeutic interventions including nicotine replacement therapy (Rose, Ross et al. 2013), methylphenidate (Stoy, Schlagenhauf et al. 2011), antidepressants (Ossewaarde, Verkes et al. 2011, Stoy, Schlagenhauf et al. 2012) and antipsychotics (Nielsen, Rostrup et al. 2012).

However, it is important to remember that MIDT is not designed to capture primary intrinsic rewards. While there appears to be substantial overlap, differences in regional brain activation particularly in the consummation stage have been described between extrinsic monetary incentives and tasks

involving intrinsic rewards such as food and sex, with the former engaging the orbitofrontal cortex and the latter the anterior insula (Sescousse, Caldú et al. 2013).

Publication 1. The neural substrate of reward anticipation in health: a meta-analysis of fMRI findings in the monetary incentive delay task

Fundamentally, understanding the aetiology of a disorder requires a robust model of healthy structure and function. Therefore, to determine how CHR subjects may deviate from health and whether CBD has any measurable effect, we first needed to describe the brain regions normally engaged during the anticipation of rewarding stimuli.

The original investigations of the MIDT were conducted in healthy adults (Knutson, Westdorp et al. 2000, Knutson, Adams et al. 2001) and found that anticipation of reward (versus neutral) was associated with activation of multiple regions already implicated in reward prediction (bilateral nucleus accumbens, bilateral caudate and left putamen). Later meta-analyses have been conducted looking at reward anticipation in healthy adults using a variety of cognitive tasks and a mixture of different incentives, such as monetary, food, points, social feedback and pleasing images (Liu, Hairston et al. 2011, Diekhof, Kaps et al. 2012, Bartra, McGuire et al. 2013). At the time of writing, there have been three published meta-analyses of the MIDT in healthy adults aside from ours. The first (Knutson and Greer 2008) contrasted anticipation win directly with anticipation lose, the second (Oldham, Murawski et al. 2018) contrasted both win and lose with neutral conditions, and the third (Dugré, Dumais et al. 2018) focused on loss anticipation and outcome contrasted to neutral. All found that regions implicated in reward prediction and the salience network were activated in anticipation.

Our study advances on the methodology of all three previous meta-analyses, because of the exclusive use of original unthresholded whole-brain group t-maps with the meta-analytic software SDM (Seed-based d Mapping, previously 'Signed Differential Mapping') (Radua and Mataix-Cols 2009, Radua, Van Den Heuvel et al. 2010, Radua and Mataix-Cols 2012, Radua, Mataix-Cols et al. 2012, Radua, Rubia et al. 2014). The data used by the afore-mentioned meta-analyses consisted of the coordinates and t-values of thresholded peaks extracted from published studies. Both Knutson et al and Oldham et al used the well-established activation likelihood estimation (ALE) technique (Turkeltaub, Eden et al. 2002). Dugre et al used the SDM software to analyse coordinate data. ALE and other peak probability methods calculate the regional frequency of reported peaks and assume equal activation. Purely coordinate-based meta-analyses (CBMA) do not fully account for within and between-study variation, because they do not include full image data and exclude all non-significant findings (Müller, Cieslik et

al. 2018). It has been shown that there is a poor similarity between CBMA and image-based meta-analysis (Salimi-Khorshidi, Smith et al. 2009). For CBMA, SDM offers significant benefits over ALE by attempting to recreate original group maps from the available data, including both hyper and hypoactivations (hence 'signed differential'), and assigning each voxel an effect size. Consequently, both published coordinate and original group map data can be combined. While the results of ALE-based meta-analysis may be interpreted as indicating the spatial convergence of previous findings, SDM-based can be interpreted as direct increase or decrease in activity in the brain (Müller, Cieslik et al. 2018).

The basic computation in SDM is the calculation of mean voxel value from the means for each study weighted by the inverse of the variance. This is subsequently thresholded by cluster size and local peak z-score. However, the software also includes additional statistical analyses, including between-group comparison, 'Jacknife' sensitivity, inter-study heterogeneity, and publication bias by funnel plot and Egger's test. Jacknife sensitivity, also known as 'leave-one-out' analysis, involves repeating the mean analysis multiple times, leaving out a single map each time. If the same region is found to be significant in most of the mean maps, then the finding is replicable. In order to simplify visual map interpretation, we created a density map of all Jacknife maps to easily inspect for areas differing in replicability as used by Luijten et al (Luijten, Schellekens et al. 2017). Inter-study heterogeneity is calculated from the sum of square differences between individual studies and the overall group, creating 'QH maps' which are be thresholded for significance. Again, to simplify interpretation we created density maps of thresholded significant heterogeneity for visual inspection. Funnel plots are a visual technique for assessing publication bias, with effect-size on the x-axis and precision (indexed by standard error in this case) on the y-axis. An unbiased plot should resemble an inverted funnel, with smaller studies scattered at the bottom and larger studies narrowing at the top. If the plot appears asymmetrical, this demonstrates bias. Egger's test investigates funnel plot asymmetry using a test for Y intercept = 0 in linear regression of precision (1/standard error) on the x-axis and standardised effects size (effect size/standard error) on the y-axis.

In 2014, we conducted a systematic literature search of 4 databases (EMBASE, MEDLINE, PsychINFO and CINAHL) using online software published by NICE (https://hdas.nice.org.uk/) for titles and abstracts containing the text 'monetary', 'reward', 'incentive', 'anticipation' and/or 'fMRI' plus variants, complemented by a full text search of PubMed (https://www.ncbi.nlm.nih.gov/pubmed/) using the same words. After screening articles for relevance, we contacted each study group offering collaboration and requesting available healthy adult group map data. Maps received were then further screened by visual inspection for orientation, the use of region-of-interest masks and for other field-

of-view restrictions before inclusion in the analysis. Published coordinate-only data were additionally extracted from the remaining articles and combined with original group maps using SDM.

Following preliminary analysis, further methodological refinement was required. Firstly, the combined data results demonstrated significant publication bias. This was controlled by simply excluding the coordinate-only data leaving pure group map data. Secondly, the sheer scale of significant findings was overwhelming with hundreds of peaks and clusters exceeding 1000 voxels. Initially we sought to use the simple false discovery rate correction (p-values reported in the paper), but this was not robust enough. Crossing scientific disciplines, we identified a solution from particle physics known as the '5-sigma' threshold (z-score>5, p<0.0000003), a concept whose equivalent has been called for in medicine (Horton 2015). Finally, we used an atlas of the human brain to accurately identify the anatomical location of peaks (Mai, Paxinos et al. 2007).

Publication 2. Cannabidiol attenuates insular dysfunction during motivational salience processing in subjects at clinical high risk for psychosis

Population sample

The second study of this thesis was an experimental design, investigating reward processing in psychosis, specifically differences in motivational salience induced by the MIDT between subjects at clinical-high risk (CHR) for psychosis and healthy controls and the acute effect of cannabidiol on motivational salience in CHR subjects.

Once psychosis is diagnosed, most individuals will receive treatment with antipsychotic medication, who's common pharmacodynamic action is D_2-R antagonism. Antipsychotic treatment is associated with structural brain changes (Vita, De Peri et al. 2015). Studying CHR subjects at risk of developing psychosis confers the advantage of antipsychotic naivety and low risk of possible neurogenerative change, offering 'cleaner' insights into the underlying aetiology. In addition, DA-ergic activity is central to reward processing models, and the CHR sample offers insight into an unmodified DA-ergic system and the effect of a cannabidiol challenge on motivational salience.

However, the CHR state is not a definitive precursor to psychosis. CHR samples have been criticised for not being representative of first-episode psychosis populations (FEP). There are high rates of false positives, falling transition rates, and differing demographics (Ajnakina, David et al. 2018) including under-representation of males (Wilson, Patel et al. 2016). In one cohort from South London, only 4.1% of FEP had had any contact with the well-established partner CHR services (Ajnakina, Morgan et al. 2017). CHR services have also been criticised for inconsistent sampling criteria and definitions of

transition (van Os and Guloksuz 2017). Given that the prevalence of subclinical psychotic symptoms has been estimated at 5% in the general population (van Os, Linscott et al. 2009), it has been proposed that attenuated psychotic symptoms are a more sensitive marker for severity of non-psychotic states (van Os and Guloksuz 2017) rather than transition to psychosis and could represent a pluripotent risk syndrome for a range of mental disorders (Yung, Woods et al. 2012).

The aim of the second experimental study was two-fold: first, to determine differences in brain activation between CHR subjects and a sample matched healthy controls, and secondly to investigate whether CBD has any detectable effect on function on identified areas of difference. The first study of this thesis produced comprehensive whole-brain maps of increased and decreased activation in reward anticipation, confirming the involvement of the striatum and salience network in motivational salience. Indeed, the resultant maps have the potential to be used as data-based region-of-interest (ROI) masks (as opposed to hypothesis-driven) for future research. However, because of the relatively small sample sizes for the experimental study, we instead chose hypothesis-driven ROI's of the core salience network (anterior cingulate gyrus and insula) and mesostriatal-medial temporal lobe.

Design

The second study was drawn from a larger project, a 3-week randomised placebo-controlled double-blind, parallel-arm pharmacological challenge and fMRI investigation of the potential of CBD as an intervention in CHR subjects. Because of the parallel arm design, the acute single dose effect of CBD could not be repeated within-subject, increasing random noise and reducing the power detect any true effects. However, because reward processing is an iterative learning operation, the parallel-arm between-subject design confers the advantage of minimising any learning effects within subjects.

Thirty-three CHR subjects were recruited from services in England and nineteen healthy controls (HC). CHR subjects were randomised to CBD (CHR-CBD, n=16) or placebo (CHR-PLB, n=17). Subjects were asked to abstain from psychoactive substances prior to scanning. Psychopathology was assessed by trained interviewers using the Comprehensive Assessment of the At-Risk Mental State. Drug use was assessed by urine sample and self-reported Cannabis Experiences Questionnaire (Barkus, Stirling et al. 2006). All subjects underwent the same MRI scanning procedure in the same scanner including the two consecutive runs of the MIDT. Blood samples were taken for plasma CBD analysis before and after the MRI scan. The MIDT consisting of 48 trials randomised to 4 anticipation conditions of win 20p, win £1, lose £1 and neutral. Behavioural performance data were collected to assist interpretation of imaging data, including mean monetary reward (£GBP), accuracy (% response on target), reaction time (ms), false-starts (premature action initiation) and any trial responses (attention, %). Imaging data were analysed using SPM8. In order to increase statistical power, all anticipation conditions of reward

and loss were combined into a 'motivational salience' condition subsequently contrasted with the neutral condition within each group. Between group pairwise analysis was initially employed, focusing on (1) differences between CHR-PLB and HC to detect differences between health and the CHR state, and (2) CHR-PLB and CHR-CBD to detect the effect of CBD in the CHR state. The groups were then compared by ANOVA to test for any linear relationship. Activity in surviving clusters was then co-analysed with behavioural data to test for correlations.

Chapter 3

The neural substrate of reward anticipation in health: a meta-analysis of fMRI findings in the monetary incentive delay task.

Wilson, R. P., Colizzi, M., Bossong, M. G., Allen, P., Kempton, M. & Bhattacharyya, S., 25 Sep 2018, Neuropsychology Review

For supplementary material please refer to Appendix 1: pp 104-140

Neuropsychology Review (2018) 28:496–506
https://doi.org/10.1007/s11065-018-9385-5

REVIEW

The Neural Substrate of Reward Anticipation in Health: A Meta-Analysis of fMRI Findings in the Monetary Incentive Delay Task

Robin Paul Wilson[1] · Marco Colizzi[1] · Matthijs Geert Bossong[1,2] · Paul Allen[1,3] · Matthew Kempton[1] · MTAC · Sagnik Bhattacharyya[1]

Received: 31 October 2017 / Accepted: 27 August 2018 / Published online: 25 September 2018

Abstract
The monetary incentive delay task breaks down reward processing into discrete stages for fMRI analysis. Here we look at anticipation of monetary gain and loss contrasted with neutral anticipation. We meta-analysed data from 15 original whole-brain group maps ($n = 346$) and report extensive areas of relative activation and deactivation throughout the whole brain. For both anticipation of gain and loss we report robust activation of the striatum, activation of key nodes of the putative salience network, including anterior cingulate and anterior insula, and more complex patterns of activation and deactivation in the central executive and default networks. On between-group comparison, we found significantly greater relative deactivation in the left inferior frontal gyrus associated with incentive valence. This meta-analysis provides a robust whole-brain map of a reward anticipation network in the healthy human brain.

Keywords Monetary incentive delay task · Anticipation or reward · Healthy adults · fMRI · Meta-analysis

Introduction

Reward processing in the brain is an iterative learning process involving goal-directed behaviour and adaptive decision-making in response to a stimulus. Stimulus presentation followed by receipt of reward increases the likelihood of a behaviour occurring again. A reward stimulus (incentive) has an intrinsic value (valence) which makes it salient, standing out from a background of stimulus bombardment. Incentives may be innately rewarding to an organism (e.g. sex, food), known as intrinsic rewards, or may be neutral at first and learnt by association, known as extrinsic rewards (e.g. money). The anticipation of a reward incentive prepares an approach behaviour, creating motivational salience, and the consumption of the reward reinforces motivational salience.

The neural mechanism of reward processing is beginning to be understood. Physiological work in primates revealed that reward prediction is mediated by dopaminergic neurons in the striatum (Schultz et al. 1997). Moreover a putative salience network has been identified by functional connectivity analysis (Seeley et al. 2007) which may be involved in choosing stimuli worthy of attention from a continuous stream of internally and externally generated inputs to the brain, thought to be anchored in the anterior cingulate and anterior insula (Uddin 2015).

The monetary incentive delay task is a widely used and validated reward processing task adapted for use in human fMRI studies to investigate motivational salience processes in health and disease. It was developed based on instrumental

Electronic supplementary material The online version of this article (https://doi.org/10.1007/s11065-018-9385-5) contains supplementary material, which is available to authorized users.

✉ Robin Paul Wilson
robin.wilson@kcl.ac.uk

[1] Department of Psychosis Studies, Institute of Psychiatry, Psychology and Neuroscience, King's College London, De Crespigny Park, London SE5 8AF, UK

[2] Department of Psychiatry, Brain Center Rudolf Magnus, University Medical Center Utrecht, Utrecht, Netherlands

[3] Cognition, Neuroscience and Neuroimaging (CNNI) Laboratory, Department of Psychology, University of Roehampton, London, UK

conditioning paradigms employed in animal studies (Schultz et al. 1997; Knutson et al. 2000). The monetary incentive delay task allows reward processing to be parsed into at least two distinct components, namely, 'anticipation' and 'feedback'. Typically, the task consists of a sequence of three visual stimulus events (Fig. 1), (1) *anticipation,* a learned visual cue representing valence (e.g. financial gain-circle, loss-square, neutral-triangle) which elicits motivational salience, (2) *the target*, another learned visual cue (e.g. rectangle) to initiate the behaviour, usually pressing a button on time (a time-dependent motor task), and (3) *feedback* in the form of text or image indicating consummation (financial gain, loss, neutral) and dependent on performance.

When studied with fMRI, the two main phases when imaging data are acquired include (1) during and after the first visual stimulus (anticipation/motivational salience) and (2) during and after the third visual stimulus (feedback/consummation). Because of individual variation in performance, the duration of target presentation may be adjusted automatically within the program such that each participant experiences approximately the same success rates, usually set at around 66%. Typically, there are three main anticipation conditions, win, neutral or lose. The anticipation conditions are coupled with five main feedback conditions dependent on type of anticipation and performance (e.g. target hit or missed), namely, 1) anticipation-win-hit, 2) anticipation-win-miss, 3) anticipation-lose-hit, 4) anticipation-lose-miss and 5) anticipation-neutral. The neutral anticipation stimulus is used as a contrast to control for aspects of visual and motor processing commonly engaged during the different conditions. There are multiple variations that can be introduced, but in this meta-analysis we focus only on the anticipation conditions stimulating positive, neutral and negative salience through monetary gain or loss.

The original investigations of the monetary incentive delay task in healthy adults (Knutson et al. 2001; Knutson et al. 2000) reported that anticipation of reward (versus neutral) was associated with activation of multiple regions including areas implicated in both reward prediction (bilateral nucleus accumbens, bilateral caudate and left putamen) and the salience network (bilateral insula, right anterior cingulate gyrus).

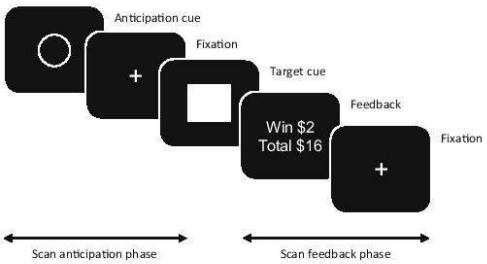

Fig. 1 Example of visual cues presented during a trial of the monetary incentive delay task

Since the original studies, many more studies have used the monetary incentive delay task to investigate brain networks engaged in reward processing. The monetary incentive delay task has mainly been used to study differences between demographic groups (e.g. adolescents and adults, males and females), clinical populations (e.g. *major* depression, psychosis) or interventions (e.g. placebo). Several whole-brain meta-analyses have been conducted looking at reward anticipation in healthy adults using a variety of tasks and a mixture of different rewards, such as monetary, food, points, social feedback and pleasing images (Liu et al. 2011; Diekhof et al. 2012; Bartra et al. 2013). We identified only two meta-analyses focusing on reward anticipation in healthy adults using solely the monetary incentive delay task. The first meta-analysis of healthy adults using the monetary incentive delay task alone (Knutson et al. 2008) contrasted anticipation win directly with anticipation lose, whereas the second, more recent meta-analyses (Oldham et al. 2018) contrasted both win and lose with neutral conditions. Both analyses found that regions implicated in reward prediction and the salience network were activated.

All of the aforementioned meta-analyses, including the two focusing only on the reward processing in healthy adults employed the activation likelihood estimation technique (Turkeltaub et al. 2002) using published text coordinates. However, coordinate-based meta-analytic approaches cannot fully account for within study and random between study variation, because they do not include the full statistical images and exclude null findings unlike image-based meta-analyses (Müller et al. 2018). Coordinate-based methods such as activation likelihood estimation treat all foci of activation equally regardless of the strength of activation, and it has been shown that there is a poor similarity between coordinate and image based meta-analysis (Salimi-Khorshidi et al. 2009). The seed-based d mapping (SDM) meta-analytic technique (Radua et al. 2012) offers significant benefits over activation likelihood estimation, because it allows both thresholded coordinates and original group map image data to be combined creating maps effect-size. Furthermore, activation likelihood estimation and SDM answer slightly different questions. While the results of activation likelihood estimation-based meta-analysis may be interpreted as indicating the spatial convergence of previous findings, seed-based d mapping-based can be interpreted as direct increase or decrease in activity in the brain (Müller et al. 2018).

The primary objective of this study was to conduct a whole brain meta-analysis of fMRI studies employing only the monetary incentive delay task in healthy adults using the seed-based d mapping technique to investigate which brain regions are activated or deactivated during monetary reward anticipation. We specifically focused on the contrasts anticipation-win minus anticipation-neutral (AWAN) and anticipation-lose

minus anticipation-neutral (ALAN), to confirm activation of regions implicated in reward processing, namely reward prediction and the salience networks.

Methods

Search Strategy and Study Selection

On 15/12/14 we searched the NICE Healthcare Database including EMBASE (Ovid), MEDLINE (Ovid), PsycINFO (Ovid) and CINAHL (EBSCO) using the terms ((“monetary” AND “incentive” AND “delay” AND “fmri”).ti,ab OR (“monetary” AND (“reward” OR “incentiv*” OR “anticipat*”) AND “fmri”).ti,ab) AND “article” [Limit to: Publication Year 2000–2014]. We complemented this with a cross-reference search of Pubmed on 16/12/14 with the general search term “monetary reward incentive anticipation fMRI”. Study inclusion criteria were (i) inclusion of healthy adults, (ii) used fMRI, (iii) used Monetary Incentive Delay Task, (iv) article available in English, (v) published in a peer-reviewed journal, (vi) conditions and contrasts of interest included, (vii) whole-brain analysis reported. We also included the placebo condition of intervention studies in healthy participants meeting criteria. Full articles were read and excluded if the above inclusion criteria were not met. The search was repeated using the same search terms and databases on 19/1/17, ranging from December 2014 onwards and excluding any repeated articles.

Data Extraction

For all the articles that satisfied study inclusion criteria, all authors or corresponding authors were contacted by published email address in March 2015 requesting whole brain maps. Research groups who sent maps were included in the Monetary incentive delay Task Analysis Consortium (MTAC) (Supplementary References 1). If no maps were available for use, we manually extracted the whole-brain only coordinates from the published article for the conditions of interest for the healthy adult sample. For all articles (both maps-received and coordinates only), information on the MRI scanner, scanning sequence and timings, parameters of the monetary incentive delay task and performance data where available were extracted manually by two researchers (Colizzi and Wilson) and cross-checked for errors. This process of contacting authors was repeated for a follow-up literature search in March 2017. If no maps were available, we did not extract published article because of positive effect-size bias detected in the first round (see Results).

Data Analysis: Seed-Based D Mapping

Meta-analysis was carried out using the seed-based d mapping software employing previously described methods (Radua et al. 2014; Radua and Mataix-Cols 2009; Radua et al. 2012, 2010). In brief, the aim of seed-based d mapping is to create voxel-level maps of effect-size measured as Hedge’s g allowing modelling of both positive and negative activations on the same map. For each reported peak coordinate and value (t, z or p), seed-based d mapping ensures surrounding voxels have a similar but smaller estimated effect size by multiplication with an un-normalised Gaussian kernel. If a voxel should have a value assigned from more than one coordinate, the values are averaged weighting by the square of the distance to each close peak. The data from each study are then weighted by the inverse of the sum of variance plus between study variance and combined using the random effects model DerSimonian-Laird estimator (DerSimonian and Laird 1986). This approach allows for studies with a larger sample size or lower variability to contribute more and creates a map of heterogeneity.

Manually extracted whole-brain coordinates and group maps were formatted for seed-based d mapping. For coordinates, this involved conversion to Tailarach, for group maps conversion to Neuroimaging Informatics Technology Initiative format, left-right correction and preprocessing including reslicing data into a common voxel size by interpolation (full width at half maximum = 20 mm). Meta-analysis produced mean maps with non-overlapping clusters of activation and deactivation for each contrast. A non-parametric approach was used where *p*-values and seed-based d mapping z-scores were created by randomisation, as opposed to standard z-scores.

In neuroimaging analyses, as well as in meta-analyses, the need for appropriate statistical thresholding to minimize the extent of false positive results must be balanced against the need for avoiding false negatives (Lieberman and Cunningham 2009). Typically, neuroimaging meta-analyses control for the false discovery rate to minimize false positive results, which we have also reported. However, it is worth noting that the choice of threshold is best guided by the specific research context (Müller et al. 2018). In the present study, we did not employ the conventional threshold, but instead combined an intensity threshold ($p < 0.005$) with a cluster extent threshold (cluster >10 voxels) that has been shown to result in acceptable Type II error rates (Lieberman and Cunningham 2009).

Thus seed-based d mapping generated mean maps were thresholded at the validated default settings $p < 0.005$, seed-based d mapping-z > 1.0, cluster>10 voxels. In seed-based d mapping, using a cluster size of 10 voxels and an uncorrected $p = 0.005$ has been shown empirically to be equivalent to corrected $p = 0.05$, optimally balancing sensitivity and specificity, and seed-based d mapping-z > 1 reduces the false positive rate (Radua et al. 2012). Given 100% parametric maps, this results in 100% sensitivity and a 3.5% false positive rate to produce the final whole brain maps of statistical significance, accompanied by an HTML document of main peaks,

p value, seed-based d mapping-z-score, MNI coordinates, number of voxels per cluster and significant sub-peaks within each cluster (also with p value and seed-based d mapping-z-score). All results at the default seed-based d mapping-z > 1 threshold are reported in the supplementary material for the interested reader, however in the main text we have reported only those results that survived a more conservative threshold (z-score ≥ 5.0). The '5-sigma' threshold for significance (Horton 2015) is a consensus agreement in other scientific disciplines, reflecting five standard deviations from the mean, or $p < 0.0000003$). We have adopted this threshold in order to further minimize the probability of detecting an effect by chance and to identify the most critical regions involved in motivational salience, reflecting high confidence that these are true positives when contrasting anticipation win or loss with neutral.

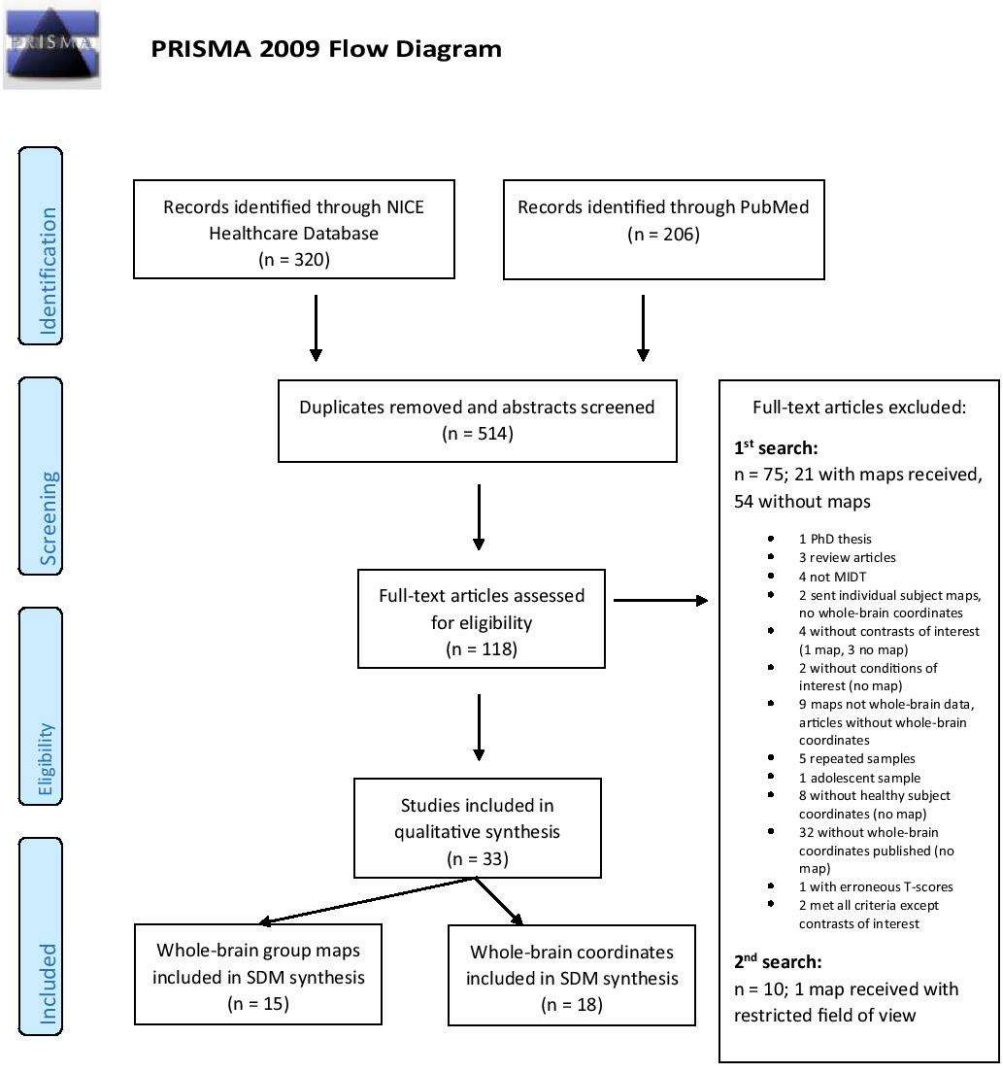

Fig. 2 PRISMA flow diagram

Table 1 Summary of available demographics for omnibus data of coordinates and group maps combined and of group maps only

contrast	n all datasets (text coordinates + group maps)	n sample size	pooled mean age (pooled SD[1])	male %	Right handed %[2]	n group maps	n sample size	pooled mean age (pooled SD[1])	male %	Right handed %[2]
AW-vs-AN	32	656	30.7 (8.15)	61.4	98.8	14	274	27.8 (6.09)	78	98.4
AL-vs-AN	21	494	31.6 (8.63)	64.8	99.3	11	246	27.4 (6.11)	71	97.8
TOTAL	33	728	30.3 (7.81)	60.6	98.8	15	346	27.4 (5.35)	76.5	98.4

[1] pooled SD excluding datasets where no SD reported; [2] mean of available data, only 25/33 sets total: 24/32 AW, 21/21 AL

Jacknife sensitivity analysis of replicability, analysis of heterogeneity and publication bias are automated within the seed-based d mapping program. Jacknife analysis involves re-analysing mean maps multiple times by leaving out a single study each time. In order to interpret the many Jacknife mean maps, we thresholded for significance, binarized the data and combined into a single overlapping density map of significant data. This allowed visual inspection of areas of low density, signifying lower replicability across studies. Inter-study heterogeneity was calculated in which Q_H statistics are converted to standard z values to create a map. This map was overlaid on the final mean map for visual inspection of areas of overlapping significant heterogeneity with areas of thresholded activation or deactivation. Publication bias was estimated using standard funnel plots and Egger's test for each reported peak. The funnel plots consisted of effect-size on the x-axis and standard error on the y-axis with bias tested using Egger's test for asymmetry of the funnel plot.

The anatomical location of the peaks were identified using the Atlas of the Human Brain and associated BrainNavigator program (Mai et al. 2007). As the atlas did not cover the cerebellum, so the Talairach Daemon (Lancaster et al. 1997; Lancaster et al. 2000) was used, following MNI to Talairach conversion.

Following mean map analysis, the two contrasts AWAN and ALAN were compared using the automated linear model analysis which calculates the between-group difference based on statistical significance after Monte Carlo randomisation. In order to study potential confounders, automated linear model meta-regression was calculated, whereby the difference between the minimum and maximum values of regressors are returned with statistical significance based on Monte Carlo randomisation.

Results

Following removal of duplicates, and screening of abstracts, from an initial list of 288 articles a final selection of 108 articles were eligible for inclusion. We contacted all corresponding authors for the 108 articles of whom 70 responded. Brain maps corresponding to 36 articles were received. Of these, 21 were excluded for reasons detailed in the Prisma flow diagram (Fig. 2).

Table 2 Anticipation win-vs-anticipation neutral main peaks for SDM z-score > 5 or < −5

Peak MNI coordinate	SDM-z	P	FDR	Voxels	Anatomical Description	n subpeaks	Egger's test p
Activation							
2,0,62	9.798	~0	>0.0001…	25,114	Right superior frontal gyrus, lateral part	169	0.910
34,40,26	6.424	~0	>0.0001…	405	Right middle frontal gyrus	9	0.919
-34,42,28	6.679	~0	>0.0001…	313	Left middle frontal gyrus	5	0.248
-16,-22,38	6.322	~0	>0.0001…	124	Left paracentral lobule	0	0.097
46,-52,-10	5.699	~0	>0.0001…	125	Right inferior temporal gyrus	2	0.139
-20,-72,10	5.476	~0	>0.0001…	83	Left occipital gyrus	1	0.123
-40,-56,-6	5.440	~0	>0.0001…	51	Left inferior temporal gyrus	0	0.354
-18,-42,-6	5.437	~0	>0.0001…	26	Left parahippocampal gyrus	0	0.910
Deactivation							
-52,-64,36	−6.434	~0	>0.0001…	4857	Left angular gyrus	12	0.670
54,-62,30	−5.253	~0	>0.0001…	1736	Right superior temporal gyrus	2	0.613

MNI (Montreal Neurological Institute), SDM-z (Signed Differential Mapping z-score), FDR (false discovery rate)

In total 15 sets of whole brain group maps were included in the meta-analysis of anticipation (Supplementary Table 1). Thirty-three articles were included in the first stage of the meta-analysis including 18 sets of whole-brain coordinates extracted from the text (Supplementary Table 1). No additional maps were included on repeating the literature search two years later. The omnibus sample size for all 33 non-overlapping samples (maps and text coordinates) was 728 healthy adults, mean age 30.3 years (SD 7.81), 60.6% male, and 98.8% right-handed (Table 1). See Supplementary Tables 1, 2 and 3 for full demographics, monetary incentive delay task specifics and fMRI acquisition and analysis for each study.

An initial omnibus analysis combined group maps and published text coordinates. However, we found significant bias for the two most significant peaks of the AWAN and ALAN contrasts (Supplementary Fig. 1, Supplementary Table 4). Given this finding and the theoretical discrepancies between coordinate and image-based meta-analysis previously discussed, we report only the *group map* meta-analysis from here on (Supplementary Table 5).

Anticipation Win Minus Anticipation Neutral

This contrast was examined in a total sample size of 274 participants (Table 1).

Activation

Eleven main peaks in eleven clusters were identified (size: 10 to 25,114 voxels, z-score: 3.967 to 9.798, Table 2, Fig. 3). Eight main peaks and 144 subpeaks exceeded $z = 5.0$. The main peak of largest cluster was located in the right superior frontal gyrus lateral part extending widely to include, amongst 140 subpeaks, the caudate and putamen bilaterally, left fundus region of caudate (proximate to nucleus accumbens) and right nucleus accumbens. The remaining main peaks $z > 5.0$ were bilateral middle frontal gyri, bilateral inferior temporal gyri, left paracentral lobule, left occipital gyrus and left parahippocampal gyrus.

Deactivation

Thirteen main peaks in thirteen clusters were identified (size: 36–4857 voxels, z-score: 1.022–6.434, Table 2, Fig. 3). Two main peaks and one subpeak exceeded $z = 5$ located in the right superior temporal gyrus and left angular gyrus.

Anticipation Lose Minus Anticipation Neutral

This contrast was examined in a combined sample of 246 participants (Table 1).

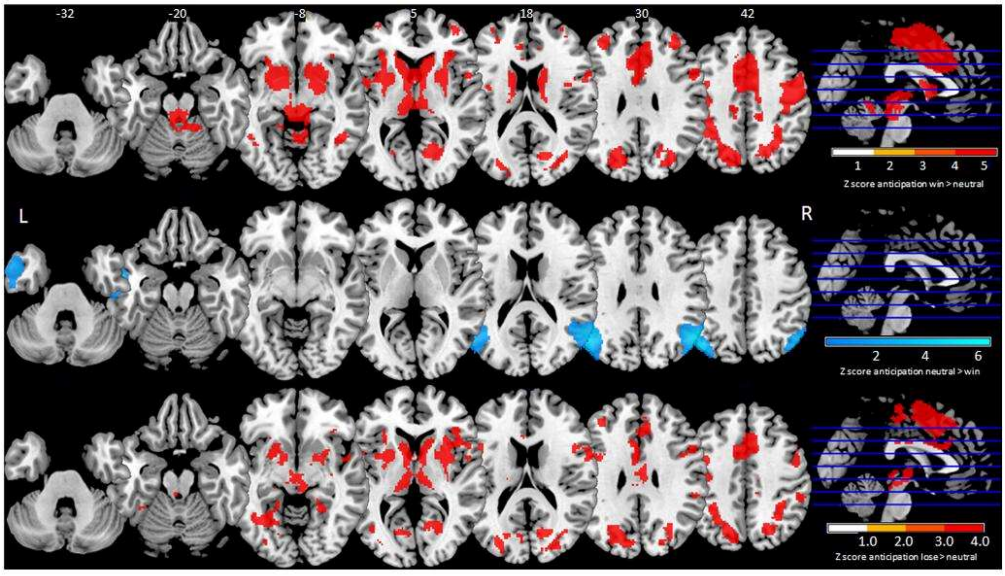

Fig. 3 Mean maps thresholded to signed differential mapping z-score > 5. Top row - anticipation win-vs-anticipation neutral with activation in red. Middle row - anticipation win-vs-anticipation neutral with deactivation in blue. Bottom row - anticipation lose-vs-anticipation neutral with activation in red

Table 3 Anticipation lose-vs-anticipation neutral main peaks for SDM z-score > 5 < −5

Peak MNI coordinate	SDM-z	P	FDR	Voxels	Anatomical Description	n subpeaks	Egger's test p
Activation							
0,18,52	6.801	~0	>0.0001…	11,315	Left superior frontal gyrus medial part	131	0.731
-28,-70,26	5.753	~0	>0.0001…	1854	Left parieto-occipital transition zone	26	0.359
30,-48,38	5.352	~0	>0.0001…	1491	Right supramarginal gyrus	25	0.185
-30,-60,-10	6.286	~0	>0.0001…	461	Left hippocampus CA1	5	0.587
52,-34,36	5.207	~0	>0.0001…	174	Right supramarginal gyrus	0	0.654
24,-46,-8	5.28	~0	>0.0001…	88	Right fusiform gyrus	0	0.620
-36,36,32	5.056	~0	>0.0001…	70	Left middle frontal gyrus	0	0.757

MNI (Montreal Neurological Institute), SDM-z (Signed Differential Mapping z-score), FDR (false discovery rate)

Activation

We found nineteen main peaks (z-score: 3.947–6.801, size: 12–11,315 voxels, Table 3, Fig. 3). Seven main peaks and 65 subpeaks exceeded z = 5.0 (Supplementary 4.3). The main peak of the largest cluster was located in the left superior frontal gyrus medial part extending widely to include, amongst 47 subpeaks, bilateral putamen and right caudate. In descending order, other main peaks z > 5 .0 were located in the left parieto-occipital transition zone, right supramarginal gyrus (2 main peaks), left hippocampus CA1, right fusiform gyrus and left middle frontal gyrus.

Deactivation

No main peaks exceeded the raised threshold z > 5, though multiple peaks were significant (Supplementary Table 5.a-d for full breakdown).

Between Group Comparison: AWAN Minus ALAN

On between-group linear model comparison between AWAN and ALAN, we found significantly greater *deactivation* in AWAN compared to ALAN in the left inferior frontal gyrus opercular part (Fig. 4, Supplementary Table 6).

Publication Bias, Heterogeneity, Sensitivity and Confounders

Funnel plots revealed no clear evidence of marked asymmetry on visual inspection for the higher thresholded main peaks for either contrast (Supplementary Fig. 1), also surviving Egger's test for bias (Tables 2 & 3). Maps of significant heterogeneity (Q_H) were overlaid on the mean maps for both contrasts to visually inspect for overlapping areas (Supplementary Fig. 2). For AWAN significant heterogeneity overlapped with activation in the bilateral ventral striatum and bilateral dorsal thalamic nuclei. For ALAN, overlap was seen in bilateral nucleus accumbens, bilateral medial superior frontal gyrus and the left precentral gyrus. Visual inspection of Jacknife analysis overlaid on the heterogeneity maps showed good replicability of all areas reported in both contrasts (Supplementary Fig. 3).

Outside of the task conditions, two independent regressors were available, namely, placebo intervention and scanner strength. Seventy of the 274 (26%) subjects in AWAN and 59 of the 246 (24%) in ALAN were given placebo (washout period 1 to 2 weeks). Overlaying heterogeneity maps for each contrast with meta-regression for placebo showed overlap with activation in AWAN in the bilateral ventral striatum, but no visual overlap in the ALAN contrast (Supplementary Fig. 4, Supplementary Table 8).

Regarding field strength, for AWAN 7 of 14 mean maps were generated using a 3 T scanner, for ALAN 5 of 11 maps were 3 T and the remainder for both 1.5 T. No areas of overlap in heterogeneity corresponded to areas of activation or deactivation in the mean maps (Supplementary Fig. 5, Supplementary Table 9).

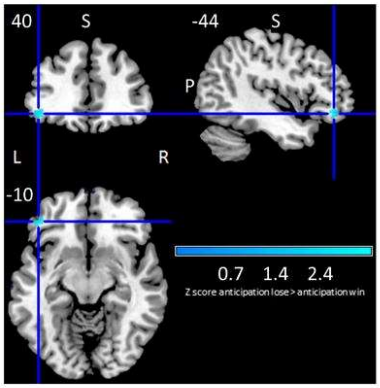

Fig. 4 Between group comparison of anticipation win-vs-neutral minus anticipation lose-vs-neutral showing relative deactivation in blue

Discussion

The aim of the present study was to investigate which regions of the brain are robustly engaged by reward processing in healthy adult humans, specifically looking at motivational salience, that is, presentation of reward incentive and preparation of approach behaviour. Using all available fMRI group-map data for the anticipation of reward and loss conditions of the monetary incentive delay task in healthy adult humans, our meta-analysis shows that there are large areas of both *activation* and *deactivation* across the whole brain in motivational salience. For the first time, we report the pattern of deactivation in anticipation of reward in the monetary incentive delay task in healthy adult humans. We also report evidence of positive effect-size bias in the anterior cingulate (AWAN) and striatum (AWAN and ALAN) in the literature.

The results presented here are consistent with those reported in a recent activation likelihood estimation based meta-analysis of reward anticipation using the monetary incentive delay task in healthy adults (Oldham et al. 2018), but we report far more extensive areas of activation involving frontal, temporal, parietal and cerebellar regions. Furthermore, we have reported on areas of relative deactivation as well as publication bias, heterogeneity, replicability, and the potential effects of placebo and scanner strength.

We have confirmed a number of regions of activation reported in the original monetary incentive delay task studies of healthy adults (Knutson et al. 2001; Knutson et al. 2000) for AWAN, including bilateral insula (left insula originally reported as motor cortex), right nucleus accumbens, nucleus accumbens, bilateral caudate, left putamen, thalamus, right amygdala, right anterior cingulate gyrus (both reported as 'right mesial prefrontal cortex'), right superior frontal gyrus medial part (reported as 'right SMA') and right cerebellum anterior lobe culmen (reported as cerebellar vermis). However, we did not find any activation in the right amygdala or left nucleus accumbens, an area of significant heterogeneity. We have also greatly extended the pattern of activity such that all previous unilateral peaks, except right amygdala, were found to be bilateral including putamen, superior frontal gyrus (medial and lateral), anterior cingulate gyrus, cerebellum anterior lobe culmen, and thalamic nuclei. We have provided greater resolution within the thalamus itself, finding activation in bilateral medial dorsal thalamic nuclei and two left ventral anterior thalamic nuclei. We report nine additional bilateral areas of activation including middle frontal gyri and inferior temporal gyri, precentral gyri, frontal operculae, paracingulate cortex, postcentral gyri, superior parietal lobules, precunei and insular gyri. We report twenty additional unilateral areas of activation (5 main peaks) including areas known to be implicated in both salience processing, such as the hippocampus (Crottaz-Herbette et al. 2005), and reward processing, such as the right parahippocampal gyrus and right inferior frontal gyrus (Brooks et al. 2013).

Interpretation

As predicted, the striatum is strongly engaged in both anticipation of reward and loss, though not clearly differentiated when comparing the two contrasts. We found significant heterogeneity in this area in the anticipation of reward across all studies which may be explained in part by placebo effects.

Both reward and loss anticipation robustly engage key nodes of the salience network including anterior insular and anterior cingulate cortex. However, a mixed picture emerged for the anterior cingulate with anticipation of reward strongly activating bilateral anterior cingulate with a single main peak of deactivation in the left anterior cingulate. In contrast, anticipation of loss strongly activated the left anterior cingulate only with no detected deactivation. This pattern of activation may be reflected in the AWAL between-group comparison (Supplementary Table 6) showing a subthreshold (cluster size 8 voxels) difference in activation in the left anterior cingulate. The anterior insula was activated bilaterally in both contrasts. The insula cortex is considered a major cortical target of ascending interoceptive and visceromotor signals passing through thalamic nuclei (Uddin 2015) found to be functionally connected to amygdala, dorsomedial thalamus, hypothalamus peri-aqueductal grey matter (Seeley et al. 2007). We confirmed activity in these regions, though seemingly a different pattern for each contrast (AWAN - bilateral dorsomedial thalamic nuclei, right periaqueductal grey matter; ALAN - right posterior hypothalamic area, left basomedial nucleus of the amygdala).

The right anterior insular cortex, in particular, is also thought to be involved in switching between two other networks, namely, the central-executive and the default-mode networks (Sridharan et al. 2008). The central-executive network is considered the neural substrate underlying cognitive processes such as inhibition, interference control, working memory and cognitive flexibility (Diamond 2013) and is thought to be anchored in the dorsolateral prefrontal and lateral parietal cortex (Sridharan et al. 2008). We found strong bilateral activation of dorsolateral prefrontal cortex in both contrasts in the bilateral middle frontal gyri and bilateral superior frontal gyri, lateral part. Regarding the lateral parietal cortex we found significant but differing patterns of activation for each contrast. In both conditions, there was bilateral activation of the superior parietal lobule and unilateral activation of the right angular gyrus. However in AWAN there was *unilateral* activation of the left supramarginal gyrus and deactivation in the *left* angular gyrus, and in ALAN *bilateral* activation of the supramarginal gyrus and unilateral deactivation of the *right* angular gyrus.

The default-mode network is considered a state of cortical activity independent of external stimuli (originally considered to be 'waking rest') convergent with areas active in resting state fMRI (Andrews-Hanna et al. 2014) and task-induced deactivation (Andrews-Hanna, 2012). This network has been

further subdivided into a 'core' anchored in the posterior cingulate cortex and anteromedial prefrontal cortex, as well as the 'medial temporal' and' dorsal medial subsystems' (Andrews-Hanna 2012). The core is associated with self-referential processes, the medial temporal subsystem corresponds to past and future autobiographical thought, episodic memory and contextual retrieval, and the dorsal medial subsystem corresponds to social cognition, story comprehension and semantic processing (Yeo et al. 2011). We found bilateral activation of the 'core' posterior cingulate in both anticipation contrasts. Regarding the medial temporal subsystem, we observed a differing pattern of activation in the ventromedial prefrontal cortex with unilateral activation of the right posterior orbital gyrus in AWAN and unilateral activation of the left intermediate orbital gyrus in ALAN. In AWAN in the medial temporal lobe, there was bilateral deactivation in the parahippocampal gyrus in conjunction with unilateral activation in the left parahippocampal gyrus. Yet in ALAN we reported unilateral activation of the left hippocampus CA1 region. With respect to the dorsomedial subsystem, on the one hand we found robust bilateral activation of the superior frontal gyrus, lateral part in both contrasts. On the other hand, we saw a mixed picture in the lateral temporal cortex. The inferior temporal gyrus was activated in both contrasts. In AWAN, there was activation in the right middle temporal gyrus, deactivation in the right middle gyrus and deactivation in the right superior temporal gyrus. In ALAN there was activation in the left middle temporal gyrus, deactivation in bilateral middle temporal gyri and deactivation in the left superior temporal gyrus.

The monetary incentive delay task is also a motor processing task and, as such, we observed broad bilateral activation of primary motor cortex (precentral gyrus), somatosensory cortex (post central gyrus), the supplementary motor area and multiple thalamic nuclei in both contrasts. The striatal region of the basal ganglia was activated, but no peaks were seen in the globus pallidus or subthalamic nuclei. Significant activity was also found in the cerebellum. In AWAN there was strong activation in bilateral anterior lobe of the cerebellum and a peak of deactivation in the right posterior lobe, but in ALAN a mixed picture of unilateral activation and deactivation in the right anterior lobe. It is known that there is an important function for the cerebellum in motivational salience, in keeping with a recent animal study (Cutando et al. 2013) suggesting a role in encoding expectation of reward, the growing understanding of the reciprocal connections between cerebellum and basal ganglia (Niendam et al. 2012) and cerebellar involvement in addiction (Moulton et al. 2014).

These observed patterns of activation are controlled by the neutral condition in which the only theoretical difference in task activation is the absence of motivational salience. Could it be that common areas of activation and deactivation are part of a motivational salience network, robustly engaging the striatum, salience network, parts of the central executive and default networks and associated motor regions? The picture emerging from the central executive and default network appears more complicated with robust activation in the posterior cingulate and dorsolateral prefrontal cortex, but a differing pattern emerging between anticipation of reward and loss in the lateral parietal cortex, ventromedial cortex, medial (including hippocampus) and lateral temporal cortex.

Between-group comparisons

The first meta-analysis of healthy controls discussed earlier compared uncontrolled anticipation of reward directly with loss (Knutson and Greer 2008). We used a different approach (between-group linear model) comparing mean group maps for two controlled conditions, AWAN and ALAN. We report only one significant peak above threshold in the left inferior frontal gyrus operculum. This region was deactivated in both conditions, but significantly more deactivated in anticipating loss than reward. Additionally, the left anterior cingulate gyrus was active in both contrasts, significantly more so anticipating reward than while anticipating loss, but just under threshold (Supplementary Table 6). The left inferior frontal gyrus has previously been implicated in response inhibition (Swick et al. 2008; Bhattacharyya et al. 2015) and the attribution of aspects of stimulus salience and attentional allocation of resources (Seeley et al. 2007; Bhattacharyya et al. 2012; Downar et al. 2002). Might this left inferior frontal activation reflect differential allocation of cognitive resources according to motivational salience or could this directly reflect a representation of valence?

Limitations

Our findings are limited by the reported sample demographics, constraints of the monetary incentive delay task, the data acquisition and analysis, the methods of meta-analysis and the brain atlas used. Across all the studies, we were only able to report sample size, age, gender and handedness. Other variables such as substance use, education, IQ, socioeconomic status and ethnicity were too inconsistently reported for any meaningful interpretation.

In terms of the monetary incentive delay task, there was significant variation across designs. The maps we received were from many different international locations including Europe, the USA, Japan and South Korea. Therefore the financial incentive could have different meanings to different samples, although superficially they appear to be similarly small amounts of money. There was inconsistent reporting of, and variation in, the duration of all the phases of each trial, including monetary incentive stimulus presentation, anticipation, target, feedback and inter-stimulus interval. The data are gathered over multiple trials varying from 44 to 180 in each study, and the target hit rate was either unreported or varied from 50% to 75% which could have influenced any neural substrate for the temporally bound reward

prediction error signal. The monetary incentive delay task is not designed to capture temporal learning or any reward prediction error signal. Variants of the monetary incentive delay task have been developed that introduce contingency, varying the predictability of reward receipt following action, and we have included a single group map in the AWAN condition introducing this (Li et al. 2014). Lastly, overall performance data was not consistently reported, preventing meaningful behavioural interpretation.

Regarding data acquisition and analysis, a variety of scanners and sequences were used in each study. There was variation in acquisition and echo time, number and thickness of slices, resolution and analysis software. All of these are documented in Supplementary Table 3 for reference. Only two potential confounders were available for statistical analysis, scanner strength and placebo condition, though meta-regression and comparison with heterogeneity and mean maps did not suggest any significant effects on our results.

The most important limitation to our method was the exclusion of over half of the studies. We felt this to be an essential step after identification of the positive effect-size bias in published coordinate-based data. The main peaks of the omnibus analysis (text coordinates and group maps) are reported in Supplementary Table 4 for reference. Secondly, because we found such a large number of significant peaks, we could not report all the data generated by this meta-analysis and applied a very conservative threshold. Subsequently, on the one hand, we feel our results are extremely robust, but on the other, many regions which may be of interest are not discussed. However, all these data are recorded in the Supplementary Table 5.

In terms of the between-group linear model comparison of AWAN and ALAN, there was a difference in gender proportion between AWAN (78%) and ALAN (71%), though this effect just fails to achieve nominal significance ($\chi 2\ (1) = 3.34$, $p = 0.07$). However, 10 of the 15 studies ($n = 194$) for which we received group maps, sent both AWAN and ALAN contrasts, such that the majority of the data was repeated-measures within-group, strengthening the results.

Finally, the brain atlas used for anatomical location, while strong on detail, is based on the dissection of a single 24 year old male brain and does not cover the cerebellum necessitating additional use of the Tailarach Daemon.

Notwithstanding these limitations, this image-based meta-analysis uses data from a large sample of healthy individuals and reveals robust engagement of brain areas that have previously been linked to the anticipation of reward as well as novel brain areas, providing a definitive map of the reward anticipation network in the healthy human brain.

Acknowledgements We would like to acknowledge the support of Joaquim Radua, Anton Albajes-Eizagirre, Christian Windischberger and Rupert Lanzenberger.

Monetary Incentive Delay Task Analysis Consortium (MTAC) (arranged in alphabetical order):

Abe, N, Barros-Loscertales, AR, Bayer, J, Beck, A, Bjork, J, Boecker, R, Bustamante, JC, Choi, JS, Delmonte, S, Dillon, D, Figee, M, Garavan, H, Hagele, C, Hermans, EJ, ICCAM Consortium, Ikeda, Y, Kappel, V, Kaufmann, C, Lamm, C, Lammertz, SE, Li, Y, Murphy, A, Nestor, L, Pecina, M, Pfabigan, D, Pizzagalli, D, Rademacher L, Admon, R, Sommer T, Stark, R, Suzuki, H, Van Amelsvoort, T, Van Hell, E, Vink M, Votinov, M, Wotruba, D.

Compliance with Ethical Standards

Conflict of Interest The authors report no financial or other conflict of interest. MB is supported by the Veni fellowship from the Netherlands Organisation for Scientific Research. PA is supported by the British Academy and MRC CiC. MK is supported by an MRC Career Development Fellowship. SB is supported by an NIHR Clinician Scientist Award and the MRC.

References

Andrews-Hanna, J. R. (2012). The brain's default network and its adaptive role in internal mentation. *Neuroscientist, 18*(3), 251–270. https://doi.org/10.1177/1073858411403316.

Andrews-Hanna, J. R., Smallwood, J., & Spreng, R. N. (2014). The default network and self-generated thought: component processes, dynamic control, and clinical relevance. *Annals of the New York Academy of Sciences, 1316*(1), 29–52.

Bartra, O., McGuire, J. T., & Kable, J. W. (2013). The valuation system: a coordinate-based meta-analysis of BOLD fMRI experiments examining neural correlates of subjective value. *Neuroimage, 76*, 412–427.

Bhattacharyya, S., Atakan, Z., Martin-Santos, R., Crippa, J. A., Kambeitz, J., Malhi, S., et al. (2015). Impairment of inhibitory control processing related to acute psychotomimetic effects of cannabis. *European Neuropsychopharmacology, 25*(1), 26–37. https://doi.org/10.1016/j.euroneuro.2014.11.018.

Bhattacharyya, S., Crippa, J. A., Allen, P., Martin-Santos, R., Borgwardt, S., Fusar-Poli, P., et al. (2012). Induction of psychosis by Δ9-tetrahydrocannabinol reflects modulation of prefrontal and striatal function during attentional salience processing. *Archives of General Psychiatry, 69*(1), 27–36. https://doi.org/10.1001/archgenpsychiatry.2011.161.

Brooks, S. J., Cedernaes, J., & Schiöth, H. B. (2013). Increased prefrontal and parahippocampal activation with reduced dorsolateral prefrontal and insular cortex activation to food images in obesity: a meta-analysis of fMRI studies. *PLoS One, 8*(4), e60393.

Crottaz-Herbette, S., Lau, K., Glover, G., & Menon, V. (2005). Hippocampal involvement in detection of deviant auditory and visual stimuli. *Hippocampus, 15*(1), 132–139.

Cutando, L., Busquets-Garcia, A., Puighermanal, E., Gomis-Gonzalez, M., Delgado-Garcia, J. M., Gruart, A., et al. (2013). Microglial activation underlies cerebellar deficits produced by repeated cannabis exposure. *The Journal of Clinical Investigation, 123*(7), 2816–2831. https://doi.org/10.1172/jci67569.

DerSimonian, R., & Laird, N. (1986). Meta-analysis in clinical trials. *Controlled Clinical Trials, 7*(3), 177–188.

Diamond, A. (2013). Executive functions. *Annual Review of Psychology, 64*, 135–168.

Diekhof, E. K., Kaps, L., Falkai, P., & Gruber, O. (2012). The role of the human ventral striatum and the medial orbitofrontal cortex in the representation of reward magnitude - an activation likelihood estimation meta-analysis of neuroimaging studies of passive reward expectancy and outcome processing. *Neuropsychologia, 50*(7), 1252–1266. https://doi.org/10.1016/j.neuropsychologia.2012.02.007.

Downar, J., Crawley, A. P., Mikulis, D. J., & Davis, K. D. (2002). A cortical network sensitive to stimulus salience in a neutral behavioral context across multiple sensory modalities. *Journal of Neurophysiology, 87*(1), 615–620.

Horton, R. (2015). Offline: What is medicine's 5 sigma? *The Lancet, 385*(9976), 1380. https://doi.org/10.1016/S0140-6736(15)60696-1.

Knutson, B., Bhanji, J. P., Cooney, R. E., Atlas, L. Y., & Gotlib, I. H. (2008). Neural responses to monetary incentives in major depression. *Biological Psychiatry, 63*(7), 686–692. https://doi.org/10.1016/j.biopsych.2007.07.023.

Knutson, B., Fong, G. W., Adams, C. M., Varner, J. L., & Hommer, D. (2001). Dissociation of reward anticipation and outcome with event-related fMRI. *Neuroreport, 12*(17), 3683–3687.

Knutson, B., & Greer, S. M. (2008). Anticipatory affect: neural correlates and consequences for choice. *Philosophical Transactions of the Royal Society of London B: Biological Sciences, 363*(1511), 3771–3786.

Knutson, B., Westdorp, A., Kaiser, E., & Hommer, D. (2000). FMRI visualization of brain activity during a monetary incentive delay task. *Neuroimage, 12*(1), 20–27. https://doi.org/10.1006/nimg.2000.0593.

Lancaster, J. L., Rainey, L. H., Summerlin, J. L., Freitas, C. S., Fox, P. T., Evans, A. C., et al. (1997). Automated labeling of the human brain: a preliminary report on the development and evaluation of a forward-transform method. *Human Brain Mapping, 5*(4), 238–242. https://doi.org/10.1002/(sici)1097-0193(1997)5:4<238::aid-hbm6>3.0.co;2-4.

Lancaster, J. L., Woldorff, M. G., Parsons, L. M., Liotti, M., Freitas, C. S., Rainey, L., et al. (2000). Automated Talairach atlas labels for functional brain mapping. *Human Brain Mapping, 10*(3), 120–131.

Li, Y., Sescousse, G., & Dreher, J.-C. (2014). Endogenous cortisol levels are associated with an imbalanced striatal sensitivity to monetary versus non-monetary cues in pathological gamblers. *Frontiers in Behavioral Neuroscience, 8*.

Lieberman, M. D., & Cunningham, W. A. (2009). Type I and Type II error concerns in fMRI research: re-balancing the scale. *Social Cognitive and Affective Neuroscience, 4*(4), 423–428. https://doi.org/10.1093/scan/nsp052.

Liu, X., Hairston, J., Schrier, M., & Fan, J. (2011). Common and distinct networks underlying reward valence and processing stages: a meta-analysis of functional neuroimaging studies. *Neuroscience and Biobehavioral Reviews, 35*(5), 1219–1236. https://doi.org/10.1016/j.neubiorev.2010.12.012.

Mai, J. K., Paxinos, G., & Voss, T. (2007). *Atlas of the human brain* (3rd ed.). San Diego: Academic Press.

Moulton, E. A., Elman, I., Becerra, L. R., Goldstein, R. Z., & Borsook, D. (2014). The Cerebellum and Addiction: Insights Gained from Neuroimaging Research. *Addiction Biology, 19*(3), 317–331.

Müller, V. I., Cieslik, E. C., Laird, A. R., Fox, P. T., Radua, J., Mataix-Cols, D., et al. (2018). Ten simple rules for neuroimaging meta-analysis. *Neuroscience & Biobehavioral Reviews, 84*, 151–161. https://doi.org/10.1016/j.neubiorev.2017.11.012.

Niendam, T. A., Laird, A. R., Ray, K. L., Dean, Y. M., Glahn, D. C., & Carter, C. S. (2012). Meta-analytic evidence for a superordinate cognitive control network subserving diverse executive functions. *Cognitive, Affective, & Behavioral Neuroscience, 12*(2), 241–268. https://doi.org/10.3758/s13415-011-0083-5.

Oldham, S., Murawski, C., Fornito, A., Youssef, G., Yucel, M., & Lorenzetti, V. (2018). The anticipation and outcome phases of reward and loss processing: A neuroimaging meta-analysis of the monetary incentive delay task. *Human Brain Mapping*. https://doi.org/10.1002/hbm.24184.

Radua, J., & Mataix-Cols, D. (2009). Voxel-wise meta-analysis of grey matter changes in obsessive–compulsive disorder. *The British Journal of Psychiatry, 195*(5), 393–402.

Radua, J., Mataix-Cols, D., Phillips, M. L., El-Hage, W., Kronhaus, D., Cardoner, N., et al. (2012). A new meta-analytic method for neuroimaging studies that combines reported peak coordinates and statistical parametric maps. *European Psychiatry, 27*(8), 605–611.

Radua, J., Rubia, K., Canales-Rodríguez, E. J., Pomarol-Clotet, E., Fusar-Poli, P., & Mataix-Cols, D. (2014). Anisotropic kernels for coordinate-based meta-analyses of neuroimaging studies. *Frontiers in Psychiatry, 5*.

Radua, J., Van Den Heuvel, O. A., Surguladze, S., & Mataix-Cols, D. (2010). Meta-analytical comparison of voxel-based morphometry studies in obsessive-compulsive disorder vs other anxiety disorders. *Archives of General Psychiatry, 67*(7), 701–711.

Salimi-Khorshidi, G., Smith, S. M., Keltner, J. R., Wager, T. D., & Nichols, T. E. (2009). Meta-analysis of neuroimaging data: a comparison of image-based and coordinate-based pooling of studies. *Neuroimage, 45*(3), 810–823. https://doi.org/10.1016/j.neuroimage.2008.12.039.

Schultz, W., Dayan, P., & Montague, P. R. (1997). A neural substrate of prediction and reward. *Science, 275*(5306), 1593–1599.

Seeley, W. W., Menon, V., Schatzberg, A. F., Keller, J., Glover, G. H., Kenna, H., et al. (2007). Dissociable intrinsic connectivity networks for salience processing and executive control. *The Journal of Neuroscience, 27*(9), 2349–2356. https://doi.org/10.1523/jneurosci.5587-06.2007.

Sridharan, D., Levitin, D. J., & Menon, V. (2008). A critical role for the right fronto-insular cortex in switching between central-executive and default-mode networks. *Proceedings of the National Academy of Sciences of the United States of America, 105*(34), 12569–12574. https://doi.org/10.1073/pnas.0800005105.

Swick, D., Ashley, V., & Turken, U. (2008). Left inferior frontal gyrus is critical for response inhibition. *BMC Neuroscience, 9*(1), 102.

Yeo, T. B., Krienen, F. M., Sepulcre, J., Sabuncu, M. R., Lashkari, D., Hollinshead, M., et al. (2011). The organization of the human cerebral cortex estimated by intrinsic functional connectivity. *Journal of Neurophysiology, 106*(3), 1125–1165.

Turkeltaub, P. E., Eden, G. F., Jones, K. M., & Zeffiro, T. A. (2002). Meta-Analysis of the Functional Neuroanatomy of Single-Word Reading: Method and Validation. *Neuroimage, 16*(3), 765–780. https://doi.org/10.1006/nimg.2002.1131.

Uddin, L. Q. (2015). Salience processing and insular cortical function and dysfunction. *Nature Reviews Neuroscience, 16*(1), 55.

Addendum

In the "The Neural Substrate of Reward Anticipation in Health: A Meta-Analysis of fMRI Findings in the Monetary Incentive Delay Task", both group map data and coordinate-based data were initially combined in an 'omnibus analysis'. On post-hoc analysis, significant bias was observed in the main peaks for both anticipation win-vs-neutral (AWAN) and anticipation lose-vs-neutral (ALAN) contrasts (Supplementary Fig. 1, Supplementary Table 4) leading to exclusion of all coordinate-based data.

In this addendum, we explore this bias and directly compare group map data with coordinate-based data using methods detailed in the section "Data Analysis: Seed-Based D Mapping" in the article.

Bias in coordinate-based data

There were 18 studies (n=382) for AWAN and 10 studies (n=228) for ALAN with coordinate-based data (see Table 1). As in the original paper, mean maps were generated and thresholded at the validated default settings (p< 0.005, SDM-z> 1.0, k>10 voxels). Bias was then estimated by funnel plot (effect size on the x-axis, standard error on the y-axis) and asymmetry assessed by Egger's test.

Table 1. Anticipation win and lose versus neutral main peaks using coordinate-based data

Peak MNI coordinate	SDM-z	P	FDR	Voxels	Anatomical Description	Egger's test p
AWAN activation (18 studies, n=382)						
-14,10,0	5.658	~0	<0.0001…	10700	Left putamen	**0.048**
4,4,28	4.121	~0	<0.0001…	3458	Right anterior cingulate	0.541
-24,-42,-26	3.611	<0.0001	0.0001	869	Left cerebellum anterior lobe*	**0.046**
12,-64,6	3.461	0.0001	0.0002	79	Left striate area	0.642
-40,26,0	2.937	0.0017	0.0020	24	Left inferior frontal gyrus orbital part	**0.043**
18,-72,-22	2.811	0.0029	0.0029	14	Right cerebellum posterior lobe*	0.414
ALAN activation (10 studies, n=228)						
0,12,10	6.035	~0	<0.0001…	7195	Left anterior cingulate gyrus**	0.869
-6,16,22	4.044	~0	<0.0001…	248	Left anterior cingulate gyrus	0.578
-6,-60,0	2.603	0.0023	0.0027	14	Left lingual gyrus	0.297
36,56,8	2.565	0.0027	0.0027	11	Right middle frontal gyrus	0.505

p< 0.005, SDM-z> 1.0, k>10 voxels, MNI (Montreal Neurological Institute), SDM-z (Signed Differential Mapping z-score), FDR (false discovery rate), *Talairach client, ** nearest grey matter structure

In the AWAN group, three peaks proved significant demonstrating evidence of bias, located in the left putamen, left cerebellum anterior lobe and left inferior frontal gyrus orbital part. No peaks demonstrated bias in ALAN.

Between-group linear comparison

The automated linear model analysis described in the methods section of the main paper was used to detect any major differences between group map data and coordinate-based data in both AWAN and ALAN.

Table 2. Between-group linear comparison of group map data minus coordinate-based data for the contrast anticipation win versus neutral

Peak MNI coordinate	SDM-z	P	FDR	Voxels	Anatomical Description
-8,-4,54	8.508	~0	<0.0001…	17237	Left superior frontal gyrus medial part
36,48,26	6.241	~0	<0.0001…	555	Right middle frontal gyrus
40,-56,-8	5.524	~0	<0.0001…	191	Right inferior temporal gyrus
-42,-58,-6	5.612	~0	<0.0001…	165	Left inferior temporal gyrus
18,-18,16	5.209	~0	<0.0001…	161	Right caudate/ventral lateral thalamic nuclei
24,2,6	6.558	~0	<0.0001…	80	Right putamen
-22,2,6	6.918	~0	<0.0001…	71	Left putamen
16,-44,-18	5.537	~0	<0.0001…	59	Right cerebellum anterior lobe*
-48,-70,34	-5.635	~0	<0.0001…	1888	Left angular gyrus
54,-64,30	-5.602	~0	<0.0001…	1295	Right angular gyrus

p< 0.005, SDM-z> 5.0, k>10 voxels, MNI (Montreal Neurological Institute), SDM-z (Signed Differential Mapping z-score), FDR (false discovery rate), *Talairach client

For the contrast AWAN, extensive areas were found to be significantly different between the two forms of data. In order to meaningfully interpret the results, the z-score ≥ 5.0 threshold was applied once again (see Table 2, Figure 1). Areas differing between the two sets of data overlapped with locations identified in the main paper for activation (superior and middle frontal gyri, inferior temporal gyri) and deactivation (angular gyri).

Figure 1. Between-group linear comparison of group map data minus coordinate-based data for the contrast anticipation win versus neutral

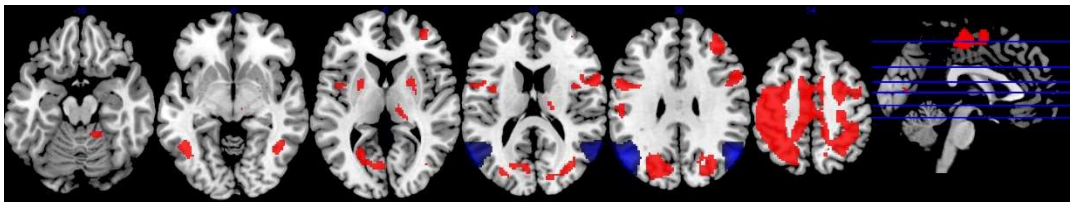

Red- relative activation, blue- relative deactivation

Table 3. Between-group linear comparison of group map data minus coordinate-based data for the contrast anticipation lose versus neutral

Peak MNI coordinate	SDM-z	P	FDR	Voxels	Anatomical Description
0,10,14	-5.179	~0	<0.0001…	139	Left caudate*

p< 0.005, SDM-z> 5.0, k>10 voxels, MNI (Montreal Neurological Institute), SDM-z (Signed Differential Mapping z-score), FDR (false discovery rate), *nearest grey matter structure

Applying the same threshold to ALAN did not yield such extensive regions, but notably a cluster including the left caudate was robustly identified as being relatively less activated in group map data (see Table 3, Figure 2).

Figure 2. Between-group linear comparison of group map data minus coordinate-based data for the contrast anticipation lose versus neutral

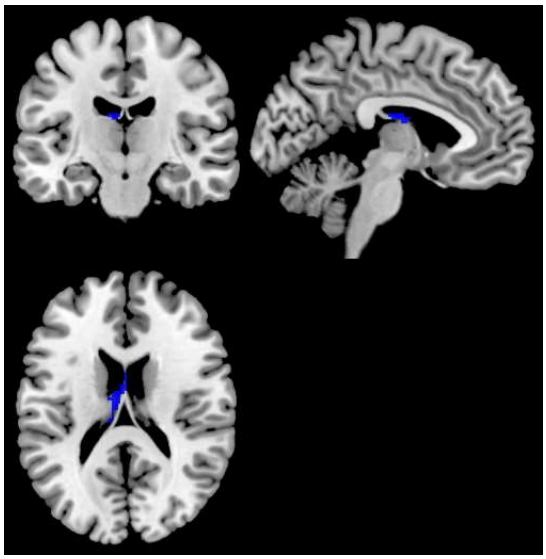

Blue- relative deactivation

Conclusion

There is some evidence of bias in the literature in reporting reward anticipation in the MIDT, which is mitigated by exclusive use of group-map data. Group maps contain far more data from across the brain including both activation and deactivation as standard, whereas coordinate-based data contains information on far fewer voxels and may exclude deactivation. Group maps contain larger sample sizes and are therefore subject to less sampling error and greater statistical power than coordinate-based data maps. In addition, because the coordinate-based data is thresholded, there is an increased probability of Type II error (rejecting a real effect) within maps.

The findings in this addendum corroborate those of Salimi-Khorshidi et al who found poor similarity between image based meta-analysis (IMBA) and coordinate-based meta-analysis (CBMA) within the same dataset (Salimi-Khorshidi, Smith et al. 2009). The results presented here infer that there is considerable type II error and sampling error in CBMA of the MIDT, which may well apply to other cognitive task-fMRI CBMA's. This is not to say that findings of CBMA are incorrect, but that they may be 'missing the big picture'.

Chapter 4

Cannabidiol attenuates insular dysfunction during motivational salience processing in subjects at clinical high risk for psychosis.

Wilson, R. P., Bossong, M. G., Appiah-Kusi, E. M., Petros, N., Brammer, M., Perez, J., Allen, P., McGuire, P. & Bhattacharyya, S., 2019, Translational Psychiatry

For supplementary material please refer to appendix 2: pp 141-145

Wilson et al. *Translational Psychiatry* (2019)9:203
https://doi.org/10.1038/s41398-019-0534-2

Translational Psychiatry

ARTICLE Open Access

Cannabidiol attenuates insular dysfunction during motivational salience processing in subjects at clinical high risk for psychosis

Robin Wilson[1], Matthijs G. Bossong[1,2], Elizabeth Appiah-Kusi[1], Natalia Petros[1], Michael Brammer[1,3], Jesus Perez[4], Paul Allen[1,5], Philip McGuire[1] and Sagnik Bhattacharyya[1]

Abstract

Accumulating evidence points towards the antipsychotic potential of cannabidiol. However, the neurocognitive mechanisms underlying the antipsychotic effect of cannabidiol remain unclear. We investigated this in a double-blind, placebo-controlled, parallel-arm study. We investigated 33 antipsychotic-naïve subjects at clinical high risk for psychosis (CHR) randomised to 600 mg oral cannabidiol or placebo and compared them with 19 healthy controls. We used the monetary incentive delay task while participants underwent fMRI to study reward processing, known to be abnormal in psychosis. Reward and loss anticipation phases were combined to examine a motivational salience condition and compared with neutral condition. We observed abnormal activation in the left insula/parietal operculum in CHR participants given placebo compared to healthy controls associated with premature action initiation. Insular activation correlated with both positive psychotic symptoms and salience perception, as indexed by difference in reaction time between salient and neutral stimuli conditions. CBD attenuated the increased activation in the left insula/parietal operculum and was associated with overall slowing of reaction time, suggesting a possible mechanism for its putative antipsychotic effect by normalising motivational salience and moderating motor response.

Introduction

The aberrant salience hypothesis of psychosis[1] postulates that hyperdopaminergia in the mesostriatal pathway leads to aberrant assignment of salience to everyday experiences and stimuli, which in turn result in psychotic symptoms. Elevated presynaptic dopamine function in the striatum is established in psychotic disorders[2] and in subjects at clinical high risk for psychosis (CHR)[3,4], and an understanding of the relationship between dopamine, aberrant salience and psychotic symptoms, particularly delusions, is emerging[5]. It has been suggested that mesostriatal dopaminergic overactivity may be driven by glutamatergic dysfunction in the medial temporal lobe (MTL)[6], and both increased hippocampal blood flow[7] and metabolism[8] have been reported in CHR subjects and established psychosis.

Dopamine signalling is fundamental to reward processing[9] which is dysfunctional in psychosis[10]. Reward processing includes the attribution of 'motivational salience', whereby the anticipation of a rewarding stimulus or incentive prepares an individual for 'approach behaviour' towards eventual consumption. Neuroimaging studies have demonstrated abnormal brain activity during cognitive tasks capturing 'motivational salience' in CHR and psychosis. Compared to healthy controls, CHR subjects have been found to have hypoactivation in the ventral striatum (VS) and midbrain[11] and right inferior parietal lobule[12], with VS activity to 'aberrant' or non-salient stimuli correlating with severity of positive psychotic symptoms[13]. Others have shown increased activation in

Correspondence: Sagnik Bhattacharyya (sagnik.2.bhattacharyya@kcl.ac.uk)
[1]Department of Psychosis Studies, Institute of Psychiatry, Psychology and Neuroscience, King's College London, London, UK
[2]Department of Psychiatry, Brain Center Rudolf Magnus, University Medical Center Utrecht, Utrecht, Netherlands
Full list of author information is available at the end of the article.

the posterior cingulate cortex (PCC), middle and superior frontal gyri (MFG, SFG)[14] and ventral pallidum and midbrain[15]. In the VS, activity while processing both non-salient[13] and salient stimuli[15] have been correlated with positive psychotic symptoms, as has activity in the right anterior insula during salient stimuli[15]. In established psychosis, meta-analysis suggests hypoactivation of the VS[16], and individual studies have reported reduced activation in the cingulate and ventral tegmentum in unmedicated patients[12,17], and in the right insula in medicated patients[12] while processing motivational salience.

While the aberrant salience hypothesis of psychosis generally focuses on midbrain and striatal function, emerging evidence points towards a key role for other brain regions. In particular, the 'salience network' (SN), anchored in the anterior cingulate (ACC) and insular cortex (IC), may play a role in selecting relevant internal and externally generated signals for higher order processing[18,19]. Altered volume, activation and dysconnectivity of components of the SN have been observed both in established psychotic disorders[12,20–22] and in CHR[23–26] prior to the onset of psychosis, with evidence of association between symptoms and both the extent of volume loss[27] and altered activation[12,28,29] of the insula. This has led to the hypothesis that psychotic symptoms arise as a result of insular dysfunction within the salience network[30].

There is evidence from healthy volunteer studies that cannabidiol (CBD), a non-psychoactive substance in cannabis, opposes the psychotomimetic effects of Δ9-tetrahydrocannabinol (Δ9-THC)[31,32], its main psychoactive ingredient. This is complemented by evidence of efficacy as an antipsychotic in some[33,34], though not all[35], clinical trials. We have recently shown that CBD may normalise MTL, midbrain and striatal dysfunction in CHR patients[36], but the precise neurocognitive mechanism of any antipsychotic effect remains unclear. Whether CBD modulates aberrant motivational salience, and whether this is linked to any antipsychotic effect remains untested.

Therefore, in this study we investigated whether there is a pattern of abnormal activation in CHR compared to healthy controls during the processing of motivationally salient stimuli, and whether a single dose of CBD attenuates this abnormal function in CHR. We selected CHR subjects, because they are antipsychotic-naïve and at risk of developing psychosis[37], thus avoiding confounding effects of dopamine antagonism. Furthermore, they are more stable than people with established psychosis and can better tolerate the demands of complex neuroimaging investigations.

We employed the monetary incentive delay task (MIDT), a reward processing task adapted for fMRI[38]. The MIDT allows reward processing to be parsed into at least two distinct components: 'anticipation' and 'feedback'. We focused on the anticipation condition, as VS activity in this condition has been linked to dopamine release[39], and the SN is robustly activated in both anticipation of reward and loss[40]. Hence, we did not limit anticipation to one specific valence (e.g. reward or loss), but combined all motivationally salient conditions, as previously reported[17,41]. Existing research in CHR using the MIDT has found abnormal activation in the PCC, MFG and SFG in reward anticipation[15], though abnormal striatal activity hasn't been detected[15,42].

Our primary hypothesis was that CHR participants would display altered activation in the core SN (IC and ACC) relative to healthy controls, and a single dose of CBD would have an opposite effect in these regions. Our secondary hypothesis was that CHR participants would display altered activation in the midbrain, striatum and hippocampus, and again CBD would have an opposite effect in these regions.

Method

Participants

Thirty-three CHR participants aged 18–35 years were recruited from early intervention services in the UK. Exclusion criteria included history of psychotic or manic episode, current DSM IV diagnosis of substance dependence (except cannabis), neurological disorder or severe intercurrent illness, unwillingness to use barrier contraception, pregnancy, and any contraindication to MRI. All participants gave written, informed consent. Participants were required to abstain from cannabis for 96 h, other recreational substances for 2 weeks, alcohol for 24 h and caffeine and nicotine for 6 h before attending. Urine samples were collected prior to drug administration to monitor for substance use and to exclude pregnancy. Nineteen healthy control (HC) participants matched for age (within 3 years), sex and ethnicity were recruited by local advertisement. All participants gave written informed consent prior to commencing the trial. The study was approved by the National Research Ethics Service Committee of London—Camberwell St Giles.

Study design and measures

This study was a randomised placebo-controlled double-blind, parallel-arm fMRI investigation of the acute effect of 600 mg oral CBD on the anticipation phase of the MIDT in subjects deemed at clinical high-risk of psychosis. Randomisation and blinding were carried out at the Maudsley Hospital Pharmacy. Psychopathology was assessed by a trained interviewer using the Comprehensive Assessment of At-Risk Mental States interview (CAARMS)[37] prior to drug administration. Plasma CBD levels were sampled 120 and 300 min after drug administration. MRI scanning took place 180 minutes after drug intake. Participants were monitored for any adverse reactions. The study took place at the Clinical Research

Facility, King's College Hospital and the Centre for Neuroimaging Sciences, Department of Neuroimaging, Institute of Psychiatry, Psychology and Neuroscience.

Monetary incentive delay task

Participants underwent two runs of the MIDT each consisting of 48 individual trials. Four conditions were used, induced by learned visual cues: neutral (£0), win small (£0.20), win large (£2.00) and lose (£2). Participants underwent standardised training prior to entering the scanner. There were 12 trials for each condition randomised into 48 trials per run, with two consecutive runs lasting 8 min each. Participants began each run with a baseline figure of £10.00 and received payment at the end of the same study day for the cumulative total won in both runs.

The cue was presented for 250 ms and the feedback for 1450 ms (see Supplementary Fig 1). Target presentation time varied for each run by ±10ms from an initial 250 ms and ranging between 150 and 300 ms to assure ~66% success for each participant. A successful hit depended on the participant responding by pressing the button during target presentation. A response prior to 100 ms after target onset was considered an unsuccessful 'false-start'. Scanning of anticipation occurred during the interval between cue and target which varied from 3700 to 4500 ms in duration. The inter-trial interval was 10 s for all trials.

Drug intervention

CHR participants were randomised to receive either oral 600 mg CBD (CHR-CBD; CBD obtained from THC Pharm, Germany) or placebo (CHR-PLB) prepared in identical capsules following a standard light breakfast. Participants were administered the capsule at ~11 a.m., 180 min before the start of scanning.

Scanning parameters

Participants underwent structural and functional MRI in a single session. Images were acquired using a General Electric Signa HDx 3.0 T MRI scanner. Structural images were acquired using a whole-brain sagittal T1-weighted scan based on Alzheimer's Disease Neuroimaging Initiative parameters (TE = 2.85 ms, TR = 6.98 ms, inversion time = 400 ms, flip angle = 11^0, voxel size 1.0 × 1.0 × 1.2 mm). 480 T2*-weighted images were acquired in two 8-min runs (TE = 30 ms, TR = 2.0 s, flip angle = 75°, 39 × 3 mm thick axial planes, 3.3 mm inter-slice gap, in-plane voxel size 3.75 × 3.75 mm).

Analysis

Imaging

fMRI data were preprocessed using SPM8 (Wellcome Trust Centre for Neuroimaging) by realignment of functional images, co-registration with the structural scan, spatial normalization into standard MNI space and smoothing by a Gaussian filter (FWHM = 8 mm). Using general linear model regression with factors time-locked to task events and convolved with a canonical hemodynamic response function, the regression coefficient (*b*-value) for each voxel was determined. There were 12 regressors in the task design: four modelling conditions of anticipation (anticipation win large £2, anticipation win small 20p, anticipation lose £2 and anticipation neutral), seven modelling feedback conditions (neutral feedback following anticipation neutral and successful or unsuccessful response feedback for the remaining six anticipation conditions) and one regressor modelling response activity for all four anticipation conditions. Within-group maps were created for salience condition by combining anticipation of all win and loss conditions and contrasting with neutral anticipation. Between-group contrasts were created comparing HC with CHR-PLB (HC-vs-CHR-PLB) and CHR-PLB with CHR-CBD (CHR-PLB-vs-CHR-CBD).

Two region-of-interest (ROI) analyses were performed using masks created for the SN and combined hippocampus-midbrain–striatum (HMS). The SN mask was created using the Pick Atlas in SPM8 by selecting human bilateral ACC and insulae. The HMS mask was defined by a previous study of CHR[7] and consisted of bilateral medial hippocampi, subicula, caudate, putamen, pallidum and midbrain. Exploratory whole-brain analysis was also conducted.

To test the hypothesis that activation in CHR-CBD would be intermediate between that of HC and CHR-PLB, we examined whether a linear relationship in brain activation (CHR-PLB > CHR-CBD > HC) existed within the ROI's and at whole-brain level by three-way ANOVA. We applied a family-wise error corrected (FWE) $p < 0.05$ threshold, corrected for volume for all analyses.

Behavioural performance

Behavioural performance was analysed for the two between-group contrasts of interest (HC-vs-CHR-PLB and CHR-PLB-vs-CHR-CBD), including five components: mean monetary reward (£GBP), accuracy (percentage response on target), reaction time (ms), false-starts (premature action initiation) and any trial responses (attention, percentage).

Pairwise independent *t*-testing was applied for mean monetary reward, pairwise ANOVA for mean reaction time, and pairwise binary logistic regression for accuracy, false-starts, delayed reaction and any trial response.

We tested for correlation between activation and behavioural performance (RT) and psychotic symptoms using the mean *b*-value for ANOVA-derived clusters.

Results

There was no significant difference between HC ($n = 19$), CHR-PLB ($n = 17$) and CHR-CBD ($n = 16$) in age,

gender, ethnicity, country of birth or handedness (see Table 1). There were no significant differences between CHR-PLB and CHR-CBD in either positive or negative symptom subscale of the CAARMS or in terms of current tobacco smoking and cannabis use. HC participants were selected to have minimal drug use history. In the CHR-CBD group, mean plasma CBD levels were 126.4 nM (sd 221.8) before and 823.0 nM (sd 881.5) after the fMRI scan.

Behavioural performance

Mean monetary reward: at the end of the 96 trials (2 runs of 48), the HC group appeared to win a higher cumulative total of money, though this was non-significant in pairwise analysis (Table 2).

Accuracy: There was a significant likelihood of increased accuracy in the salience condition compared to neutral in both HC-vs-CHR-PLB ($p < 0.001$) and CHR-PLB-vs-CHR-CBD ($p < 0.001$). There was a trend toward impaired accuracy in CHR-PLB compared to HC across all stimuli conditions ($p = 0.085$), but there was no interaction between salience and group. There was no significant difference between CHR-PLB and CHR-CBD or group by condition interaction.

Reaction time (see Fig. 1): RT shortened significantly in the salience condition compared to the neutral stimuli condition for both HC-vs-CHR-PLB ($p < 0.001$) and CHR-PLB-vs-CHR-CBD ($p < 0.001$). Regarding HC-vs-CHR-PLB, there was a trend-level interaction between group and condition ($p = 0.085$) such that the acceleration of response (as indexed by shorter RT) while viewing salient stimuli compared to neutral stimuli was greater in HC than in CHR-PLB. RT was significantly slower overall in CHR-CBD than CHR-PLB ($p < 0.001$).

False-starts (premature action initiation): CHR-PLB were significantly more likely to produce false-starts than HC ($p < 0.001$) and CHR-CBD at trend-level

Table 1 Sample characteristics

	HC ($n = 19$)	CHR-CBD ($n = 16$)	CHR-PLB ($n = 17$)	Pairwise analysis	
				HC-vs-CHR-PLB	CHR-PLB-vs-CHR-CBD
Age/yr (sd)	23.9 (4.15)	22.7 (5.08)	24.1 (4.48)	$p = 0.91$[a]	$p = 0.42$[a]
Ethnicity %					
White	57.9	62.5	41.2	$p = 0.59$	p = 0.43[b]
Black White	26.3	12.5	29.4		
Asian	0	0	5.9		
Mixed	15.8	25	23.5		
UK born %	57.9	68.8	82.4	$p = 0.26$[b]	$p = 0.51$[b]
Years education (sd)	17.0 (1.58)	14.5 (3.06)	11.9 (3.44)	**$P < 0.01$[a]**	$p = 0.09$[a]
Gender % (male)	57.9	62.5	41.2	$p = 0.32$[b]	$p = 0.22$[b]
UDS % (positive)	0	63	47	Not compared[c]	$p = 0.45$[b]
THC	0	13	29		
Morphine	0	6	0		
Benzodiazepine	0	0	6		
Phencyclidine	0	0	6		
Missing	0	19	12		
Current smoker % (yes)	10.5	31.3	56.3	Not compared[c]	$p = 0.14$[b]
Current cannabis use %	0	43.8	41.2	Not compared[c]	$p = 0.88$[b]
Handedness % (right)	94.7	87.5	100	$p = 0.38$[b]	$p = 0.16$[b]
CAARMS score (sd)					
Positive symptoms	NA	40.19 (20.79)	42.94 (29.46)	NA	$p = 0.75$[a]
Negative symptoms	NA	23.25 (16.49)	28.41 (10.17)	NA	$p = 0.43$[a]

HC healthy control group, *CHR-CBD* clinical-high risk cannabidiol group, *CHR-PLB* clinical-high risk placebo group, *CAARMS* comprehensive assessment of at-risk mental state
[a]Independent *t*-test
[b]Pearson chi-squared test
[c]HC were selected to have minimal drug use and hence were not compared with CHR participants on these parameters
Bold values indicates statistical significance in respective tests

Table 2 Behavioural performance

	HC	CHR-CBD	CHR-PLB	Pairwise analysis	
				HC-vs-CHR-PLB	HC-vs-CHR-PLB
Mean monetary reward £GBP (SD)	41.00 (6.63)	37.48 (12.14)	36.13 (11.97)	$p = 0.150$[a]	$p = 0.751$[a]
Accuracy (successful hits on target) %					
Overall	63.5	60.4	59.3	Group exp(B) = 1.147 (CI 0.981–1.341), $p = 0.085$[b] Condition exp(B) = 0.639 (CI 0.546–0.747), **$p < 0.001$**[b] Condition ✲ group exp(B) = 0.841 (CI 0.615–1.149), $p = 0.276$[b]	Group exp(B) = 0.985 (CI 0.837–1.159), $p = 0.855$[b] Condition exp(B) = 0.616 (CI 0.0.523–0.724), **$p < 0.001$**[b] Condition ✲ group exp(B) = 0.780 (CI 0.564–1.080), $p = 0.134$[b]
Neutral	53.9	49.2	52.7		
Salience	66.7	64.1	61.5		
Mean reaction time/ms > 100 ms (SD)					
Overall	243.13 (44.97)	251.31 (52.19)	245.70 (46.82)	Group F(1,3275) = 0.207, $p = 0.649$[c] Condition F(1,3275) = 36.60, **$p < 0.001$**[3] Condition ✲ group F(1,3275) = 2.974, $p = 0.085$[c]	Group F(1,3151) = 16.67, **$p < 0.001$**[c] Condition F(1,3151) = 51.500, **$p < 0.001$**[c] Condition ✲ group F(1,3151) = 0.000, $p = 0.992$[c]
Neutral	254.32 (49.36)	262.68 (58.60)	251.93 (52.02)		
Salience	239.69 (42.97)	248.00 (49.72)	243.79 (44.96)		
False starts %					
Overall	0.9	1.8	3.2	Group exp(B) = 4.630, (CI 2.054–10.437), **$p < 0.001$**[b] Condition exp(B) = 1.446 (CI 0.642–3.260), $p = 0.374$[b] Condition ✲ group exp(B) = 2.224 (CI 0.438–11.303), $p = 0.335$[b]	Group exp(B) = 1.678 (CI 0.970–2.902), $p = 0.064$[b] Condition exp(B) = 0.875 (CI 0.506–1.513), $p = 0.632$[b] Condition ✲ group exp(B) = 0.814 (CI 0.272–2.435), $p = 0.712$[b]
Neutral	0.5	2.2	3.2		
Salience	1.0	1.7	3.1		
Delayed response %					
Overall	33.2	32.8	35.0	Group exp(B) = 0.995, (CI 0.843–1.175), $p = 0.953$[b] Condition exp(B) = 0.733 (CI 0.621–0.866, **$p < 0.001$**[b] Condition ✲ group exp(B) = 0.816 (CI 0.585–1.139), $p = 0.232$[b]	Group exp(B) = 1.035 (CI 0.867–1.235), $p = 0.704$[b] Condition exp(B) = 0.747 (CI 0.626–0.892), **$p = 0.001$**[b] Condition ✲ group exp(B) = 0.848 (CI 0.595–1.208), $p = 0.362$[b]
Neutral	40.3	39.6	38.8		
Salience	31.0	30.8	33.9		
Trial response %					
Overall	96.8	93.0	96.6	Group exp(B) = 0.939, (CI 0.624–1.415), $p = 0.765$[b] Condition exp(B) = 7.667 (CI 5.092–11.546), **$p < 0.001$**[b] Condition ✲ group exp(B) = 0.810 (CI 0.488–2.507), $p = 0.810$[b]	Group exp(B) = 2.330 (CI 1.635–3.321), **$p < 0.001$**[b] Condition exp(B) = 5.754 (CI 4.037–8.202), **$p < 0.001$**[b] Condition ✲ group exp(B) = 0.623 (CI 0.307–1.265), $p = 0.190$[b]
Neutral	90.8	84.1	90.7		
Salience	98.8	96.0	98.6		

HC healthy control group, *CHR-CBD* clinical-high risk cannabidiol group, *CHR-PLB* clinical-high risk placebo group
[a]Independent *t*-test
[b]Pairwise binary logistic regression
[c]Analysis of variance
Bold values indicates that the result of the statistical test was significant

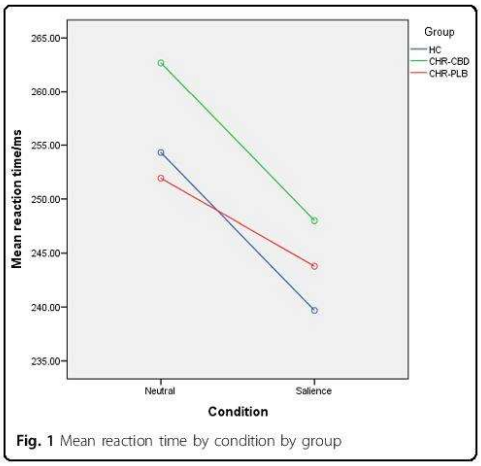

Fig. 1 Mean reaction time by condition by group

($p = 0.064$). There were no significant effects of condition or group by condition interaction in either HC-vs-CHR-PLB or CHR-PLB-vs-CHR-CBD.

Trial response: in both pairwise analyses, subjects were more likely to respond in the salience condition (HC-vs-CHR-PLB $p < 0.001$; CHR-PLB-vs-CHR-CBD $p < 0.001$). There was no difference between CHR-PLB and HC, but CHR-CBD was significantly less likely to respond than CHR-PLB ($p < 0.001$). There was no group by condition interaction in either HC-vs-CHR-PLB or CHR-PLB-vs-CHR-CBD.

Imaging

A single participant in the CBD group was excluded from imaging analysis because of inattention to all neutral trials with a subsequent lack of corresponding contrasts, such that the imaging sample sizes were 19 (HC), 15 (CHR-CBD) and 17 (CHR-PLB).

Task network (HC only)

In HC, salience condition was associated with activation in both SN and HMS masks and across the whole brain (see Supplementary Table 1).

HC-vs-CHR-PLB

Within the SN (Table 3, Fig. 2), the bilateral frontal operculae (FO; left: $k = 12$ voxels, $T = 4.77$, $p = 0.002$; right: $k = 18$ voxels, $T = 4.47$, $p = 0.006$) and the left insula converging with left parietal operculum (PO; $k = 13$ voxels, $T = 4.11$, $p = 0.019$) were significantly more active in CHR-PLB compared to HC during salient compared to neutral condition. No areas met significance threshold for HMS. At whole-brain level (Supplementary Table 2, Fig. 2), the following regions were significantly more active in CHR-PLB: the left SFG medial part ($k = 141$ voxels, $T = 6.55$, $p < 0.001$), a cluster spanning the left inferior frontal gyrus opercular part and left FO ($T = 5.47$, $p = 0.002$; $T = 5.26$, $p = 0.004$), and the left superior temporal gyrus ($k = 13$ voxels, $T = 5.06$, $p = 0.009$).

Table 3 Salience network analysis for salience-vs-neutral contrast

Region	Peak coordinate (MNI)			Cluster size	*p* value
	x	*y*	*z*		
Pairwise comparison CHR-PLB > HC					
Left frontal operculum	−42	14	12	12	0.002
Right frontal operculum	42	14	12	18	0.006
Left insula/parietal operculum	−32	−16	22	13	0.019
Pairwise comparison CHR-PLB > CHR-CBD					
Left insula/claustrum	−30	−16	20	3	0.035
Three-way ANOVA CHR-PLB > CHR-CBD > HC					
Left frontal operculum	−42	14	22	6	0.007
Left insula/parietal operculum	−32	−16	22	26	0.009

Small volume corrected, family wise error-corrected $p < 0.05$, $k \geq 3$ voxels
HC healthy control group, *CHR-CBD* clinical-high risk cannabidiol group, *CHR-PLB* clinical-high risk placebo group

CHR-PLB-vs-CHR-CBD

Within the SN (Table 3, Fig. 2), the left insula/claustrum ($k = 3$ voxels, $T = 3.98$, $p = 0.035$) was more active in CHR-PLB compared to CHR-CBD during salient relative to neutral condition. No areas met significance threshold for HMS. At whole-brain level (Supplementary Table 2, Fig. 2), the right SFG lateral part was more active in CHR-PLB ($k = 3$ voxels, $T = 4.99$, $p = 0.025$), and the right cerebellum posterior lobe was more active in CHR-CBD ($k = 6$ voxels, $T = 5.03$, $p = 0.022$).

Between-group linear analysis

ANOVA of the SN (CHR-PLB > CHR-CBD > HC; Table 3, Fig. 2) during salient relative neutral condition generated two significant peaks. The largest was located in the left insula/PO ($k = 26$ voxels, $F = 20.13$, $p = 0.009$) with the exact same peak coordinate reported in HC-vs-CHR-PLB (−32, −16, 22). The second was located in the left FO ($k = 6$ voxels, $F = 20.65$, $p = 0.007$). Mean b-values for each group confirmed increased activation in CHR-PLB compared to HC, with CHR-CBD intermediate. No areas met significance threshold for HMS. Exploratory whole-brain ANOVA (CHR-PLB > CHR-CBD > HC; Supplementary Table 2, Fig. 2), generated a significant peak in the left SFG medial part close to the HC-vs-CHR-PLB peak (−10,

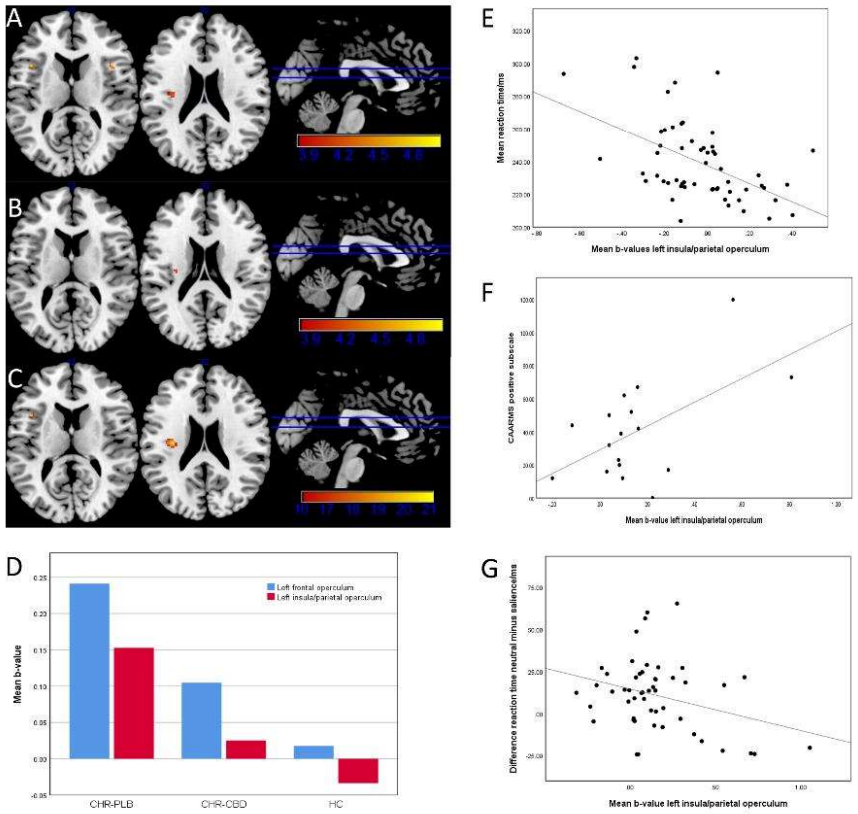

Fig. 2 Salience network region-of-interest analysis of salience>neutral contrast (small-volume corrected, $p < 0.05$ FWE-corrected at voxel level, $k \geq 3$ voxels). **a** Pairwise comparison CHR-PLB>HC with clusters in bilateral frontal operculae and left insula/parietal operculum. **b** Pairwise comparison CHR-PLB>CHR-CBD with cluster in left insula/claustrum. **c** Three-way ANOVA CHR-PLB>CHR-CBD>HC with clusters in left frontal operculum and left insula/parietal operculum. **d** Mean *b*-value parameter estimates extracted from the two clusters generated by ANOVA for each group (CHR-PLB, CHR-CBD, and HC) showing increased activation in CHR-PLB relative to HC with CHR-CBD intermediate in the left frontal operculum and left insula/parietal operculum. **e** Negative correlation between mean b-value from ANOVA-derived cluster of left insula/parietal operculum and mean reaction time for salience condition in HC. **f** Positive correlation between mean b-value from ANOVA-derived cluster of left insula/parietal operculum and CAARMS positive subscale in CHR-PLB. **g** Negative correlation between mean b-value from ANOVA-derived cluster of left insula/parietal operculum and difference in mean reaction time between neutral and salience condition in CHR-PLB

22, 58, $k = 18$ voxels, $F = 27.56$, $p = 0.006$). Mean *b*-values again confirmed increased activation in PLB relative to HC, with CBD to be intermediate.

Relationship between behavioural performance and imaging

Within the SN, there was a negative correlation with activity in the left insula/PO in HC ($r = -0.503$, $p < 0.001$, CI = −0.737 to 0.270; Fig. 2), which was absent in CHR. In CHR-PLB, there was a negative correlation between the *b*-values and mean RT difference between salience and neutral conditions ($r = -0.308$, $p = 0.028$, CI = −0.581 to −0.034; Fig. 2), which was absent in CHR-CBD. Please see Supplementary Analysis for whole brain.

Relationship between psychopathology and imaging

Within the SN, there was a positive correlation ($r = 0.569$, $p = 0.017$, CI = 0.117 to 1.022) between CAARMS positive score in CHR-PLB and left insula/PO activation (Fig. 2).

Discussion

In this study, we investigated differences in brain function and behaviour between healthy controls and CHR subjects and examined the effect of a single dose of CBD relative to placebo condition in CHR subjects while processing motivationally salient stimuli. We confirmed our primary hypothesis of abnormal activation within the salience network in CHR-PLB compared to HC, which was modulated by a single dose of CBD. Compared to HC, CHR-PLB had increased activation in the left insula/PO and bilateral FO, associated with premature action initiation. CBD appeared to attenuate activation in the proximate left insula/claustrum, associated with an overall slowing of reaction time. We also established a linear relationship in activation of the left insula/PO and left FO between CHR-PLB, CHR-CBD and HC, with activation intermediate in CHR-CBD. However, we found no differences in activation in the hippocampus-midbrain-striatum between either HC and CHR-PLB or CHR-PLB and CHR-CBD.

Shorter RT during salient compared to neutral stimuli across all groups is consistent with previous literature[43] and indicates that RT acceleration during the MIDT may be an index of salience perception. In HC, left insula/PO activity negatively correlated with RT during salient stimuli. This may indicate that insular activation is a proxy measure of salience perception and is consistent with the idea that the insula detects salient stimuli to guide behaviour[18]. Such a relationship was absent in the CHR-PLB group. In contrast, activation at this site in CHR-PLB negatively correlated with the RT acceleration during salient compared to neutral stimuli (as indexed by mean RT difference between neutral and salience conditions), indicating that the higher the insular activation, the slower was the acceleration. This may imply that greater insular activation in CHR-PLB relative to HC was associated impaired discrimination of salience in CHR patients and could be a marker of aberrant motivational salience processing. Furthermore, activation at this site positively correlated with CAARMS positive symptoms in CHR-PLB, directly linking aberrant motivational salience processing with psychopathology.

The left insula/PO site of abnormal activation is posteriorly situated and overlaps with the primary site of somatosensory interoceptive input, relaying information to the anterior insula for higher order processing[19] and switching between the default and central executive networks[44,45]. Left insula function has been implicated in both the generation of psychotic symptoms[28,29,46] and in antipsychotic treatment[28,47]. Our results extend previous literature by showing that increased activation within the SN was associated with both aberrant processing of motivationally salient stimuli and psychotic symptoms in patients in the very early stages of psychosis. A single dose of CBD attenuated activation in this region, such that it was intermediate between CHR-PLB and HC. However, CBD did not have any effect on striatal or MTL function in the present study, unlike our previous report[36]. This may reflect the different cognitive activation tasks used in the two studies, as in our previous study, we employed a verbal learning task. Here, we did not identify altered striatal or MTL function in CHR-PLB when compared to HC, and a lack of CBD effect may be a consequence. It has been suggested that while the striatum is involved in attribution of motivational salience to stimuli[1], the insula may be involved with 'proximal salience', thought to involve the evaluation of stimuli[30]. Previous studies in CHR patients did not detect any evidence of altered striatal activity[15,42], consistent with absence of altered striatal activation during the anticipation of motivationally salient stimuli in CHR-PLB relative to HC here. Whether the lack of an effect of diagnosis (CHR-PLB vs HC contrast) or treatment (CBD) on striatal function in the present study reflects a specific dysfunction in 'proximal salience', as opposed to motivational salience, and a specific CBD effect on the former, remains to be tested.

The precise molecular mechanism of action of CBD remains unclear. There is evidence that CBD may be a negative allosteric modulator at the CB1 receptor[48]. As CB1 is a presynaptic G-protein coupled inhibitory receptor, CBD could promote neurotransmitter release by inhibiting presynaptic agonism induced by retrograde endocannabinoid messengers. CBD may also enhance endocannabinoid tone by inhibiting breakdown of the CB1 agonist anandamide by fatty acid amide hydrolase[49]. In light of evidence of CB1 receptor alteration in the insula in schizophrenia[50,51], any antipsychotic effect of CBD may also be through modulation of endocannabinoid dysfunction within the insula.

Limitations

The present results should be considered in light of certain limitations. Using a within-subject, repeated measures design would have been ideal instead of the cross-sectional design that we have employed, as that would have allowed us to directly test whether CBD normalised altered insular function in CHR patients. Logistical complexities of carrying out such a study influenced our design choice. It is also worth noting that the CHR and HC groups differed in terms of years in education, current cannabis and other drug use that may have influenced brain activation differences between the two groups.

Conclusion

In summary, results presented here suggest that altered function of the insular cortex, a core component of the salience network, may underlie aberrant salience

processing and psychotic symptoms in patients at clinical high-risk of psychosis and that a single dose of CBD may attenuate some of this dysfunction. Future studies need to investigate whether such effects may underlie the antipsychotic effects of CBD observed following a period of treatment.

Acknowledgements
This study was supported by grant MR/J012149/1 (S.B., P.M.) from the Medical Research Council. S.B. was supported by NIHR Clinician Scientist Award NIHR CS-11-001 and P.A. by MRC CiC when this work was carried out. M.G.B. was supported by a Veni fellowship from the Netherlands Organisation for Scientific Research.

Author details
[1]Department of Psychosis Studies, Institute of Psychiatry, Psychology and Neuroscience, King's College London, London, UK. [2]Department of Psychiatry, Brain Center Rudolf Magnus, University Medical Center Utrecht, Utrecht, Netherlands. [3]Centre for Neuroimaging Sciences, Department of Neuroimaging, Institute of Psychiatry, Psychology, and Neuroscience, King's College London, London, UK. [4]CAMEO Early Intervention Service, Cambridgeshire and Peterborough NHS Foundation Trust, Cambridge, UK. [5]Cognition, Neuroscience and Neuroimaging (CNNI) Laboratory, Department of Psychology, University of Roehampton, London, UK

Conflict of interest
The authors declare that they have no conflict of interest.

Supplementary Information accompanies this paper at (https://doi.org/10.1038/s41398-019-0534-2).

Received: 19 March 2019 Accepted: 20 June 2019
Published online: 22 August 2019

References

1. Kapur, S. Psychosis as a state of aberrant salience: a framework linking biology, phenomenology, and pharmacology in schizophrenia. *Am. J. Psychiatry* **160**, 13–23 (2003).
2. Howes, O. D. et al. The nature of dopamine dysfunction in schizophrenia and what this means for treatment. *Arch. Gen. Psychiatry* **69**, 776–786 (2012).
3. Egerton, A. et al. Presynaptic striatal dopamine dysfunction in people at ultra-high risk for psychosis: findings in a second cohort. *Biol. Psychiatry* **74**, 106–112 (2013).
4. Howes, O. D. et al. Dopamine synthesis capacity before onset of psychosis: a prospective [18F]-DOPA PET imaging study. *Am. J. Psychiatry* **168**, 1311–1317 (2011).
5. Winton-Brown, T. T., Fusar-Poli, P., Ungless, M. A. & Howes, O. D. Dopaminergic basis of salience dysregulation in psychosis. *Trends Neurosci.* **37**, 85–94 (2014).
6. Modinos, G., Allen, P., Grace, A. A. & McGuire, P. Translating the MAM model of psychosis to humans. *Trends Neurosci.* **38**, 129–138 (2015).
7. Allen, P. et al. Resting hyperperfusion of the hippocampus, midbrain, and basal ganglia in people at high risk for psychosis. *Am. J. Psychiatry* **173**, 392–399 (2015).
8. Schobel Scott, A. et al. Imaging patients with psychosis and a mouse model establishes a spreading pattern of hippocampal dysfunction and implicates glutamate as a driver. *Neuron.* **78**, 81–93 (2013).
9. Schultz, W. Dopamine reward prediction-error signalling: a two-component response. *Nat. Rev. Neurosci.* **17**, 183–195 (2016).
10. Strauss, G. P., Waltz, J. A. & Gold, J. M. A review of reward processing and motivational impairment in schizophrenia. *Schizophr. Bull.* **40**, S107–S116 (2014).
11. Schmidt, A. et al. Longitudinal alterations in motivational salience processing in ultra-high-risk subjects for psychosis. *Psychol. Med.* **47**, 243–254 (2017).
12. Smieskova, R. et al. Modulation of motivational salience processing during the early stages of psychosis. *Schizophr. Res.* **166**, 17–23 (2015).
13. Roiser, J. P., Howes, O. D., Chaddock, C. A., Joyce, E. M. & McGuire, P. Neural and behavioral correlates of aberrant salience in individuals at risk for psychosis. *Schizophr. Bull.* **39**, 1328–1336 (2012).
14. Winton-Brown, T. et al. Altered activation and connectivity in a hippocampal-basal ganglia-midbrain circuit during salience processing in subjects at ultra high risk for psychosis. *Transl. Psychiatry* **7**, e1245 (2017).
15. Wotruba, D. et al. Symptom dimensions are associated with reward processing in unmedicated persons at risk for psychosis. *Front Behav. Neurosci.* **8**, 382 (2014).
16. Radua, J. et al. Ventral striatal activation during reward processing in psychosis: a neurofunctional meta-analysis. *JAMA psychiatry* **72**, 1243–1251 (2015).
17. Nielsen, M. Ø. et al. Alterations of the brain reward system in antipsychotic naïve schizophrenia patients. *Biol. Psychiatry* **71**, 898–905 (2012).
18. Seeley, W. W. et al. Dissociable intrinsic connectivity networks for salience processing and executive control. *J. Neurosci.* **27**, 2349–2356 (2007).
19. Uddin, L. Q. Salience processing and insular cortical function and dysfunction. *Nat. Rev. Neurosci.* **16**, 55 (2015).
20. Baiano, M. et al. Anterior cingulate volumes in schizophrenia: a systematic review and a meta-analysis of MRI studies. *Schizophr. Res.* **93**, 1–12 (2007).
21. Shepherd, A. M., Matheson, S. L., Laurens, K. R., Carr, V. J. & Green, M. J. Systematic meta-analysis of insula volume in schizophrenia. *Biol. Psychiatry* **72**, 775–784 (2012).
22. O'Neill, A., Mechelli, A. & Bhattacharyya, S. Dysconnectivity of large-scale functional networks in early psychosis: a meta-analysis. *Schizophr. Bull.* **45**, 579–590 (2018)
23. Fornito, A. et al. Anatomic abnormalities of the anterior cingulate cortex before psychosis onset: an MRI study of ultra-high-risk individuals. *Biol. Psychiatry* **64**, 758–765 (2008).
24. Takahashi, T. et al. Insular cortex gray matter changes in individuals at ultra-high-risk of developing psychosis. *Schizophr. Res.* **111**, 94–102 (2009).
25. Wang, C. et al. Disrupted salience network functional connectivity and white-matter microstructure in persons at risk for psychosis: findings from the LYRIKS study. *Psychol. Med.* **46**, 2771–2783 (2016).
26. Wotruba, D. et al. Aberrant coupling within and across the default mode, task-positive, and salience network in subjects at risk for psychosis. *Schizophr. Bull.* **40**, 1095–1104 (2014).
27. Takahashi, T. et al. Follow-up MRI study of the insular cortex in first-episode psychosis and chronic schizophrenia. *Schizophr. Res.* **108**, 49–56 (2009).
28. Walter, A. et al. Altered insular function during aberrant salience processing in relation to the severity of psychotic symptoms. *Front Psychiatry* **7**, 189 (2016).
29. Thusius, N., Romanowicz, M., Mlynek, K. & Sola, C. Prolonged psychosis associated with left insular stroke: talking to God in the walls. *Psychosomatics.* **59**, 618–621 (2018)
30. Palaniyappan, L. & Liddle, P. F. Does the salience network play a cardinal role in psychosis? An emerging hypothesis of insular dysfunction. *J. Psychiatry Neurosci.* **37**, 17–27 (2012)
31. Bhattacharyya, S. et al. Opposite effects of delta-9-tetrahydrocannabinol and cannabidiol on human brain function and psychopathology. *Neuropsychopharmacology* **35**, 764–774 (2010).
32. Englund, A. et al. Cannabidiol inhibits THC-elicited paranoid symptoms and hippocampal-dependent memory impairment. *J. Psychopharmacol.* **27**, 19–27 (2013).
33. Leweke, F. M. et al. Cannabidiol enhances anandamide signaling and alleviates psychotic symptoms of schizophrenia. *Transl. Psychiatry* **2**, e94 (2012).
34. McGuire, P. et al. Cannabidiol (CBD) as an adjunctive therapy in schizophrenia: a multicenter randomized controlled trial. *Am. J. Psychiatry* **175**, 225–231 (2018).
35. Boggs, D. L. et al. The effects of cannabidiol (CBD) on cognition and symptoms in outpatients with chronic schizophrenia a randomized placebo controlled trial. *Psychopharmacology* **235**, 1923–1932 (2018).
36. Bhattacharyya, S. et al. Effect of cannabidiol on medial temporal, midbrain, and striatal dysfunction in people at clinical high risk of psychosis: a randomized clinical trial. *JAMA Psychiatry* **75**, 1107–1117 (2018).
37. Yung, A. R. et al. Mapping the onset of psychosis: the comprehensive assessment of at-risk mental states. *Aust. N. Z. J. Psychiatry* **39**, 964–971 (2005).
38. Knutson, B., Westdorp, A., Kaiser, E. & Hommer, D. FMRI visualization of brain activity during a monetary incentive delay task. *Neuroimage* **12**, 20–27 (2000).

39. Schott, B. H. et al. Mesolimbic functional magnetic resonance imaging activations during reward anticipation correlate with reward-related ventral striatal dopamine release. *J. Neurosci.* **28**, 14311–14319 (2008).
40. Wilson, R. P. et al. The neural substrate of reward anticipation in health: a meta-analysis of fmri findings in the monetary incentive delay task. *Neuropsychol. Rev.* **28**, 496–506 (2018)
41. Nielsen, M. O. et al. Improvement of brain reward abnormalities by antipsychotic monotherapy in schizophrenia. *Arch. Gen. Psychiatry* **69**, 1195–1204 (2012).
42. Juckel, G. et al. Ventral striatal activation during reward processing in subjects with ultra-high risk for schizophrenia. *Neuropsychobiology* **66**, 50–56 (2012).
43. Mir, P. et al. Motivation and movement: the effect of monetary incentive on performance speed. *Exp. Brain Res.* **209**, 551–559 (2011).
44. Sridharan, D., Levitin, D. J. & Menon, V. A critical role for the right fronto-insular cortex in switching between central-executive and default-mode networks. *Proc. Natl Acad. Sci. USA* **105**, 12569–12574 (2008).
45. Menon, V. & Uddin, L. Q. Saliency, switching, attention and control: a network model of insula function. *Brain Struct. Funct.* **214**, 655–667 (2010).
46. Raij, T. T., Mantyla, T., Mantere, O., Kieseppa, T. & Suvisaari, J. Cortical salience network activation precedes the development of delusion severity. *Psychol. Med.* **46**, 2741–2748 (2016).
47. Radua, J. et al. Multimodal meta-analysis of structural and functional brain changes in first episode psychosis and the effects of antipsychotic medication. *Neurosci. Biobehav. Rev.* **36**, 2325–2333 (2012).
48. Laprairie, R., Bagher, A., Kelly, M. & Denovan-Wright, E. Cannabidiol is a negative allosteric modulator of the cannabinoid CB1 receptor. *Br. J. Pharmacol.* **172**, 4790–4805 (2015).
49. Bisogno, T. et al. Molecular targets for cannabidiol and its synthetic analogues: effect on vanilloid VR1 receptors and on the cellular uptake and enzymatic hydrolysis of anandamide. *Br. J. Pharmacol.* **134**, 845–852 (2001).
50. Ranganathan, M. et al. Reduced brain cannabinoid receptor availability in schizophrenia. *Biol. Psychiatry* **79**, 997–1005 (2016).
51. Ceccarini, J. et al. Increased ventral striatal CB1 receptor binding is related to negative symptoms in drug-free patients with schizophrenia. *NeuroImage* **79**, 304–312 (2013).

Chapter 5

Discussion

For the discussion, the article titles for chapters 3 and 4 are abbreviated as such:

- Chapter 3: "The neural substrate of reward anticipation in health: a meta-analysis of fMRI findings in the monetary incentive delay task" is referred to as the *MS meta-analysis*
- Chapter 4: "Cannabidiol attenuates insular dysfunction during motivational salience processing in subjects at clinical high risk for psychosis" is referred to as the *CBD study*

Summary of findings

In this thesis, we set out to determine the neural substrate of motivational salience in healthy adults using fMRI, whether motivational salience is affected in the clinic high-risk (CHR) for psychosis state and the effect of modulation by cannabidiol. In the MS meta-analysis, we established a definitive and robust map of motivational salience in healthy adults based on original group map data capturing the anticipation phase of the Monetary Incentive Delay Task (MIDT). We also established that the core salience network (SN), comprising the anterior cingulate gyrus (ACG) and insula, is fundamental to motivational salience (MS). In the experimental CBD study, we demonstrated functional differences during MS between CHR participants and matched healthy controls (HC) in the core SN. We found abnormal activation in the core SN and superior frontal gyrus (SFG) medial part in CHR subjects, and attenuation of these regions by acute administration of oral CBD associated with change in behavioural performance toward.

The MS meta-analysis

This was the first published fMRI meta-analysis exclusively using original group map data to study the MIDT and MS, and the first to report regions of both relative activation and deactivation. We have robustly shown more extensive involvement of cortical and subcortical regions than has been reported before, and we have established a fundamental role for the SN in MS. From a total of fifteen international whole-brain group maps (n=346), we have found that MS involves activity in the striatum, the SN, the central executive network (CEN), default network (DN) and the cerebellum.

The SN, DN and CEN have been labelled the 'three core neurocognitive networks', because they are intrinsically coupled and engaged during waking rest and task activity (Menon 2011). The SN is thought to detect salient events or stimuli and facilitate switching between the DN (waking rest) and the CEN (working memory, attention) (Sridharan, Levitin et al. 2008, Goulden, Khusnulina et al. 2014).The relationship between the anterior insula and dorsal ACG (dACG) lies at the core of this network (White,

Joseph et al. 2010) and has been coined the 'alerting insula and updating cingulate', whereby the anterior insula signals the presence of behaviourally relevant events to the dACG which updates attention settings (Han, Eaton et al. 2018).

Regarding the CEN, we found robust and consistent activation in the bilateral dorsolateral prefrontal cortex (PFC) and bilateral superior parietal lobule, with a mix of activation and deactivation in angular and supramarginal gyri. Regarding the DN, this has been theorised to consist of three functional subdivisions, the 'core' posterior cingulate concerned with self-referential processes, the 'medial temporal subsystem' concerned with episodic memory and contextual retrieval, and the 'dorsal medial subsystem' involved with semantic processing (Andrews-Hanna, Smallwood et al. 2014). The core posterior cingulate was consistently activated in loss and reward. However, activity in the 'medial temporal subsystem' was heterogenous, specifically in the ventromedial prefrontal cortex, parahippocampal gyri and hippocampi. Within the 'dorsal medial subsystem', the bilateral supplementary motor area (SMA) converging with dorsomedial PFC were consistently activated with heterogenous activity in the lateral temporal cortex.

We also confirmed a role for the cerebellum in MS, with heterogenous activity in both reward and loss conditions. There is increasing evidence of cerebellar involvement in reward processing. Climbing fibres (projecting from the inferior olivary nucleus of the medulla to deep cerebellar nuclei and Purkinje cells) encode prediction error signal (Ohmae and Medina 2015) and expected reward valence (Larry, Yarkoni et al. 2019), and both climbing fibres and anterior cerebellar granule cells encode reward expectation (Wagner, Kim et al. 2017, Kostadinov, Beau et al. 2019). Recently, direct projections have been found from deep cerebellar nuclei to the ventral tegmental area in mice (Carta, Chen et al. 2019) linking the cerebellum to mesostriatal projections.

Comparison of anticipation of reward and loss revealed greater relative deactivation of the left inferior frontal gyrus (IFG) orbital part in anticipation of reward- suggesting a role in valence processing. The orbital part of the IFG lies adjacent to the lateral orbital gyrus and can be considered part of the lateral orbitofrontal cortex (LOFC). The LOFC has been found to encode predicted reward value (Howard, Gottfried et al. 2015), reward value on consummation (Sescousse, Redouté et al. 2010), and is involved in decisions based on reward value and probability (Rogers, Owen et al. 1999). It has also been reported that the LOFC is active on presentation of novel stimuli encoding reward, yet suppressed on repeated presentation of the same stimulus, thereby encoding a representation of that stimulus (Klein-Flügge, Barron et al. 2013). Our findings concur with suppression on repeated presentation, but extend our understanding, because the degree of relative deactivation appears to encode reward or loss.

A second significant peak was identified in the left ACG (though beneath publication threshold) showing overall activation, relatively greater in anticipation of reward than loss. The dACG is sensitive to change in reward valence (Bush, Vogt et al. 2002), has a role in performance monitoring (Holroyd, Nieuwenhuis et al. 2004), enhancing attention to task relevant stimuli (Weissman, Gopalakrishnan et al. 2004) and optimising cognitive performance dependent on predicted demand informed by previous behaviour (Sheth, Mian et al. 2012). Recently it has been shown that the dACG may compare past positive and negative rewards representing predicted reward (Wittmann, Kolling et al. 2016). The dual roles of reward processing and modulation of cognition have been united in the 'expected value of control (EVC) theory', whereby dACG evaluates expected future benefits from given cost of control intensity and is involved in downstream control allocation and behaviour (Shenhav, Cohen et al. 2016). Our findings support the reported sensitivity of the dACG to valence in the context of MS, which may in turn coordinate attentional resources and facilitate switching from the DN to CEN.

The inferior frontal gyri are also critical in response inhibition, a core component of the CEN and the reward anticipation phase of the MIDT when waiting for the target to present. There is a body of evidence for the role of the IFG in response inhibition. It has been hypothesised that the right IFG applies a brake to motor response which may be influenced by salience (Aron, Robbins et al. 2014). There is also neuropsychological evidence of a specific role for the left IFG, as lesions have been shown to impair response inhibition in the Go/No go task (Swick, Ashley et al. 2008).

In summary, during MS, the dACG is relatively activated and the LOFC relatively deactivated. This may represent a dACG-LOFC axis encoding learned reward valence. During anticipation of reward, dACG activation and LOFC deactivation are more significant than during anticipation of loss. Could greater dACG activation coordinate suppression in the LOFC associated with differential motor response inhibition?

Finally, as discussed in the addendum to Chapter 3, we demonstrated evidence of bias and type II error in the literature reporting reward anticipation in the MIDT which could extend to all published fMRI coordinate-based meta-analyses (CBMA). We therefore propose that methodological consideration be given to prioritising image-based meta-analyses (IBMA) in future to avoid 'missing the big picture'.

The CBD study

In this double-blind randomised placebo-controlled parallel-arm study, thirty-three antipsychotic-naïve CHR subjects ingested either 600mg oral cannabidiol (CHR-CBD) or placebo (CHR-PLB) and

underwent the MIDT during fMRI. Nineteen age and sex-matched healthy adults were recruited as controls. During analysis, the anticipation conditions of reward and loss were combined to create a condition of motivational salience. Results were analysed at exploratory whole-brain level and within hypothesis-driven a priori regions-of-interest (ROI) using masks encompassing: 1) hippocampus-midbrain-striatum, and 2) core SN (bilateral ACG and insulae). Two pair-wise comparisons were analysed between i) HC and CHR-PLB and ii) CHR-PLB and CHR-CBD. A linear relationship between the three groups was investigated by 3-way ANOVA. Correlations with behavioural performance were restricted to ANOVA-generated clusters. Significant differences in all tests were identified in the core SN and at whole-brain level but were notably absent in the hippocampus-midbrain-striatum.

Within the core SN, compared to HC, CHR-PLB subjects demonstrated increased activity in the bilateral frontal operculae (FO) and left insula/parietal operculum (Ins/PO). In the whole-brain analysis, CHR-PLB exhibited increased activation in the left superior frontal gyrus (SFG) medial part, left IFG/FO and left superior temporal/supramarginal gyri.

Compared to CHR-CBD, left Ins/PO activation was again increased in CHR-PLB. At the whole-brain level, CHR-PLB had relatively increased activity in the right SFG lateral part and decreased activity in the right cerebellum posterior lobe.

A linear relationship was present between the three groups in the core SN and whole-brain levels, but not in the hippocampus-midbrain-striatum. Two clusters located in the left FO and left Ins/PO were significant within the core SN and one cluster in the left SFG medial part at whole-brain level. Surprisingly, we did not find any differences between the three groups in the ACG, given the solid body of evidence for pathology in psychotic disorders. In all three clusters, activation was greatest in CHR-PLB, least in HC, with CHR-CBD intermediate, suggesting that abnormal hyperactivity in CHR-PLB was attenuated by CBD.

In the HC group, there was a negative correlation between left Ins/PO activation and reaction time in the salience condition, directly implicating this area in the detection of salience and preparation of a motor response. Furthermore, in the CHR-PLB group, left Ins/PO activation correlated positively with positive psychotic symptoms and negatively with mean difference in reaction time, linking abnormal psychopathology and impaired salience detection with hyperactivation in the same area of insular cortex.

The insula is a region of cortex folded within the lateral sulcus bordering the frontal, temporal and parietal lobes. The areas of cortex covering and confluent with the insula are known as the frontal, temporal or parietal operculae (Latin for ‘little lid’) respectively. The insula is considered an integration

hub of sensorimotor, visceral, interoceptive, cognitive and emotional information processing (Gogolla 2017, Uddin, Nomi et al. 2017). Structural connectivity has shown extensive connections to cortical areas including frontal, parietal, temporal cortices and cingulate cortex (Ghaziri, Tucholka et al. 2017). Resting state functional connectivity suggests two regionally defined patterns of connectivity moving from anterior to posterior insula on a continuum (Tian and Zalesky 2018). The anterior insula has a pattern of connectivity to the ACG, middle frontal, inferior frontal, temporoparietal cortex and cerebellum, whereas the posterior pattern connects to posterior cingulate, sensorimotor and premotor cortex, SMA, temporal and occipital cortex (Cauda, D'Agata et al. 2011, Cauda, Costa et al. 2012).

Insula function within the salience network during task performance is typically considered to be lateralised to the right side, specifically to the right anterior insula (Cauda, Costa et al. 2012). However, we have found that differences between CHR-PLB and HC are predominantly lateralised to the left insula with associated activation of left SMA, inferior frontal and temporoparietal cortex. This could reflect abnormal activation of the DN during motivational salience in CHR subjects. It has been reported that functional connectivity is altered between the three core neurocognitive networks in schizophrenia (Manoliu, Riedl et al. 2013), and that dysconnectivity between the SN and DN may be a core deficit of early psychosis (O'Neill, Mechelli et al. 2018). Contralaterally, reduced functional connectivity between the midbrain and right insula has also been reported during reward consummation in psychosis (Gradin, Waiter et al. 2013).

Administration of CBD attenuated the hyperactivation observed in the left Ins/PO of CHR associated with reduced activation of the right dorsolateral PFC and increased activation in the right cerebellum. This suggests modulation of connectivity by CBD in the insula, an effect previously reported in other brain areas during attentional salience (Bhattacharyya, Falkenberg et al. 2014). The dorsolateral PFC is part of the CEN and is known to exhibit dysfunction in schizophrenia (Lewis, Hashimoto et al. 2005). It has been reported that the dorsolateral PFC exerts an inhibitory influence on the anterior insula which in turn exerts an excitatory influence on the dorsolateral PFC forming a feedback loop between the SN and CEN which is diminished in schizophrenia (Palaniyappan, Simmonite et al. 2013).

The cerebellum also falls within the anterior insula connectivity pattern. Cerebellar motor dysfunction has long been recognised in psychosis, but the role the cerebellum plays is relatively under-investigated compared to regions such as the striatum (Bernard and Mittal 2014). The MS meta-analysis confirmed cerebellar involvement in MS in health, and the CBD study has shown an effect of CBD on cerebellar activity in CHR. Furthermore, CB1 density is high in the cerebellum, including on climbing fibres (Hu and Mackie 2015) which are implicated in reward processing.

CBD also attenuated hyperactivation of the left SMA, a region high in CB1 density (Hu and Mackie 2015). Activation in this cluster positively correlated with reaction time in the salience condition, suggesting that attenuation of this region improved reaction time, despite the overall main effect of CBD slowing reaction times. The SMA is considered part of the DN and has also been linked to reward expectancy (Campos, Breznen et al. 2005). The SMA has been linked to motor readiness (Chen, Scangos et al. 2010), timing of motor response (Mita, Mushiake et al. 2009), behavioural response selection and inhibition (Simmonds, Pekar et al. 2008), motor planning, execution and sequence processing (Cona and Semenza 2017). CHR-PLB generated more premature motor responses (false-starts) than both HC and CHR-CBD (trend level). Therefore, hyperactivation of the SMA in CHR may be involved in impaired timing or response inhibition leading to premature motor response in CHR, improved on administration of CBD.

What does this tell us about the role of motivational salience in early psychosis? It is important to recall that the CHR state is not an established disorder, but a clinically heterogenous group of help-seeking young adults experiencing mild symptoms akin to schizophrenia. As previously discussed, it could be that attenuated or brief limited psychotic symptoms may be representative of the severity of other non-psychotic disorders, especially in the young. In addition, the HC group were selected on the basis of low rates of substance use, and it is feasible that the differences that we have observed could be attributed to higher rates of substance use.

It is important to consider that other neurotransmitter systems have also been implicated in motivational salience using the same paradigm of drug intervention during MIDT and fMRI. Most pertinent to psychosis is dopamine and the antipsychotic class of drugs. All antipsychotics share the pharmacodynamic property of D2R antagonism. 'Typical' first-generation antipsychotics primarily exert effects via potent dopaminergic antagonism and are more associated with extrapyramidal side effects, whereas 'atypical' second-generation antipsychotics target additional neurotransmitter systems such as serotonin and noradrenaline with fewer extrapyramidal side effects. Olanzapine (an atypical) has been shown to attenuate VS activation in healthy controls (Abler, Erk et al. 2007). However, VS hypoactivation is recognised during motivational salience in patients with schizophrenia (Radua, Schmidt et al. 2015). Atypical antipsychotics appear to both enhance VS activation compared to typicals (Juckel, Schlagenhauf et al. 2006, Schlagenhauf, Juckel et al. 2008) and normalise (Simon, Biller et al. 2010, Nielsen, Rostrup et al. 2012). This action may be related to activity in alternative neurotransmitter systems to dopamine, and in fact both the serotonin/noradrenaline reuptake inhibitor duloxetine and noradrenaline/dopamine reuptake inhibitor bupropion have been shown to increase VS activation in healthy controls (Ossewaarde, Verkes et al. 2011, Ikeda, Funayama et al.

2019). The theme of variation in striatal activation is common to these studies, however we found no difference in striatal activation on CBD administration.

Therefore, we cannot draw any specific conclusion about the underlying aetiology of primary psychotic disorders, though we can offer insights into the relationship between symptoms and motivational salience. In the same vein, we cannot infer that CBD may prevent the onset of a psychotic disorder, but it may potentially alleviate symptoms. We can confirm that the endocannabinoid system is involved in motivational salience and that CBD may have therapeutic properties in improving motivational salience in CHR.

Limitations and methodological considerations

The fMRI/cognitive task paradigm

The main limitation of fMRI is a lack of understanding the mechanism of neurovascular coupling and the haemodynamic response, which itself varies across the cortex. On average, in $1mm^3$ of cortex, there are up to 30,000 neurons, probably slightly more glial cells, 10^9 synapses, 4km of axon and 0.4km of dendrites (Logothetis 2008, von Bartheld, Bahney et al. 2016). Thus each fMRI voxel represents a highly complex population of cells and connections. The haemodynamic response is likely a function of net excitation/inhibition in local excitatory-inhibitory micro-networks of neurons (Logothetis 2008). The relationship between neuronal activity, neurovascular coupling, haemodynamics and the BOLD signal have been described by a generative model, though this is beyond the scope of this thesis (Havlicek, Roebroeck et al. 2015).

Contrasting within-task conditions is based on the assumption that brain function consists of discrete cognitive processes, and that subtracting one condition from another, such as subtracting anticipation neutral from anticipation win, equates to the removal of discrete cognitive processes of interest. Furthermore, in fMRI, contrasting conditions relies on the idea of 'pure insertion', that such cognitive function evokes unique brain activity which is independent of other cognitive functions and activity in the brain. However, the brain is a non-linear system and this assumption has been experimentally challenged and critiqued (Friston, Price et al. 1996).

MS meta-analysis

We did not register the protocol for the meta-analysis in advance, for example with the National Institute for Health Research (NIHR) International Prospective Register of Systematic Reviews

(PROSPERO- https://www.crd.york.ac.uk/prospero/). There were also only enough resources for a single-rater for study selection, increasing risk of selection bias. Due to the extensive findings, we introduced the extremely conservative 'z5' concept as a post-hoc threshold borrowed from other scientific disciplines. This post-hoc analysis introduced a risk of confirmation bias during interpretation and an increased type II error, although all results at the original threshold are published in the supplementary material. Therefore, the main function of our maps will be to provide guidance for exploration of the role of more refined areas the brain in the context of motivational salience. To that effect, we have generated a number of masks available for use as "data-based ROI's" in future analysis.

There were insufficient data for analysis of behavioural performance and highly variable parameters in image acquisition and analysis preventing any meaningful regression analyses and identification of confounding variables. It's also important to recognise we analysed secondary 'monetary' reward, and the anticipation conditions of the MIDT are not designed to capture other important elements of reward processing such as prediction error signal, consummation or learning.

Finally, the findings have been interpreted in the context of brain networks owing to the sheer number of peaks of activation, but the meta-analysis itself was a mass univariate analysis, not a multivariate analysis of functional connectivity designed to elicit network changes. This could introduce a further risk of confirmation bias.

CBD study

For fMRI, our sample sizes were small resulting in low statistical power and probable inflation of brain-behaviour correlation, particularly at whole-brain level (Cremers, Wager et al. 2017). A recent analysis of data from the Human Connectome Project demonstrated that most fMRI studies are insufficiently powered to detect reasonable effect sizes despite improvements in power over time (Poldrack, Baker et al. 2017). However, it has been argued that pharmaco-fMRI studies have detected consistent and reproducible effects in disease specific networks (Wandschneider and Koepp 2016). In the CBD study, we combined conditions of reward and loss anticipation to increase power, but this necessarily prevented investigation of valence and any differences between reward-approach behaviour and loss-avoidance behaviour.

Moreover, the use of placebo in the CHR-PLB sample introduced a major confounder when comparing with HC who were not subjected to any intervention. In the MS meta-analysis, we reported significant placebo effect in the anticipation phase of the meta-analysis (Supplementary Fig 4, Supplementary Table 8) most significant in the ventral striatum and cerebellum. To control for this in the CBD study

we could have administered placebo to the HC group or recruited a further sample of CHR subjects without placebo. However, this was not practicable, as there are ethical implications in the first instance, and adopting the second scenario would have necessarily reduced the overall CHR sample size due to recruitment limitations.

Implications for clinical practice

The MS meta-analysis shows that extensive cortical, subcortical and cerebellar regions are involved in motivational salience and reward processing, particularly the 'three core neurocognitive networks'. This provides a neurocognitive basis for investigating differences in psychiatric disorders where reward processing is involved and for pharmaco-fMRI trials of therapeutic agents.

The CBD study adds to existing literature on the complex relationship between cannabis and psychosis, suggesting a potential common neural substrate for substance use and psychosis within the salience network. Through cannabinoid modulation of motivational salience, the endocannabinoid system is implicated in psychopathology and reward processing abnormalities in psychosis.

The development of CBD as a drug is potentially ground-breaking. Traditional dopaminergic antipsychotics are associated with major side effects including loss of cortical volume (Emsley, Asmal et al. 2017), extra-pyramidal and metabolic side effects. CBD could be the first effective non-dopaminergic antipsychotic agent. In addition, the absence of findings in hippocampus-midbrain-striatum, traditionally at the core of the aetiology and treatment of psychosis, may represent a paradigm shift from mesostriatal dopamine to alternative neurotransmitter systems and cognitive networks such as the salience network.

The CBD study contributes to phase II evidence for the effectiveness of CBD as an antipsychotic. Pharmaco-fMRI studies offer the advantage of detecting effects on brain function without subjective symptom relief and with more consistent and objective data from smaller sample sizes (Wandschneider and Koepp 2016). Phase III trials principally demonstrate effectiveness, safety, side effects and comparison with other existing treatments. There are several patient groups where evidence warrants further phase III trials of CBD, particularly in early psychosis. The antipsychotic potential of CBD augurs well for the prevention and treatment of the high proportion first-episode psychosis attributable to high-potency cannabis use (Di Forti, Quattrone et al. 2019).

Future research

In relation to future studies of the MIDT, we have generated data-based masks, as opposed to hypothesis-driven region-of-interest, available for the analysis of the anticipation phase. Regarding the methodology of future imaging meta-analyses, we have introduced the concept of the 'z5' threshold borrowed from other scientific disciplines. We have contributed the evidence in the literature of bias and Type II error in neuroimaging coordinate based meta-analyses, so that the design of future imaging meta-analyses should consider image-based meta-analysis (IBMA). Feedback data from the MIDT should be subject to IBMA. Other cognitive aspects of reward processing not directly captured in this MS meta-analysis or by the standard MIDT itself, such as value encoding, reward prediction error signal and learning also need further investigation, and subsequently, the functional connectivity for each aspect should be determined.

Given the pre-eminence of striatal dopamine in theories of psychosis and reward processing, the relationship between the 'three core neurocognitive networks' and striatal dopamine deserves further scrutiny. Dopamine synthesis capacity has already been linked to functional connectivity in the salience network in healthy adults (McCutcheon, Nour et al. 2018).

There should be further investigation of the potential common neural substrate of motivational salience and psychopathology, particularly the finding of impaired salience detection associated with insular hyperactivation. Functional connectivity between the identified regions might reveal an 'aberrant salience network'. Of specific relevance, von Economo neurons are found almost exclusively in the ACG and frontoinsular cortex (Watson, Jones et al. 2006, Fajardo, Escobar et al. 2008) and density is reduced in the ACG in early onset schizophrenia (Brüne, Schöbel et al. 2010). What role might these neurons play in CHR, psychopathology and motivational salience?

The CBD study findings could be expanded by investigation of motivational salience using similar methodology in a longitudinal cohort of CHR focusing on subjects who transition to a psychotic disorder, or in a first-episode/early psychosis sample. It is also important to analyse the effect of continued treatment with CBD, in the CHR sample and others, as this is only an acute challenge.

Perhaps the most significant contribution of this thesis to future research could be as background evidence for phase III clinical trials of CBD in psychosis to determine its efficacy, safety and tolerability profile. Finally, there needs to be further research into the role of the endocannabinoid system in severe mental illness, psychopathology and reward processing. Specifically relating to CBD, its effect on endocannabinoids, the mechanism and site of action are yet to be elucidated.

Chapter 6

References

Abel, E. L. (1980). "Marijuana: The first twelve thousand years." New York. Kap. I.
Abler, B., S. Erk and H. Walter (2007). "Human reward system activation is modulated by a single dose of olanzapine in healthy subjects in an event-related, double-blind, placebo-controlled fMRI study." Psychopharmacology (Berl) **191**(3): 823-833.
Abler, B., H. Walter, S. Erk, H. Kammerer and M. Spitzer (2006). "Prediction error as a linear function of reward probability is coded in human nucleus accumbens." NeuroImage **31**(2): 790-795.
Addington, J., N. Case, M. M. Saleem, A. M. Auther, B. A. Cornblatt and K. S. Cadenhead (2014). "Substance use in clinical high risk for psychosis: a review of the literature." Early intervention in psychiatry **8**(2): 104-112.
Addington, J., D. Piskulic, L. Liu, J. Lockwood, K. S. Cadenhead, T. D. Cannon, B. A. Cornblatt, T. H. McGlashan, D. O. Perkins, L. J. Seidman, M. T. Tsuang, E. F. Walker, C. E. Bearden, D. H. Mathalon and S. W. Woods (2017). "Comorbid diagnoses for youth at clinical high risk of psychosis." Schizophrenia Research **190**: 90-95.
Adovasio, J. M., O. Soffer and B. Klima (1996). "Upper Palaeolithic fibre technology: interlaced woven finds from Pavlov I, Czech Republic, c. 26,000 years ago." Antiquity **70**(269): 526-534.
Aizpurua-Olaizola, O., U. Soydaner, E. Öztürk, D. Schibano, Y. Simsir, P. Navarro, N. Etxebarria and A. Usobiaga (2016). "Evolution of the cannabinoid and terpene content during the growth of Cannabis sativa plants from different chemotypes." Journal of natural products **79**(2): 324-331.
Ajnakina, O., A. S. David and R. M. Murray (2018). "'At risk mental state' clinics for psychosis – an idea whose time has come – and gone!" Psychological Medicine: 1-6.
Ajnakina, O., C. Morgan, C. Gayer-Anderson, S. Oduola, F. Bourque, S. Bramley, J. Williamson, J. H. MacCabe, P. Dazzan, R. M. Murray and A. S. David (2017). "Only a small proportion of patients with first episode psychosis come via prodromal services: a retrospective survey of a large UK mental health programme." BMC Psychiatry **17**(1): 308.
Allen, P., J. Luigjes, O. D. Howes, A. Egerton, K. Hirao, I. Valli, J. Kambeitz, P. Fusar-Poli, M. Broome and P. McGuire (2012). "Transition to psychosis associated with prefrontal and subcortical dysfunction in ultra high-risk individuals." Schizophrenia bulletin **38**(6): 1268-1276.
Anderson, E. (1952). "Plants, Life and Man." Boston, MA: Little, Brown.
Andréasson, S., P. Allebeck, A. Engström and U. Rydberg (1987). "Cannabis and schizophrenia. A longitudinal study of Swedish conscripts." Lancet **2**(8574): 1483-1486.
Andrews-Hanna, J. R., J. Smallwood and R. N. Spreng (2014). "The default network and self-generated thought: component processes, dynamic control, and clinical relevance." Annals of the New York Academy of Sciences **1316**(1): 29-52.
Aron, A. R., T. W. Robbins and R. A. Poldrack (2014). "Inhibition and the right inferior frontal cortex: one decade on." Trends in Cognitive Sciences **18**(4): 177-185.
Arseneault, L., M. Cannon, R. Poulton, R. Murray, A. Caspi and T. E. Moffitt (2002). "Cannabis use in adolescence and risk for adult psychosis: longitudinal prospective study." BMJ **325**(7374): 1212-1213.
Attwell, D. and C. Iadecola (2002). "The neural basis of functional brain imaging signals." Trends Neurosci **25**(12): 621-625.
Balodis, I. M., H. Kober, P. D. Worhunsky, M. C. Stevens, G. D. Pearlson and M. N. Potenza (2012). "Diminished frontostriatal activity during processing of monetary rewards and losses in pathological gambling." Biol Psychiatry **71**(8): 749-757.
Barkus, E. J., J. Stirling, R. S. Hopkins and S. Lewis (2006). "Cannabis-induced psychosis-like experiences are associated with high schizotypy." Psychopathology **39**(4): 175-178.
Barnett, J. H., U. Werners, S. M. Secher, K. E. Hill, R. Brazil, K. Masson, D. E. Pernet, J. B. Kirkbride, G. K. Murray, E. T. Bullmore and P. B. Jones (2007). "Substance use in a population-based clinic sample of people with first-episode psychosis." Br J Psychiatry **190**: 515-520.
Barron, A., E. Søvik and J. Cornish (2010). "The Roles of Dopamine and Related Compounds in Reward-Seeking Behavior Across Animal Phyla." Frontiers in Behavioral Neuroscience **4**(163).

Bartra, O., J. T. McGuire and J. W. Kable (2013). "The valuation system: a coordinate-based meta-analysis of BOLD fMRI experiments examining neural correlates of subjective value." Neuroimage **76**: 412-427.
Beck, A., F. Schlagenhauf, T. Wüstenberg, J. Hein, T. Kienast, T. Kahnt, K. Schmack, C. Hägele, B. Knutson, A. Heinz and J. Wrase (2009). "Ventral striatal activation during reward anticipation correlates with impulsivity in alcoholics." Biol Psychiatry **66**(8): 734-742.
Bernard, J. A. and V. A. Mittal (2014). "Cerebellar-motor dysfunction in schizophrenia and psychosis-risk: the importance of regional cerebellar analysis approaches." Front Psychiatry **5**: 160.
Bhattacharyya, S., J. A. Crippa, P. Allen, R. Martin-Santos, S. Borgwardt, P. Fusar-Poli, K. Rubia, J. Kambeitz, C. O'Carroll, M. L. Seal, V. Giampietro, M. Brammer, A. W. Zuardi, Z. Atakan and P. K. McGuire (2012). "Induction of psychosis by Δ9-tetrahydrocannabinol reflects modulation of prefrontal and striatal function during attentional salience processing." Arch Gen Psychiatry **69**(1): 27-36.
Bhattacharyya, S., I. Falkenberg, R. Martin-Santos, Z. Atakan, J. A. Crippa, V. Giampietro, M. Brammer and P. McGuire (2014). "Cannabinoid Modulation of Functional Connectivity within Regions Processing Attentional Salience." Neuropsychopharmacology **40**: 1343.
Bhattacharyya, S., P. D. Morrison, P. Fusar-Poli, R. Martin-Santos, S. Borgwardt, T. Winton-Brown, C. Nosarti, C. M. O' Carroll, M. Seal, P. Allen, M. A. Mehta, J. M. Stone, N. Tunstall, V. Giampietro, S. Kapur, R. M. Murray, A. W. Zuardi, J. A. Crippa, Z. Atakan and P. K. McGuire (2010). "Opposite effects of delta-9-tetrahydrocannabinol and cannabidiol on human brain function and psychopathology." Neuropsychopharmacology **35**(3): 764-774.
Bhattacharyya, S., R. Wilson, E. Appiah-Kusi and et al. (2018). "Effect of cannabidiol on medial temporal, midbrain, and striatal dysfunction in people at clinical high risk of psychosis: A randomized clinical trial." JAMA Psychiatry.
Bloomfield, M. A., E. Mouchlianitis, C. J. Morgan, T. P. Freeman, H. V. Curran, J. P. Roiser and O. D. Howes (2016). "Salience attribution and its relationship to cannabis-induced psychotic symptoms." Psychol Med **46**(16): 3383-3395.
Bloomfield, M. A. P., C. J. A. Morgan, A. Egerton, S. Kapur, H. V. Curran and O. D. Howes (2014). "Dopaminergic Function in Cannabis Users and Its Relationship to Cannabis-Induced Psychotic Symptoms." Biological Psychiatry **75**(6): 470-478.
Bloomfield, M. A. P., C. J. A. Morgan, S. Kapur, H. V. Curran and O. D. Howes (2014). "The link between dopamine function and apathy in cannabis users: an [18F]-DOPA PET imaging study." Psychopharmacology **231**(11): 2251-2259.
Bossong, M. G., M. Antoniades, M. Azis, C. Samson, B. Quinn, I. Bonoldi, G. Modinos, J. Perez, O. D. Howes, J. M. Stone, P. Allen and P. McGuire (2019). "Association of Hippocampal Glutamate Levels With Adverse Outcomes in Individuals at Clinical High Risk for PsychosisAssociation of Hippocampal Glutamate Levels With Outcomes in People at Risk for PsychosisAssociation of Hippocampal Glutamate Levels With Outcomes in People at Risk for Psychosis." JAMA Psychiatry **76**(2): 199-207.
Bossong, M. G., M. A. Mehta, B. N. M. van Berckel, O. D. Howes, R. S. Kahn and P. R. A. Stokes (2015). "Further human evidence for striatal dopamine release induced by administration of Δ9-tetrahydrocannabinol (THC): selectivity to limbic striatum." Psychopharmacology **232**(15): 2723-2729.
Brancato, A., A. Cavallaro, G. Lavanco, F. Plescia and C. Cannizzaro (2018). "Reward-related limbic memory and stimulation of the cannabinoid system: An upgrade in value attribution?" Journal of Psychopharmacology **32**(2): 204-214.
Brüne, M., A. Schöbel, R. Karau, A. Benali, P. M. Faustmann, G. Juckel and E. Petrasch-Parwez (2010). "Von Economo neuron density in the anterior cingulate cortex is reduced in early onset schizophrenia." Acta Neuropathologica **119**(6): 771-778.
Brunette, M. F., K. T. Mueser, S. Babbin, P. Meyer-Kalos, R. Rosenheck, C. U. Correll, C. Cather, D. G. Robinson, N. R. Schooler, D. L. Penn, J. Addington, S. E. Estroff, J. Gottlieb, S. M. Glynn, P. Marcy, J. Robinson and J. M. Kane (2018). "Demographic and clinical correlates of substance use disorders in first episode psychosis." Schizophrenia Research **194**: 4-12.

Budney, A. J., J. R. Hughes, B. A. Moore and R. Vandrey (2004). "Review of the validity and significance of cannabis withdrawal syndrome." Am J Psychiatry **161**(11): 1967-1977.
Budney, A. J., R. Roffman, R. S. Stephens and D. Walker (2007). "Marijuana dependence and its treatment." Addict Sci Clin Pract **4**(1): 4-16.
Bush, G., B. A. Vogt, J. Holmes, A. M. Dale, D. Greve, M. A. Jenike and B. R. Rosen (2002). "Dorsal anterior cingulate cortex: a role in reward-based decision making." Proceedings of the National Academy of Sciences **99**(1): 523-528.
Bustamante, J. C., A. Barros-Loscertales, V. Costumero, P. Fuentes-Claramonte, P. Rosell-Negre, N. Ventura-Campos, J. J. Llopis and C. Avila (2014). "Abstinence duration modulates striatal functioning during monetary reward processing in cocaine patients." Addict Biol **19**(5): 885-894.
Callaghan, R. C., J. K. Cunningham, P. Allebeck, T. Arenovich, G. Sajeev, G. Remington, I. Boileau and S. J. Kish (2012). "Methamphetamine use and schizophrenia: A population-based cohort study in California." American Journal of Psychiatry **169**(4): 389-396.
Campos, M., B. Breznen, K. Bernheim and R. Andersen (2005). "Supplementary motor area encodes reward expectancy in eye-movement tasks." Journal of neurophysiology **94**(2): 1325-1335.
Cannon, T. D., Y. Chung, G. He, D. Sun, A. Jacobson, T. G. van Erp, S. McEwen, J. Addington, C. E. Bearden, K. Cadenhead, B. Cornblatt, D. H. Mathalon, T. McGlashan, D. Perkins, C. Jeffries, L. J. Seidman, M. Tsuang, E. Walker, S. W. Woods and R. Heinssen (2015). "Progressive reduction in cortical thickness as psychosis develops: a multisite longitudinal neuroimaging study of youth at elevated clinical risk." Biol Psychiatry **77**(2): 147-157.
Cantwell, R., J. Brewin, C. Glazebrook, T. Dalkin, R. Fox, I. Medley and G. Harrison (1999). "Prevalence of substance misuse in first-episode psychosis." Br J Psychiatry **174**: 150-153.
Carod-Artal, F. (2013). "Psychoactive plants in ancient Greece."
Carta, I., C. H. Chen, A. L. Schott, S. Dorizan and K. Khodakhah (2019). "Cerebellar modulation of the reward circuitry and social behavior." Science **363**(6424): eaav0581.
Cascini, F., C. Aiello and G. Di Tanna (2012). "Increasing delta-9-tetrahydrocannabinol (Δ-9-THC) content in herbal cannabis over time: systematic review and meta-analysis." Current drug abuse reviews **5**(1): 32-40.
Caspi, A., T. E. Moffitt, M. Cannon, J. McClay, R. Murray, H. Harrington, A. Taylor, L. Arseneault, B. Williams, A. Braithwaite, R. Poulton and I. W. Craig (2005). "Moderation of the effect of adolescent-onset cannabis use on adult psychosis by a functional polymorphism in the catechol-O-methyltransferase gene: longitudinal evidence of a gene X environment interaction." Biol Psychiatry **57**(10): 1117-1127.
Cauda, F., T. Costa, D. M. Torta, K. Sacco, F. D'Agata, S. Duca, G. Geminiani, P. T. Fox and A. Vercelli (2012). "Meta-analytic clustering of the insular cortex: characterizing the meta-analytic connectivity of the insula when involved in active tasks." Neuroimage **62**(1): 343-355.
Cauda, F., F. D'Agata, K. Sacco, S. Duca, G. Geminiani and A. Vercelli (2011). "Functional connectivity of the insula in the resting brain." NeuroImage **55**(1): 8-23.
Ceccarini, J., M. De Hert, R. Van Winkel, J. Peuskens, G. Bormans, L. Kranaster, F. Enning, D. Koethe, F. M. Leweke and K. Van Laere (2013). "Increased ventral striatal CB1 receptor binding is related to negative symptoms in drug-free patients with schizophrenia." NeuroImage **79**: 304-312.
Chen, C. H., J. Suckling, B. R. Lennox, C. Ooi and E. T. Bullmore (2011). "A quantitative meta-analysis of fMRI studies in bipolar disorder." Bipolar disorders **13**(1): 1-15.
Chen, X., K. W. Scangos and V. Stuphorn (2010). "Supplementary motor area exerts proactive and reactive control of arm movements." Journal of Neuroscience **30**(44): 14657-14675.
Choi, J. S., Y. C. Shin, W. H. Jung, J. H. Jang, D. H. Kang, C. H. Choi, S. W. Choi, J. Y. Lee, J. Y. Hwang and J. S. Kwon (2012). "Altered brain activity during reward anticipation in pathological gambling and obsessive-compulsive disorder." PLoS One **7**(9): e45938.
Chong, H. Y., S. L. Teoh, D. B.-C. Wu, S. Kotirum, C.-F. Chiou and N. Chaiyakunapruk (2016). "Global economic burden of schizophrenia: a systematic review." Neuropsychiatric disease and treatment **12**: 357-373.

Colizzi, M. and S. Bhattacharyya (2018). "Cannabis use and the development of tolerance: a systematic review of human evidence." Neuroscience & Biobehavioral Reviews **93**: 1-25.
Colizzi, M., E. Carra, S. Fraietta, J. Lally, D. Quattrone, S. Bonaccorso, V. Mondelli, O. Ajnakina, P. Dazzan, A. Trotta, L. Sideli, A. Kolliakou, F. Gaughran, M. Khondoker, A. S. David, R. M. Murray, J. H. MacCabe and M. Di Forti (2016). "Substance use, medication adherence and outcome one year following a first episode of psychosis." Schizophrenia Research **170**(2): 311-317.
Colizzi, M., P. McGuire, V. Giampietro, S. Williams, M. Brammer and S. Bhattacharyya (2018). "Previous cannabis exposure modulates the acute effects of delta-9-tetrahydrocannabinol on attentional salience and fear processing." Experimental and clinical psychopharmacology.
Colizzi, M., P. McGuire, R. G. Pertwee and S. Bhattacharyya (2016). "Effect of cannabis on glutamate signalling in the brain: A systematic review of human and animal evidence." Neuroscience & Biobehavioral Reviews **64**: 359-381.
Cona, G. and C. Semenza (2017). "Supplementary motor area as key structure for domain-general sequence processing: A unified account." Neuroscience & Biobehavioral Reviews **72**: 28-42.
Correll, C. U., B. Galling, A. Pawar, A. Krivko, C. Bonetto, M. Ruggeri, T. J. Craig, M. Nordentoft, V. H. Srihari, S. Guloksuz, C. L. M. Hui, E. Y. H. Chen, M. Valencia, F. Juarez, D. G. Robinson, N. R. Schooler, M. F. Brunette, K. T. Mueser, R. A. Rosenheck, P. Marcy, J. Addington, S. E. Estroff, J. Robinson, D. Penn, J. B. Severe and J. M. Kane (2018). "Comparison of Early Intervention Services vs Treatment as Usual for Early-Phase Psychosis: A Systematic Review, Meta-analysis, and Meta-regression." JAMA Psychiatry **75**(6): 555-565.
Costumero, V., A. Barros-Loscertales, J. C. Bustamante, N. Ventura-Campos, P. Fuentes and C. Avila (2013). "Reward sensitivity modulates connectivity among reward brain areas during processing of anticipatory reward cues." Eur J Neurosci **38**(3): 2399-2407.
Cremers, H. R., T. D. Wager and T. Yarkoni (2017). "The relation between statistical power and inference in fMRI." PLoS One **12**(11): e0184923.
D'Souza, D. C., E. Perry, L. MacDougall, Y. Ammerman, T. Cooper, Y. T. Wu, G. Braley, R. Gueorguieva and J. H. Krystal (2004). "The psychotomimetic effects of intravenous delta-9-tetrahydrocannabinol in healthy individuals: implications for psychosis." Neuropsychopharmacology **29**(8): 1558-1572.
da Silva Alves, F., N. Schmitz, M. Figee, N. Abeling, G. Hasler, J. van der Meer, A. Nederveen, L. de Haan, D. Linszen and T. van Amelsvoort (2011). "Dopaminergic modulation of the human reward system: a placebo-controlled dopamine depletion fMRI study." Journal of Psychopharmacology **25**(4): 538-549.
Damiano, C. R., J. Aloi, K. Dunlap, C. J. Burrus, M. G. Mosner, R. V. Kozink, R. E. McLaurin, O. A. Mullette-Gillman, R. M. Carter, S. A. Huettel, F. J. McClernon, A. Ashley-Koch and G. S. Dichter (2014). "Association between the oxytocin receptor (OXTR) gene and mesolimbic responses to rewards." Mol Autism **5**(1): 7.
Das-Munshi, J., C.-K. Chang, R. Dutta, C. Morgan, J. Nazroo, R. Stewart and M. J. Prince (2017). "Ethnicity and excess mortality in severe mental illness: a cohort study." The Lancet Psychiatry **4**(5): 389-399.
Davies, C., A. Cipriani, J. P. Ioannidis, J. Radua, D. Stahl, U. Provenzani, P. McGuire and P. Fusar-Poli (2018). "Lack of evidence to favor specific preventive interventions in psychosis: a network meta-analysis." World Psychiatry **17**(2): 196-209.
Davies, C., D. Oliver, A. De Micheli, G. Rutigliano, I. Bonoldi, M. Cappucciati, M. Rocchetti, V. Ramella-Cravaro, P. Fusar-Poli, L. Gavaghan, P. McGuire and R. Patel (2017). "Diagnostic and Prognostic Significance of DSM-5 Attenuated Psychosis Syndrome in Services for Individuals at Ultra High Risk for Psychosis." Schizophrenia Bulletin **44**(2): 264-275.
Davies, C., Y. Paloyelis, G. Rutigliano, M. Cappucciati, A. De Micheli, V. Ramella-Cravaro, U. Provenzani, M. Antoniades, G. Modinos, D. Oliver, D. Stahl, S. Murguia, F. Zelaya, P. Allen, S. Shergill, P. Morrison, S. Williams, D. Taylor, P. McGuire and P. Fusar-Poli (2019). "Oxytocin modulates hippocampal perfusion in people at clinical high risk for psychosis." Neuropsychopharmacology.

de Greck, M., L. Scheidt, A. F. Bölter, J. Frommer, C. Ulrich, E. Stockum, B. Enzi, C. Tempelmann, T. Hoffmann and G. Northoff (2011). "Multimodal psychodynamic psychotherapy induces normalization of reward related activity in somatoform disorder." World Journal of Biological Psychiatry **12**(4): 296-308.
de Leeuw, M., R. S. Kahn and M. Vink (2015). "Fronto-striatal dysfunction during reward processing in unaffected siblings of schizophrenia patients." Schizophr Bull **41**(1): 94-103.
De Luca, M. A., V. Valentini, Z. Bimpisidis, F. Cacciapaglia, P. Caboni and G. Di Chiara (2014). "Endocannabinoid 2-Arachidonoylglycerol Self-Administration by Sprague-Dawley Rats and Stimulation of in vivo Dopamine Transmission in the Nucleus Accumbens Shell." Frontiers in Psychiatry **5**(140).
Degenhardt, L. and W. Hall (2001). "The association between psychosis and problematical drug use among Australian adults: findings from the National Survey of Mental Health and Well-Being." Psychol Med **31**(4): 659-668.
Demjaha, A., A. Egerton, R. M. Murray, S. Kapur, O. D. Howes, J. M. Stone and P. K. McGuire (2014). "Antipsychotic Treatment Resistance in Schizophrenia Associated with Elevated Glutamate Levels but Normal Dopamine Function." Biological Psychiatry **75**(5): e11-e13.
Demjaha, A., J. M. Lappin, D. Stahl, M. X. Patel, J. H. MacCabe, O. D. Howes, M. Heslin, U. A. Reininghaus, K. Donoghue, B. Lomas, M. Charalambides, A. Onyejiaka, P. Fearon, P. Jones, G. Doody, C. Morgan, P. Dazzan and R. M. Murray (2017). "Antipsychotic treatment resistance in first-episode psychosis: prevalence, subtypes and predictors." Psychological Medicine **47**(11): 1981-1989.
Demjaha, A., R. M. Murray, P. K. McGuire, S. Kapur and O. D. Howes (2012). "Dopamine synthesis capacity in patients with treatment-resistant schizophrenia." American Journal of Psychiatry **169**(11): 1203-1210.
Deshmukh, R. R. and P. L. Sharma (2012). "Stimulation of accumbens shell cannabinoid CB1 receptors by noladin ether, a putative endocannabinoid, modulates food intake and dietary selection in rats." Pharmacological Research **66**(3): 276-282.
Devane, W. A., L. Hanus, A. Breuer, R. G. Pertwee, L. A. Stevenson, G. Griffin, D. Gibson, A. Mandelbaum, A. Etinger and R. Mechoulam (1992). "Isolation and structure of a brain constituent that binds to the cannabinoid receptor." Science **258**(5090): 1946-1949.
Di Forti, M., D. Quattrone, T. P. Freeman, G. Tripoli, C. Gayer-Anderson, H. Quigley, V. Rodriguez, H. E. Jongsma, L. Ferraro, C. La Cascia, D. La Barbera, I. Tarricone, D. Berardi, A. Szöke, C. Arango, A. Tortelli, E. Velthorst, M. Bernardo, C. M. Del-Ben, P. R. Menezes, J.-P. Selten, P. B. Jones, J. B. Kirkbride, B. P. F. Rutten, L. de Haan, P. C. Sham, J. van Os, C. M. Lewis, M. Lynskey, C. Morgan, R. M. Murray, S. Amoretti, M. Arrojo, G. Baudin, S. Beards, M. Bernardo, J. Bobes, C. Bonetto, B. Cabrera, A. Carracedo, T. Charpeaud, J. Costas, D. Cristofalo, P. Cuadrado, C. M. Díaz-Caneja, A. Ferchiou, N. Franke, F. Frijda, E. García Bernardo, P. Garcia-Portilla, E. González, K. Hubbard, S. Jamain, E. Jiménez-López, M. Leboyer, G. López Montoya, E. Lorente-Rovira, C. Marcelino Loureiro, G. Marrazzo, C. Martínez, M. Matteis, E. Messchaart, M. D. Moltó, J. Nacher, M. S. Olmeda, M. Parellada, J. González Peñas, B. Pignon, M. Rapado, J.-R. Richard, J. J. Rodríguez Solano, L. Roldán Díaz, M. Ruggeri, P. A. Sáiz, E. Sánchez, J. Sanjuán, C. Sartorio, F. Schürhoff, F. Seminerio, R. Shuhama, L. Sideli, S. A. Stilo, F. Termorshuizen, S. Tosato, A.-M. Tronche, D. van Dam and E. van der Ven (2019). "The contribution of cannabis use to variation in the incidence of psychotic disorder across Europe (EU-GEI): a multicentre case-control study." The Lancet Psychiatry.
Di Marzo, V., T. Bisogno and L. De Petrocellis (2005). The Biosynthesis, Fate and Pharmacological Properties of Endocannabinoids. Cannabinoids. R. G. Pertwee. Berlin, Heidelberg, Springer Berlin Heidelberg**:** 147-185.
Díaz-Caneja, C. M., L. Pina-Camacho, A. Rodríguez-Quiroga, D. Fraguas, M. Parellada and C. Arango (2015). "Predictors of outcome in early-onset psychosis: a systematic review." Npj Schizophrenia **1**: 14005.
Diekhof, E. K., L. Kaps, P. Falkai and O. Gruber (2012). "The role of the human ventral striatum and the medial orbitofrontal cortex in the representation of reward magnitude - an activation likelihood

estimation meta-analysis of neuroimaging studies of passive reward expectancy and outcome processing." Neuropsychologia **50**(7): 1252-1266.
Docherty, J. P., D. P. Van Kammen, S. G. Siris and S. R. Marder (1978). "Stages of onset of schizophrenic psychosis." The American Journal of Psychiatry.
Dugré, J. R., A. Dumais, N. Bitar and S. Potvin (2018). "Loss anticipation and outcome during the Monetary Incentive Delay Task: a neuroimaging systematic review and meta-analysis." PeerJ **6**: e4749-e4749.
Dujourdy, L. and F. Besacier (2017). "A study of cannabis potency in France over a 25 years period (1992–2016)." Forensic Science International **272**: 72-80.
ElSohly, M. A., Z. Mehmedic, S. Foster, C. Gon, S. Chandra and J. C. Church (2016). "Changes in Cannabis Potency Over the Last 2 Decades (1995–2014): Analysis of Current Data in the United States." Biological Psychiatry **79**(7): 613-619.
Emsley, R., L. Asmal, S. du Plessis, B. Chiliza, L. Phahladira and S. Kilian (2017). "Brain volume changes over the first year of treatment in schizophrenia: relationships to antipsychotic treatment." Psychol Med **47**(12): 2187-2196.
Englund, A., P. D. Morrison, J. Nottage, D. Hague, F. Kane, S. Bonaccorso, J. M. Stone, A. Reichenberg, R. Brenneisen, D. Holt, A. Feilding, L. Walker, R. M. Murray and S. Kapur (2013). "Cannabidiol inhibits THC-elicited paranoid symptoms and hippocampal-dependent memory impairment." J Psychopharmacol **27**(1): 19-27.
Enzi, B., M. A. Edel, S. Lissek, S. Peters, R. Hoffmann, V. Nicolas, M. Tegenthoff, G. Juckel and C. Saft (2012). "Altered ventral striatal activation during reward and punishment processing in premanifest Huntington's disease: a functional magnetic resonance study." Exp Neurol **235**(1): 256-264.
Eranti, S. V., J. H. MacCabe, H. Bundy and R. M. Murray (2013). "Gender difference in age at onset of schizophrenia: a meta-analysis." Psychol Med **43**(1): 155-167.
Excellence, N. I. f. C. (2016). "Implementing the early intervention in psychosis access and waiting time standard: Guidance."
Fajardo, C., M. I. Escobar, E. Buriticá, G. Arteaga, J. Umbarila, M. F. Casanova and H. Pimienta (2008). "Von Economo neurons are present in the dorsolateral (dysgranular) prefrontal cortex of humans." Neuroscience Letters **435**(3): 215-218.
Fergusson, D. M. and J. M. Boden (2008). "Cannabis use and later life outcomes." Addiction **103**(6): 969-976; discussion 977-968.
Foglia, E., T. Schoeler, E. Klamerus, K. Morgan and S. Bhattacharyya (2017). "Cannabis use and adherence to antipsychotic medication: a systematic review and meta-analysis." Psychological medicine **47**(10): 1691-1705.
Freeman, T. and W. Swift (2016). "Cannabis potency: the need for global monitoring." Addiction **111**(2): 376-377.
Friston, K. J., C. J. Price, P. Fletcher, C. Moore, R. S. J. Frackowiak and R. J. Dolan (1996). "The Trouble with Cognitive Subtraction." NeuroImage **4**(2): 97-104.
Funayama, T., Y. Ikeda, A. Tateno, H. Takahashi, Y. Okubo, H. Fukayama and H. Suzuki (2014). "Modafinil augments brain activation associated with reward anticipation in the nucleus accumbens." Psychopharmacology (Berl) **231**(16): 3217-3228.
Gaoni, Y. and R. Mechoulam (1964). "Isolation, Structure, and Partial Synthesis of an Active Constituent of Hashish." Journal of the American Chemical Society **86**(8): 1646-1647.
Gaston, T. E. and D. Friedman (2017). "Pharmacology of cannabinoids in the treatment of epilepsy." Epilepsy & Behavior **70**: 313-318.
Gerard, C., C. Mollereau, G. Vassart and M. Parmentier (1990). "Nucleotide sequence of a human cannabinoid receptor cDNA." Nucleic acids research **18**(23): 7142.
Ghaziri, J., A. Tucholka, G. Girard, J.-C. Houde, O. Boucher, G. Gilbert, M. Descoteaux, S. Lippé, P. Rainville and D. K. Nguyen (2017). "The corticocortical structural connectivity of the human insula." Cerebral cortex **27**(2): 1216-1228.

Giuffrida, A., F. M. Leweke, C. W. Gerth, D. Schreiber, D. Koethe, J. Faulhaber, J. Klosterkötter and D. Piomelli (2004). "Cerebrospinal anandamide levels are elevated in acute schizophrenia and are inversely correlated with psychotic symptoms." Neuropsychopharmacology **29**(11): 2108-2114.
Gogolla, N. (2017). "The insular cortex." Current Biology **27**(12): R580-R586.
Goulden, N., A. Khusnulina, N. J. Davis, R. M. Bracewell, A. L. Bokde, J. P. McNulty and P. G. Mullins (2014). "The salience network is responsible for switching between the default mode network and the central executive network: Replication from DCM." NeuroImage **99**: 180-190.
Gouvêa, E. S., A. F. Santos Filho, V. K. Ota, V. Mrad, A. Gadelha, R. A. Bressan, Q. Cordeiro and S. I. Belangero (2017). "The role of the CNR1 gene in schizophrenia: a systematic review including unpublished data." Revista Brasileira de Psiquiatria **39**(2): 160-171.
Gradin, V. B., G. Waiter, A. O'Connor, L. Romaniuk, C. Stickle, K. Matthews, J. Hall and J. Douglas Steele (2013). "Salience network-midbrain dysconnectivity and blunted reward signals in schizophrenia." Psychiatry Res **211**(2): 104-111.
Hall, W. and L. Degenhardt (2007). "Prevalence and correlates of cannabis use in developed and developing countries." Current opinion in Psychiatry **20**(4): 393-397.
Han, S. W., H. P. Eaton and R. Marois (2018). "Functional Fractionation of the Cingulo-opercular Network: Alerting Insula and Updating Cingulate." Cerebral Cortex **29**(6): 2624-2638.
Harrison, B. J. and C. Pantelis (2010). Cognitive Subtraction. Encyclopedia of Psychopharmacology. I. P. Stolerman. Berlin, Heidelberg, Springer Berlin Heidelberg**:** 323-323.
Havlicek, M., A. Roebroeck, K. Friston, A. Gardumi, D. Ivanov and K. Uludag (2015). "Physiologically informed dynamic causal modeling of fMRI data." NeuroImage **122**: 355-372.
Helfand, A. I., C. M. Olsen and C. J. Hillard (2017). "Cannabinoid Receptor 1 and Fatty Acid Amide Hydrolase Contribute to Operant Sensation Seeking in Mice." Int J Mol Sci **18**(8).
Hernandez, G. and J. F. Cheer (2011). "Extinction learning of rewards in the rat: is there a role for CB1 receptors?" Psychopharmacology **217**(2): 189-197.
Hillman, E. M. C. (2014). "Coupling Mechanism and Significance of the BOLD Signal: A Status Report." Annual Review of Neuroscience **37**(1): 161-181.
Hjorthøj, C., A. E. Stürup, J. J. McGrath and M. Nordentoft (2017). "Years of potential life lost and life expectancy in schizophrenia: a systematic review and meta-analysis." The Lancet Psychiatry **4**(4): 295-301.
Holroyd, C. B., S. Nieuwenhuis, N. Yeung, L. Nystrom, R. B. Mars, M. G. H. Coles and J. D. Cohen (2004). "Dorsal anterior cingulate cortex shows fMRI response to internal and external error signals." Nature Neuroscience **7**(5): 497-498.
Horder, J., C. J. Harmer, P. J. Cowen and C. McCabe (2010). "Reduced neural response to reward following 7 days treatment with the cannabinoid CB1 antagonist rimonabant in healthy volunteers." Int J Neuropsychopharmacol **13**(8): 1103-1113.
Horton, R. (2015). "Offline: What is medicine's 5 sigma?" The Lancet **385**(9976): 1380.
Howard, J. D., J. A. Gottfried, P. N. Tobler and T. Kahnt (2015). "Identity-specific coding of future rewards in the human orbitofrontal cortex." Proceedings of the National Academy of Sciences **112**(16): 5195-5200.
Howes, O., R. McCutcheon and J. Stone (2015). "Glutamate and dopamine in schizophrenia: An update for the 21st century." Journal of Psychopharmacology **29**(2): 97-115.
Howes, O. D., S. K. Bose, F. Turkheimer, I. Valli, A. Egerton, L. R. Valmaggia, R. M. Murray and P. McGuire (2011). "Dopamine synthesis capacity before onset of psychosis: a prospective [18F]-DOPA PET imaging study." Am J Psychiatry **168**(12): 1311-1317.
Howes, O. D., A. Egerton, V. Allan, P. McGuire, P. Stokes and S. Kapur (2009). "Mechanisms underlying psychosis and antipsychotic treatment response in schizophrenia: insights from PET and SPECT imaging." Current pharmaceutical design **15**(22): 2550-2559.
Howes, O. D., J. Kambeitz, E. Kim, D. Stahl, M. Slifstein, A. Abi-Dargham and S. Kapur (2012). "The nature of dopamine dysfunction in schizophrenia and what this means for treatment." Arch Gen Psychiatry **69**(8): 776-786.

Howes, O. D., R. McCutcheon, O. Agid, A. de Bartolomeis, N. J. van Beveren, M. L. Birnbaum, M. A. Bloomfield, R. A. Bressan, R. W. Buchanan, W. T. Carpenter, D. J. Castle, L. Citrome, Z. J. Daskalakis, M. Davidson, R. J. Drake, S. Dursun, B. H. Ebdrup, H. Elkis, P. Falkai, W. W. Fleischacker, A. Gadelha, F. Gaughran, B. Y. Glenthoj, A. Graff-Guerrero, J. E. Hallak, W. G. Honer, J. Kennedy, B. J. Kinon, S. M. Lawrie, J. Lee, F. M. Leweke, J. H. MacCabe, C. B. McNabb, H. Meltzer, H. J. Moller, S. Nakajima, C. Pantelis, T. Reis Marques, G. Remington, S. L. Rossell, B. R. Russell, C. O. Siu, T. Suzuki, I. E. Sommer, D. Taylor, N. Thomas, A. Ucok, D. Umbricht, J. T. Walters, J. Kane and C. U. Correll (2017). "Treatment-Resistant Schizophrenia: Treatment Response and Resistance in Psychosis (TRRIP) Working Group Consensus Guidelines on Diagnosis and Terminology." Am J Psychiatry **174**(3): 216-229.

Hu, S. S. and K. Mackie (2015). "Distribution of the Endocannabinoid System in the Central Nervous System." Handb Exp Pharmacol **231**: 59-93.

Hunt, G. E., M. M. Large, M. Cleary, H. M. X. Lai and J. B. Saunders (2018). "Prevalence of comorbid substance use in schizophrenia spectrum disorders in community and clinical settings, 1990–2017: Systematic review and meta-analysis." Drug and Alcohol Dependence **191**: 234-258.

Iannotti, F. A., V. Di Marzo and S. Petrosino (2016). "Endocannabinoids and endocannabinoid-related mediators: targets, metabolism and role in neurological disorders." Progress in lipid research **62**: 107-128.

Iffland, K. and F. Grotenhermen (2017). "An update on safety and side effects of cannabidiol: a review of clinical data and relevant animal studies." Cannabis and Cannabinoid Research **2**(1): 139-154.

Ikeda, Y., T. Funayama, A. Tateno, H. Fukayama, Y. Okubo and H. Suzuki (2019). "Bupropion increases activation in nucleus accumbens during anticipation of monetary reward." Psychopharmacology (Berl) **236**(12): 3655-3665.

Jääskeläinen, E., P. Juola, N. Hirvonen, J. J. McGrath, S. Saha, M. Isohanni, J. Veijola and J. Miettunen (2012). "A Systematic Review and Meta-Analysis of Recovery in Schizophrenia." Schizophrenia Bulletin **39**(6): 1296-1306.

Jaffe, A. E., Y. Gao, A. Deep-Soboslay, R. Tao, T. M. Hyde, D. R. Weinberger and J. E. Kleinman (2015). "Mapping DNA methylation across development, genotype and schizophrenia in the human frontal cortex." Nature Neuroscience **19**: 40.

James, S. L., D. Abate, K. H. Abate, S. M. Abay, C. Abbafati, N. Abbasi, H. Abbastabar, F. Abd-Allah, J. Abdela, A. Abdelalim, I. Abdollahpour, R. S. Abdulkader, Z. Abebe, S. F. Abera, O. Z. Abil, H. N. Abraha, L. J. Abu-Raddad, N. M. E. Abu-Rmeileh, M. M. K. Accrombessi, D. Acharya, P. Acharya, I. N. Ackerman, A. A. Adamu, O. M. Adebayo, V. Adekanmbi, O. O. Adetokunboh, M. G. Adib, J. C. Adsuar, K. A. Afanvi, M. Afarideh, A. Afshin, G. Agarwal, K. M. Agesa, R. Aggarwal, S. A. Aghayan, S. Agrawal, A. Ahmadi, M. Ahmadi, H. Ahmadieh, M. B. Ahmed, A. N. Aichour, I. Aichour, M. T. E. Aichour, T. Akinyemiju, N. Akseer, Z. Al-Aly, A. Al-Eyadhy, H. M. Al-Mekhlafi, R. M. Al-Raddadi, F. Alahdab, K. Alam, T. Alam, A. Alashi, S. M. Alavian, K. A. Alene, M. Alijanzadeh, R. Alizadeh-Navaei, S. M. Aljunid, A. a. Alkerwi, F. Alla, P. Allebeck, M. M. L. Alouani, K. Altirkawi, N. Alvis-Guzman, A. T. Amare, L. N. Aminde, W. Ammar, Y. A. Amoako, N. H. Anber, C. L. Andrei, S. Androudi, M. D. Animut, M. Anjomshoa, M. G. Ansha, C. A. T. Antonio, P. Anwari, J. Arabloo, A. Arauz, O. Aremu, F. Ariani, B. Armoon, J. Ärnlöv, A. Arora, A. Artaman, K. K. Aryal, H. Asayesh, R. J. Asghar, Z. Ataro, S. R. Atre, M. Ausloos, L. Avila-Burgos, E. F. G. A. Avokpaho, A. Awasthi, B. P. Ayala Quintanilla, R. Ayer, P. S. Azzopardi, A. Babazadeh, H. Badali, A. Badawi, A. G. Bali, K. E. Ballesteros, S. H. Ballew, M. Banach, J. A. M. Banoub, A. Banstola, A. Barac, M. A. Barboza, S. L. Barker-Collo, T. W. Bärnighausen, L. H. Barrero, B. T. Baune, S. Bazargan-Hejazi, N. Bedi, E. Beghi, M. Behzadifar, M. Behzadifar, Y. Béjot, A. B. Belachew, Y. A. Belay, M. L. Bell, A. K. Bello, I. M. Bensenor, E. Bernabe, R. S. Bernstein, M. Beuran, T. Beyranvand, N. Bhala, S. Bhattarai, S. Bhaumik, Z. A. Bhutta, B. Biadgo, A. Bijani, B. Bikbov, V. Bilano, N. Bililign, M. S. Bin Sayeed, D. Bisanzio, B. F. Blacker, F. M. Blyth, I. R. Bou-Orm, S. Boufous, R. Bourne, O. J. Brady, M. Brainin, L. C. Brant, A. Brazinova, N. J. K. Breitborde, H. Brenner, P. S. Briant, A. M. Briggs, A. N. Briko, G. Britton, T. Brugha, R. Buchbinder, R. Busse, Z. A. Butt, L. Cahuana-Hurtado, J. Cano, R. Cárdenas, J. J. Carrero, A. Carter, F. Carvalho, C. A. Castañeda-Orjuela, J. Castillo Rivas, F. Castro, F. Catalá-López, K. M. Cercy, E. Cerin, Y. Chaiah, A. R. Chang, H.-Y. Chang, J.-C. Chang, F. J. Charlson, A. Chattopadhyay, V. K. Chattu, P.

Chaturvedi, P. P.-C. Chiang, K. L. Chin, A. Chitheer, J.-Y. J. Choi, R. Chowdhury, H. Christensen, D. J. Christopher, F. M. Cicuttini, L. G. Ciobanu, M. Cirillo, R. M. Claro, D. Collado-Mateo, C. Cooper, J. Coresh, P. A. Cortesi, M. Cortinovis, M. Costa, E. Cousin, M. H. Criqui, E. A. Cromwell, M. Cross, J. A. Crump, A. F. Dadi, L. Dandona, R. Dandona, P. I. Dargan, A. Daryani, R. Das Gupta, J. Das Neves, T. T. Dasa, G. Davey, A. C. Davis, D. V. Davitoiu, B. De Courten, F. P. De La Hoz, D. De Leo, J.-W. De Neve, M. G. Degefa, L. Degenhardt, S. Deiparine, R. P. Dellavalle, G. T. Demoz, K. Deribe, N. Dervenis, D. C. Des Jarlais, G. A. Dessie, S. Dey, S. D. Dharmaratne, M. T. Dinberu, M. A. Dirac, S. Djalalinia, L. Doan, K. Dokova, D. T. Doku, E. R. Dorsey, K. E. Doyle, T. R. Driscoll, M. Dubey, E. Dubljanin, E. E. Duken, B. B. Duncan, A. R. Duraes, H. Ebrahimi, S. Ebrahimpour, M. M. Echko, D. Edvardsson, A. Effiong, J. R. Ehrlich, C. El Bcheraoui, M. El Sayed Zaki, Z. El-Khatib, H. Elkout, I. R. F. Elyazar, A. Enayati, A. Y. Endries, B. Er, H. E. Erskine, B. Eshrati, S. Eskandarieh, A. Esteghamati, S. Esteghamati, H. Fakhim, V. Fallah Omrani, M. Faramarzi, M. Fareed, F. Farhadi, T. A. Farid, C. S. E. s. Farinha, A. Farioli, A. Faro, M. S. Farvid, F. Farzadfar, V. L. Feigin, N. Fentahun, S.-M. Fereshtehnejad, E. Fernandes, J. C. Fernandes, A. J. Ferrari, G. T. Feyissa, I. Filip, F. Fischer, C. Fitzmaurice, N. A. Foigt, K. J. Foreman, J. Fox, T. D. Frank, T. Fukumoto, N. Fullman, T. Fürst, J. M. Furtado, N. D. Futran, S. Gall, M. Ganji, F. G. Gankpe, A. L. Garcia-Basteiro, W. M. Gardner, A. K. Gebre, A. T. Gebremedhin, T. G. Gebremichael, T. F. Gelano, J. M. Geleijnse, R. Genova-Maleras, Y. C. D. Geramo, P. W. Gething, K. E. Gezae, K. Ghadiri, K. Ghasemi Falavarjani, M. Ghasemi-Kasman, M. Ghimire, R. Ghosh, A. G. Ghoshal, S. Giampaoli, P. S. Gill, T. K. Gill, I. A. Ginawi, G. Giussani, E. V. Gnedovskaya, E. M. Goldberg, S. Goli, H. Gómez-Dantés, P. N. Gona, S. V. Gopalani, T. M. Gorman, A. C. Goulart, B. N. G. Goulart, A. Grada, M. E. Grams, G. Grosso, H. C. Gugnani, Y. Guo, P. C. Gupta, R. Gupta, R. Gupta, T. Gupta, B. Gyawali, J. A. Haagsma, V. Hachinski, N. Hafezi-Nejad, H. Haghparast Bidgoli, T. B. Hagos, G. B. Hailu, A. Haj-Mirzaian, A. Haj-Mirzaian, R. R. Hamadeh, S. Hamidi, A. J. Handal, G. J. Hankey, Y. Hao, H. L. Harb, S. Harikrishnan, J. M. Haro, M. Hasan, H. Hassankhani, H. Y. Hassen, R. Havmoeller, C. N. Hawley, R. J. Hay, S. I. Hay, A. Hedayatizadeh-Omran, B. Heibati, D. Hendrie, A. Henok, C. Herteliu, S. Heydarpour, D. T. Hibstu, H. T. Hoang, H. W. Hoek, H. J. Hoffman, M. K. Hole, E. Homaie Rad, P. Hoogar, H. D. Hosgood, S. M. Hosseini, M. Hosseinzadeh, M. Hostiuc, S. Hostiuc, P. J. Hotez, D. G. Hoy, M. Hsairi, A. S. Htet, G. Hu, J. J. Huang, C. K. Huynh, K. M. Iburg, C. T. Ikeda, B. Ileanu, O. S. Ilesanmi, U. Iqbal, S. S. N. Irvani, C. M. S. Irvine, S. M. S. Islam, F. Islami, K. H. Jacobsen, L. Jahangiry, N. Jahanmehr, S. K. Jain, M. Jakovljevic, M. Javanbakht, A. U. Jayatilleke, P. Jeemon, R. P. Jha, V. Jha, J. S. Ji, C. O. Johnson, J. B. Jonas, J. J. Jozwiak, S. B. Jungari, M. Jürisson, Z. Kabir, R. Kadel, A. Kahsay, R. Kalani, T. Kanchan, M. Karami, B. Karami Matin, A. Karch, C. Karema, N. Karimi, S. M. Karimi, A. Kasaeian, D. H. Kassa, G. M. Kassa, T. D. Kassa, N. J. Kassebaum, S. V. Katikireddi, N. Kawakami, A. K. Karyani, M. M. Keighobadi, P. N. Keiyoro, L. Kemmer, G. R. Kemp, A. P. Kengne, A. Keren, Y. S. Khader, B. Khafaei, M. A. Khafaie, A. Khajavi, I. A. Khalil, E. A. Khan, M. S. Khan, M. A. Khan, Y.-H. Khang, M. Khazaei, A. T. Khoja, A. Khosravi, M. H. Khosravi, A. A. Kiadaliri, D. N. Kiirithio, C.-I. Kim, D. Kim, P. Kim, Y.-E. Kim, Y. J. Kim, R. W. Kimokoti, Y. Kinfu, A. Kisa, K. Kissimova-Skarbek, M. Kivimäki, A. K. S. Knudsen, J. M. Kocarnik, S. Kochhar, Y. Kokubo, T. Kolola, J. A. Kopec, S. Kosen, G. A. Kotsakis, P. A. Koul, A. Koyanagi, M. A. Kravchenko, K. Krishan, K. J. Krohn, B. Kuate Defo, B. Kucuk Bicer, G. A. Kumar, M. Kumar, H. H. Kyu, D. P. Lad, S. D. Lad, A. Lafranconi, R. Lalloo, T. Lallukka, F. H. Lami, V. C. Lansingh, A. Latifi, K. M.-M. Lau, J. V. Lazarus, J. L. Leasher, J. R. Ledesma, P. H. Lee, J. Leigh, J. Leung, M. Levi, S. Lewycka, S. Li, Y. Li, Y. Liao, M. L. Liben, L.-L. Lim, S. S. Lim, S. Liu, R. Lodha, K. J. Looker, A. D. Lopez, S. Lorkowski, P. A. Lotufo, N. Low, R. Lozano, T. C. D. Lucas, L. R. Lucchesi, R. Lunevicius, R. A. Lyons, S. Ma, E. R. K. Macarayan, M. T. Mackay, F. Madotto, H. Magdy Abd El Razek, M. Magdy Abd El Razek, D. P. Maghavani, N. B. Mahotra, H. T. Mai, M. Majdan, R. Majdzadeh, A. Majeed, R. Malekzadeh, D. C. Malta, A. A. Mamun, A.-L. Manda, H. Manguerra, T. Manhertz, M. A. Mansournia, L. G. Mantovani, C. C. Mapoma, J. C. Maravilla, W. Marcenes, A. Marks, F. R. Martins-Melo, I. Martopullo, W. März, M. B. Marzan, T. P. Mashamba-Thompson, B. B. Massenburg, M. R. Mathur, K. Matsushita, P. K. Maulik, M. Mazidi, C. McAlinden, J. J. McGrath, M. McKee, M. M. Mehndiratta, R. Mehrotra, K. M. Mehta, V. Mehta, F. Mejia-Rodriguez, T. Mekonen, A. Melese, M. Melku, M. Meltzer, P. T. N. Memiah, Z. A. Memish, W. Mendoza, D. T. Mengistu, G. Mengistu, G. A. Mensah, S. T. Mereta, A. Meretoja, T. J. Meretoja, T. Mestrovic, N. M. G. Mezerji, B.

Miazgowski, T. Miazgowski, A. I. Millear, T. R. Miller, B. Miltz, G. K. Mini, M. Mirarefin, E. M. Mirrakhimov, A. T. Misganaw, P. B. Mitchell, H. Mitiku, B. Moazen, B. Mohajer, K. A. Mohammad, N. Mohammadifard, M. Mohammadnia-Afrouzi, M. A. Mohammed, S. Mohammed, F. Mohebi, M. Moitra, A. H. Mokdad, M. Molokhia, L. Monasta, Y. Moodley, M. Moosazadeh, G. Moradi, M. Moradi-Lakeh, M. Moradinazar, P. Moraga, L. Morawska, I. Moreno Velásquez, J. Morgado-Da-Costa, S. D. Morrison, M. M. Moschos, S. M. Mousavi, K. B. Mruts, A. A. Muche, K. F. Muchie, U. O. Mueller, O. S. Muhammed, S. Mukhopadhyay, K. Muller, J. E. Mumford, M. Murhekar, J. Musa, K. I. Musa, G. Mustafa, A. F. Nabhan, C. Nagata, M. Naghavi, A. Naheed, A. Nahvijou, G. Naik, N. Naik, F. Najafi, L. Naldi, H. S. Nam, V. Nangia, J. R. Nansseu, B. R. Nascimento, G. Natarajan, N. Neamati, I. Negoi, R. I. Negoi, S. Neupane, C. R. J. Newton, J. W. Ngunjiri, A. Q. Nguyen, H. T. Nguyen, H. L. T. Nguyen, H. T. Nguyen, L. H. Nguyen, M. Nguyen, N. B. Nguyen, S. H. Nguyen, E. Nichols, D. N. A. Ningrum, M. R. Nixon, N. Nolutshungu, S. Nomura, O. F. Norheim, M. Noroozi, B. Norrving, J. J. Noubiap, H. R. Nouri, M. Nourollahpour Shiadeh, M. R. Nowroozi, E. O. Nsoesie, P. S. Nyasulu, C. M. Odell, R. Ofori-Asenso, F. A. Ogbo, I.-H. Oh, O. Oladimeji, A. T. Olagunju, T. O. Olagunju, P. R. Olivares, H. E. Olsen, B. O. Olusanya, K. L. Ong, S. K. Ong, E. Oren, A. Ortiz, E. Ota, S. S. Otstavnov, S. Øverland, M. O. Owolabi, M. P A, R. Pacella, A. H. Pakpour, A. Pana, S. Panda-Jonas, A. Parisi, E.-K. Park, C. D. H. Parry, S. Patel, S. Pati, S. T. Patil, A. Patle, G. C. Patton, V. R. Paturi, K. R. Paulson, N. Pearce, D. M. Pereira, N. Perico, K. Pesudovs, H. Q. Pham, M. R. Phillips, D. M. Pigott, J. D. Pillay, M. A. Piradov, M. Pirsaheb, F. Pishgar, O. Plana-Ripoll, D. Plass, S. Polinder, S. Popova, M. J. Postma, A. Pourshams, H. Poustchi, D. Prabhakaran, S. Prakash, V. Prakash, C. A. Purcell, M. B. Purwar, M. Qorbani, D. A. Quistberg, A. Radfar, A. Rafay, A. Rafiei, F. Rahim, K. Rahimi, A. Rahimi-Movaghar, V. Rahimi-Movaghar, M. Rahman, M. H. u. Rahman, M. A. Rahman, S. U. Rahman, R. K. Rai, F. Rajati, U. Ram, P. Ranjan, A. Ranta, P. C. Rao, D. L. Rawaf, S. Rawaf, K. S. Reddy, R. C. Reiner, N. Reinig, M. B. Reitsma, G. Remuzzi, A. M. N. Renzaho, S. Resnikoff, S. Rezaei, M. S. Rezai, A. L. P. Ribeiro, S. R. Robinson, L. Roever, L. Ronfani, G. Roshandel, A. Rostami, G. A. Roth, A. Roy, E. Rubagotti, P. S. Sachdev, N. Sadat, B. Saddik, E. Sadeghi, S. Saeedi Moghaddam, H. Safari, Y. Safari, R. Safari-Faramani, M. Safdarian, S. Safi, S. Safiri, R. Sagar, A. Sahebkar, M. A. Sahraian, H. S. Sajadi, N. Salam, J. S. Salama, P. Salamati, K. Saleem, Z. Saleem, Y. Salimi, J. A. Salomon, S. S. Salvi, I. Salz, A. M. Samy, J. Sanabria, Y. Sang, D. F. Santomauro, I. S. Santos, J. V. Santos, M. M. Santric Milicevic, B. P. Sao Jose, M. Sardana, A. R. Sarker, N. Sarrafzadegan, B. Sartorius, S. Sarvi, B. Sathian, M. Satpathy, A. R. Sawant, M. Sawhney, S. Saxena, M. Saylan, E. Schaeffner, M. I. Schmidt, I. J. C. Schneider, B. Schöttker, D. C. Schwebel, F. Schwendicke, J. G. Scott, M. Sekerija, S. G. Sepanlou, E. Serván-Mori, S. Seyedmousavi, H. Shabaninejad, A. Shafieesabet, M. Shahbazi, A. A. Shaheen, M. A. Shaikh, M. Shams-Beyranvand, M. Shamsi, M. Shamsizadeh, H. Sharafi, K. Sharafi, M. Sharif, M. Sharif-Alhoseini, M. Sharma, R. Sharma, J. She, A. Sheikh, P. Shi, K. Shibuya, M. Shigematsu, R. Shiri, R. Shirkoohi, K. Shishani, I. Shiue, F. Shokraneh, H. Shoman, M. G. Shrime, S. Si, S. Siabani, T. J. Siddiqi, I. D. Sigfusdottir, R. Sigurvinsdottir, J. P. Silva, D. G. A. Silveira, N. S. V. Singam, J. A. Singh, N. P. Singh, V. Singh, D. N. Sinha, E. Skiadaresi, E. L. N. Slepak, K. Sliwa, D. L. Smith, M. Smith, A. M. Soares Filho, B. H. Sobaih, S. Sobhani, E. Sobngwi, S. S. Soneji, M. Soofi, M. Soosaraei, R. J. D. Sorensen, J. B. Soriano, I. N. Soyiri, L. A. Sposato, C. T. Sreeramareddy, V. Srinivasan, J. D. Stanaway, D. J. Stein, C. Steiner, T. J. Steiner, M. A. Stokes, L. J. Stovner, M. L. Subart, A. Sudaryanto, M. a. B. Sufiyan, B. F. Sunguya, P. J. Sur, I. Sutradhar, B. L. Sykes, D. O. Sylte, R. Tabarés-Seisdedos, S. K. Tadakamadla, B. T. Tadesse, N. Tandon, S. G. Tassew, M. Tavakkoli, N. Taveira, H. R. Taylor, A. Tehrani-Banihashemi, T. G. Tekalign, S. W. Tekelemedhin, M. G. Tekle, H. Temesgen, M.-H. Temsah, O. Temsah, A. S. Terkawi, M. Teweldemedhin, K. R. Thankappan, N. Thomas, B. Tilahun, Q. G. To, M. Tonelli, R. Topor-Madry, F. Topouzis, A. E. Torre, M. Tortajada-Girbés, M. Touvier, M. R. Tovani-Palone, J. A. Towbin, B. X. Tran, K. B. Tran, C. E. Troeger, T. C. Truelsen, M. K. Tsilimbaris, D. Tsoi, L. Tudor Car, E. M. Tuzcu, K. N. Ukwaja, I. Ullah, E. A. Undurraga, J. Unutzer, R. L. Updike, M. S. Usman, O. A. Uthman, M. Vaduganathan, A. Vaezi, P. R. Valdez, S. Varughese, T. J. Vasankari, N. Venketasubramanian, S. Villafaina, F. S. Violante, S. K. Vladimirov, V. Vlassov, S. E. Vollset, K. Vosoughi, I. S. Vujcic, F. S. Wagnew, Y. Waheed, S. G. Waller, Y. Wang, Y.-P. Wang, E. Weiderpass, R. G. Weintraub, D. J. Weiss, F. Weldegebreal, K. G. Weldegwergs, A. Werdecker, T. E. West, H. A. Whiteford, J. Widecka, T. Wijeratne, L. B. Wilner, S. Wilson, A. S.

Winkler, A. B. Wiyeh, C. S. Wiysonge, C. D. A. Wolfe, A. D. Woolf, S. Wu, Y.-C. Wu, G. M. A. Wyper, D. Xavier, G. Xu, S. Yadgir, A. Yadollahpour, S. H. Yahyazadeh Jabbari, T. Yamada, L. L. Yan, Y. Yano, M. Yaseri, Y. J. Yasin, A. Yeshaneh, E. M. Yimer, P. Yip, E. Yisma, N. Yonemoto, S.-J. Yoon, M. Yotebieng, M. Z. Younis, M. Yousefifard, C. Yu, V. Zadnik, Z. Zaidi, S. B. Zaman, M. Zamani, Z. Zare, A. J. Zeleke, Z. M. Zenebe, K. Zhang, Z. Zhao, M. Zhou, S. Zodpey, I. Zucker, T. Vos and C. J. L. Murray (2018). "Global, regional, and national incidence, prevalence, and years lived with disability for 354 diseases and injuries for 195 countries and territories, 1990–2017: a systematic analysis for the Global Burden of Disease Study 2017." The Lancet **392**(10159): 1789-1858.

Jansma, J. M., H. H. van Hell, L. J. Vanderschuren, M. G. Bossong, G. Jager, R. S. Kahn and N. F. Ramsey (2013). "THC reduces the anticipatory nucleus accumbens response to reward in subjects with a nicotine addiction." Transl Psychiatry **3**: e234.

Jiang, R., S. Yamaori, S. Takeda, I. Yamamoto and K. Watanabe (2011). "Identification of cytochrome P450 enzymes responsible for metabolism of cannabidiol by human liver microsomes." Life Sciences **89**(5): 165-170.

Juckel, G., F. Schlagenhauf, M. Koslowski, D. Filonov, T. Wüstenberg, A. Villringer, B. Knutson, T. Kienast, J. Gallinat and J. Wrase (2006). "Dysfunction of ventral striatal reward prediction in schizophrenic patients treated with typical, not atypical, neuroleptics." Psychopharmacology **187**(2): 222-228.

Kappel, V., R. C. Lorenz, M. Streifling, B. Renneberg, U. Lehmkuhl, A. Strohle, H. Salbach-Andrae and A. Beck (2014). "Effect of brain structure and function on reward anticipation in children and adults with attention deficit hyperactivity disorder combined subtype." Soc Cogn Affect Neurosci.

Kapur, S. (2003). "Psychosis as a state of aberrant salience: a framework linking biology, phenomenology, and pharmacology in schizophrenia." Am J Psychiatry **160**(1): 13-23.

Kaufmann, C., J. C. Beucke, F. Preusse, T. Endrass, F. Schlagenhauf, A. Heinz, G. Juckel and N. Kathmann (2013). "Medial prefrontal brain activation to anticipated reward and loss in obsessive-compulsive disorder." Neuroimage Clin **2**: 212-220.

Keith, S. J. and S. M. Matthews (1991). "The diagnosis of schizophrenia: A review of onset and duration issues." Schizophrenia Bulletin **17**(1): 51-67.

Kelleher, I., H. Keeley, P. Corcoran, F. Lynch, C. Fitzpatrick, N. Devlin, C. Molloy, S. Roddy, M. C. Clarke, M. Harley, L. Arseneault, C. Wasserman, V. Carli, M. Sarchiapone, C. Hoven, D. Wasserman and M. Cannon (2012). "Clinicopathological significance of psychotic experiences in non-psychotic young people: evidence from four population-based studies." Br J Psychiatry **201**(1): 26-32.

Kempton, M. (2006). MRI and neuropsychological investigations in euthymic patients with bipolar disorder, University of London.

Kirk, U., K. W. Brown and J. Downar (2014). "Adaptive neural reward processing during anticipation and receipt of monetary rewards in mindfulness meditators." Soc Cogn Affect Neurosci.

Kirkbride, J. B., A. Errazuriz, T. J. Croudace, C. Morgan, D. Jackson, J. Boydell, R. M. Murray and P. B. Jones (2012). "Incidence of schizophrenia and other psychoses in England, 1950–2009: a systematic review and meta-analyses." PloS one **7**(3): e31660.

Klein-Flügge, M. C., H. C. Barron, K. H. Brodersen, R. J. Dolan and T. E. J. Behrens (2013). "Segregated encoding of reward–identity and stimulus–reward associations in human orbitofrontal cortex." Journal of Neuroscience **33**(7): 3202-3211.

Klein, C., E. Karanges, A. Spiro, A. Wong, J. Spencer, T. Huynh, N. Gunasekaran, T. Karl, L. E. Long, X.-F. Huang, K. Liu, J. C. Arnold and I. S. McGregor (2011). "Cannabidiol potentiates Δ9-tetrahydrocannabinol (THC) behavioural effects and alters THC pharmacokinetics during acute and chronic treatment in adolescent rats." Psychopharmacology **218**(2): 443-457.

Knutson, B., C. M. Adams, G. W. Fong and D. Hommer (2001). "Anticipation of increasing monetary reward selectively recruits nucleus accumbens." J Neurosci **21**(16): RC159.

Knutson, B., J. P. Bhanji, R. E. Cooney, L. Y. Atlas and I. H. Gotlib (2008). "Neural responses to monetary incentives in major depression." Biol Psychiatry **63**(7): 686-692.

Knutson, B., G. W. Fong, C. M. Adams, J. L. Varner and D. Hommer (2001). "Dissociation of reward anticipation and outcome with event-related fMRI." Neuroreport **12**(17): 3683-3687.
Knutson, B., G. W. Fong, S. M. Bennett, C. M. Adams and D. Hommer (2003). "A region of mesial prefrontal cortex tracks monetarily rewarding outcomes: characterization with rapid event-related fMRI." Neuroimage **18**(2): 263-272.
Knutson, B. and S. M. Greer (2008). "Anticipatory affect: neural correlates and consequences for choice." Philosophical Transactions of the Royal Society of London B: Biological Sciences **363**(1511): 3771-3786.
Knutson, B. and A. Heinz (2015). "Probing Psychiatric Symptoms with the Monetary Incentive Delay Task." Biological Psychiatry **77**(5): 418-420.
Knutson, B., A. Westdorp, E. Kaiser and D. Hommer (2000). "FMRI visualization of brain activity during a monetary incentive delay task." Neuroimage **12**(1): 20-27.
Koethe, D., A. Giuffrida, D. Schreiber, M. Hellmich, F. Schultze-Lutter, S. Ruhrmann, J. Klosterkötter, D. Piomelli and F. M. Leweke (2009). "Anandamide elevation in cerebrospinal fluid in initial prodromal states of psychosis." Br J Psychiatry **194**(4): 371-372.
Koob, G. F. and N. D. Volkow (2016). "Neurobiology of addiction: a neurocircuitry analysis." The Lancet Psychiatry **3**(8): 760-773.
Kostadinov, D., M. Beau, M. B. Pozo and M. Häusser (2019). "Predictive and reactive reward signals conveyed by climbing fiber inputs to cerebellar Purkinje cells." Nature Neuroscience.
Lally, J., O. Ajnakina, B. Stubbs, M. Cullinane, K. C. Murphy, F. Gaughran and R. M. Murray (2017). "Remission and recovery from first-episode psychosis in adults: systematic review and meta-analysis of long-term outcome studies." Br J Psychiatry **211**(6): 350-358.
Lambert, M., P. Conus, D. I. Lubman, D. Wade, H. Yuen, S. Moritz, D. Naber, P. D. McGorry and B. G. Schimmelmann (2005). "The impact of substance use disorders on clinical outcome in 643 patients with first-episode psychosis." Acta Psychiatr Scand **112**(2): 141-148.
Laprairie, R., A. Bagher, M. Kelly and E. Denovan-Wright (2015). "Cannabidiol is a negative allosteric modulator of the cannabinoid CB1 receptor." British journal of pharmacology **172**(20): 4790-4805.
Laredo, S. A., W. R. Marrs and L. H. Parsons (2017). Endocannabinoid Signaling in Reward and Addiction: From Homeostasis to Pathology. Endocannabinoids and Lipid Mediators in Brain Functions, Springer**:** 257-318.
Large, M., S. Sharma, M. T. Compton, T. Slade and O. Nielssen (2011). "Cannabis use and earlier onset of psychosis: a systematic meta-analysis." Archives of General Psychiatry **68**(6): 555-561.
Larry, N., M. Yarkoni, A. Lixenberg and M. Joshua (2019). "Cerebellar climbing fibers encode expected reward size." bioRxiv: 533653.
Lawn, W., T. P. Freeman, R. A. Pope, A. Joye, L. Harvey, C. Hindocha, C. Mokrysz, A. Moss, M. B. Wall, M. A. Bloomfield, R. K. Das, C. J. Morgan, D. J. Nutt and H. V. Curran (2016). "Acute and chronic effects of cannabinoids on effort-related decision-making and reward learning: an evaluation of the cannabis 'amotivational' hypotheses." Psychopharmacology (Berl) **233**(19-20): 3537-3552.
Leweke, F. M., A. Giuffrida, D. Koethe, D. Schreiber, B. M. Nolden, L. Kranaster, M. A. Neatby, M. Schneider, C. W. Gerth, M. Hellmich, J. Klosterkötter and D. Piomelli (2007). "Anandamide levels in cerebrospinal fluid of first-episode schizophrenic patients: Impact of cannabis use." Schizophrenia Research **94**(1): 29-36.
Leweke, F. M., A. Giuffrida, U. Wurster, H. M. Emrich and D. Piomelli (1999). "Elevated endogenous cannabinoids in schizophrenia." Neuroreport **10**(8): 1665-1669.
Leweke, F. M., D. Piomelli, F. Pahlisch, D. Muhl, C. W. Gerth, C. Hoyer, J. Klosterkötter, M. Hellmich and D. Koethe (2012). "Cannabidiol enhances anandamide signaling and alleviates psychotic symptoms of schizophrenia." Transl Psychiatry **2**: e94.
Lewis, D. A., T. Hashimoto and D. W. Volk (2005). "Cortical inhibitory neurons and schizophrenia." Nat Rev Neurosci **6**(4): 312-324.
Leyton, M. and P. Vezina (2013). "Striatal ups and downs: their roles in vulnerability to addictions in humans." Neuroscience & Biobehavioral Reviews **37**(9): 1999-2014.

Li, Y., G. Sescousse and J.-C. Dreher (2014). "Endogenous cortisol levels are associated with an imbalanced striatal sensitivity to monetary versus non-monetary cues in pathological gamblers." Frontiers in behavioral neuroscience **8**.
Lindquist, M. A., J. Meng Loh, L. Y. Atlas and T. D. Wager (2009). "Modeling the hemodynamic response function in fMRI: efficiency, bias and mis-modeling." NeuroImage **45**(1 Suppl): S187-S198.
Linscott, R. and J. Van Os (2013). "An updated and conservative systematic review and meta-analysis of epidemiological evidence on psychotic experiences in children and adults: on the pathway from proneness to persistence to dimensional expression across mental disorders." Psychological medicine **43**(6): 1133-1149.
Liu, X., J. Hairston, M. Schrier and J. Fan (2011). "Common and distinct networks underlying reward valence and processing stages: a meta-analysis of functional neuroimaging studies." Neurosci Biobehav Rev **35**(5): 1219-1236.
Logothetis, N. K. (2008). "What we can do and what we cannot do with fMRI." Nature **453**(7197): 869.
López-Moreno, J. A., V. Echeverry-Alzate and K.-M. Bühler (2011). "The genetic basis of the endocannabinoid system and drug addiction in humans." Journal of Psychopharmacology **26**(1): 133-143.
Luijten, M., A. F. Schellekens, S. Kühn, M. J. Machielse and G. Sescousse (2017). "Disruption of reward processing in addiction : An image-based meta-analysis of functional magnetic resonance imaging studies." JAMA Psychiatry **74**(4): 387-398.
Lutz, K. and M. Widmer (2014). "What can the monetary incentive delay task tell us about the neural processing of reward and punishment." Neuroscience and Neuroeconomics **3**: 33-35.
Mai, J., G. Paxinos and T. Voss (2007). A**tlas of the Human Brain**, Academic Press.
Manoliu, A., V. Riedl, A. Zherdin, M. Mühlau, D. Schwerthöffer, M. Scherr, H. Peters, C. Zimmer, H. Förstl and J. Bäuml (2013). "Aberrant dependence of default mode/central executive network interactions on anterior insular salience network activity in schizophrenia." Schizophrenia bulletin **40**(2): 428-437.
Manzanares, J., D. Cabañero, N. Puente, M. S. García-Gutiérrez, P. Grandes and R. Maldonado (2018). "Role of the endocannabinoid system in drug addiction." Biochemical pharmacology.
Marconi, A., M. Di Forti, C. M. Lewis, R. M. Murray and E. Vassos (2016). "Meta-analysis of the Association Between the Level of Cannabis Use and Risk of Psychosis." Schizophr Bull **42**(5): 1262-1269.
Matheson, S. L., A. M. Shepherd, R. M. Pinchbeck, K. R. Laurens and V. J. Carr (2012). "Childhood adversity in schizophrenia: a systematic meta-analysis." Psychological Medicine **43**(2): 225-238.
Matsuda, L. A., S. J. Lolait, M. J. Brownstein, A. C. Young and T. I. Bonner (1990). "Structure of a cannabinoid receptor and functional expression of the cloned cDNA." Nature **346**: 561.
Mátyás, F., G. M. Urbán, M. Watanabe, K. Mackie, A. Zimmer, T. F. Freund and I. Katona (2008). "Identification of the sites of 2-arachidonoylglycerol synthesis and action imply retrograde endocannabinoid signaling at both GABAergic and glutamatergic synapses in the ventral tegmental area." Neuropharmacology **54**(1): 95-107.
Mazzoncini, R., K. Donoghue, J. Hart, C. Morgan, G. A. Doody, P. Dazzan, P. B. Jones, K. Morgan, R. M. Murray and P. Fearon (2010). "Illicit substance use and its correlates in first episode psychosis." Acta Psychiatrica Scandinavica **121**(5): 351-358.
McCutcheon, R. A., M. M. Nour, T. Dahoun, S. Jauhar, F. Pepper, P. Expert, M. Veronese, R. A. Adams, F. Turkheimer, M. A. Mehta and O. D. Howes (2018). "Mesolimbic Dopamine Function Is Related to Salience Network Connectivity: An Integrative Positron Emission Tomography and Magnetic Resonance Study." Biological Psychiatry.
McGorry, P. (1993). "Early Psychosis Prevention and Intervention Centre." Australasian Psychiatry **1**(1): 32-34.
McGuire, P., P. Robson, W. J. Cubala, D. Vasile, P. D. Morrison, R. Barron, A. Taylor and S. Wright (2018). "Cannabidiol (CBD) as an Adjunctive Therapy in Schizophrenia: A Multicenter Randomized Controlled Trial." Am J Psychiatry **175**(3): 225-231.

McPartland, J. M., M. Duncan, V. Di Marzo and R. G. Pertwee (2015). "Are cannabidiol and Δ9-tetrahydrocannabivarin negative modulators of the endocannabinoid system? A systematic review." British journal of pharmacology **172**(3): 737-753.
McRobbie, D. W., E. A. Moore, M. J. Graves and M. R. Prince (2003). MRI From Picture to Proton, Cambridge University Press.
McRobbie, D. W., E. A. Moore, M. J. Graves and M. R. Prince (2006). MRI: Prom Picture to Proton, UK, Cambridge: Cambridge University Press. Pg.
Mechoulam, R., S. Ben-Shabat, L. Hanus, M. Ligumsky, N. E. Kaminski, A. R. Schatz, A. Gopher, S. Almog, B. R. Martin and D. R. Compton (1995). "Identification of an endogenous 2-monoglyceride, present in canine gut, that binds to cannabinoid receptors." Biochemical pharmacology **50**(1): 83-90.
Mechoulam, R., L. O. Hanuš, R. Pertwee and A. C. Howlett (2014). "Early phytocannabinoid chemistry to endocannabinoids and beyond." Nature Reviews Neuroscience **15**: 757.
Mehmedic, Z., S. Chandra, D. Slade, H. Denham, S. Foster, A. S. Patel, S. A. Ross, I. A. Khan and M. A. ElSohly (2010). "Potency trends of Δ9-THC and other cannabinoids in confiscated cannabis preparations from 1993 to 2008." Journal of forensic sciences **55**(5): 1209-1217.
Melis, M., A. L. Muntoni and M. Pistis (2012). "Endocannabinoids and the processing of value-related signals." Frontiers in pharmacology **3**: 7.
Menon, V. (2011). "Large-scale brain networks and psychopathology: a unifying triple network model." Trends in Cognitive Sciences **15**(10): 483-506.
Merritt, K., A. Egerton, M. J. Kempton, M. J. Taylor and P. K. McGuire (2016). "Nature of Glutamate Alterations in Schizophrenia: A Meta-analysis of Proton Magnetic Resonance Spectroscopy StudiesNature of Glutamate Alterations in SchizophreniaNature of Glutamate Alterations in Schizophrenia." JAMA Psychiatry **73**(7): 665-674.
Miller, B. J., P. Buckley, W. Seabolt, A. Mellor and B. Kirkpatrick (2011). "Meta-analysis of cytokine alterations in schizophrenia: clinical status and antipsychotic effects." Biol Psychiatry **70**(7): 663-671.
Mita, A., H. Mushiake, K. Shima, Y. Matsuzaka and J. Tanji (2009). "Interval time coding by neurons in the presupplementary and supplementary motor areas." Nature Neuroscience **12**: 502.
Mitchell, J. E. and L. A. Dahlgren (1986). "Prevalence of smoking among psychiatric outpatients." Am J psychiatry **143**(8): 993-997.
Modinos, G., P. Allen, A. A. Grace and P. McGuire (2015). "Translating the MAM model of psychosis to humans." Trends in neurosciences **38**(3): 129-138.
Modinos, G., F. Şimşek, M. Azis, M. Bossong, I. Bonoldi, C. Samson, B. Quinn, J. Perez, M. R. Broome, F. Zelaya, D. J. Lythgoe, O. D. Howes, J. M. Stone, A. A. Grace, P. Allen and P. McGuire (2018). "Prefrontal GABA levels, hippocampal resting perfusion and the risk of psychosis." Neuropsychopharmacology.
Moore, B. A., E. M. Augustson, R. P. Moser and A. J. Budney (2005). "Respiratory effects of marijuana and tobacco use in a US sample." Journal of general internal medicine **20**(1): 33-37.
Moreno-Küstner, B., C. Martin and L. Pastor (2018). "Prevalence of psychotic disorders and its association with methodological issues. A systematic review and meta-analyses." PloS one **13**(4): e0195687.
Morgan, C. J. and H. V. Curran (2008). "Effects of cannabidiol on schizophrenia-like symptoms in people who use cannabis." Br J Psychiatry **192**(4): 306-307.
Morgan, C. J. A., T. P. Freeman, J. Powell and H. V. Curran (2016). "AKT1 genotype moderates the acute psychotomimetic effects of naturalistically smoked cannabis in young cannabis smokers." Translational Psychiatry **6**: e738.
Morgan, C. J. A., E. Page, C. Schaefer, K. Chatten, A. Manocha, S. Gulati, H. V. Curran, B. Brandner and F. M. Leweke (2018). "Cerebrospinal fluid anandamide levels, cannabis use and psychotic-like symptoms." British Journal of Psychiatry **202**(5): 381-382.
Morrison, P. D., V. Zois, D. A. McKeown, T. D. Lee, D. W. Holt, J. F. Powell, S. Kapur and R. M. Murray (2009). "The acute effects of synthetic intravenous Delta9-tetrahydrocannabinol on psychosis, mood and cognitive functioning." Psychol Med **39**(10): 1607-1616.

Mouchlianitis, E., R. McCutcheon and O. D. Howes (2016). "Brain-imaging studies of treatment-resistant schizophrenia: a systematic review." The Lancet Psychiatry **3**(5): 451-463.
Müller, V. I., E. C. Cieslik, A. R. Laird, P. T. Fox, J. Radua, D. Mataix-Cols, C. R. Tench, T. Yarkoni, T. E. Nichols, P. E. Turkeltaub, T. D. Wager and S. B. Eickhoff (2018). "Ten simple rules for neuroimaging meta-analysis." Neuroscience & Biobehavioral Reviews **84**: 151-161.
Munro, S., K. L. Thomas and M. Abu-Shaar (1993). "Molecular characterization of a peripheral receptor for cannabinoids." Nature **365**(6441): 61.
Murray, G. K., L. Clark, P. R. Corlett, A. D. Blackwell, R. Cools, P. B. Jones, T. W. Robbins and L. Poustka (2008). "Incentive motivation in first-episode psychosis: a behavioural study." BMC Psychiatry **8**: 34.
Murray, G. K., P. R. Corlett, L. Clark, M. Pessiglione, A. D. Blackwell, G. Honey, P. B. Jones, E. T. Bullmore, T. W. Robbins and P. C. Fletcher (2007). "Substantia nigra/ventral tegmental reward prediction error disruption in psychosis." Molecular Psychiatry **13**: 267.
Murray, R. M., V. Bhavsar, G. Tripoli and O. Howes (2017). "30 Years on: How the Neurodevelopmental Hypothesis of Schizophrenia Morphed Into the Developmental Risk Factor Model of Psychosis." Schizophrenia Bulletin **43**(6): 1190-1196.
Nestor, L., R. Hester and H. Garavan (2010). "Increased ventral striatal BOLD activity during non-drug reward anticipation in cannabis users." Neuroimage **49**(1): 1133-1143.
Nielsen, M. O., E. Rostrup, S. Wulff, N. Bak, B. V. Broberg, H. Lublin, S. Kapur and B. Glenthoj (2012). "Improvement of brain reward abnormalities by antipsychotic monotherapy in schizophrenia." Arch Gen Psychiatry **69**(12): 1195-1204.
Nielsen, M. Ø., E. Rostrup, S. Wulff, N. Bak, H. Lublin, S. Kapur and B. Glenthøj (2012). "Alterations of the Brain Reward System in Antipsychotic Naïve Schizophrenia Patients." Biological Psychiatry **71**(10): 898-905.
Nielsen, S. M., N. G. Toftdahl, M. Nordentoft and C. Hjorthoj (2017). "Association between alcohol, cannabis, and other illicit substance abuse and risk of developing schizophrenia: a nationwide population based register study." Psychol Med **47**(9): 1668-1677.
Nordentoft, M., J. Ø. Rasmussen, M. Melau, C. R. Hjorthøj and A. A. Thorup (2014). "How successful are first episode programs? A review of the evidence for specialized assertive early intervention." Current opinion in psychiatry **27**(3): 167-172.
O'Neill, A., A. Mechelli and S. Bhattacharyya (2018). "Dysconnectivity of Large-Scale Functional Networks in Early Psychosis: A Meta-analysis." Schizophrenia Bulletin: sby094-sby094.
Ogawa, S., T. M. Lee, A. R. Kay and D. W. Tank (1990). "Brain magnetic resonance imaging with contrast dependent on blood oxygenation." Proceedings of the National Academy of Sciences of the United States of America **87**(24): 9868-9872.
Ohmae, S. and J. F. Medina (2015). "Climbing fibers encode a temporal-difference prediction error during cerebellar learning in mice." Nature Neuroscience **18**: 1798.
Oldham, S., C. Murawski, A. Fornito, G. Youssef, M. Yucel and V. Lorenzetti (2018). "The anticipation and outcome phases of reward and loss processing: A neuroimaging meta-analysis of the monetary incentive delay task." Hum Brain Mapp.
Oleson, E. B., M. V. Beckert, J. T. Morra, C. S. Lansink, R. Cachope, R. A. Abdullah, A. L. Loriaux, D. Schetters, T. Pattij, M. F. Roitman, A. H. Lichtman and J. F. Cheer (2012). "Endocannabinoids shape accumbal encoding of cue-motivated behavior via CB1 receptor activation in the ventral tegmentum." Neuron **73**(2): 360-373.
Olney, J. W. and N. B. Farber (1995). "Glutamate receptor dysfunction and schizophrenia." Arch Gen Psychiatry **52**(12): 998-1007.
Ossewaarde, L., S. Qin, H. J. Van Marle, G. A. van Wingen, G. Fernández and E. J. Hermans (2011). "Stress-induced reduction in reward-related prefrontal cortex function." Neuroimage **55**(1): 345-352.
Ossewaarde, L., R. J. Verkes, E. J. Hermans, S. C. Kooijman, M. Urner, I. Tendolkar, G. A. van Wingen and G. Fernandez (2011). "Two-week administration of the combined serotonin-noradrenaline reuptake inhibitor duloxetine augments functioning of mesolimbic incentive processing circuits." Biol Psychiatry **70**(6): 568-574.

Ossewaarde, L., R. J. Verkes, E. J. Hermans, S. C. Kooijman, M. Urner, I. Tendolkar, G. A. van Wingen and G. Fernández (2011). "Two-Week Administration of the Combined Serotonin-Noradrenaline Reuptake Inhibitor Duloxetine Augments Functioning of Mesolimbic Incentive Processing Circuits." Biological Psychiatry **70**(6): 568-574.
Palaniyappan, L., M. Simmonite, Thomas P. White, Elizabeth B. Liddle and Peter F. Liddle (2013). "Neural Primacy of the Salience Processing System in Schizophrenia." Neuron **79**(4): 814-828.
Pecina, M., M. Martinez-Jauand, T. Love, J. Heffernan, P. Montoya, C. Hodgkinson, C. S. Stohler, D. Goldman and J. K. Zubieta (2014). "Valence-specific effects of BDNF Val66Met polymorphism on dopaminergic stress and reward processing in humans." J Neurosci **34**(17): 5874-5881.
Penny, W., K. Friston, J. Ashburner, S. Kiebel and T. Nichols (2007). Statistical Parametric Mapping: The Analysis of Functional Brain Images, Academic Press.
Penttilä, M., E. Jääskeläinen, N. Hirvonen, M. Isohanni and J. Miettunen (2014). "Duration of untreated psychosis as predictor of long-term outcome in schizophrenia: systematic review and meta-analysis." The British Journal of Psychiatry **205**(2): 88-94.
Pertwee, R. (2008). "The diverse CB1 and CB2 receptor pharmacology of three plant cannabinoids: Δ9-tetrahydrocannabinol, cannabidiol and Δ9-tetrahydrocannabivarin." British journal of pharmacology **153**(2): 199-215.
Pertwee, R. G. (2008). "The diverse CB1 and CB2 receptor pharmacology of three plant cannabinoids: delta9-tetrahydrocannabinol, cannabidiol and delta9-tetrahydrocannabivarin." Br J Pharmacol **153**(2): 199-215.
Pertwee, R. G. (2015). Endocannabinoids and their pharmacological actions. Endocannabinoids, Springer**:** 1-37.
Pfabigan, D. M., E. M. Seidel, R. Sladky, A. Hahn, K. Paul, A. Grahl, M. Kublbock, C. Kraus, A. Hummer, G. S. Kranz, C. Windischberger, R. Lanzenberger and C. Lamm (2014). "P300 amplitude variation is related to ventral striatum BOLD response during gain and loss anticipation: an EEG and fMRI experiment." Neuroimage **96**: 12-21.
Piomelli, D. (2014). "More surprises lying ahead. The endocannabinoids keep us guessing." Neuropharmacology **76**: 228-234.
Plichta, M. M. and A. Scheres (2014). "Ventral–striatal responsiveness during reward anticipation in ADHD and its relation to trait impulsivity in the healthy population: A meta-analytic review of the fMRI literature." Neuroscience & Biobehavioral Reviews **38**: 125-134.
Poldrack, R. A., C. I. Baker, J. Durnez, K. J. Gorgolewski, P. M. Matthews, M. R. Munafò, T. E. Nichols, J. B. Poline, E. Vul and T. Yarkoni (2017). "Scanning the horizon: towards transparent and reproducible neuroimaging research." Nat Rev Neurosci **18**(2): 115-126.
Pollak, T. A., R. McCormack, M. Peakman, T. R. Nicholson and A. S. David (2013). "Prevalence of anti-N-methyl-d-aspartate (NMDA) receptor antibodies in patients with schizophrenia and related psychoses: a systematic review and meta-analysis." Psychological Medicine **44**(12): 2475-2487.
Radua, J. and D. Mataix-Cols (2009). "Voxel-wise meta-analysis of grey matter changes in obsessive–compulsive disorder." The British Journal of Psychiatry **195**(5): 393-402.
Radua, J. and D. Mataix-Cols (2012). "Meta-analytic methods for neuroimaging data explained." Biology of mood & anxiety disorders **2**(1): 6.
Radua, J., D. Mataix-Cols, M. L. Phillips, W. El-Hage, D. M. Kronhaus, N. Cardoner and S. Surguladze (2012). "A new meta-analytic method for neuroimaging studies that combines reported peak coordinates and statistical parametric maps." Eur Psychiatry **27**(8): 605-611.
Radua, J., K. Rubia, E. J. Canales-Rodríguez, E. Pomarol-Clotet, P. Fusar-Poli and D. Mataix-Cols (2014). "Anisotropic kernels for coordinate-based meta-analyses of neuroimaging studies." Frontiers in psychiatry **5**.
Radua, J., A. Schmidt, S. Borgwardt, A. Heinz, F. Schlagenhauf, P. McGuire and P. Fusar-Poli (2015). "Ventral striatal activation during reward processing in psychosis: a neurofunctional meta-analysis." JAMA psychiatry **72**(12): 1243-1251.

Radua, J., O. A. Van Den Heuvel, S. Surguladze and D. Mataix-Cols (2010). "Meta-analytical comparison of voxel-based morphometry studies in obsessive-compulsive disorder vs other anxiety disorders." Archives of general psychiatry **67**(7): 701-711.
Ranganathan, M., J. Cortes-Briones, R. Radhakrishnan, H. Thurnauer, B. Planeta, P. Skosnik, H. Gao, D. Labaree, A. Neumeister, B. Pittman, T. Surti, Y. Huang, R. E. Carson and D. C. D'Souza (2016). "Reduced Brain Cannabinoid Receptor Availability in Schizophrenia." Biol Psychiatry **79**(12): 997-1005.
Regier, D. A., M. E. Farmer, D. S. Rae and et al. (1990). "Comorbidity of mental disorders with alcohol and other drug abuse: Results from the epidemiologic catchment area (eca) study." JAMA **264**(19): 2511-2518.
Rogers, R. D., A. M. Owen, H. C. Middleton, E. J. Williams, J. D. Pickard, B. J. Sahakian and T. W. Robbins (1999). "Choosing between small, likely rewards and large, unlikely rewards activates inferior and orbital prefrontal cortex." Journal of Neuroscience **19**(20): 9029-9038.
Roiser, J. P., O. D. Howes, C. A. Chaddock, E. M. Joyce and P. McGuire (2012). "Neural and behavioral correlates of aberrant salience in individuals at risk for psychosis." Schizophrenia bulletin **39**(6): 1328-1336.
Roiser, J. P., K. E. Stephan, H. E. M. den Ouden, T. R. E. Barnes, K. J. Friston and E. M. Joyce (2008). "Do patients with schizophrenia exhibit aberrant salience?" Psychological Medicine **39**(2): 199-209.
Romanczuk-Seiferth, N., S. Koehler, C. Dreesen, T. Wustenberg and A. Heinz (2014). "Pathological gambling and alcohol dependence: neural disturbances in reward and loss avoidance processing." Addict Biol.
Rose, E. J., T. J. Ross, B. J. Salmeron, M. Lee, D. M. Shakleya, M. A. Huestis and E. A. Stein (2013). "Acute nicotine differentially impacts anticipatory valence- and magnitude-related striatal activity." Biol Psychiatry **73**(3): 280-288.
Russo, E. B. (2007). "History of cannabis and its preparations in saga, science, and sobriquet." Chemistry & biodiversity **4**(8): 1614-1648.
Saji, K., Y. Ikeda, W. Kim, Y. Shingai, A. Tateno, H. Takahashi, Y. Okubo, H. Fukayama and H. Suzuki (2013). "Acute NK(1) receptor antagonist administration affects reward incentive anticipation processing in healthy volunteers." Int J Neuropsychopharmacol **16**(7): 1461-1471.
Salimi-Khorshidi, G., S. M. Smith, J. R. Keltner, T. D. Wager and T. E. Nichols (2009). "Meta-analysis of neuroimaging data: a comparison of image-based and coordinate-based pooling of studies." Neuroimage **45**(3): 810-823.
Schizophrenia Working Group of the Psychiatric Genomics, C., S. Ripke, B. M. Neale, A. Corvin, J. T. R. Walters, K.-H. Farh, P. A. Holmans, P. Lee, B. Bulik-Sullivan, D. A. Collier, H. Huang, T. H. Pers, I. Agartz, E. Agerbo, M. Albus, M. Alexander, F. Amin, S. A. Bacanu, M. Begemann, R. A. Belliveau Jr, J. Bene, S. E. Bergen, E. Bevilacqua, T. B. Bigdeli, D. W. Black, R. Bruggeman, N. G. Buccola, R. L. Buckner, W. Byerley, W. Cahn, G. Cai, D. Campion, R. M. Cantor, V. J. Carr, N. Carrera, S. V. Catts, K. D. Chambert, R. C. K. Chan, R. Y. L. Chen, E. Y. H. Chen, W. Cheng, E. F. C. Cheung, S. Ann Chong, C. Robert Cloninger, D. Cohen, N. Cohen, P. Cormican, N. Craddock, J. J. Crowley, D. Curtis, M. Davidson, K. L. Davis, F. Degenhardt, J. Del Favero, D. Demontis, D. Dikeos, T. Dinan, S. Djurovic, G. Donohoe, E. Drapeau, J. Duan, F. Dudbridge, N. Durmishi, P. Eichhammer, J. Eriksson, V. Escott-Price, L. Essioux, A. H. Fanous, M. S. Farrell, J. Frank, L. Franke, R. Freedman, N. B. Freimer, M. Friedl, J. I. Friedman, M. Fromer, G. Genovese, L. Georgieva, I. Giegling, P. Giusti-Rodríguez, S. Godard, J. I. Goldstein, V. Golimbet, S. Gopal, J. Gratten, L. de Haan, C. Hammer, M. L. Hamshere, M. Hansen, T. Hansen, V. Haroutunian, A. M. Hartmann, F. A. Henskens, S. Herms, J. N. Hirschhorn, P. Hoffmann, A. Hofman, M. V. Hollegaard, D. M. Hougaard, M. Ikeda, I. Joa, A. Julià, R. S. Kahn, L. Kalaydjieva, S. Karachanak-Yankova, J. Karjalainen, D. Kavanagh, M. C. Keller, J. L. Kennedy, A. Khrunin, Y. Kim, J. Klovins, J. A. Knowles, B. Konte, V. Kucinskas, Z. Ausrele Kucinskiene, H. Kuzelova-Ptackova, A. K. Kähler, C. Laurent, J. Lee Chee Keong, S. Hong Lee, S. E. Legge, B. Lerer, M. Li, T. Li, K.-Y. Liang, J. Lieberman, S. Limborska, C. M. Loughland, J. Lubinski, J. Lönnqvist, M. Macek Jr, P. K. E. Magnusson, B. S. Maher, W. Maier, J. Mallet, S. Marsal, M. Mattheisen, M. Mattingsdal, R. W. McCarley, C. McDonald, A. M. McIntosh, S. Meier, C. J. Meijer, B. Melegh, I. Melle, R. I. Mesholam-Gately, A. Metspalu, P. T. Michie, L. Milani, V. Milanova,

Y. Mokrab, D. W. Morris, O. Mors, K. C. Murphy, R. M. Murray, I. Myin-Germeys, B. Müller-Myhsok, M. Nelis, I. Nenadic, D. A. Nertney, G. Nestadt, K. K. Nicodemus, L. Nikitina-Zake, L. Nisenbaum, A. Nordin, E. O'Callaghan, C. O'Dushlaine, F. A. O'Neill, S.-Y. Oh, A. Olincy, L. Olsen, J. Van Os, C. Pantelis, G. N. Papadimitriou, S. Papiol, E. Parkhomenko, M. T. Pato, T. Paunio, M. Pejovic-Milovancevic, D. O. Perkins, O. Pietiläinen, J. Pimm, A. J. Pocklington, J. Powell, A. Price, A. E. Pulver, S. M. Purcell, D. Quested, H. B. Rasmussen, A. Reichenberg, M. A. Reimers, A. L. Richards, J. L. Roffman, P. Roussos, D. M. Ruderfer, V. Salomaa, A. R. Sanders, U. Schall, C. R. Schubert, T. G. Schulze, S. G. Schwab, E. M. Scolnick, R. J. Scott, L. J. Seidman, J. Shi, E. Sigurdsson, T. Silagadze, J. M. Silverman, K. Sim, P. Slominsky, J. W. Smoller, H.-C. So, C. A. Spencer, E. A. Stahl, H. Stefansson, S. Steinberg, E. Stogmann, R. E. Straub, E. Strengman, J. Strohmaier, T. Scott Stroup, M. Subramaniam, J. Suvisaari, D. M. Svrakic, J. P. Szatkiewicz, E. Söderman, S. Thirumalai, D. Toncheva, S. Tosato, J. Veijola, J. Waddington, D. Walsh, D. Wang, Q. Wang, B. T. Webb, M. Weiser, D. B. Wildenauer, N. M. Williams, S. Williams, S. H. Witt, A. R. Wolen, E. H. M. Wong, B. K. Wormley, H. Simon Xi, C. C. Zai, X. Zheng, F. Zimprich, N. R. Wray, K. Stefansson, P. M. Visscher, W. Trust Case-Control Consortium, R. Adolfsson, O. A. Andreassen, D. H. R. Blackwood, E. Bramon, J. D. Buxbaum, A. D. Børglum, S. Cichon, A. Darvasi, E. Domenici, H. Ehrenreich, T. Esko, P. V. Gejman, M. Gill, H. Gurling, C. M. Hultman, N. Iwata, A. V. Jablensky, E. G. Jönsson, K. S. Kendler, G. Kirov, J. Knight, T. Lencz, D. F. Levinson, Q. S. Li, J. Liu, A. K. Malhotra, S. A. McCarroll, A. McQuillin, J. L. Moran, P. B. Mortensen, B. J. Mowry, M. M. Nöthen, R. A. Ophoff, M. J. Owen, A. Palotie, C. N. Pato, T. L. Petryshen, D. Posthuma, M. Rietschel, B. P. Riley, D. Rujescu, P. C. Sham, P. Sklar, D. St Clair, D. R. Weinberger, J. R. Wendland, T. Werge, M. J. Daly, P. F. Sullivan and M. C. O'Donovan (2014). "Biological insights from 108 schizophrenia-associated genetic loci." Nature **511**: 421.

Schlagenhauf, F., G. Juckel, M. Koslowski, T. Kahnt, B. Knutson, T. Dembler, T. Kienast, J. Gallinat, J. Wrase and A. Heinz (2008). "Reward system activation in schizophrenic patients switched from typical neuroleptics to olanzapine." Psychopharmacology (Berl) **196**(4): 673-684.

Schmidt, A., L. Palaniyappan, R. Smieskova, A. Simon, A. Riecher-Rössler, U. E. Lang, P. Fusar-Poli, P. McGuire and S. J. Borgwardt (2016). "Dysfunctional insular connectivity during reward prediction in patients with first-episode psychosis." Journal of psychiatry & neuroscience : JPN **41**(6): 367-376.

Schoeler, T., A. Monk, M. B. Sami, E. Klamerus, E. Foglia, R. Brown, G. Camuri, A. C. Altamura, R. Murray and S. Bhattacharyya (2016). "Continued versus discontinued cannabis use in patients with psychosis: a systematic review and meta-analysis." The Lancet Psychiatry **3**(3): 215-225.

Schoeler, T., N. Petros, M. Di Forti, E. Klamerus, E. Foglia, O. Ajnakina, C. Gayer-Anderson, M. Colizzi, D. Quattrone, I. Behlke, S. Shetty, P. McGuire, A. S. David, R. Murray and S. Bhattacharyya (2016). "Effects of continuation, frequency, and type of cannabis use on relapse in the first 2 years after onset of psychosis: an observational study." The Lancet Psychiatry **3**(10): 947-953.

Schultz, W. (2017). "Reward prediction error." Current Biology **27**(10): R369-R371.

Schultz, W., P. Dayan and P. R. Montague (1997). "A neural substrate of prediction and reward." Science **275**(5306): 1593-1599.

Scuderi, C., D. D. Filippis, T. Iuvone, A. Blasio, A. Steardo and G. Esposito (2009). "Cannabidiol in medicine: a review of its therapeutic potential in CNS disorders." Phytotherapy Research: An International Journal Devoted to Pharmacological and Toxicological Evaluation of Natural Product Derivatives **23**(5): 597-602.

Sescousse, G., X. Caldú, B. Segura and J.-C. Dreher (2013). "Processing of primary and secondary rewards: A quantitative meta-analysis and review of human functional neuroimaging studies." Neuroscience & Biobehavioral Reviews **37**(4): 681-696.

Sescousse, G., J. Redouté and J.-C. Dreher (2010). "The architecture of reward value coding in the human orbitofrontal cortex." Journal of neuroscience **30**(39): 13095-13104.

Shanahan, W. J., I. R. Falloon, M. Laporta and H. A. Krekorian (1990). "The Buckingham Project—the description of a home based mental health service." Irish Journal of Psychological Medicine **7**(2): 151-153.

Shenhav, A., J. D. Cohen and M. M. Botvinick (2016). "Dorsal anterior cingulate cortex and the value of control." Nature Neuroscience **19**: 1286.
Sheth, S. A., M. K. Mian, S. R. Patel, W. F. Asaad, Z. M. Williams, D. D. Dougherty, G. Bush and E. N. Eskandar (2012). "Human dorsal anterior cingulate cortex neurons mediate ongoing behavioural adaptation." Nature **488**: 218.
Simmonds, D. J., J. J. Pekar and S. H. Mostofsky (2008). "Meta-analysis of Go/No-go tasks demonstrating that fMRI activation associated with response inhibition is task-dependent." Neuropsychologia **46**(1): 224-232.
Simon, J. J., A. Biller, S. Walther, D. Roesch-Ely, C. Stippich, M. Weisbrod and S. Kaiser (2010). "Neural correlates of reward processing in schizophrenia — Relationship to apathy and depression." Schizophrenia Research **118**(1–3): 154-161.
Smieskova, R., J. P. Roiser, C. A. Chaddock, A. Schmidt, F. Harrisberger, K. Bendfeldt, A. Simon, A. Walter, P. Fusar-Poli, P. K. McGuire, U. E. Lang, A. Riecher-Rössler and S. Borgwardt (2015). "Modulation of motivational salience processing during the early stages of psychosis." Schizophr Res **166**(1-3): 17-23.
Solinas, M., Z. Justinova, S. R. Goldberg and G. Tanda (2006). "Anandamide administration alone and after inhibition of fatty acid amide hydrolase (FAAH) increases dopamine levels in the nucleus accumbens shell in rats." Journal of neurochemistry **98**(2): 408-419.
Spreckelmeyer, K. N., S. Krach, G. Kohls, L. Rademacher, A. Irmak, K. Konrad, T. Kircher and G. Grunder (2009). "Anticipation of monetary and social reward differently activates mesolimbic brain structures in men and women." Soc Cogn Affect Neurosci **4**(2): 158-165.
Sridharan, D., D. J. Levitin and V. Menon (2008). "A critical role for the right fronto-insular cortex in switching between central-executive and default-mode networks." Proc Natl Acad Sci U S A **105**(34): 12569-12574.
Stella, N., P. Schweitzer and D. Piomelli (1997). "A second endogenous cannabinoid that modulates long-term potentiation." Nature **388**: 773.
Stone, J. M., P. D. Morrison and L. S. Pilowsky (2007). "Glutamate and dopamine dysregulation in schizophrenia--a synthesis and selective review." J Psychopharmacol **21**(4): 440-452.
Stoy, M., F. Schlagenhauf, L. Schlochtermeier, J. Wrase, B. Knutson, U. Lehmkuhl, M. Huss, A. Heinz and A. Strohle (2011). "Reward processing in male adults with childhood ADHD--a comparison between drug-naive and methylphenidate-treated subjects." Psychopharmacology (Berl) **215**(3): 467-481.
Stoy, M., F. Schlagenhauf, P. Sterzer, F. Bermpohl, C. Hägele, K. Suchotzki, K. Schmack, J. Wrase, R. Ricken, B. Knutson, M. Adli, M. Bauer, A. Heinz and A. Ströhle (2012). "Hyporeactivity of ventral striatum towards incentive stimuli in unmedicated depressed patients normalizes after treatment with escitalopram." Journal of Psychopharmacology **26**(5): 677-688.
Sullivan, P. F., K. S. Kendler and M. C. Neale (2003). "Schizophrenia as a complex trait: evidence from a meta-analysis of twin studies." Arch Gen Psychiatry **60**(12): 1187-1192.
Swick, D., V. Ashley and U. Turken (2008). "Left inferior frontal gyrus is critical for response inhibition." BMC neuroscience **9**(1): 102.
Taylor, L., B. Gidal, G. Blakey, B. Tayo and G. Morrison (2018). "A Phase I, Randomized, Double-Blind, Placebo-Controlled, Single Ascending Dose, Multiple Dose, and Food Effect Trial of the Safety, Tolerability and Pharmacokinetics of Highly Purified Cannabidiol in Healthy Subjects." CNS Drugs.
Tham, M., O. Yilmaz, M. Alaverdashvili, M. E. M. Kelly, E. M. Denovan-Wright and R. B. Laprairie (2018). "Allosteric and orthosteric pharmacology of cannabidiol and cannabidiol-dimethylheptyl at the type 1 and type 2 cannabinoid receptors." Br J Pharmacol.
Tian, Y. and A. Zalesky (2018). "Characterizing the functional connectivity diversity of the insula cortex: Subregions, diversity curves and behavior." NeuroImage **183**: 716-733.
Treadway, M. T., J. W. Buckholtz and D. H. Zald (2013). "Perceived stress predicts altered reward and loss feedback processing in medial prefrontal cortex." Front Hum Neurosci **7**: 180.

Turkeltaub, P. E., G. F. Eden, K. M. Jones and T. A. Zeffiro (2002). "Meta-Analysis of the Functional Neuroanatomy of Single-Word Reading: Method and Validation." NeuroImage **16**(3): 765-780.
Uddin, L. Q., J. S. Nomi, B. Hébert-Seropian, J. Ghaziri and O. Boucher (2017). "Structure and Function of the Human Insula." J Clin Neurophysiol **34**(4): 300-306.
UNODC World Drug Report 2018 (United Nations publication, Sales No. E.18.XI.9).
Vaidya, J. G., B. Knutson, D. S. O'Leary, R. I. Block and V. Magnotta (2013). "Neural sensitivity to absolute and relative anticipated reward in adolescents." PLoS One **8**(3): e58708.
Valmaggia, L. R., M. Byrne, F. Day, M. R. Broome, L. Johns, O. Howes, P. Power, S. Badger, P. Fusar-Poli and P. K. McGuire (2018). "Duration of untreated psychosis and need for admission in patients who engage with mental health services in the prodromal phase." British Journal of Psychiatry **207**(2): 130-134.
van Hell, H. H., G. Jager, M. G. Bossong, A. Brouwer, J. M. Jansma, L. Zuurman, J. van Gerven, R. S. Kahn and N. F. Ramsey (2012). "Involvement of the endocannabinoid system in reward processing in the human brain." Psychopharmacology (Berl) **219**(4): 981-990.
van Hell, H. H., M. Vink, L. Ossewaarde, G. Jager, R. S. Kahn and N. F. Ramsey (2010). "Chronic effects of cannabis use on the human reward system: an fMRI study." European neuropsychopharmacology **20**(3): 153-163.
van Kesteren, C. F. M. G., H. Gremmels, L. D. de Witte, E. M. Hol, A. R. Van Gool, P. G. Falkai, R. S. Kahn and I. E. C. Sommer (2017). "Immune involvement in the pathogenesis of schizophrenia: a meta-analysis on postmortem brain studies." Translational Psychiatry **7**: e1075.
Van Os, J., M. Bak, M. Hanssen, R. V. Bijl, R. De Graaf and H. Verdoux (2002). "Cannabis use and psychosis: A longitudinal population-based study." American Journal of Epidemiology **156**(4): 319-327.
van Os, J. and S. Guloksuz (2017). "A critique of the "ultra-high risk" and "transition" paradigm." World psychiatry : official journal of the World Psychiatric Association (WPA) **16**(2): 200-206.
van Os, J., R. J. Linscott, I. Myin-Germeys, P. Delespaul and L. Krabbendam (2009). "A systematic review and meta-analysis of the psychosis continuum: evidence for a psychosis proneness–persistence–impairment model of psychotic disorder." Psychological Medicine **39**(2): 179-195.
van Os, J. and U. Reininghaus (2016). "Psychosis as a transdiagnostic and extended phenotype in the general population." World Psychiatry **15**(2): 118-124.
Vink, M., M. van den Heuvel, M. Raemakers, R. Mandl, B. Neggers, L. Kushan, N. Ramsey and T. Gladwin (2007). Preprocessing and Analysis of Functional MRI Data. Rudolf Magnus Institute of Neuroscience, University Medical Center Utrecht.
Vita, A., L. De Peri, G. Deste, S. Barlati and E. Sacchetti (2015). "The Effect of Antipsychotic Treatment on Cortical Gray Matter Changes in Schizophrenia: Does the Class Matter? A Meta-analysis and Meta-regression of Longitudinal Magnetic Resonance Imaging Studies." Biological Psychiatry **78**(6): 403-412.
von Bartheld, C. S., J. Bahney and S. Herculano-Houzel (2016). "The search for true numbers of neurons and glial cells in the human brain: A review of 150 years of cell counting." The Journal of comparative neurology **524**(18): 3865-3895.
Wagner, M. J., T. H. Kim, J. Savall, M. J. Schnitzer and L. Luo (2017). "Cerebellar granule cells encode the expectation of reward." Nature **544**(7648): 96-100.
Wandschneider, B. and M. J. Koepp (2016). "Pharmaco fMRI: Determining the functional anatomy of the effects of medication." Neuroimage Clin **12**: 691-697.
Watson, K. K., T. K. Jones and J. M. Allman (2006). "Dendritic architecture of the von Economo neurons." Neuroscience **141**(3): 1107-1112.
Weiland, B. J., M. M. Heitzeg, D. Zald, C. Cummiford, T. Love, R. A. Zucker and J. K. Zubieta (2014). "Relationship between impulsivity, prefrontal anticipatory activation, and striatal dopamine release during rewarded task performance." Psychiatry Res **223**(3): 244-252.
Weinberger, D. R. (1987). "Implications of normal brain development for the pathogenesis of schizophrenia." Arch Gen Psychiatry **44**(7): 660-669.

Weissman, D. H., A. Gopalakrishnan, C. J. Hazlett and M. G. Woldorff (2004). "Dorsal Anterior Cingulate Cortex Resolves Conflict from Distracting Stimuli by Boosting Attention toward Relevant Events." Cerebral Cortex **15**(2): 229-237.
White, T. P., V. Joseph, S. T. Francis and P. F. Liddle (2010). "Aberrant salience network (bilateral insula and anterior cingulate cortex) connectivity during information processing in schizophrenia." Schizophr Res **123**(2-3): 105-115.
Wijayendran, S. B., A. O'Neill and S. Bhattacharyya (2016). "The effects of cannabis use on salience attribution: a systematic review." Acta Neuropsychiatrica **30**(1): 43-57.
Wilson, R. P., R. Patel and S. Bhattacharyya (2016). "Do fewer males present to clinical high-risk services for psychosis relative to first-episode services?" Early Intervention in Psychiatry: n/a-n/a.
Winton-Brown, T. T., P. Fusar-Poli, M. A. Ungless and O. D. Howes (2014). "Dopaminergic basis of salience dysregulation in psychosis." Trends Neurosci **37**(2): 85-94.
Wisdom, J. P., J. I. Manuel and R. E. Drake (2011). "Substance use disorder among people with first-episode psychosis: a systematic review of course and treatment." Psychiatr Serv **62**(9): 1007-1012.
Wittmann, M. K., N. Kolling, R. Akaishi, B. K. H. Chau, J. W. Brown, N. Nelissen and M. F. S. Rushworth (2016). "Predictive decision making driven by multiple time-linked reward representations in the anterior cingulate cortex." Nature Communications **7**: 12327.
Wotruba, D., K. Heekeren, L. Michels, R. Buechler, J. J. Simon, A. Theodoridou, S. Kollias, W. Rossler and S. Kaiser (2014). "Symptom dimensions are associated with reward processing in unmedicated persons at risk for psychosis." Front Behav Neurosci **8**: 382.
Wu, C. C., G. R. Samanez-Larkin, K. Katovich and B. Knutson (2014). "Affective traits link to reliable neural markers of incentive anticipation." Neuroimage **84**: 279-289.
Yung, A. R., P. D. McGorry, C. A. McFarlane, H. J. Jackson, G. C. Patton and A. Rakkar (1996). "Monitoring and care of young people at incipient risk of psychosis." Schizophr Bull **22**(2): 283-303.
Yung, A. R., S. W. Woods, S. Ruhrmann, J. Addington, F. Schultze-Lutter, B. A. Cornblatt, G. P. Amminger, A. Bechdolf, M. Birchwood, S. Borgwardt, T. D. Cannon, L. de Haan, P. French, P. Fusar-Poli, M. Keshavan, J. Klosterkötter, J. S. Kwon, P. D. McGorry, P. McGuire, M. Mizuno, A. P. Morrison, A. Riecher-Rössler, R. K. R. Salokangas, L. J. Seidman, M. Suzuki, L. Valmaggia, M. van der Gaag, S. J. Wood and T. H. McGlashan (2012). "Whither the Attenuated Psychosis Syndrome?" Schizophrenia Bulletin **38**(6): 1130-1134.
Yung, A. R., H. P. Yuen, P. D. McGorry, L. J. Phillips, D. Kelly, M. Dell'Olio, S. M. Francey, E. M. Cosgrave, E. Killackey, C. Stanford, K. Godfrey and J. Buckby (2005). "Mapping the onset of psychosis: the Comprehensive Assessment of At-Risk Mental States." Aust N Z J Psychiatry **39**(11-12): 964-971.
Zendulka, O., G. Dovrtelová, K. Nosková, M. Turjap, A. Sulcová, L. Hanus and J. Jurica (2016). "Cannabinoids and cytochrome P450 interactions." Current drug metabolism **17**(3): 206-226.
Zhang, W.-N., S.-H. Chang, L.-Y. Guo, K.-L. Zhang and J. Wang (2013). "The neural correlates of reward-related processing in major depressive disorder: A meta-analysis of functional magnetic resonance imaging studies." Journal of Affective Disorders **151**(2): 531-539.
Zona, L. C., B. R. Fry, J. A. LaLonde and H. C. Cromwell (2017). "Effects of anandamide administration on components of reward processing during free choice." Pharmacology Biochemistry and Behavior **158**: 14-21.
Zuardi, A. W., S. L. Morais, F. S. Guimarães and R. Mechoulam (1995). "Antipsychotic effect of cannabidiol." The Journal of Clinical Psychiatry **56**(10): 485-486.

Appendices

Appendix 1

Supplementary References 1: Monetary Incentive Delay Task Analysis Consortium (MTAC) listed in alphabetical order

Abe, N, Barros-Loscertales, AR (Costumero et al. 2013), Bayer, J, Beck, A, Bjork, J, Boecker, R, Bustamante, JC (Bustamante et al. 2014), Choi, JS (Choi et al. 2012), Delmonte, S, Dillon, D, Figee, M, Gallagher, L, Garavan, H (Nestor et al. 2010), Hagele, C, Hermans, EJ, ICCAM Consortium, Ikeda, Y (Saji et al. 2013, Funayama et al. 2014), Kappel, V (Kappel et al. 2014), Kaufmann, C (Kaufmann et al. 2013), Lamm, C (Pfabigan et al. 2014), Lammertz, SE (Pfabigan et al. 2014), Li, Y (Li et al. 2014), Murphy, A, Nestor, L (Nestor et al. 2010), Pecina, M (Pecina et al. 2014), Pfabigan, D (Pfabigan et al. 2014), Pizzagalli, D, Rademacher L, Roee, A, Stark, R, Suzuki, H (Saji et al. 2013, Funayama et al. 2014), Van Amselvoort, T (da Silva Alves et al. 2011), Van Hell, E (van Hell et al. 2012, Jansma et al. 2013), Vink M (de Leeuw et al. 2015), Votinov, M, Wotruba, D

Supplementary Table 1. Available demographics for all 33 studies included in omnibus analysis including coordinate-based and group map data sources

Author	Country	Data (maps or coordinates)	n	Age (SD)	Male %	Right-handed %	Smoking	Alcohol	Drugs	Years education	FSIQ	SES	Ethnicity
De Leeuw (de Leeuw, Kahn et al. 2015)	Netherlands	Maps	29	30.3 (1.7)	41	100	1/29	n/a	3 CU last12/12	n/a	117 (3)	n/a	n/a
Bustamante (Bustamante, Barros-Loscertales et al. 2014)	Spain	Maps	18	37.4 (8.2)	100	100	n/a	n/a	0	9.56 (2.2)	n/a	n/a	n/a
Funayama (Funayama, Ikeda et al. 2014)	Japan	Maps	20	29.9 (n/a)	60	100	n/a	n/a	n/a	n/a	n/a	n/a	n/a
Kappel (Kappel, Lorenz et al. 2014)	Germany	Maps	20	23.7 (3.4)	100	100	6/20	304.3g/month ± 284.2	n/a	12.1 (1.4)	108 (11.3)	5.55	n/a
Li (Li, Sescousse et al. 2014)	France	Maps	20	31 (7.3)	100	100	0.1 (0.3) Fagerstrom test nicotine dependence	4.2 (3.5) Alcohol use disorders identification test	n/a	13.2 (1.7)	n/a	n/a	n/a
Pecina (Pecina, Martinez-Jauand et al. 2014)	USA	Maps	72	26 (4.24*)	53	n/a	n/a	<5 drinks/week	0	n/a	n/a	n/a	75% Caucasian, 18% African American
Pfabigan (Pfabigan, Seidel et al. 2014)	Austria	Maps	25	23.8 (3.6)	48	100	n/a	n/a	n/a	n/a	n/a	n/a	n/a
Costumero (Costumero,	Spain	Maps	44	23.4 (4.1)	100	98	n/a	n/a	0	13.8 (22)	n/a	n/a	n/a

Barros-Loscertales et al. 2013)													
Jansma (Jansma, van Hell et al. 2013)	Netherlands	Maps	11	21.2 (2.65*)	100	n/a	0.06 cigs/day	13.2u/week	22.6 times cannabis used in last year, other illicit 0.73	n/a	105 (1.5)	n/a	n/a
Kaufmann (Kaufmann, Beucke et al. 2013)	Germany	Maps	19	34.9 (11.8)	42	84	n/a	n/a	0 last 3/12	n/a	107 (12)	n/a.	n/a
Saji (Saji, Ikeda et al. 2013)	Japan	Maps	18	29.6 (6.94)	56	100	n/a	n/a	n/a	n/a	n/a	n/a	n/a
Choi (Choi, Shin et al. 2012)	Korea	Maps	15	26.6 (4.29)	100	100	9.3 cigs/day (8 smokers)	0	0	14.27 (1.4)	114 (7.1)	n/a	n/a
Van Hell (van Hell, Jager et al. 2012)	Netherlands	Maps	11	21.7 (2.3)	100	n/a	3 cigs/week (SD 8.4, 0-28)	16.7 U/week (SD 8.7, 2-40)	CU 17.9 times last 12/12 (SD 13.4, 5-52), other SU 1.3 /lifetime (SD 1.6, 0-4)	n/a	105 (6)	n/a	n/a
Da Silva Alves (da Silva Alves, Schmitz et al. 2011)	Netherlands	Maps	10	35.8 (10.4)	100	100	n/a	0	0	14.8 (2.3)	n/a	n/a	n/a
Nestor (Nestor, Hester et al. 2010)	Ireland	Maps	14	23.1 (4.49*)	79	100	10 cigs/day (SD 2.4), 15/30 days used (SD 4.2)	7.8 (SD 1.4)	CU 3 lifetime joints (SD 0.6); hallucinogenic x2 lifetime (SD 0.4); MDMA 3.6 lifetime use (SD 0.9); cocaine 4.8 lifetime (SD 0.3); amphetamine 3.3 lifetime (SD 1.2)	16.1 (0.4)	123 (0.8)	n/a	n/a
Damiano (Damiano, Aloi et al. 2014)	USA	Coords	31	23.58 (3.15)	45	100	n/a	n/a	n/a	n/a	109 (2.46)	n/a	Non-Hispanic Caucasian, USA

Balodis (Balodis, Kober et al. 2012)	USA	Coords	14	37.1 (11.3)	71	93	2 current smokers	no past alcohol abuse/dependence	monitored prescan	n/a	107 (13.2)	n/a	n/a
Enzi (Enzi, Edel et al. 2012)	Germany	Coords	15	34.7 (8.3)	53	100	n/a	n/a	n/a	14.94 (1.9)	n/a	n/a	n/a
Wu (Wu, Samanez-Larkin et al. 2014)	USA	Coords	49	50 (16.5)	47	106	n/a	n/a	n/a	n/a	n/a	n/a	n/a
Kirk (Kirk, Brown et al. 2014)	USA	Coords	44	36.5 (9.7)	45	n/a	n/a	n/a	n/a	15.2 (1.7)	n/a	2.7 (see note)	n/a
Romanczuk-Seiferth (Romanczuk-Seiferth, Koehler et al. 2014)	Germany	Coords	17	37.41 (11.76)	100	n/a	8.03±8.30 cigarettes/day	134.50±151.51 grams of alcohol 7 month	no drug dependence	11.35 (1.5)	n/a	n/a	n/a
Weiland (Weiland, Heitzeg et al. 2014)	USA	Coords	12	30.9 (9)	0	100	"non-smoking"		no substance abuse/dependence, exposure last 6/12 to CNS prescription or illicit drug	n/a	n/a	n/a	n/a
Treadway (Treadway, Buckholtz et al. 2013)	USA	Coords	38	22 (4**)	53	n/a	n/a	n/a	n/a	n/a	n/a	n/a	n/a
Vaidya (Vaidya, Knutson et al. 2013)	USA	Coords	18	27.72 (1.36)	50	100	n/a	n/a	n/a	n/a	n/a	n/a	n/a
Ossewaarde (Ossewaarde, Verkes et al. 2011)	Netherlands	Coords	19	24.6 (7.1)	47	n/a	n/a	n/a	monitored prescan	n/a	n/a	n/a	n/a
Ossewaarde (Ossewaarde, Qin et al. 2011)	Netherlands	Coords	13	20 (1.8)	0	100	n/a	n/a	n/a	n/a	n/a	n/a	n/a
Beck (Beck, Schlagenhauf et al. 2009)	Germany	Coords	19	41.68 (8.97)	100	100	9.68 cigs/day (sd8.65)	4.06kg pure alcohol/year (SD 4.27)	n/a	11.65 (1.7)	108 (7.91)	6.06	n/a

Knutson (Knutson, Fong et al. 2003)	USA	Coords	12	31 (n/a)	50	100	n/a	n/a	n/a	n/a	n/a	n/a	n/a
De Greck (de Greck, Scheidt et al. 2011)	Germany	Coords	20	37 (10.6)	40	80	n/a	n/a	n/a	n/a	n/a	n/a	n/a
Spreckelmeyer (Spreckelmeyer, Krach et al. 2009)	Germany	Coords	32	28.5 (7.25**)	50	100	"non-smoking"	n/a	n/a	n/a	n/a	n/a	n/a
Knutson (Knutson, Bhanji et al. 2008)	USA	Coords	12	28.67 (4.25)	33	n/a	n/a	No alcohol abuse last 6/12, no Hx alcohol dependence	no substance abuse last 6/12, no Hx substance dependence	n/a	n/a	n/a	n/a
Knutson (Knutson, Fong et al. 2001)	USA	Coords	9	26.45 (5.85)	22	100	n/a	n/a	n/a	n/a	n/a	n/a	n/a
Knutson (Knutson, Adams et al. 2001)	USA	Coords	8	31 (n/a)	50	100	n/a	n/a	n/a	n/a	n/a	n/a	n/a

SD (standard deviation), FSIQ (full scale intelligence quotient), SES (socioeconomic status), CU (cannabis use)

Supplementary Table 2: Monetary incentive delay task parameters for all 33 studies included in omnibus analysis including coordinate-based and group map data sources

Author	monetary incentive	Placebo	Trial duration /ms	No. trials	Task duration /s	t stimulus /ms	t anticipation /ms	t target /ms	t delay /ms	t feedback /ms	t inter stimulus interval /ms	Planned hit rate %	Contrasts (-vs-neutal)
De Leeuw (de Leeuw, Kahn et al. 2015)	€1	N	9571	60	575	750	779-6729	.	.	.	1029-6979	50	AW, FWH, FWM
Bustamante (Bustamante, Barros-Loscertales et al. 2014)	€0.2, 3	N	8000	120	960	500	2000-2250	100	2000-4000	1500	2000-4000	75	AW, AL,
Funayama (Funayama, Ikeda et al. 2014)	¥20, 100, 500	Y (2 week washout)	.	180	.	2000	2000-2500	160-470	1130-1940	1900	.	66	AW, AL, FWH, FWM, FLH, FLM
Kappel (Kappel, Lorenz et al. 2014)	*0.2, 1, 5	N	6000	144	1320	250	2000-2500	160-260	.	1650	.	66	AW
Li (Li, Sescousse et al. 2014)*	€1,2,3,10,11,12	N	.	171	.	2500	1500-4500	1000	.	1500	2000-5000	.	AW, FWH, FWM
Pecina (Pecina, Martinez-Jauand et al. 2014)	USD $0.2, 1, 5	N	6000	144	.	.	.	.	.	.	.	.	AL
Pfabigan (Pfabigan, Seidel et al. 2014)	€2	N	.	100	.	1000	2000-2500	264+/-		1000	3000-7000	50	AW, AL
Costumero (Costumero, Barros-Loscertales et al. 2013)	€0.2, 3	N	.	120	960	500	2000-2250	100	2000-4000	1500	2000-4000	.	AW, AL
Jansma (Jansma, van Hell et al. 2013)	€0.1, 5	Y (2 week washout)	.	44	711	500	4300-10300	280+/-	.	1000	1000-21000	50	AWS, AL,

Kaufmann (Kaufmann, Beucke et al. 2013)	€0.1, 0.6, 3	N	11600	144	696	250	3740-4240	150-500	1420-1720	1870	3280-3780	66	AW, AL, FWH, FWM, FLH, FLM
Saji (Saji, Ikeda et al. 2013)	¥0, 100, 300	Y (1 week washout)	4370	144	780	250	2000-2500	160-260	.	1650	1000	66	AW, AL
Choi (Choi, Shin et al. 2012)	~~₩~~1000	N	.	.	1076.4	350	4180-4480	200-500	.	1500	5170-9850	.	AW, AL
Van Hell (van Hell, Jager et al. 2012)	€0, 2	Y (2 week washout)	8000	48	.	.	4300-10300	.	.	.	0-30000	50	AW, FWH
Da Silva Alves (da Silva Alves, Schmitz et al. 2011)	€0.2, 1, 5	Y (8 day washout	6000	144	6000	250	2000-2500	160-260	.	1650	5000	66	AW, AL
Nestor (Nestor, Hester et al. 2010)	€0, 0.5	N	6000-18000	81	1020	2000-8000 (stimulus merged with anticipation)		400	.	1500	2000-8000	50	AW, AL, FWH, FWM, FLH, FLM
Damiano (Damiano, Aloi et al. 2014)	USD $1	N	12000	80	.	2000	2000-2500	500	.	3000	.	67	AW
Balodis (Balodis, Kober et al. 2012)	USD $1, 5	N	12000	110	1200	1000	3000-5000	.	4000-6000	1200	.	66	AW, AL
Enzi (Enzi, Edel et al. 2012)	€0.1, 0.6, 3	N	.	90	.	250	3740-4240	160-360	1500-2200	1650	4000	67	AW, AL
Wu (Wu, Samanez-Larkin et al. 2014)	USD $0.50, 5	N	10000	90	.	2000	2000-2500	150-500	.	2000	2000-6000	66	AW, AL
Kirk (Kirk, Brown et al. 2014)	USD $0, 1, 5	N	2500	96	.	2500	2000-2500	160-260	500	2000	1000-1500	66	AW, AL
Romanczuk-Seiferth (Romanczuk-Seiferth, Koehler et al. 2014)	€1	N	9500	75	712.5	500	2000-4500	150-500	1000-3000	1500	4000-7000	67	AW, AL
Weiland (Weiland, Heitzeg et al. 2014)	USD $0.20, 1, 5	N	6000	72	2x300	2000	2000	200-300	1700-1800	.	.	66	AW

Treadway (Treadway, Buckholtz et al. 2013)	USD $0.2, 1, 5	N	.	180	4x464	1000	2000-2500	160-260	.	1650	.	66	AW, AL, FWH, FLM
Vaidya (Vaidya, Knutson et al. 2013)	USD $.20, $1 and $5.00		.	162	3x600	.	.	.	.	.	4000	66	AW
Ossewaarde (Ossewaarde, Verkes et al. 2011)	€1	N	10000 (mean)	50	750	3500-8500 (stimulus merged with anticipation)		150-500 (+10ms if previous miss, -20ms if previous hit))	1200-5300	500	.	33	AW
Ossewaarde (Ossewaarde, Qin et al. 2011)	€1	N	10000 (mean)	50	750	3500-8500 (stimulus merged with anticipation)		150-500 (+10ms if previous miss, -20ms if previous hit))	1200-5300	500	.	33	AW
Beck (Beck, Schlagenhauf et al. 2009)	€0.1, 0.6, 3	N	7690	144	840	250	2250-2750	200-1000	.	1650	3530	67	AW, AL
Knutson (Knutson, Fong et al. 2003)	USD $0.20, 1, 5	N	6000	144	2x432	250	2000-2500	160-260	.	1650	.	66	AW, AL
De Greck (de Greck, Scheidt et al. 2011)	€1	N	.	180	1890	250	2250-2750	200-500	.	1650	4000-5000	66	AW
Spreckelmeyer (Spreckelmeyer, Krach et al. 2009)	€0.20, 1, 3	N	.	88	840	240	2250-2750	160-260	.	1650	2500-5000	66	AW
Knutson (Knutson, Bhanji et al. 2008)	USD $0.20, 1, 5	N	6000	180	1080	250	2000-2500	160-360	.	1650	.	66	AW, AL
Knutson (Knutson, Fong et al. 2001)	USD $1	N	6000	54	324	250	2000-2500	160-260	.	1650	.	66	AW
Knutson (Knutson, Adams et al. 2001)	USD $0.20, 1, 5	N	6000	144	2x600	250	2000-2500	160-260	.	1650	.	66	AW, AL

* uncertainty included in anticipation (probability of reward if successful 25, 75, 100%, and 'low' or 'high' intensity monetary reward), reaction to target based on visual discrimination within fixed time, not speed reaction time; AW (anticipation win), AL (anticipation lose), FWH (feedback win hit), FWM (feedback win miss), FLH (feedback lose hit), FLM (feedback lose miss)

Supplementary Table 3: fMRI data acquisition and analysis parameters for all 33 studies included in omnibus analysis including coordinate-based and group map data sources

	Scanner	**Sequence**	**Strength /Tesla**	**TR /ms**	**TE /ms**	**Software**	**FWHM /mm**	**No. slices**	**Slice thickness /mm**	**Resolution (resampled)**	**Corrected**	**Threshold**
De Leeuw (de Leeuw, Kahn et al. 2015)	Philips Achieva	2D EPI-SENSE (sensitivity encoding)	3	1600	23	SPM5	8	30	.	4mm isotropic voxel	n/a	n/a
Bustamante (Bustamante, Barros-Loscertales et al. 2014)	Siemens Avanto	T2 * gradient	1.5	2000	30	SPM8	8	30	3.5	(3x3x3mm)	n/a	n/a
Funayama (Funayama, Ikeda et al. 2014)	Phillips Electronics Intera Achieva Nova	GE-EPI	1.5	2000	40	SPM8	8	28	5	(2x2x2mm)	n/a	n/a
Kappel (Kappel, Lorenz et al. 2014)	GE Signa	T2*-weighted in-/out-spiral pulse	3	2300	27	SPM8	.	29	.	.	n/a	n/a
Li (Li, Sescousse et al. 2014)	Siemens Sonata	GE-EPI	1.5	2500	60	SPM2	10	26	.	3.4x3.4x4mm	n/a	n/a
Pecina (Pecina, Martinez-Jauand et al. 2014)	General Electric Signa	T2* weighted pulse sequence (single-shot combined spiral in/out, GE)	3	2000	30	SPM8	6	29	4	.	n/a	n/a
Pfabigan (Pfabigan, Seidel et al. 2014)	Siemens TIMTrio	Gradient-recalled EPI-sequence with distortion correction	3	1800	38	SPM8	8	23	.	1.5x1.5x3mm	n/a	n/a
Costumero (Costumero, Barros-	Siemens Avanto	EPI	1.5	2000	30	SPM5	6	30	3.5	($3mm^3$)	n/a	n/a

Loscertales et al. 2013)												
Jansma (Jansma, van Hell et al. 2013)	Philips Achieva	SENSE PRESTO	3	22.5	33.2	SPM5	8	40	.	4mm isotropic voxel	n/a	n/a
Kaufmann (Kaufmann, Beucke et al. 2013)	Siemens Sonata	GE-EPI	1.5	1870	40	SPM8	8	33	.	3x3x3.5mm	n/a	n/a
Saji (Saji, Ikeda et al. 2013)	Phillips Electronics Intera Achieva Nova	GE-EPI	1.5	2000	40	SPM8	8	28	5	(2x2x2mm)	n/a	n/a
Choi (Choi, Shin et al. 2012)	Siemens Avanto	GE-EPI	1.5	2340	52	SPM8	4	25	.	(3x3x3mm)	n/a	n/a
Van Hell (van Hell, Jager et al. 2012)	Philips Achieva with Quasar dual gradient set	SENSE-PRESTO echo-shifting sequence	3	22.5	33.2	SPM5	8	40	.	4mm isotropic voxel	n/a	n/a
Da Silva Alves (da Silva Alves, Schmitz et al. 2011)	Philips Intera	T2*-weighted GE-EPI	3	2000	30	SPM5	8	35	3	3x3x3mm	n/a	n/a
Nestor (Nestor, Hester et al. 2010)	Philips Intera Achieva	T2* weighted EPI	3	2000	35	AFNI	3mm isotropic rms Gaussian kernel	32	3.5	.	n/a	n/a
Damiano (Damiano, Aloi et al. 2014)	General Electric Health Technologies 3-T MR750 scanner	SENSE spiral pulse sequence	3	2000	30	Preprocessing-FEAT, MCFLIRT, FLIRT, FMRIB's Improved Linear Model, whole brain FLAME (FMRIB Local Analysis of Mixed Effects)	5	32	.	$4mm^3$	Corrected	Clusterwise Z>5.25, 'corrected' significance P<0.05
Balodis (Balodis, Kober et al. 2012)	Siemens 3 Tesla scanner (Trio; Siemens AG)	T2*-weighted BOLD sequence	3	1500	27	SPM5	6	25	4	.	Corrected	AlphaSim combined cluster & voxelwise FWE P<0.05

Enzi (Enzi, Edel et al. 2012)	1.5 Siemens Magnetom Symphony (standard imaging head coil)	EPI	1.5	1900	45	SPM5	8	22	.	(3×3×3mm)	Corrected	Voxelwise FDR p<0.05
Wu (Wu, Samanez-Larkin et al. 2014)	General Electric	T2*-sensitive spiral in/out pulse sequence	1.5	2000	40	AFNI	4	24	4	3.75x3.75mm (inplane resolution)	Uncorrected	p<0.001, k>16
Kirk (Kirk, Brown et al. 2014)	Siemens Trio	EPI	3	2000	25	SPM8	8	37	4	3.4x3.4x4.0mm	Corrected	FDR p<0.01, k>10
Romanczuk-Seiferth (Romanczuk-Seiferth, Koehler et al. 2014)	Siemens Magnetom TIM Trio	GE-EPI	3	2500	35	SPM8	8	39	.	3.5x3.5x3mm	Uncorrected	P<0.001, k>10
Weiland (Weiland, Heitzeg et al. 2014)	General Electric Signa	T2*-weighted single shot combined spiral in/out sequences	3	2000	30	SPM8	6	29	4	.	Corrected	Clusterwise FDR p<0.001
Treadway (Treadway, Buckholtz et al. 2013)	Phillips Achieva	GE-EPI	3	2000	25	SPM5	6	30	2.5	(2mm isotropic voxel)	Corrected	SPM5 cluster correction procedure p<0.05
Vaidya (Vaidya, Knutson et al. 2013)	Siemens Trio	EPI	3	2000	30	AFNI	4	27	3.75	3.75x3.75mm inplane resolution (2mm isotropic voxel)	Corrected	Monte Carlo simulations using AFNI 3dAlphaSim (uncorrected p<0.005, k>89) corrected alpha of 0.05
Ossewaarde (Ossewaarde, Verkes et al. 2011)	Siemens Avanto	GE-EPI	1.5	2340	35	SPM5	8	32	3.5	(2x2x2mm)	Corrected	FWE corrected p<0.05
Ossewaarde (Ossewaarde, Qin et al. 2011)	Siemens TIM Trio	GE-EPI	3	1890	25	SPM5	8	37	3	(2x2x2mm)	Corrected	FWE corrected p<0.001

Beck (Beck, Schlagenhauf et al. 2009)	Siemens Magnetom Vision	GE-EPI	1.5	1870	40	SPM5	8	18	.	4x4x3.3mm	Uncorrected	P<0.001, k>10
Knutson (Knutson, Fong et al. 2003)	General Electric MRI scanner (standard quadrature head coil)	GE	1.5	2000	40	AFNI	4	22	3.8	3.75x3.75mm inplane resolution	Uncorrected	p<0.0001
De Greck (de Greck, Scheidt et al. 2011)	General Electric Sigma Horizon (standard circular polarized head coil)	GE-EPI	1.5	2000	35	AFNI	.	23	5	.	Corrected	FDR p<0.0005, k>15
Spreckelmeyer (Spreckelmeyer, Krach et al. 2009)	Phillips Medical Systems, Achieva	EPI	1.5	2000	50	SPM5	6	22	3.8	4x4x4mm	Corrected	FWE p<0.05
Knutson (Knutson, Bhanji et al. 2008)	General Electric MRI scanner (standard quadrature head coil)	T2*-sensitive in-/out- spiral pulse sequence	1.5	.	40	AFNI	4	24	4	$4mm^3$	Uncorrected	P<0.0001
Knutson (Knutson, Fong et al. 2001)	General Electric MRI scanner (standard quadrature head coil)	GE	1.5	2000	40	AFNI	4	16	7	3.75x3.75mm (inplane resolution)	Uncorrected	P<0.0001
Knutson (Knutson, Adams et al. 2001)	General Electric MRI scanner (standard quadrature head coil)	GE	1.5	2000	40	AFNI	4	16	3.8	3.75x3.75mm (inplane resolution)	Uncorrected	P<0.05

TR (acquisition time), TE (echo time), FWHM (full width at half maximum), FWE (family-wise error corrected), FDR (false discovery rate)

Supplementary Figure 1: Funnel plots for the highest peaks in AWAN and ALAN with Egger's test for asymmetry

Anticipation win-vs-neutral: peak 1 for all 33 studies included in omnibus analysis including coordinate-based and group map data with effect size on the x-axis, standard error on the y-axis and Egger's test beneath

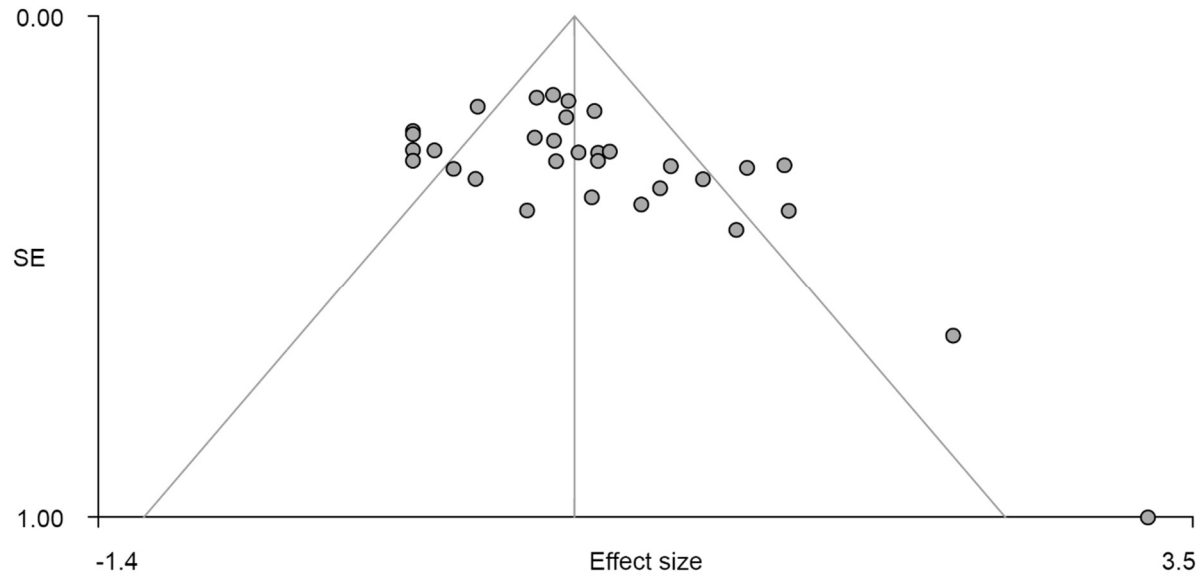

Egger test: Bias: 2.64, t: 2.90, df: 30, **p=0.007**

Anticipation win-vs-neutral: peak 1 for all 14 studies involving group map data with effect size on the x-axis, standard error on the y-axis and Egger's test beneath

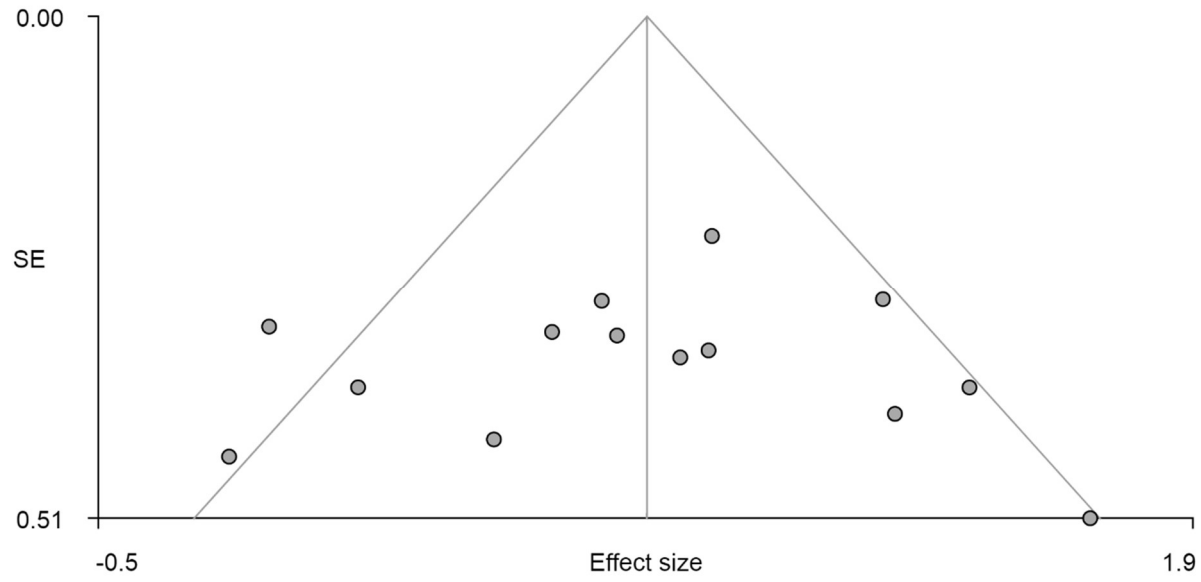

Egger test: Bias: -0.23, t: -0.12, df: 12, p=0.910

Anticipation win-vs-neutral: peak 2 for all 33 studies included in omnibus analysis including coordinate-based and group map data with effect size on the x-axis, standard error on the y-axis and Egger's test beneath

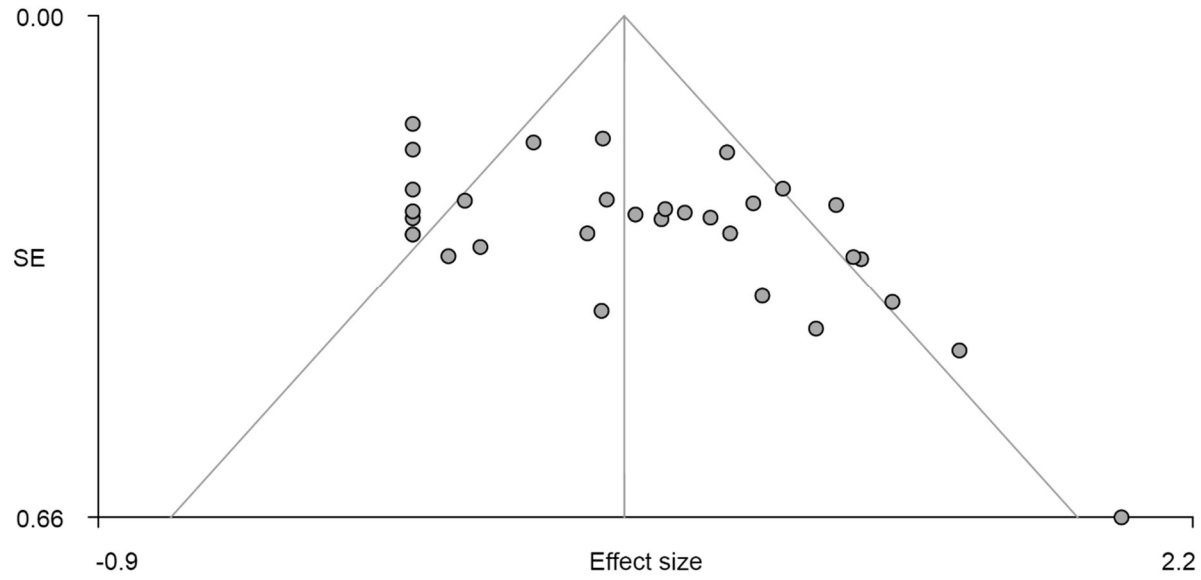

Egger test: Bias: 2.96, t: 2.97, df: 30, **p=0.006**

Anticipation win-vs-neutral: peak 2 for all 14 studies involving group map data with effect size on the x-axis, standard error on the y-axis and Egger's test beneath

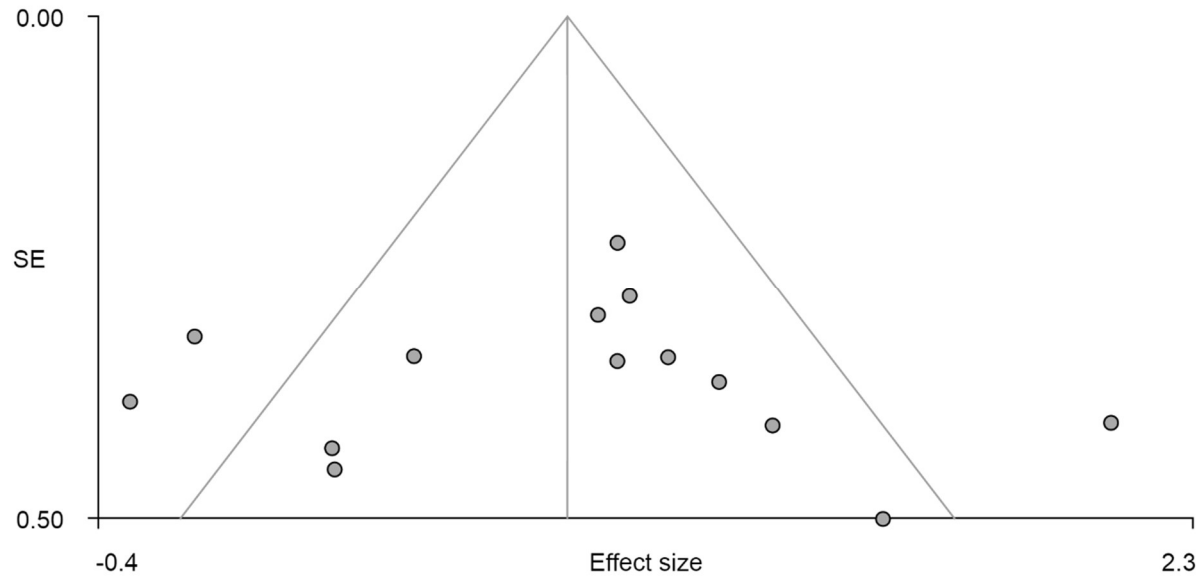

Egger test: Bias: 0.24, t: 0.10, df: 12, p=0.919

Anticipation lose-vs-neutral: peak 1 for all 33 studies included in omnibus analysis including coordinate-based and group map data with effect size on the x-axis, standard error on the y-axis and Egger's test beneath

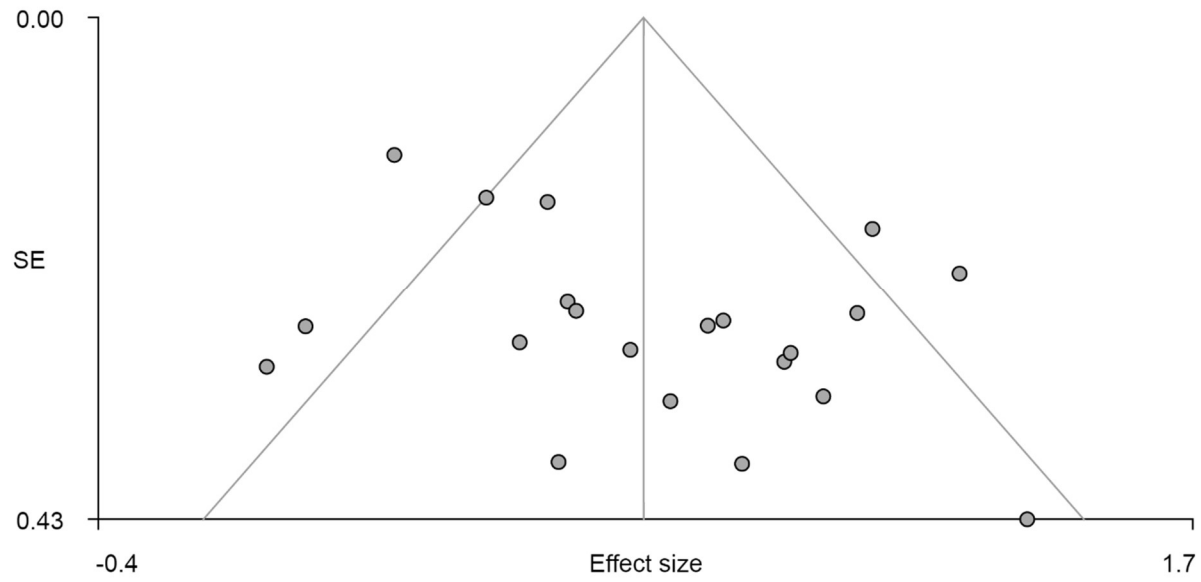

Egger test: Bias: 2.09, t: 2.08, df: 19, **p=0.051**

Anticipation lose-vs-neutral: peak 1 for all 11 studies involving group map data with effect size on the x-axis, standard error on the y-axis and Egger's test beneath

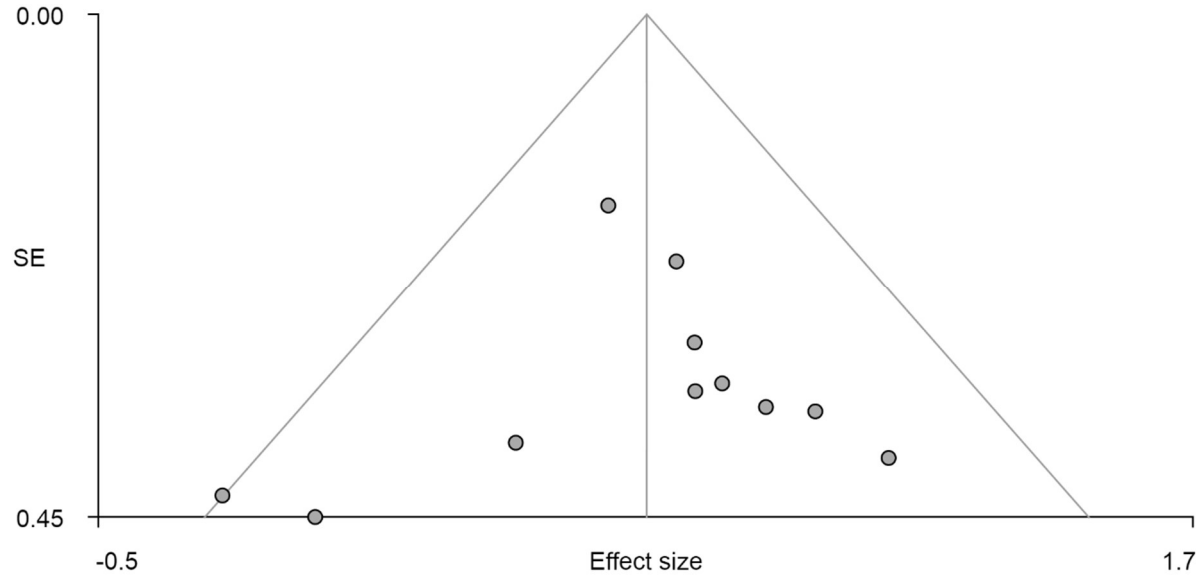

Egger test: Bias: -0.36, t: -0.36, df: 9, p=0.731

Supplementary Table 4: Omnibus results for text coordinates and maps combined- main peaks

Anticipation win-vs-neutral maps/text activation main peaks

Peak MNI coordinate	SDM-z	P	FDR	Voxels	Anatomical Description	Egger's test p
-14,10,0	8.552	~0	0	15262	Left fundus region of putamen	**0.007**
0,8,44	7.131	~0	0	5872	Right anterior cingulate	**0.006**
12,-64,6	5.062	~0	0	839	Right striate area	0.960
-24,-36,-26	4.603	0.000196099	0.000484	401	Left cerebellum anterior lobe, culmen*	0.928
-58,-14,22	4.505	0.000356078	0.000738	86	Left postcentral gyrus	0.723
52,0,42	4.113	0.002441049	0.003262	79	Right precentral gyrus	0.124
26,-6,62	4.044	0.003349364	0.003965	26	Right superior frontal gyrus lateral part	0.174
40,54,10	4.062	0.00312227	0.003785	21	Right middle frontal gyrus	0.691
-20,-48,-34	4.082	0.002843618	0.003625	11	Left cerebellum, anterior lobe*	0.505
-10,-24,40	3.967	0.00459826	0.004789	10	Left paracentral lobule	0.066
44,-6,52	3.968	0.004567325	0.004789	10	Right middle frontal gyrus	0.313

MNI (Montreal Neurological Institute), SDM-z (Signed Differential Mapping z-score), FDR (false discovery rate), *Talairach client

Anticipation win-vs-neutral maps/text deactivation main peaks

Peak MNI coordinate	SDM-z	P	FDR	Voxels	Anatomical Description	Egger's test p
-52,-64,36	-3.723	~0	0	5546	Left angular gyrus	0.405
-22,24,48	-2.503	~0	0	4953	Left superior frontal gyrus, lateral part	0.917
56,-62,30	-3.417	~0	0	1901	Right superior temporal gyrus	0.149
10,-52,30	-2.521	~0	0	1980	Right posterior cingulate	0.486
-48,34,-12	-2.59	~0	0	1094	Left inferior frontal gyrus, orbital part	0.936
62,-4,-18	-1.555	~0	0	1542	Right middle temporal gyrus*	0.734
40,-12,14	-1.249	0.000005186	0.00000583	129	Right precentral gyrus	0.381
-28,-14,-24	-1.001	0.000010312	0.0000103	76	Left parahippocampal gyrus	0.770
0,-38,72	-1.226	0.000005186	0.00000583	76	Right postcentral gyrus*	0.789

MNI (Montreal Neurological Institute), SDM-z (Signed Differential Mapping z-score), FDR (false discovery rate), *nearest grey matter structure

Anticipation lose-vs-neutral maps/text activation all peaks

Peak MNI coordinate	SDM-z	P	FDR	Voxels	Anatomical Description	Egger's test p
16,8,10	7.27	~0	0	12127	Right medial caudate/putamen	**0.051**
-6,16,22	6.273	~0	0	3500	Left anterior cingulate gyrus	0.554
-14,-72,38	4.362	0.00023222	0.000483	593	Left parieto-occipital transition zone	0.270
-6,-62,4	4.085	0.000851512	0.001352	367	Left occipital gyrus	0.786
-30,-58,-8	4.674	0.000067115	0.000181	204	Left fusiform gyrus	0.343
20,-68,42	4.251	0.000376761	0.000659	190	Right superior parietal lobule	0.301
48,-2,42	3.841	0.002002418	0.002313	154	Right precentral gyrus	0.052
34,52,4	4.267	0.000361264	0.000655	88	Right middle frontal gyrus	0.595
4,-54,-10	3.88	0.001728892	0.002147	58	Right Cerebellum, Anterior Lobe, Culmen*	0.097
38,46,20	3.842	0.001986921	0.002313	41	Right middle frontal gyrus	**0.049**
52,12,32	4.055	0.000985742	0.001518	38	Right inferior frontal gyrus, opercular part	0.441
22,-44,-8	3.93	0.001398563	0.001906	37	Right fusiform gyrus	0.854
30,-82,14	3.913	0.00151211	0.001973	30	Right occipital gyri	0.161
10,-78,12	3.847	0.001940489	0.002313	29	Right striate area	0.158
24,-80,28	3.798	0.002353311	0.002665	28	Right parieto-occipital transition zone	0.446
26,-20,-8	4.735	0.000046432	0.000135	17	Right claustrum	0.965
-50,-36,38	3.675	0.003643513	0.003712	11	Left supramarginal gyrus	0.104

MNI (Montreal Neurological Institute), SDM-z (Signed Differential Mapping z-score), FDR (false discovery rate), *Talairach client

Anticipation lose-vs-neutral maps/text deactivation all peaks

Peak MNI coordinate	SDM-z	P	FDR	Voxels	Anatomical Description	Egger's test p
-26,26,48	-2.168	~0	0	4534	Left middle frontal gyrus	0.779
-52,-66,32	-2.877	~0	0	*2334*	Left superior temporal gyrus	0.174
58,-62,28	-2.943	~0	0	2031	Right superior temporal gyrus	0.553
-6,-60,28	-2.178	~0	0	1925	Left precuneus	0.194
-60,-12,-16	-1.663	0.000005186	0.0000178	1081	Left middle temporal gyrus	0.410
60,0,-18	-1.515	0.000020623	0.0000527	615	Right middle temporal gyrus	0.792
-44,38,-18	-1.776	0.000005186	0.0000178	394	Left inferior frontal gyrus, orbital part*	0.739
2,-56,66	-1.557	0.000010312	0.0000334	406	Right precuneus	**0.048**
-16,-16,-26	-1.45	0.000025809	0.0000619	110	Left entorhinal cortex	0.097
34,38,-12	-1.12	0.000185788	0.00031	60	Right lateral orbital gyrus	0.497

MNI (Montreal Neurological Institute), SDM-z (Signed Differential Mapping z-score), FDR (false discovery rate), *nearest grey matter structure

Supplementary Table 5: Only Group Map Results

Anticipation win-vs-neutral activation maps only all peaks

Peak MNI coordinate	SDM-z	P	FDR	Voxels	Anatomical Description	Egger's test p
2,0,62	9.798	~0	0	25114	Right superior frontal gyrus, lateral part	0.910

MNI coordinate	SDM-Z	P	FDR		Description
-2,6,46	9.655	~0		0	Left anterior cingulate
-56,2,34	8.871	~0		0	Left precentral gyrus
-10,-4,54	8.749	~0		0	Left paracentral lobule
10,6,52	8.711	~0		0	Right superior frontal gyrus medial part
-56,2,24	8.652	~0		0	Left precentral gyrus
10,6,12	8.605	~0		0	Right medial caudate
8,14,2	8.554	~0		0	Right nucleus accumbens
-12,-2,50	8.511	~0		0	Left superior frontal gyrus medial part
10,12,6	8.417	~0		0	Right medial caudate
-10,4,14	8.416	~0		0	Left medial caudate
-22,4,8	8.362	~0		0	Left putamen
-14,6,12	8.268	~0		0	Left medial caudate
-56,0,40	8.261	~0		0	Left precentral gyrus
-12,10,34	8.153	~0		0	Left anterior cingulate
26,2,8	8.152	~0		0	Right putamen
-22,-2,54	8.145	~0		0	Left superior frontal gyrus lateral part
24,2,0	8.013	~0		0	Right putamen
-38,-10,42	7.988	~0		0	Left middle frontal gyrus
-4,8,6	7.937	~0		0	Left fundus region of caudate
-18,20,2	7.92	~0		0	Left putamen
-58,-18,44	7.837	~0		0	Left postcentral gyrus
-22,14,0	7.82	~0		0	Left putamen
-22,12,-4	7.758	~0		0	Left prepiriform claustrum
2,-28,-2	7.699	~0		0	Right periaqueductal grey matter*
-18,6,-2	7.661	~0		0	Left putamen
-54,-4,44	7.575	~0		0	Left precentral gyrus
-26,-24,58	7.524	~0		0	Left postcentral gyrus
-28,-24,64	7.456	~0		0	Left postcentral gyrus
14,-8,14	7.322	~0		0	Right medial caudate
-30,24,10	7.274	~0		0	Left insular gyrus
-6,4,34	7.252	~0		0	Left anterior cingulate
4,-28,-10	7.223	~0		0	Right pretectal area
-18,-66,36	7.217	~0		0	Left precuneus
22,-4,-4	7.167	~0		0	Right putamen
10,12,44	7.136	~0		0	Right superior frontal gyrus medial part
-6,16,26	7.121	~0		0	Left anterior cingulate
-12,8,0	6.997	~0		0	Left fundus region of caudate
-46,-8,54	6.9	~0		0	Left precentral gyrus

-16,14,0	6.888	~0	0	Left reticular thalamic nucleus*
38,2,14	6.876	~0	0	Right frontal operculum
-32,-44,62	6.864	~0	0	Left superior parietal lobule
-52,-10,50	6.838	~0	0	Left precentral gyrus
-30,-40,44	6.828	~0	0	Left postcentral gyrus
-38,-4,52	6.823	~0	0	Left middle frontal gyrus
-54,-14,20	6.82	~0	0	Left parietal operculum
30,-4,48	6.812	~0	0	Right middle frontal gyrus
34,-2,48	6.786	~0	0	Right middle frontal gyrus
38,-2,50	6.773	~0	0	Right middle frontal gyrus
-30,-8,66	6.728	~0	0	Left superior frontal gyrus lateral part
-14,-78,40	6.706	~0	0	Left parieto-occipital transition zone
14,-22,64	6.642	~0	0	Right precentral gyrus
-32,-14,66	6.619	~0	0	Left precentral gyrus
30,-26,48	6.61	~0	0	Right precentral gyrus
-42,-28,58	6.593	~0	0	Left postcentral gyrus
-38,-32,56	6.591	~0	0	Left postcentral gyrus
-26,2,46	6.591	~0	0	Left middle frontal gyrus
36,-20,40	6.584	~0	0	Right postcentral gyrus
-10,-16,14	6.574	~0	0	Left ventral lateral posterior thalamic
-34,-34,62	6.567	~0	0	Left postcentral gyrus
46,-4,52	6.562	~0	0	Right middle frontal gyrus
24,-70,6	6.552	~0	0	Right occiptal gyri
-26,-32,54	6.534	~0	0	Left postcentral gyrus
-8,-26,12	6.517	~0	0	Left medial dorsal thalamic nucleus
-18,-74,40	6.505	~0	0	Left parieto-occipital transition zone
-12,-30,60	6.498	~0	0	Left precentral gyrus
-2,0,12	6.486	~0	0	Left medial septal nucleus
-14,-24,12	6.471	~0	0	Left pulvinar
-48,-24,48	6.447	~0	0	Left postcentral gyrus
6,-30,-18	6.435	~0	0	Right cerebellum anterior lobe culmen**
-54,-22,44	6.352	~0	0	Left posterior central gyrus
14,-14,40	6.332	~0	0	Right posterior cingulate
-10,-12,8	6.275	~0	0	Left ventral anterior thalamic nucleus
20,18,-8	6.187	~0	0	Right posterior orbital gyrus
-12,-34,66	6.181	~0	0	Left postcentral gyrus
2,-16,-2	6.179	~0	0	Right ventral anterior thalamic nucleus**
10,-40,-14	6.152	~0	0	Right cerebellum anterior lobe culmen**
-2,-18,52	6.133	~0	0	Left paracentral lobule
-24,4,66	6.114	~0	0	Left superior frontal gyrus lateral part
24,-74,22	6.098	~0	0	Right precuneus
-42,0,10	6.09	~0	0	Left frontal operculum
8,34,30	6.081	~0	0	Right anterior cingulate
-48,-20,56	6.067	~0	0	Left postcentral gyrus
-2,-30,-20	6.06	~0	0	Left cerebellum anterior lobe culmen**
14,-32,60	6.047	~0	0	Right postcentral gyrus

-46,-34,40	6.039	~0	0	Left supramarginal gyrus
-26,-76,28	6.023	~0	0	Left parieto-occipital transition zone
-6,-34,-14	6.009	~0	0	Left cerebellum anterior lobe culmen**
44,-6,58	5.991	~0	0	Right middle frontal gyrus
12,-30,56	5.963	~0	0	Right precentral gyrus
14,-32,64	5.952	~0	0	Right postcentral gyrus
26,-6,58	5.948	~0	0	Right superior frontal gyrus
30,-54,38	5.948	~0	0	Right superior parietal lobule
-12,-20,0	5.921	~0	0	Left paracentral lobule
14,-44,-18	5.905	~0	0	Right cerebellum anterior lobe culmen**
-8,-32,54	5.889	~0	0	Left precenral gyrus
-48,-36,52	5.865	~0	0	Left supramarginal gyrus
-10,-36,52	5.85	~0	0	Left paracentral lobule
-40,-34,42	5.824	~0	0	Left supramarginal gyrus
-28,-6,4	5.809	~0	0	Left putamen
8,-20,10	5.807	~0	0	Right medial dorsal thalamic
38,-66,16	5.738	~0	0	Right middle temporal gyrus
-4,-26,64	5.711	~0	0	Left paracentral lobule
-34,4,4	5.709	~0	0	Left claustrum
6,14,26	5.699	~0	0	Right anterior cingulate
-16,-60,52	5.62	~0	0	Left superior parietal lobule
-60,2,12	5.615	~0	0	Left precentral gyrus
-18,-14,22	5.594	~0	0	Left caudate
28,-54,52	5.57	~0	0	Right superior parietal lobule
30,-76,26	5.566	~0	0	Right angular gyrus
-24,-56,48	5.543	~0	0	Left superior parietal lobule
48,-18,40	5.473	~0	0	Right precentral gyrus
-52,2,0	5.458	~0	0	Left planum polare
-18,-10,20	5.443	~0	0	Left caudate
54,12,32	5.423	~0	0	Right inferior frontal gyrus opercular part
-18,-16,70	5.421	~0	0	Left precentral gyrus
-26,-54,42	5.42	~0	0	Left superior parietal lobule
-12,-30,72	5.389	~0	0	Left postcentral gyrus
36,26,8	5.347	~0	0	Right inferior frontal gyrus orbital part
12,-42,48	5.321	~0	0	Right paracentral lobule
56,8,38	5.312	~0	0	Right inferior frontal gyrus opercular part
8,22,26	5.299	~0	0	Right subcallosal gyrus
30,24,6	5.295	~0	0	Right insular gyrus
-52,-22,20	5.287	~0	0	Left parietal operculum
8,-48,-10	5.243	~0	0	Right cerebellum anterior lobe culmen**
0,-48,-18	5.229	~0	0	Right posterior cingulate
34,-74,14	5.218	~0	0	Right middle temporal gyrus
36,22,12	5.203	~0	0	Right inferior frontal gyrus triangular part
28,-50,44	5.196	~0	0	Right superior parietal lobule
58,8,14	5.178	~0	0	Right precentral gyrus
22,-64,42	5.148	~0	0	Right superior parietal lobule

14,-30,46	5.118	~0		0	Right paracentral lobule	
32,-76,10	5.094	~0		0	Right occiptal gyri*	
22,-64,46	5.088	~0		0	Right superior parietal lobule	
36,-74,10	5.088	~0		0	Right middle temporal gyrus	
4,-54,-10	5.087	~0		0	Right cerebellum anterior lobe culmen**	
16,-64,52	5.079	~0		0	Right superior parietal lobule	
38,-28,46	5.073	~0		0	Right postcentral gyrus	
-26,-66,52	5.059	~0		0	Left superior parietal lobule	
26,-62,34	5.034	~0		0	Right angular gyrus	
18,-66,34	5.014	~0		0	Right precuneus	
-8,36,16	4.986	0.0011096	0.001370382			
-10,-10,-14	4.975	0.001140535	0.001402126			
38,-70,20	4.957	0.001186967	0.001439399			
18,-26,8	4.951	0.001186967	0.001439399			
18,-10,70	4.946	0.001217961	0.00146301			
22,-62,32	4.936	0.001228273	0.00146301			
-10,-70,46	4.93	0.001238585	0.001468765			
14,-32,40	4.913	0.001290202	0.001523234			
18,-60,4	4.911	0.001305699	0.001534769			
12,-64,54	4.907	0.001321197	0.001546204			
52,8,2	4.841	0.001491487	0.001730383			
12,-12,50	4.825	0.001579225	0.001808685			
18,-28,4	4.823	0.001605034	0.001830422			
52,0,16	4.814	0.001641154	0.001863683			
0,-22,-18	4.789	0.00174433	0.001964204			
-18,-88,18	4.774	0.001806259	0.00202278			
12,-78,12	4.733	0.001961112	0.002180822			
42,6,22	4.711	0.002038538	0.002257554			
14,-72,36	4.666	0.002275944	0.002499807			
40,10,22	4.657	0.002301693	0.00251777			
24,-60,28	4.649	0.002342999	0.002542201			
16,-58,48	4.643	0.002379119	0.002570983			
10,-74,38	4.628	0.002482355	0.002671772			
46,4,18	4.608	0.00258559	0.002744316			
18,-50,56	4.582	0.002750695	0.002857311			
6,-6,32	4.51	0.003210008	0.003308777			
16,-76,40	4.479	0.003478408	0.003517786			
48,6,26	4.457	0.003653884	0.003681357			
34,-46,56	4.387	0.004293799	0.004309881			
34,40,26	6.424	~0		0	405	Right middle frontal gyrus	0.919
40,54,6	5.306	~0		0	Right middle frontal gyrus		
34,40,34	5.123	~0		0	Right middle frontal gyrus		
32,54,12	4.945	0.001223087	0.00146301				
-34,42,28	6.679	~0		0			
-32,38,20	5.437	~0		0			
-34,52,14	4.829	0.001553416	0.001786762				

-32,60,0	4.79	0.001739204	0.001964204			
-34,56,0	4.688	0.002172709	0.002396239			
-32,44,10	4.48	0.003452599	0.003504911			
-34,42,28	6.679	~0	0	313	Left middle frontal gyrus	0.248
-32,38,20	5.437	~0		0	Left middle frontopolar gyrus	
-34,52,14	4.829	0.001553416	0.001786762			
-32,60,0	4.79	0.001739204	0.001964204			
-34,56,0	4.688	0.002172709	0.002396239			
-32,44,10	4.48	0.003452599	0.003504911			
-16,-22,38	6.322	~0	0	124	Left paracentral lobule	0.097
46,-52,-10	5.699	~0	0	125	Right inferior temporal gyrus	0.139
40,-56,-8	5.495	~0		0	Right inferior temporal gyrus	
46,-46,-10	4.956	0.001186967	0.001439399			
-20,-72,10	5.476	~0	0	83	Left occipital gyri	0.123
-20,-70,4	4.604	0.002590716	0.002744316			
-40,-56,-6	5.440	~0	0	51	Left inferior temporal gyrus	0.354
-18,-42,-6	5.437	~0	0	26	Left parahippocampal gyrus	0.910
-6,-30,28	4.082	~0	0	19	Left posterior cingulate	0.184
-24,-56,8	3.967	~0	0	18	Left striate	0.864
-44,-42,-12	3.968	~0	0	10	Left planum polare	0.740

MNI (Montreal Neurological Institute), SDM-z (Signed Differential Mapping z-score), FDR (false discovery rate), *nearest grey matter structure, **Talairach client

Anticipation win-vs-neutral maps only deactivation all peaks

Peak MNI coordinate	**SDM-z**	**P**	**FDR**	**Voxels**	**Anatomical Description**	**Egger's test p**
-52,-64,36	-6.434	~0	0	4857	Left angular gyrus	0.670
-58,-58,28	-4.852	~0		0		
-58,-62,22	-4.649	~0		0		
-60,-18,-12	-3.097	~0		0		
-56,0,-24	-2.751	~0		0		
-58,-10,-14	-2.724	~0		0		

-62,-10,-20	-2.709	~0		0		
-60,-32,-8	-2.506	0.000005186		7.64E-06		
-54,6,-30	-2.484	0.000005186		7.64E-06		
-60,-26,-10	-2.306	0.000005186		7.64E-06		
-68,-50,4	-1.105	0.000356078		0.000465507		
-60,-50,44	-0.7	0.001537919		0.001776562		
-60,-68,6	-0.461	0.003297746		0.003386191		
-44,36,-12	-4.623	~0	0	5739	Left inferior frontal gyrus orbital part	0.074
-40,16,48	-4.104	~0		0		
-22,24,48	-3.667	~0		0		
-56,24,14	-3.035	~0		0		
-16,48,34	-3.031	~0		0		
-12,30,54	-2.617	~0		0		
-14,60,18	-2.424	0.000005186		7.64E-06		
20,26,48	-2.319	0.000005186		7.64E-06		
20,28,52	-2.262	0.000005186		7.64E-06		
-4,58,20	-2.231	0.000010312		1.51E-05		
-12,36,48	-1.922	0.000025809		3.72E-05		
-16,54,26	-1.789	0.000041306		5.89E-05		
-4,56,-8	-1.538	0.000092924		0.000131072		
18,42,46	-1.513	0.00009805		0.000136152		
16,46,42	-1.357	0.000165164		0.000225837		
36,24,48	-1.277	0.000221908		0.000298851		
12,54,34	-1.256	0.000237405		0.00031654		
10,56,26	-1.034	0.000474811		0.000611776		
-52,22,32	-0.647	0.001811445		0.00202278		
44,16,50	-0.336	0.004613757		0.004613757		
54,-62,30	-5.253	~0	0	1736	Right superior temporal gyrus	0.613
58,-58,30	-5.248	~0		0	Right superior temporal gyrus	
42,-54,22	-2.989	~0		0		
-8,-52,32	-3.102	~0	0	2159	Left precuneus	0.756
8,-52,32	-3.068	~0		0		
0,-60,30	-2.934	~0		0		
12,-52,12	-1.985	0.000025809		3.72E-05		
-10,-54,14	-1.923	0.000025809		3.72E-05		
62,-10,-20	-1.797	0.000041306	5.89E-05	807	Right middle temporal gyrus	0.570
60,-4,-16	-1.77	0.000046432		6.58E-05		
54,-8,-28	-1.525	0.00009805		0.000136152		
48,6,-42	-1.497	0.00009805		0.000136152		
50,4,-28	-1.243	0.000247717		0.000327035		
48,0,-32	-1.088	0.000376761		0.000490155		
46,-12,-32	-0.873	0.000846386		0.00105503		
52,-8,-34	-0.867	0.000846386		0.00105503		
48,-16,-36	-0.757	0.001217961		0.00146301		
48,-8,-40	-0.548	0.002518475		0.002689049		
66,-18,-20	-0.443	0.003442287		0.003504911		

40,-12,12	-2.812	~0	0	228	Right precentral gyrus	0.928
26,-18,-24	-1.421	0.000139356	0.000192512	353	Right parahippocampal gyrus	0.750
28,-10,-24	-1.347	0.00017029	0.000230494			
22,-6,-24	-1.261	0.000227094	0.000304306			
-24,-8,-24	-2.488	0.000005186	7.64E-06	213	Left parahippocampal gyrus	0.842
18,-84,-48	-1.022	0.000521243	0.000662053	236	Right cerebellum posterior lobe inferior semi-lunar lobule**	0.297
28,-82,-50	-1.007	0.000552177	0.000698035			
22,-84,-48	-0.981	0.000583172	0.000733756			
40,-70,-54	-0.573	0.002327502	0.002535653			
42,-66,-48	-0.526	0.002662957	0.002787783			
42,-62,-48	-0.456	0.003344178	0.003420762			
0,32,0	-1.185	0.000289023	0.000379697	90	Left anterior cingulate	0.608
0,24,-8	-0.506	0.002859116	0.002958468			
0,-38,72	-1.35	0.00017029	0.000230494	63	Left paracentral lobule	0.252
2,-48,70	-0.531	0.002642334	0.002787783			
6,-50,70	-0.527	0.002662957	0.002787783			
2,-60,64	-0.517	0.002750695	0.002857311			
-24,-40,8	-1.401	0.000149667	0.000205696	42	Left dentate gyrus	0.116
-24,-42,4	-1.249	0.000242531	0.000321774			
-20,-38,12	-1.056	0.00043869	0.000567966			
-32,-46,0	-1.027	0.000495434	0.000635293			
-16,-36,12	-0.807	0.001057982	0.001312681			
32,6,-36	-1.022	0.000521243	0.000665625	36	Right fusiform gyrus*	**0.039**

MNI (Montreal Neurological Institute), SDM-z (Signed Differential Mapping z-score), FDR (false discovery rate), *nearest grey matter structure, **Talairach client

Anticipation lose-vs-neutral activation maps only all peaks

Peak MNI coordinate	SDM-z	P	FDR	Voxels	Anatomical Description	Egger's test
0,18,52	6.801	~0	0	11315	Left superior frontal gyrus medial part	0.731
2,-12,-2	6.254	~0	0		Right posterior hypothalamic area	
32,-20,0	6.019	~0	0		Right putamen	
-24,2,6	5.993	~0	0		Left putamen	
6,-12,30	5.978	~0	0		Right posterior cingulate	

-58,2,28	5.801	~0	0	Left precentral gyrus
2,-28,-2	5.793	~0	0	Right pretectal area
-46,4,20	5.793	~0	0	Left inferior frontal gyrus opercular part
-52,6,44	5.75	~0	0	Left precentral gyrus
-48,12,18	5.739	~0	0	Left inferior frontal gyrus opercular part
-26,8,-2	5.672	~0	0	Left prepiriform claustrum
-14,-22,-2	5.666	~0	0	Left ventroposterior inferior thalamic nucleus
-6,2,30	5.657	~0	0	Left anterior cingulate
12,-12,12	5.634	~0	0	Right ventroanterior thalamic nucleus
28,-6,8	5.61	~0	0	Right putamen
-22,8,-2	5.593	~0	0	Left putamen
26,-2,8	5.567	~0	0	Right putamen
32,14,8	5.554	~0	0	Right insula
-12,-20,2	5.518	~0	0	Left ventrolateral posterior thalamic nucleus
16,16,2	5.48	~0	0	Right putamen
40,30,2	5.474	~0	0	Right inferior frontal gyrus triangular part
52,12,34	5.444	~0	0	Right inferior frontal gyrus opercular part
-14,-18,12	5.429	~0	0	Left ventrolateral posterior thalamic nucleus
20,2,6	5.35	~0	0	Right putamen
26,2,8	5.338	~0	0	Right putamen
16,8,10	5.337	~0	0	Right caudate
6,12,56	5.327	~0	0	Right superior frontal gyrus medial part
30,0,12	5.325	~0	0	Right claustrum
-18,-28,8	5.187	~0	0	Left lateral pulvinar
2,28,48	5.181	~0	0	Left superior frontal gyrus medial part
12,-30,56	5.172	~0	0	Right precentral gyrus
-28,-10,60	5.167	~0	0	Left superior frontal gyrus lateral part
-4,8,56	5.161	~0	0	Left superior frontal gyrus medial part
-8,6,46	5.159	~0	0	Left superior frontal gyrus medial part
-4,2,62	5.157	~0	0	Left superior frontal gyrus medial part
38,30,8	5.126	~0	0	Right inferior frontal gyrus triangular part
-16,-6,-12	5.12	~0	0	Left amygdala (basomedial nucleus)
-18,-24,10	5.094	~0	0	Left ventroposterior lateral thalamic nucleus
-6,18,22	5.082	~0	0	Left anterior cingulate
-4,6,62	5.08	~0	0	Left superior frontal gyrus medial part
-4,10,26	5.067	~0	0	Left anterior cingulate
-12,12,42	5.056	~0	0	Left superior frontal gyrus medial part
-50,0,14	5.052	~0	0	Left precentral gyrus
-4,6,44	5.05	~0	0	Left anterior cingulate
-22,-22,58	5.037	~0	0	Left postcentral gyrus
20,-26,10	5.036	~0	0	Right ventroposterior lateral thalamic nucleus
8,-2,64	5.026	~0	0	Right superior frontal gyrus lateral part
-46,-2,48	5.014	~0	0	Left middle frontal gyrus
40,12,24	4.993	0.0001549	0.0003437	

-10,14,0	4.986	0.0001549	0.0003437
30,-12,8	4.979	0.00016	0.0003437
-4,-24,64	4.975	0.00016	0.0003437
-52,-36,36	4.968	0.00016	0.0003437
-12,8,12	4.968	0.00016	0.0003437
2,0,64	4.918	0.0001703	0.0003589
26,18,0	4.916	0.0001755	0.0003607
28,4,54	4.896	0.0001806	0.0003631
44,16,8	4.889	0.0001806	0.0003631
-14,10,0	4.886	0.0001806	0.0003631
12,-16,38	4.868	0.000191	0.0003786
-46,-8,54	4.86	0.0001961	0.0003864
18,12,0	4.857	0.0002064	0.0003996
-50,-8,50	4.852	0.0002064	0.0003996
-30,-10,66	4.851	0.0002116	0.000405
-12,4,0	4.84	0.0002271	0.0004296
-12,6,4	4.837	0.0002271	0.0004296
20,4,64	4.826	0.0002322	0.0004296
8,-22,-8	4.802	0.000258	0.0004695
44,18,2	4.802	0.000258	0.0004695
4,44,34	4.796	0.0002632	0.0004764
-20,-30,-2	4.795	0.0002683	0.000483
-36,-4,56	4.79	0.0002838	0.0005054
-2,-24,-12	4.783	0.0002993	0.0005199
-34,-8,56	4.774	0.0003045	0.0005199
60,10,18	4.75	0.0003406	0.0005735
-36,-6,60	4.719	0.0003716	0.0006187
-26,22,-2	4.703	0.0003819	0.0006297
32,0,48	4.697	0.0003871	0.0006318
6,30,32	4.689	0.0004026	0.0006508
14,-26,0	4.682	0.0004077	0.0006559
-4,-20,54	4.644	0.0004748	0.0007423
10,26,24	4.644	0.0004748	0.0007423
6,24,24	4.638	0.0004799	0.0007433
-32,-10,46	4.627	0.0005006	0.0007659
-40,2,32	4.625	0.0005006	0.0007659
58,2,14	4.62	0.0005057	0.0007659
-10,-30,68	4.605	0.0005109	0.0007699
2,26,26	4.596	0.0005264	0.0007896
-36,4,8	4.568	0.000578	0.0008517
44,-4,50	4.56	0.0005832	0.0008517
50,2,-6	4.559	0.0005832	0.0008517
-28,28,-4	4.556	0.0005832	0.0008517
44,10,14	4.505	0.0006812	0.0009736
-4,-30,-18	4.472	0.000769	0.0010896
-36,2,32	4.468	0.0007793	0.0010996

52,0,14	4.434	0.000867	0.0011833			
14,0,14	4.428	0.0008876	0.0012065			
14,-18,66	4.424	0.000898	0.0012156			
50,-2,42	4.415	0.0009134	0.0012265			
-36,24,12	4.414	0.0009134	0.0012265			
16,-4,16	4.412	0.0009186	0.0012285			
-56,-32,48	4.368	0.0010322	0.0013586			
64,4,12	4.357	0.0010683	0.0013951			
52,2,6	4.335	0.0011405	0.0014664			
-52,6,2	4.321	0.0011973	0.0015217			
-20,6,60	4.31	0.001218	0.0015305			
-32,24,12	4.3	0.0012799	0.0016023			
22,-4,54	4.298	0.001285	0.0016027			
-18,22,-2	4.29	0.001316	0.0016352			
52,14,2	4.274	0.0014089	0.0017312			
-34,8,28	4.271	0.0014296	0.00175			
50,4,0	4.251	0.0015121	0.0018377			
54,2,2	4.224	0.0016618	0.0019623			
8,0,2	4.202	0.0017443	0.002031			
38,6,12	4.193	0.0017753	0.0020581			
10,-12,-16	4.169	0.0018786	0.0021571			
2,-24,28	4.156	0.0019508	0.0022088			
-44,-40,56	4.151	0.0019714	0.0022088			
-30,28,6	4.15	0.0019714	0.0022088			
14,-4,-12	4.146	0.0019766	0.0022088			
42,2,-16	4.145	0.0019766	0.0022088			
12,-40,54	4.136	0.0020334	0.0022495			
40,0,8	4.121	0.0021263	0.0023445			
38,0,-6	4.118	0.0021417	0.0023538			
60,12,26	4.096	0.0022656	0.0024817			
-24,2,60	4.07	0.0024204	0.0026169			
-4,24,16	4.065	0.0024514	0.0026418			
-44,-20,60	3.998	0.0030758	0.0032209			
-36,-6,10	3.971	0.0033597	0.0034744			
-16,-12,60	3.954	0.0035197	0.0036174			
12,-32,42	3.94	0.0036642	0.0037201			
-50,-24,56	3.915	0.003948	0.0039599			
-28,-70,26	5.753	~0	0	1854	Left parieto-occipital transition zone	0.359
-24,-72,26	5.529	~0	0		Left precuneus	
-16,-76,38	5.339	~0	0		Left parieto-occipital transition zone	
-18,-72,40	5.306	~0	0		Left parieto-occipital transition zone	
-18,-72,10	5.261	~0	0		Left striate area	
-14,-72,10	5.162	~0	0		Left striate area	
-18,-66,36	5.139	~0	0		Left parieto-occipital transition zone	
-30,-46,38	5.129	~0	0		Left superior parietal lobule	
-10,-72,14	5.123	~0	0		Left striate area	

-26,-50,44	5.101	~0	0		Left superior parietal lobule	
-32,-48,44	5.023	~0	0		Left supramarginal gyrus	
-28,-58,40	4.973	0.00016	0.0003437			
-36,-78,6	4.777	0.000304	0.0005199			
-24,-84,12	4.776	0.000304	0.0005199			
-16,-72,32	4.77	0.000304	0.0005199			
-22,-68,52	4.705	0.000382	0.0006297			
-36,-78,10	4.646	0.000459	0.0007249			
-26,-82,18	4.61	0.000506	0.0007659			
-10,-82,28	4.494	0.000702	0.000999			
-36,-86,14	4.435	0.000862	0.0011833			
-30,-78,-6	4.285	0.001352	0.0016675			
-30,-84,-2	4.231	0.001595	0.0019037			
-16,-94,12	4.226	0.001641	0.0019447			
-12,-96,8	4.04	0.00273	0.0028952			
-20,-58,50	4.019	0.002916	0.0030632			
-34,-38,48	3.945	0.003618	0.0036957			
-28,-84,6	3.944	0.003633	0.0036997			
30,-48,38	5.352	~0	0	1491	Right supramarginal gyrus	0.185
30,-54,38	5.207	~0	0		Right superior parietal lobule	
34,-68,22	5.06	~0	0		Right angular gyrus	
20,-68,42	5.016	~0	0		Right angular gyrus	
22,-68,38	4.986	0.000155	0.0003437			
22,-80,26	4.984	0.000155	0.0003437			
22,-78,22	4.957	0.000165	0.0003522			
24,-68,2	4.882	0.000181	0.0003631			
24,-62,0	4.867	0.000191	0.0003786			
30,-80,14	4.777	0.000304	0.0005199			
26,-64,32	4.745	0.000356	0.0005957			
28,-72,26	4.668	0.000434	0.0006915			
20,-70,14	4.666	0.000434	0.0006915			
8,-66,10	4.562	0.000583	0.0008517			
22,-84,18	4.433	0.000867	0.0011833			
36,-50,52	4.37	0.001032	0.0013586			
12,-72,16	4.354	0.001079	0.0013981			
28,-60,-2	4.325	0.001192	0.0015208			
10,-78,12	4.316	0.001202	0.0015219			
34,-76,10	4.316	0.001208	0.0015237			
14,-64,4	4.232	0.001584	0.0018974			
38,-66,16	4.219	0.001677	0.0019733			
14,-90,20	4.172	0.001873	0.0021571			
28,-64,8	4.071	0.00242	0.0026169			
26,-64,24	4.05	0.002637	0.0028145			
38,-50,60	3.987	0.003169	0.0032875			
-30,-60,-10	6.286	~0	0	461	Left hippocampus CA1	0.587

-42,-56,-10	5.687	~0	0		Left inferior temporal gyrus	
-38,-58,-8	5.664	~0	0		Left inferior temporal gyrus	
-42,-66,4	5.069	~0	0		Left middle temporal gyrus	
-18,-44,-8	4.526	0.000645	0.0009338			
-18,-74,-6	4.517	0.000666	0.0009559			
52,-34,36	5.207	~0	0	174	Right supramarginal gyrus	0.654
24,-46,-8	5.28	~0	0	88	Right fusiform gyrus	0.62
36,42,26	4.457	0.0007948	0.0011074	83	Right middle frontal gyrus	0.184
46,-56,-8	4.827	0.0002322	0.0004296	78	Right inferior temporal gyrus	0.143
40,-58,-8	4.751	0.000341	0.0005735			
-36,36,32	5.056	~0	0	70	Left middle frontal gyrus	0.757
32,-20,66	4.829	0.0002322	0.0004296	57	Right precentral gyrus	0.67
-12,-24,36	4.827	0.0002322	0.0004296	44	Left posterior cingulate	0.075
-6,-26,40	4.147	0.001971	0.0022088			
-32,-24,14	4.524	0.0006606	0.0009523	41	Left insula	0.938
-34,-20,-2	4.137	0.002028	0.0022495			
-36,-22,6	4.046	0.002678	0.0028491			
-36,-36,58	4.381	0.0010064	0.0013351	40	Left postcentral gyrus	0.285
-50,-24,18	4.336	0.0011405	0.0014664	39	Left parietal operculum	0.754
-54,-22,22	4.242	0.001553	0.0018736			
-14,-42,50	4.215	0.0016876	0.0019788	36	Left paracingulate	0.074
-8,-40,52	4.189	0.00178	0.0020581			
56,-16,38	4.237	0.0015585	0.0018736	20	Right postcentral gyrus	0.407
-26,48,-10	4.617	0.0005057	0.0007659	14	Left intermediate orbital gyrus	0.65
4,-40,56	4.055	0.0025804	0.0027629	14	Right paracingulate	0.071
8,-40,54	3.992	0.003259			Right paracingulate	
6,-44,54	3.963	0.0035599			Right paracingulate	
2,-48,-16	3.947	0.0035868	0.0036751	12	Right cerebellum anterior lobe culmen**	0.058

MNI (Montreal Neurological Institute), SDM-z (Signed Differential Mapping z-score), FDR (false discovery rate), *nearest grey matter structure, **Talairach client

Anticipation lose-vs-neutral maps only deactivation all peaks

Peak MNI coordinate	SDM-z	P	FDR	Voxels	Anatomical Description	Egger's test p
8,64,16	-3.4	~0	0	5037	Right superior frontopolar gyrus	0.435
12,60,24	-2.838	~0	0			
10,56,24	-2.79	~0	0			
-4,62,18	-2.494	~0	0			

-2,34,0	-2.42	~0	0			
-26,26,48	-2.389	~0	0			
20,62,24	-2.381	~0	0			
-8,60,8	-2.33	~0	0			
2,54,-14	-2.266	~0	0			
18,30,50	-2.235	~0	0			
-12,60,24	-2.234	~0	0			
-2,54,16	-2.206	~0	0			
-36,16,44	-2.151	0.000005186	1.56E-05			
-42,12,52	-2.12	0.000005186	1.56E-05			
-14,38,44	-2.034	0.000030994	9.22E-05			
-8,60,30	-2.024	0.00003612	0.000105508			
-20,38,38	-1.973	0.000041306	0.000117563			
16,40,42	-1.937	0.000051618	0.000140892			
0,22,-8	-1.933	0.000051618	0.000140892			
30,30,52	-1.912	0.000051618	0.000140892			
-6,56,0	-1.863	0.000072241	0.000182244			
-6,48,-4	-1.863	0.000072241	0.000182244			
-16,50,30	-1.831	0.000072241	0.000182244			
-8,42,-6	-1.825	0.000077426	0.000192409			
-18,46,30	-1.775	0.00009805	0.000240078			
38,24,52	-1.668	0.000159979	0.000343742			
-16,54,30	-1.657	0.000159979	0.000343742			
42,18,48	-1.611	0.000175476	0.000360701			
-10,24,56	-1.581	0.000206411	0.000399621			
-6,58,34	-1.299	0.000799954	0.001109936			
-34,10,58	-1.225	0.001047671	0.001373521			
-20,60,6	-1.121	0.001548231	0.001873626			
-12,44,24	-1.105	0.001620471	0.001927203			
30,18,60	-1.088	0.001728892	0.002020074			
26,20,60	-1.047	0.001955926	0.002208761			
-26,30,56	-0.984	0.002353311	0.002569353			
-12,56,38	-0.977	0.002399802	0.002611549			
-20,58,12	-0.932	0.002828121	0.002989728			
-52,-66,32	-3.609	~0	0	2191	Left superior temporal gyrus	0.199
-54,-62,40	-3.588	~0	0			
-36,-74,44	-3.146	~0	0			
-42,-72,44	-3.082	~0	0			
-34,-78,42	-2.919	~0	0			
-48,-58,26	-2.778	~0	0			
-38,-68,42	-2.739	~0	0			
-62,-54,22	-1.982	0.000041306	0.000117563			
-42,-84,24	-1.897	0.000061929	0.000164979			
-62,-48,30	-1.304	0.000789583	0.001107355			
-14,-52,32	-2.661	~0	0	1974	Left precuneus	0.456
-12,-48,28	-2.59	~0	0			

-6,-60,28	-2.569	~0	0			
-4,-50,10	-2.353	~0	0			
-12,-56,26	-2.343	~0	0			
4,-60,30	-2.331	~0	0			
2,-44,10	-1.795	0.000092924	0.000229213			
52,-68,34	-4.054	~0	0	1609	Right angular gyrus	0.790
58,-62,30	-3.977	~0	0			
52,-64,30	-3.606	~0	0			
60,-58,30	-3.57	~0	0			
62,-56,16	-3.062	~0	0			
64,-52,14	-3.011	~0	0			
60,-60,12	-2.733	~0	0			
68,-40,2	-2.003	0.00003612	0.000105508			
66,-48,-2	-1.891	0.000061929	0.000164979			
66,-44,4	-1.883	0.000061929	0.000164979			
66,-32,0	-1.842	0.000072241	0.000182244			
70,-30,0	-1.819	0.000077426	0.000192409			
-60,-12,-16	-2.375	~0	0	1105	Left middle temporal gyrus	0.333
-64,-18,-18	-2.179	~0	0			
-54,-10,-32	-2.133	0.000005186	1.56E-05			
-54,-6,-26	-1.943	0.000051618	0.000140892			
-48,12,-36	-1.377	0.000588357	0.000855558			
-54,4,-32	-1.3	0.000794768	0.001107355			
-64,-40,-8	-1.292	0.000820577	0.001133826			
-60,-40,-8	-1.256	0.000970244	0.001292365			
-48,6,-38	-1.162	0.001321197	0.001635534			
-60,-6,-6	-1.049	0.001935303	0.002208761			
-42,16,-40	-0.787	0.004417658	0.004417658			
58,0,-18	-2.752	~0	0	577	Right middle temporal gyrus	0.986
66,-12,0	-1.872	0.000072241	0.000182244			
54,-6,-30	-1.759	0.000103235	0.000247318			
52,10,-32	-1.692	0.00013417	0.000312438			
54,12,-24	-1.618	0.000175476	0.000360701			
42,18,-40	-1.577	0.000211596	0.000404951			
44,0,-34	-1.569	0.000237405	0.000436773			
48,6,-42	-1.496	0.000340641	0.0005735			
50,4,-32	-1.424	0.000479937	0.000743344			
64,-4,-2	-1.038	0.002028227	0.002249523			
-44,38,-18	-2.156	0.000005186	1.56E-05	413	Left inferior frontal gyrus orbital part*	0.862
-54,24,8	-1.997	0.000041306	0.000117563			
-48,28,4	-1.951	0.000046432	0.000131033			
-40,32,-16	-1.692	0.00013417	0.000312438			
-48,30,-2	-1.668	0.000159979	0.000343742			
-48,34,-12	-1.548	0.000283837	0.000505442			
-38,44,-16	-0.896	0.003153265	0.003281366			

-16,-16,-26	-2.75	~0	0	337	Left entorhinal cortex	0.862
-22,-10,-22	-2.343	~0	0			
-22,2,-24	-1.697	0.00013417	0.000312438			
2,-58,66	-1.88	0.000072241	0.000182244	302	Right paracingulate gyrus	**0.006**
4,-62,64	-1.855	0.000072241	0.000182244			
4,-82,44	-1.766	0.000103235	0.000247318			
0,-76,52	-1.536	0.000294149	0.000519926			
2,-90,30	-1.528	0.000304461	0.000519926			
-2,-74,58	-1.457	0.00040257	0.000650756			
4,-88,34	-1.38	0.000577986	0.000851738			
-6,-68,64	-0.847	0.003684819	0.003729619			
20,-26,-26	-1.436	0.000459313	0.000724887	124	Right cerebellum anterior lobe culmen**	0.929
24,-20,-26	-1.215	0.001078606	0.001398082			
18,-18,-26	-1.2	0.001156032	0.00148061			
20,-20,-20	-0.953	0.002570093	0.002760777			
12,-12,-24	-0.928	0.002848744	0.003001999			
34,38,-12	-1.766	0.000103235	0.000247318	96	Right lateral orbital gyrus	0.255
42,38,-18	-1.648	0.00017029	0.000358902			
-30,-32,-20	-1.601	0.000175476	0.000360701	39	Left fusiform gyrus	0.903
4,-28,74	-1.139	0.001434684	0.001749999	14	Right precentral gyrus	**0.026**
2,-38,74	-0.834	0.003818989	0.003853707			
-2,-40,72	-0.828	0.00389123	0.003914742			
56,28,18	-1.716	0.000123858	0.000294605	12	Right inferior frontal gyrus opercular part *	0.201
20,-36,12	-1.473	0.000387073	0.00063184	10	Right stria terminalis	0.957

MNI (Montreal Neurological Institute), SDM-z (Signed Differential Mapping z-score), FDR (false discovery rate), *nearest grey matter structure, **Talairach client

Supplementary Table 6: Between Group Linear Comparison anticipation win-vs-neutral minus anticipation lose-vs-neutral

MNI coordinate	SDM-z	P	FDR	Voxels	Description
-6,38,18	2.923	0.003034532	0.004327869	8	Left anterior cingulate
-44,38,-10	-2.776	0.000676095	0.004327869	36	Left inferior frontal gyrus orbital part

MNI (Montreal Neurological Institute), SDM-z (Signed Differential Mapping z-score), FDR (false discovery rate)

Supplementary Table 7: Hetereogeneity QH Stats Converted to SDM z-scores

Anticipation win-vs-neutral

Peak MNI coordinate	SDM-z	Voxels	Anatomical Description
-30,-92,-4	8.371	3305	Left occipital gyrus
34,-88,-2	7.99	3090	Right occipital gyrus
10,4,-6	7.171	1000	Right nucleus basalis
30,20,-6	6.915	611	Right posterior orbital gyrus
-38,20,0	6.439	192	Left inferior frontal gyrus orbital part
-42,-22,54	5.703	150	Left postcentral gyrus
-10,10,-6	5.784	95	Left nucleus accumbens
-14,-10,66	5.793	87	Left superior frontal gyrus lateral part
-4,-54,64	6.154	62	Left superior parietal lobule
-30,-58,52	5.376	54	Left superior parietal lobule
-54,6,12	5.658	38	Left inferior frontal gyrus opercular part
50,4,34	5.295	38	Right precentral gyrus
-52,8,-6	5.39	34	Left superior temporal gyrus
-12,-72,-4	5.782	33	Left occipital gyrus
-22,-24,-8	5.869	32	Left lateral geniculate nucleus
32,-12,-6	5.992	24	Right limitans claustrum
2,-66,0	5.726	23	Right cerebellum anterior lobe culmen
-10,-16,42	5.334	17	Left posterior cingulate
-10,-12,56	5.351	16	Left superior frontal gyrus lateral part
2,-12,68	5.392	13	Right superior frontal gyrus lateral part
-40,-64,24	5.295	13	Left angular gyrus
60,8,22	5.295	13	Right precentral gyrus
-50,-26,54	5.574	11	Left postcentral gyrus
-60,-32,32	5.167	11	Left parietal operculum

MNI (Montreal Neurological Institute), SDM-z (Signed Differential Mapping z-score)

Anticipation lose-vs-neutral

Peak MNI coordinate	SDM-z	Voxels	Anatomical Description
-42,-22,48	7.021	1171	Left postcentral gyrus
-6,-8,50	6.745	593	Left paracentral lobule
2,-52,-20	6.807	400	Right cerebellum anterior lobe culmen*
10,6,2	6.221	192	Right fundus of the caudate
38,-8,54	6.057	117	Right precentral gyrus*

-4,-24,-6	6.704	87	Left red nucleus
-8,6,0	5.715	79	Left nucleus accumbens
-24,-96,-8	5.654	37	Left occipital gyrus
6,-48,36	5.544	35	Right posterior cingulat
-18,-60,16	5.702	15	Left occipital gyrus
32,24,2	5.295	14	Right inferior frontal gyrus opercular part
56,-60,24	5.295	11	Right superior temporal gyrus
0,40,-14	5.368	11	Left straight gyrus
-8,-82,4	5.295	10	Left occipital gyrus

MNI (Montreal Neurological Institute), SDM-z (Signed Differential Mapping z-score)

Supplementary Figure 2: Binarised thresholded overlay map of heterogeneity and mean map activation and deactivation

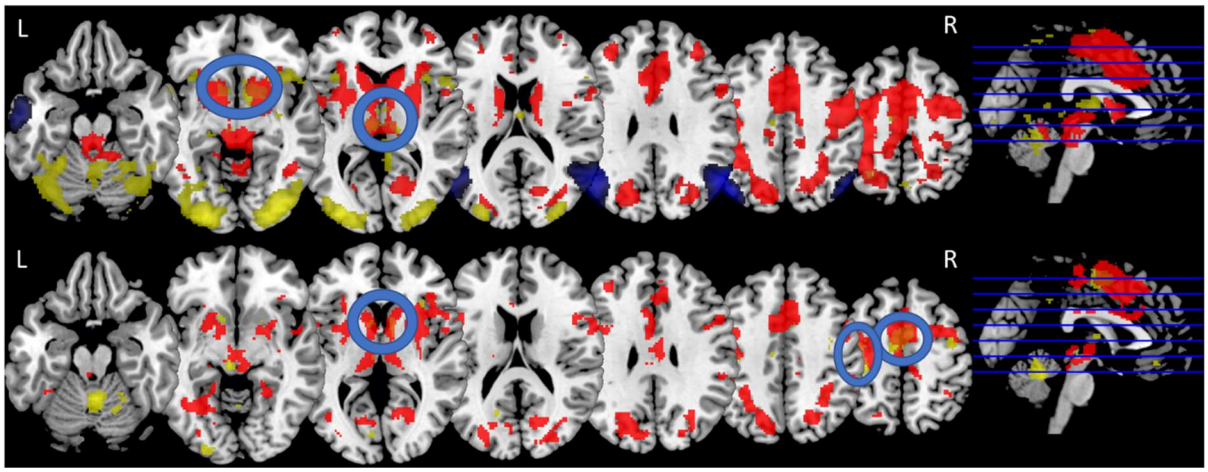

Top row anticipation win-vs-neutral; bottom anticipation lose-vs-neutral; heterogeneity is yellow, activation is red, deactivation is blue, blue circles indicate visual overlap

Supplementary Figure 3: Binarised Jacknife density maps with mean maps of activation and deactivation separated out to enhance visual inspection

Anticipation win-vs-neutral

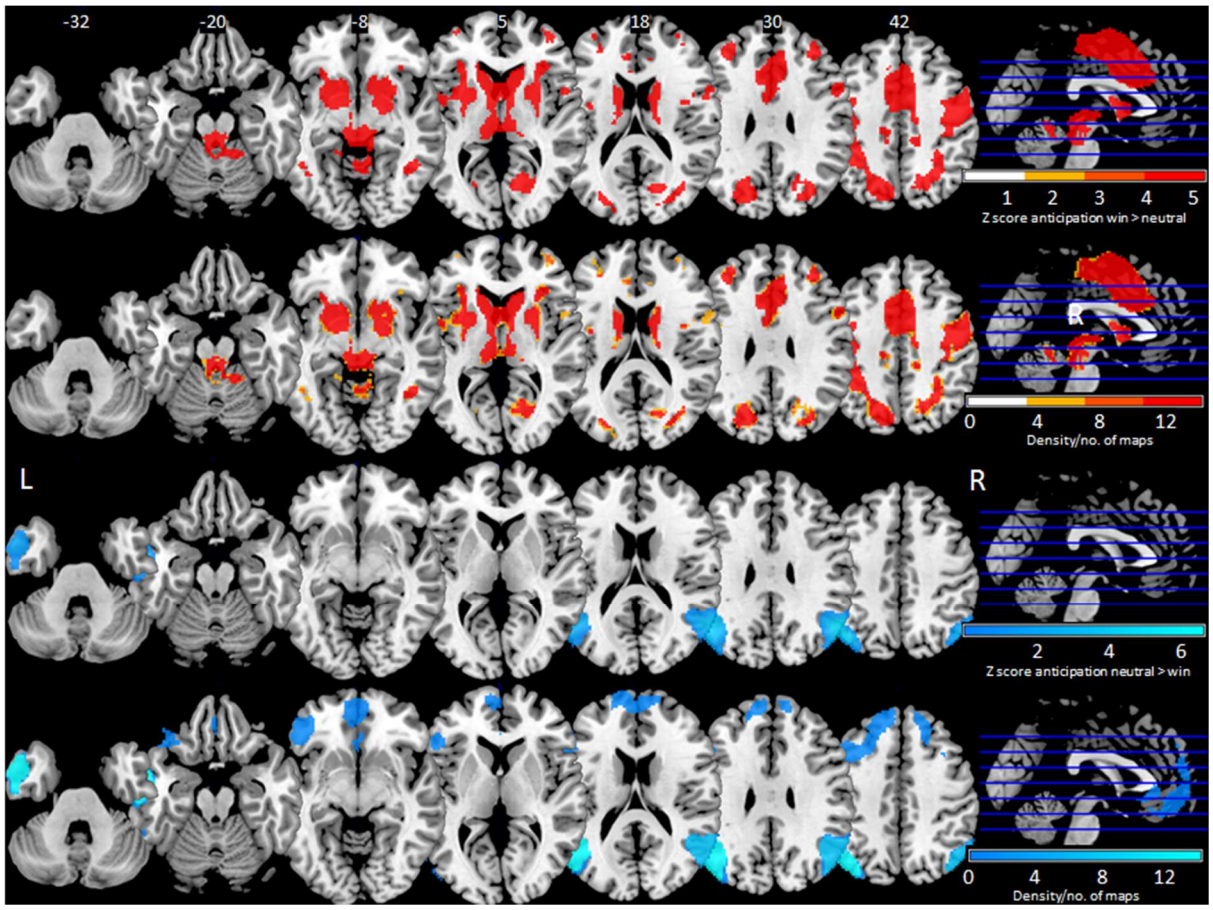

Descending from the top row: mean map activation, Jacknife density map activation, mean map deactivation, Jacknife density map deactivation

Anticipation lose-vs-neutral

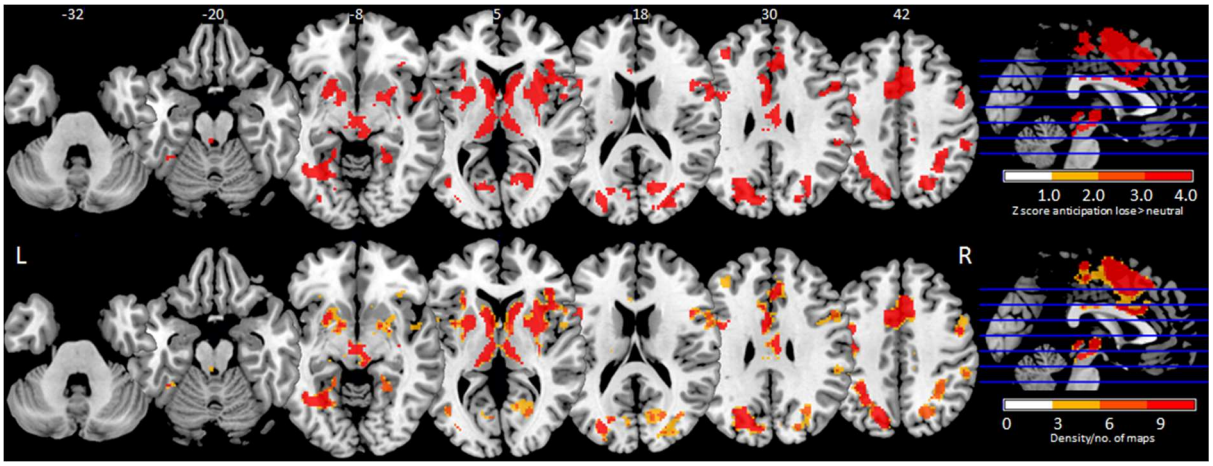

Top row: mean map activation, bottom row Jacknife density map deactivation

Supplementary Figure 4: Meta-regression for placebo effect with mean map heterogeneity overlaid

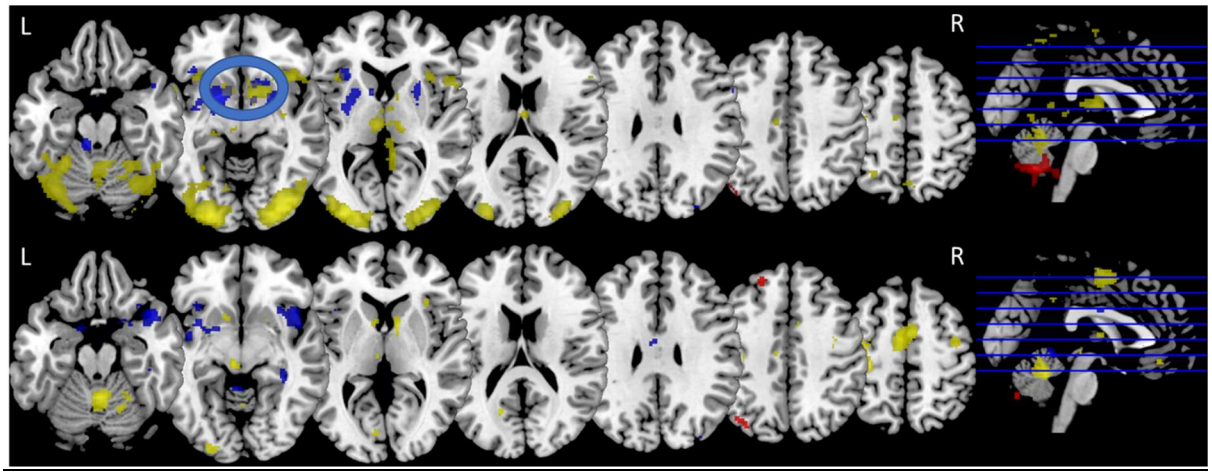

Top row- anticipation win-vs-neutral; bottom anticipation lose-vs-neutral; heterogeneity in yellow, activation red, deactivation blue, blue circles indicate visual overlap

Supplementary Table 8: Meta-regression for Placebo Effect

Anticipation win-vs-neutral

Peak MNI coordinate	SDM-z	Voxels	Anatomical description
0,-60,-42	3.649	2614	Left cerebellum posterior lobe**
-46,-72,40	2.738	28	Left angular gyrus
28,24,48	2.322	22	Right middle frontal gyrus
-16,2,-8	-4.112	991	Left substriatal terminal island (encompassing ventral striatum)
24,0,-8	-3.421	212	Right putamen
12,12,-12	-3.855	152	Right posteromedial orbital lobule
-36,26,-12	-3.152	151	Left inferior frontal gyrus orbital part
-8,-34,-18	-3.963	80	Left cerebellum anterior lobe**
32,-84,30	-3.351	65	Right occipital gyrus
-56,-2,12	-3.064	65	Left precentral gyrus
46,12,-18	-3.091	30	Right middle temporal gyrus
60,8,34	-3.200	15	Right inferior frontal gyrus opercular part*
48,6,-30	-3.003	15	Right inferior temporal gyrus
-44,-20,22	-2.882	15	Left frontal operculum
-4,-4,28	-3.114	10	Left posterior cingulate gyrus

MNI (Montreal Neurological Institute), SDM-z (Signed Differential Mapping z-score), *nearest grey matter structure, **Talairach client

Anticipation lose-vs-neutral

Peak MNI coordinate	SDM-z	Voxels	Anatomical description

16,-64,-52	3.268	123	Right cerebellum posterior lobe*
-22,36,46	3.125	109	Left superior frontal gyrus lateral part
-6,-72,-40	3.341	57	Left cerebellum posterior lobe*
-12,-58,-56	2.759	43	Left cerebellum posterior lobe*
-36,-72,44	2.879	33	Left angular gyrus
-14,60,12	2.943	30	Left middle frontopolar gyrus
-8,56,28	2.912	13	Left superior frontal gyrus medial part
-20,56,24	2.672	11	Left superior frontal gyrus lateral part
-50,-60,42	2.667	10	Left supramarginal gyrus

MNI (Montreal Neurological Institute), SDM-z (Signed Differential Mapping z-score), *Talairach client

Supplementary Figure 5: Meta-regression for Field Strength with Mean Map Heterogeneity Overlay

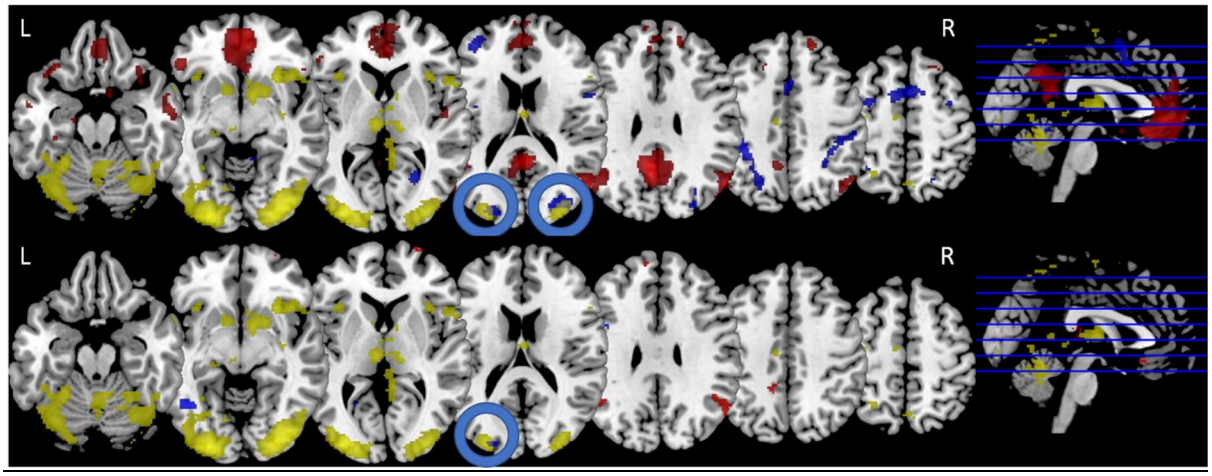

Top row: anticipation win-vs-neutral; bottom: anticipation lose-vs-neutral; heterogeneity in yellow, activation red, deactivation blue, blue circles indicate visual overlap

Supplementary Table 9: Meta-regression for Field Strength

Anticipation win-vs-anticipation neutral

Peak MNI coordinate	SDM-z	Voxels	Anatomical description
-56,-56,36	2.533	105	Left supramarginal gyrus
-14,-46,38	2.837	101	Left posterior cingulate gyrus
56,-58,34	2.424	93	Right superior temporal gyrus
24,68,0	2.544	32	Right inferior frontopolar gyrus
0,-30,14	2.55	20	Left thalamus
-2,26,-12	2.126	19	Left straight gyrus
-6,54,34	2.184	18	Left superior frontal gyrus, lateral part
-48,-54,-12	-5.115	127	Left inferior temporal gyrus
-22,-50,0	-4.309	56	Left lingual gyrus
-22,-88,16	-4.485	34	Left occipital gyri
-40,4,34	-3.747	30	Left precentral gyrus
-20,-38,-28	-4.214	13	Left cerebellum anterior lobe culmen
-6,-68,8	-3.511	12	Left striate area

MNI (Montreal Neurological Institute), SDM-z (Signed Differential Mapping z-score)

Anticipation lose-vs-anticipation neutral

Peak MNI coordinate	SDM-z	Voxels	Anatomical description
-4,34,-14	4.495	2513	Left straight gyrus
-4,-56,30	5.278	1405	Left posterior cingulate gyrus
-52,-66,32	4.104	661	Left angular gyrus
-66,-34,-6	3.917	616	Left middle temporal gyrus
54,-64,28	5.038	507	Right superior temporal gyrus
48,0,-32	3.305	297	Right inferior temporal gyrus
-48,30,-10	3.515	256	Left inferior frontal gyrus, orbital part
18,46,42	3.325	122	Right superior frontal gyrus, lateral part
36,18,-32	2.709	85	Right inferior temporopolar region
8,8,-16	2.544	56	Right anterior olfactory nucleus
-30,-38,-16	3.241	52	Left fusiform gyrus
-42,18,48	3.078	50	Left middle frontal gyrus
34,26,-18	2.603	52	Right posterior orbital gyrus
-18,-14,-24	2.983	30	Left entorhinal cortex
24,26,58	2.514	30	Right superior frontal gyrus, lateral part
50,26,-4	2.532	21	Right inferior frontal gyrus, triangular part
-6,42,30	2.284	21	Left superior frontal gyrus, medial part
50,-10,4	2.553	20	Right anterior transverse temporal gyrus
-32,-14,-24	2.355	17	Left parahippocampal gyrus
58,-24,-22	2.32	16	Right inferior temporal gyrus

-18,30,44	2.427	14	Left superior frontal gyrus, lateral part
-48,-32,52	-5.857	1642	Left supramarginal gyrus
8,6,62	-5.31	613	Right superior frontal gyrus, medial part
28,-50,46	-4.397	418	Right superior parietal lobule
-52,4,14	-5.091	372	Right precentral gyrus
28,-84,22	-5.509	344	Right parietal-occipital transition zone
-38,44,22	-4.45	196	Left middle frontal gyrus
-22,-90,18	-5.226	100	Left occipital gyri
24,-60,6	-4.524	50	Right striate area
-42,-2,50	-4.27	46	Left middle frontal gyrus
38,36,34	-4.364	42	Right middle frontal gyrus
60,8,14	-4.408	44	Right precentral gyrus
-16,-18,72	-5.059	25	Left precentral gyrus
8,-6,70	-4.806	19	Right superior frontal gyrus, lateral part
34,0,54	-3.864	22	Right middle frontal gyrus
-30,-76,24	-3.828	15	Left angular gyrus
36,50,24	-3.725	15	Right middle frontal gyrus
-62,-16,16	-3.506	14	Left reticular thalamic nucleus
0,-50,-12	-3.42	13	Left cerebellum, anterior lobe culmen
62,-40,36	-3.762	11	Right superior temporal gyrus

MNI (Montreal Neurological Institute), SDM-z (Signed Differential Mapping z-score)

Appendix 2

Figure 1. Example of MIDT visual cue sequence

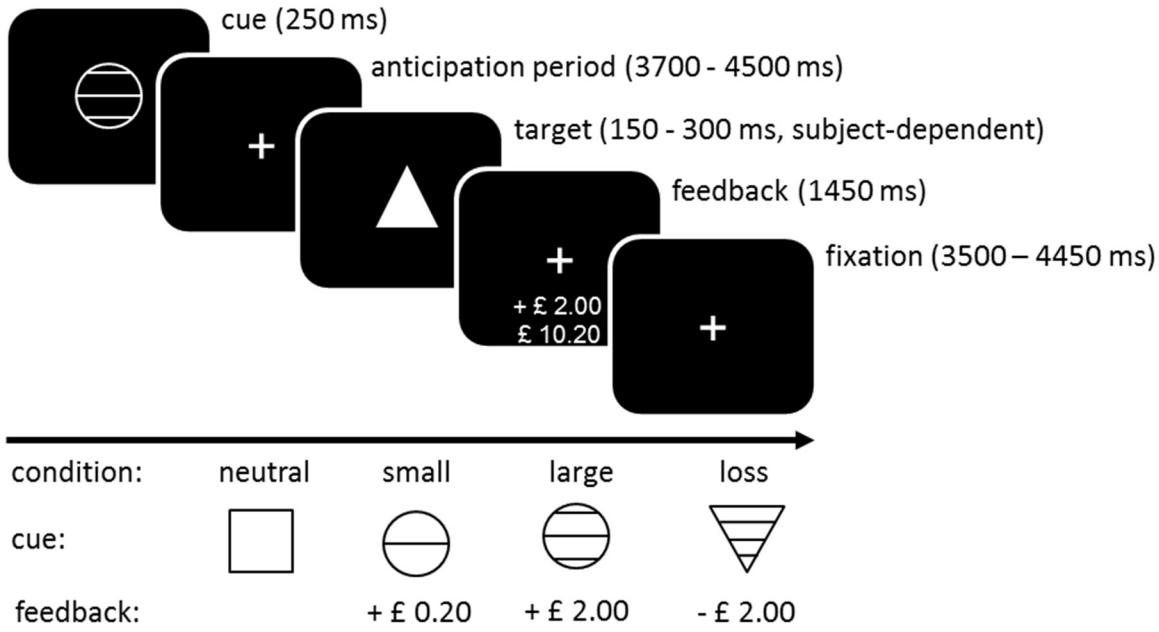

Table 1. Brain regions activated by the monetary incentive delay task in healthy controls

Region	Peak coordinate (MNI)			Cluster size	p(FWE-corr)
	x	y	z		
Core salience network ROI analysis					
Right parietal operculum	34	-40	18	47	0.001
	32	-32	14		0.003
Left insula	-30	-38	18	19	0.002
Right insula/inferior frontal gyrus triangular part	32	22	12	11	0.018
Hippocampus-midbrain-striatum ROI analysis					
Right amygdala	20	-8	-6	3578	<0.001
	20	-12	4		
	-14	-26	-18		
Wholebrain analysis					
Left precentral gyrus	-54	-2	44	6853	<0.001
	-20	-2	56		<0.001
	14	4	56		<0.001
Right amygdala	18	-8	-8	6767	<0.001
	20	-14	4		<0.001
	-18	-18	6		<0.001
Left occipital gyrus (nearest GM)	-34	-50	6	909	<0.001
	-24	-70	6		<0.001
	16	-82	8		<0.001
Right anterior cingulate	14	20	32	98	<0.001
Left occipital gyrus	-28	-94	8	70	0.002
Left paracentral lobule	-16	-24	40	28	0.006
Left cerebellum posterior lobe	-16	-44	-44	33	0.007
Right cerebellum posterior lobe	32	-66	-28	95	0.013
	22	-62	-26		0.019
	36	-76	-26		0.037
Right lateral orbital gyrus	30	34	0	22	0.014
Left paracentral lobule	-8	-44	58	33	0.015
Left superior parietal lobule	-18	-54	58	13	0.015
Right inferior frontal gyrus orbital part	28	24	10	21	0.015
	28	36	12		0.033
Right superior parietal lobule	16	-70	56	20	0.024
Right occipital gyrus	8	2	42	13	0.032
Right cerebellum posterior lobe	20	-46	-44	11	0.033

Table 1. Brain regions activated by the monetary incentive delay task in healthy controls for motivational salience (salience>neutral) in salience network region of interest (ROI), hippocampus-midbrain-striatum ROI and whole-brain. 1-sample t-test, FWE-corrected p<0.05, k>10 voxels

Table 2. Wholebrain analysis for salience-vs-neutral contrast

Region	Peak coordinate (MNI)			Cluster size	p
	x	y	z		
Pairwise comparison CHR-PLB>HC					
Left superior frontal gyrus medial part	-8	24	58	141	<0.001
Left inferior frontal gyrus opercular part	-54	20	20	65	0.002
(Left frontal operculum)	-44	16	12		0.004
Left superior temporal gyrus/supramarginal gyrus	-54	-54	30	13	0.009
Pairwise comparison CHR-PLB>CHR-CBD					
Right superior frontal gyrus lateral part	20	-4	48	3	0.025
Pairwise comparison CHR-CBD>CHR-PLB					
Right cerebellum posterior lobe	6	-82	-38	6	0.022
3-way ANOVA CHR-PLB>CHR-CBD>HC					
Left superior frontal gyrus medial part	-10	22	58	18	0.006

Table 2. Wholebrain analysis for salience-vs-neutral contrast. Family wise error-corrected p<0.05, k≥3voxels. Abbreviations: HC=healthy control group, CHR-CBD=clinical-high risk cannabidiol group, CHR-PLB=clinical-high risk placebo group.

Figure 2. Whole-brain analysis of salience>neutral contrast

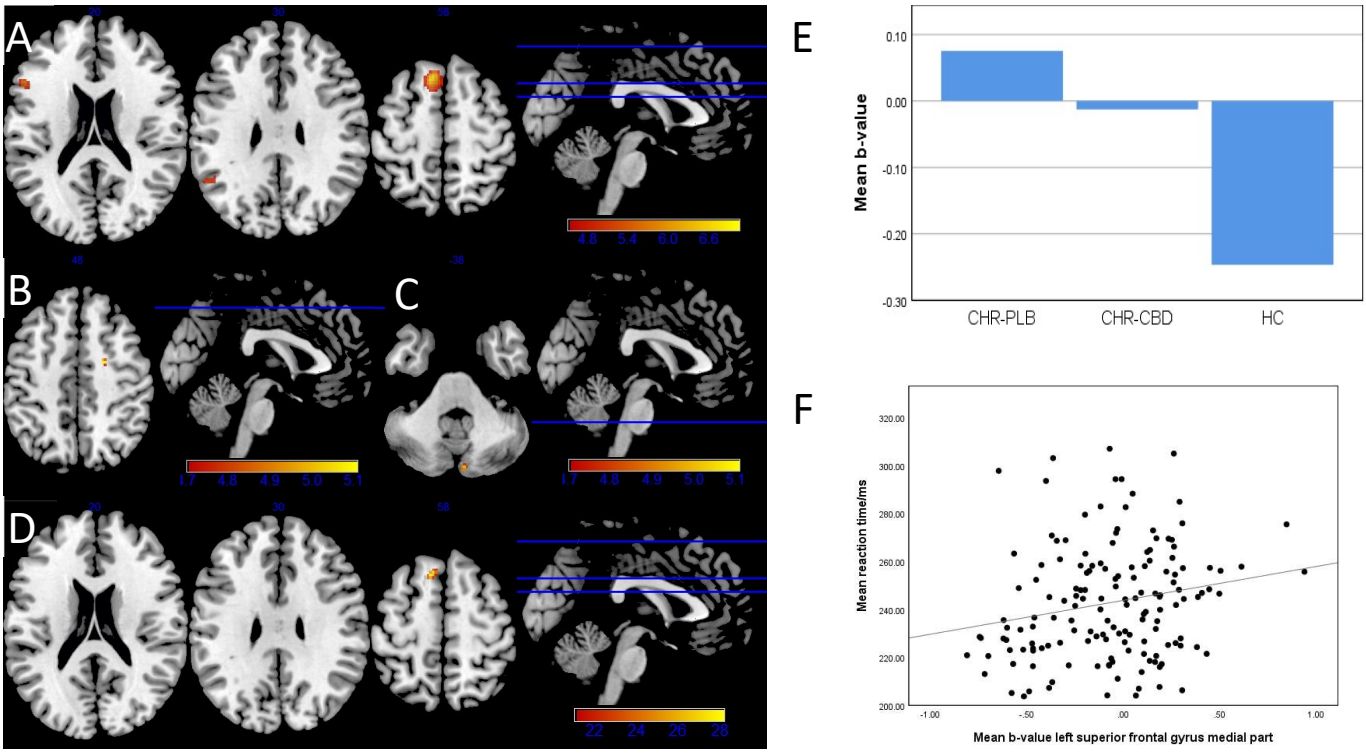

Figure 2. Whole-brain analysis of salience>neutral contrast (small-volume corrected, p<0.05 FWE-corrected at voxel level, k≥3 voxels). (A) Pairwise comparison CHR-PLB>HC with clusters in left superior frontal gyrus medial part, left inferior frontal gyrus opercular part extending to left frontal operculum and left superior temporal gyrus. (B) Pairwise comparison CHR-PLB>CHR-CBD with cluster in right superior frontal gyrus lateral part. (C) Pairwise comparison CHR-CBD>CHR-PLB with cluster in right cerebellum posterior lobe. (D) 3-way ANOVA CHR-PLB>CHR-CBD>HC with cluster in left superior frontal gyrus medial part. (E) Mean b-value parameter estimates extracted from ANOVA-derived cluster in the left superior frontal gyrus medial part for each group (CHR-PLB, CHR-CBD, and HC) showing increased activation in CHR-PLB relative to HC with CHR-CBD intermediate. (F) Positive correlation between mean b-value from ANOVA-derived cluster of left superior frontal gyrus medial part and mean reaction time for salience condition in CHR-CBD.

Supplementary Analysis

In the exploratory whole-brain analysis, we report increased activation in the left SFGM, left IFGOP and left STG in HC-vs-CHR-PLB. In CHR-PLB-vs-CHR-CBD there was relative deactivation of the right SFGL and increased activation in the right cerebellum. A linear relationship was confirmed by ANOVA in the left SFGM, with CBD attenuating activation. This in turn correlated with reaction time during salience (r=0.377, p=0.011, CI=0.093-0.662; Supplementary Table 2, Supplementary Figure 2) absent in CHR-PLB and HC. CBD was associated with an overall slowing of motor response, suggesting a role modulating premature action. The pre-SMA region is thought to be critical to behavioural response selection and inhibition in measures of response inhibition (Simmonds, Pekar et al. 2008).